ΠΑΝΕΠΙΣΤΗΜΙΟ ΚΡΗΤΗΣ

ΙΑΤΡΙΚΗ ΣΧΟΛΗ

ΤΟΜΕΑΣ ΒΑΣΙΚΩΝ ΕΠΙΣΤΗΜΩΝ

ΕΡΓΑΣΤΗΡΙΟ ΒΙΟΧΗΜΕΙΑΣ

Διδακτορική διατριβή

Ο ρόλος πρωτεολυτικών μηχανισμών στον μεταβολισμό λιπιδίων

Κωνσταντίνα Γεωργιλά

Επιβλέπων Καθηγητής: Αριστείδης Γ. Ηλιόπουλος

Ηράκλειο, 2020

UNIVERSITY OF CRETE

SCHOOL OF MEDICINE

DEPARTMENT OF BASIC SCIENCES

Ph.D. thesis

The role of proteolytic systems in the control of lipid metabolism

Konstantina Georgila

Supervisor: Aristides G. Eliopoulos

Heraklion, 2020

ΕΥΧΑΡΙΣΤΙΕΣ

Θα ήθελα να ευχαριστήσω θερμά, τον επιβλέποντα Καθηγητή μου Δρ. Αριστείδη Γ. Ηλιόπουλο που έδωσε την δυνατότητα να εκπαιδευτώ και να εργαστώ σε ένα εργαστήριό υψηλής επιστημονικής στάθμης όπως το δικό του. Του οφείλω ευγνωμοσύνη καθώς με καθοδήγησε με ενδιαφέρον στις επιστημονικές μου αναζητήσεις, υποστήριξε την ερευνητική μου δραστηριότητα, δημιουργώντας τις προϋποθέσεις για την ομαλή πορεία του διδακτορικού μου και φρόντισε για την ανάπτυξη των επιμέρους ερευνητικών μου δεξιοτήτων, συντελώντας σημαντικά στην εξέλιξή μου ως ερευνήτρια. Τον ευχαριστώ ακόμη για την αμέριστη εμπιστοσύνη που μου έδειξε, την αξιοθαύμαστη υπομονή του, και την ενθάρρυνση που μου παρείχε με γενναιοδωρία στις στιγμές απογοήτευσής μου. Πάνω απ' όλα όμως τον ευχαριστώ διότι ως υπόδειγμα ακαδημαϊκού δασκάλου και μέντορα δημιούργησε έμπνευση και όραμα για την όλη ερευνητική μου πορεία.

Η ποιότητα του χαρακτήρα του, η εγγενής ευγένεια, το ήθος και η οξύτητα και το βάθος του πνεύματός του είναι χαρακτηριστικά του τα οποία θαυμάζω, και αισθάνομαι τυχερή διότι είχα την μοναδική ευκαιρία να μαθητεύσω υπό την επίβλεψη του.

Θέλω να ευχαριστήσω τον Καθηγητή Δρ. Χρήστο Τσατσάνη και την Καθηγήτρια Δρ. Δόμνα Καραγωγέως, μέλη της Τριμελούς μου Συμβουλευτικής Επιτροπής, διότι ήταν πάντα διαθέσιμοι και βοηθητικοί για οποιοδήποτε ζήτημα πρόκυπτε.

Οφείλω ένα μεγάλο ευχαριστώ στους Αναπληρωτές Καθηγητές κυρίους Δρ. Χαμηλό και Δρ. Δράκο, με τους οποίους είχαμε μια εξαιρετική συνεργασία. Ήταν πάντα πρόθυμοι να συζητήσουν τα επιστημονικά μου ερωτήματα και με στήριξαν όχι μόνο στις ερευνητικές μου δράσεις αλλά και ως γιατροί όταν χρειάστηκε.

Ευχαριστώ τον Καθηγητή Δρ. Καρδάση Δημήτρη, και την Αναπληρωτρια Καθηγητρια Δρ. Νικολετοπούλου Βασιλική, μέλη της Επταμελούς μου Εξεταστικής Επιτροπής, για τις πολύτιμες συμβουλές τους και τις εποικοδομητικές συζητήσεις μας.

Ιδιαίτερες ευχαριστίες στον Καθηγητή Δρ. Μπούμπα Δημήτρη, ο οποίος με καθοδήγησε και με στήριξε κατά τη διάρκεια των μεταπτυχιακών μου σπουδών.

Ένα ξεχωριστό ευχαριστώ σε όλα τα μέλη του εργαστηρίου μας ειδικά τη Ζωή Βενέτη, τη Δήμητρα Βύρλα και τον Ηλία Σταγάκη για το κλίμα συνεργασίας και συναδελφικότητας που προήγαγε και την επιστημονική πρόοδο. Ευχαριστώ πολύ και τους εκπαιδευομένους μου, τη Κατερίνα, τον Αλέξανδρο, τη Στυλιανή και φυσικά τον Μιχάλη μου, τους νεότερους επιστήμονες που επέβλεψα κατά τις προπτυχιακές ή μεταπτυχιακές τους εργασίες στο εργαστήριο και οι οποίοι με την επιστημονική τους περιέργεια τόνωναν την ενέργεια μου και μοιράστηκαν το πάθος για την επιστήμη αλλά και πολλές ώρες εργαστηριακής εργασίας. Ήταν ιδιαίτερη τύχη

και χαρά να εργάζομαι με τον Μιχάλη Γούνη, ο οποίος με τον ευχάριστο χαρακτήρα του και τη λεπτομερή του εργασία ήταν πολύτιμος συνεργάτης. Αλησμόνητη θα είναι και η συμπόρευση μας με τον εξαιρετικό συνάδελφο και αναντικατάστατο φίλο Δρ. Δημήτρη Θεοφιλάτο, που απ το διπλανό εργαστήριο συμπαραστεκόταν στις αγωνίες μου και μοιραζόταν μαζί μου σκέψεις και βλέψεις επιστημονικές και όχι μόνο.

Κατά τη διάρκεια της διδακτορικής μου διατριβής μοιράστηκα τα άγχη και τα όνειρα μου με σπουδαίους φίλους που συμπαραστάθηκαν στη προσπάθειά μου. Θα ήθελα να ευχαριστήσω λοιπόν τον Άρη, το Γιώργο, την Έφη, τη Λένα, τη Μαργαρίτα και τη Μαρία για τη πίστη τους σε μένα και για την πολύτιμη στήριξή τους.

Ακόμη θα ήθελα να ευχαριστήσω τη μητέρα μου γιατί ήταν αυτή που επίμονα με παρακίνησε στην απόκτηση αυτού του τίτλου, με υποστήριζε έμπρακτα σε αυτή τη διαδρομή και με ενέπνεε με τη δική της αγάπη για την έρευνα. Πολλά ευχαριστώ στην αδερφή μου και την οικογένειά της γιατί με τη δική τους αγάπη, στήριξή και κριτική έγινα καλύτερη σε όλα τα επίπεδα. Θα ήθελα να ευχαριστήσω και τον πατέρα μου ο οποίος, ως υπέρτατο ηθικό στοιχείο, προσπαθούσε να με προστατεύσει από κακοτοπιές του ακαδημαϊκού τοπίου και μου υπενθύμιζέ και έμπρακτα τις αξίες της ζωής που ως κέντρο έχουν τον ίδιο τον άνθρωπο. Τέλος θα ήθελα να ευχαριστήσω τον σύντροφό μου και τον γιο μου, που δίνουν νόημα σε ότι κάνω και με την αγάπη και την αφοσίωση τους με ενισχύουν σε κάθε μου διάβημα.

Τέλος, θα ήθελα να σημειώσω ότι η συγγραφή της διδακτορικής μου διατριβής συνέπεσε με την περίοδο κατά την οποία περίμενα τον ερχομό του παιδιού μου αλλά και με την εξάπλωση μιας πρωτοφανούς παγκόσμιας πανδημίας με περιοριστικά μετρά απομόνωσης, ενώ η ολοκλήρωση της εργασίας και η προετοιμασία της παρουσίασης με βρίσκει πανευτυχή με το μωρό μου αγκαλιά και ταυτίζεται χρονικά με τη μερική άρση των περιορισμών. Αυτά τα γεγονότα και η συγκύριες με έκαναν ακόμη μια φορά να σκεφτώ τη σπουδαιότητα της επιστήμης μας για την ανθρωπότητα και με παρακίνησαν με αίσθημα αισιοδοξίας να συνεχίσω να ενεργώ και να πορεύομαι με σεβασμό για τη ζωή και να εργάζομαι με οξύνοια και αγάπη για το κοινό καλό, υποστηρίζοντας τις θεμελιώδεις επιδιώξεις μου, να γίνομαι καλύτερη επιστήμονας και άνθρωπος.

Στη μητέρα και στην αδερφή μου

Table of Contents

ΠΕΡΙΛΗΨΗ 1
ABSTRACT 6
1. INTRODUCTION 10
1.1 Apolipoprotein A-I 10
1.1.1 ApoA-I as a major protein component of high-density lipoprotein 10
1.1.2 ApoA-I regulation 11
1.1.3 ApoA-I in liver pathologies 13
1.2 The autophagic pathway 15
1.3 Mechanism regulating lipid metabolism in the liver 20
2. MATERIALS AND METHODS 28
2.1 Reagents and antibodies 28
2.2 Cell culture and transfection assays 29
2.3 Primary mouse hepatocytes isolation and mouse liver samples 30
2.4 Immunoblotting and densinometric analysis 31
2.5 Immunoprecipitation 32
2.6 Meausurement of secreted ApoA-I levels (ELISA) 32
2.7 MTT Cell Proliferation Assay 32
2.8 Immunofluorescence staining 33
2.9 Electron Microscopy 34
2.10 Proteasome Activity Assay 35
2.11 RNA extraction, cDNA synthesis and q-PCR, RNAseq 35
2.12 Statistical analysis 36
3. AIM OF THE STUDY 37
4. RESULTS 38
4.1 Chapter 1 38
4.1.1 Steatosis is associated with elevated levels of ApoA-I. 38
4.1.2 Autophagy but not proteasomal inhibitors lead to intracellular ApoA-I accumulation. 39
4.1.3 Autophagic pathway components associate with ApoA-I. 41
4.1.4 Genetic inhibition of autophagic pathway components leads to impaired ApoA-I proteolysis. 43
4.1.5 Starvation leads to inhibition of *de novo* synthesis of ApoA-I rather than autophagy-mediated ApoA-I degradation. 44
4.1.6 mTORC1 signaling is required for basal ApoA-I expression. 48
4.1.7 Metformin reduces ApoA-I levels by downregulating apolipoprotein gene expression. 50

4.1.8 Discussion (Chapter 1) 52
4.2 Chapter 2 56
4.2.1 ApoA-I physiologically acts to suppress intracellular lipid overload by affecting LD homeostasis. 56
4.2.2 The transcriptome of HepG2 hepatoma cells depleted for ApoA-I is enriched for upregulated genes related to lipid and cholesterol metabolism. 57
4.2.3 The transcriptome of HepG2 hepatoma cells depleted for ApoA-I is enriched for downregulated genes related to cell cycle and survival processes. 61
4.2.4 ApoA-I impacts on lipid metabolism by regulating cholesterol and lipid synthesis gene expression upon autophagic inhibition. 64
4.2.5 Autophagy inhibition modulates lipid synthesis gene expression through SREBP2. 66
4.2.6 Intracellular ApoA-I regulates lipid synthesis gene expression by impacting on FOXO activity through Akt phosphorylation. 67
4.2.7 ApoA-I physiologically functions to suppress Akt phosphorylation and activity by mTORC2 signaling modulation. 70
4.2.8 ApoA-I physically interact with Akt. 72
4.2.9 ApoA-I impacts cell death. 72
4.2.10 ApoA1 depletion confers resistance to lipotoxicity and attenuates ER-stress gene expression. 73
4.2.11 Discussion (chapter 2) 75
5. DISCUSSION 78
6. REFERENCES 83

ΠΕΡΙΛΗΨΗ

Η απολιποπρωτεΐνη Α1 (ApoA-I) , ως κύριο συστατικό της HDL, εμπλέκεται στην αντίστροφη μεταφορά χοληστερόλης, ενώ παράλληλα παρουσιάζει αντιθρομβωτικές, αντιοξειδωτικές, αντιφλεγμονώδεις και ανοσορυθμιστικές ιδιότητες, οι οποίες είναι συναφείς του προστατευτικού της ρόλο σε καρδιαγγειακές, φλεγμονώδεις και κακοήθεις παθολογίες.

Οι στόχοι αυτής της διδακτορικής διατριβής είναι (1) ο προσδιορισμός μετα-μεταγραφικών μηχανισμών ρύθμισης των ενδοκυττάριων επιπέδων της ApoA-I και (2) η διερεύνηση πιθανών ενδοκυττάριων λειτουργιών της, φαινόμενα τα οποία έχουν ελάχιστα διερευνηθεί.

Το αντικείμενο της μελέτης που περιγράφεται στο κεφάλαιο 1 σχετίζεται με τη ρύθμιση της ApoA-I στα ηπατοκύτταρα από μετα-μεταγραφικούς μηχανισμούς και πρωτεολυτικά συστήματα. Χρησιμοποιήσαμε την καρκινική σειρά ηπατοκυττάρων HepG2 και πρωτογενή ηπατοκύτταρα ποντικού ως *in vitro* μοντέλο για τη μελέτη της επίδρασης γενετικών και χημικών παρεμποδιστών της αυτοφαγίας και του πρωτεοσώματος, και εξετάσαμε την ApoA-I με ανοσοαποτύπωση, ανοσοφθορισμό και ηλεκτρονική μικροσκοπία. Διαφορετικές συνθήκες ανάπτυξης εφαρμόστηκαν σε συνδυασμό με παρεμποδιστές του mTOR προκειμένου να προσομοιάσουμε την επίδραση περιορισμένων θρεπτικών σε σύγκριση με επάρκεια θρεπτικών στη ρύθμιση της ApoA-I. Η έκφραση της ApoA-I στο ήπαρ μελετήθηκε σε ποντίκια που θράφηκαν με δίαιτα υψηλών λιπαρών και παρουσιάζουν παρεμπόδιση της αυτοφαγίας. Τα αποτελέσματα μας κατέδειξαν ότι η φαρμακολογική παρεμπόδιση της αυτοφαγίας και όχι του πρωτεοσώματος συνεπάγεται τη συσσώρευση της ApoA-I στα ηπατοκύτταρα. Για να εξετάσουμε λεπτομερώς τα μοριακά μονοπάτια που διέπουν την αποικοδόμηση της ApoA-I από την αυτοφαγία χρησιμοποιήσαμε γενετική αποσιώπηση σημαντικών ρυθμιστών της αυτοφαγικής μηχανής και παρακολουθήσαμε τα επίπεδα έκφρασης της ApoA-I. Παρατηρήσαμε ότι η πρωτεόλυση της ApoA-I διέπεται από ένα κανονικό μονοπάτι αυτοφαγίας στο οποίο συμμετέχει η Beclin1, η ULK1 και η πρωτεΐνη p62 που φαίνεται να στοχεύει την ApoA-I στα αυτοφαγοσώματα. Στη συνέχεια αναλύσαμε τα επίπεδα της ApoA-I υπό συνθήκες περιορισμένων θρεπτικών, οι οποίες επάγουν αυτοφαγία ενώ παράλληλα μπλοκάρουν αναβολικές διαδικασίες, όπως η μετάφραση, μέσω του

mTORC1 μονοπατιού. Διαπιστώσαμε ότι εφαρμόζοντας στέρηση θρεπτικών παρατηρείται ότι η καταστολή της σύνθεσης της ApoA-I επικρατεί στη ρύθμιση των επιπέδων της πρωτεΐνης σε σχέση με την επίδραση της πρωτεόλυσης της ApoA-I μέσω της αυτοφαγίας. Αυτά τα δεδομένα αναδεικνύουν τη μεγάλη συνεισφορά μετα-μεταγραφικών μηχανισμών στη ρύθμιση των επιπέδων της ApoA-I στην οποία εμπλέκεται η εξαρτωμένη mTORC1 σηματοδότηση που αναλόγως με τις συνθήκες διαθέσιμων θρεπτικών καθορίζει την αυτοφαγία ή την πρωτεϊνική σύνθεση ως το κύριο μηχανισμό ελέγχου των επίπεδών της. Δεδομένου του εδραιωμένου ρόλου της ApoA-I στην αντίστροφη μεταφορά χοληστερόλης, η ρύθμιση αυτή της ApoA-I θα μπορούσε να αντανακλά μια ηπατική απάντηση σε οργανικές απαιτήσεις για την διατήρηση των αποθηκών χοληστερόλης και λιπιδίων υπό αντίξοες θρεπτικές συνθήκες.

Καθώς παρατηρήσαμε ότι η έκφραση της ApoA-I σε ηπατοκύτταρα μπορεί να ρυθμιστεί ανάλογα στη διαθεσιμότητα των θρεπτικών, μας ενδιέφερε να μελετήσουμε αν η ApoA-I μπορεί να λειτουργήσει ως διαμεσολαβητικό μόριο ανταποκρινόμενο στις μεταβολικές ανάγκες του κυττάρου. Στο κεφάλαιο 2 παρουσιάζονται τα αποτελέσματα της μελέτης που εστιάζει στην αποσαφήνιση πιθανής ενδοκυττάριας λειτουργίας της ApoA-I στη ρύθμιση του λιπιδικού μεταβολισμού. Με αφορμή τις δημοσιευμένες παρατηρήσεις (1) ότι η καταστολή της αυτοφαγίας οδηγεί σε συσσώρευση μεγάλου μεγέθους λιπιδικών σταγόνων σε κυτταρικά συστήματα και σε στεάτωση σε πειραματικά μοντέλα, (2) ότι η απαλοιφή της ApoA-I σε ποντίκια που έχουν θραφεί με δίαιτα υψηλών λιπαρών οδηγεί σε στεάτωση και (3) ότι η ApoA-I συσσωρεύεται όταν παρεμποδίζεται η αυτοφαγία, υποθέσαμε ότι η ενδοκυττάρια ApoA-I θα μπορούσε φυσιολογικά να λειτουργήσει κατασταλτικά στην υπέρμετρη συγκέντρωση λιπιδίων και χοληστερόλης υπό συνθήκες αυτοφαγικής παρεμπόδισης. Πράγματι, βρήκαμε ότι η αποσιώπηση της ApoA-I σε κυτταρική σειρά ηπατοκυττάρων HepG2 συνεπάγεται την συσσώρευση μεγάλων λιπιδικών σταγόνων, ένα φαινόμενο το οποίο ενισχύθηκε από ταυτόχρονη παρεμπόδιση της αυτοφαγίας. Η δράση της ApoA-I στον έλεγχο του ενδοκυττάριου λιπιδικού φορτίου είναι ανεξάρτητη της αυτοφαγίας, καθώς η αποσιώπηση της ApoA-I δεν επηρέασε σημαντικά την αυτοφαγική ροή. Για να συγκεντρώσουμε πληροφορίες σχετικά με το μηχανισμό με τον οποίο η ApoA-I επηρεάζει τις ενδοκυττάριες λιπιδικές αποθήκες, διερευνήσαμε το μεταγράφωμα κυττάρων στα οποία έχει

γίνει γενετική αποσιώπηση της ApoA-I. Η βιοπληροφορική ανάλυση κατέδειξε εμπλουτισμό βιολογικών διαδικασιών που σχετίζονται με το μεταβολισμό λιπιδίων και χοληστερόλης και συσχέτιση με τη νόσο του λιπώδους ήπατος και άλλων μεταβολικών νοσημάτων. Είναι ενδιαφέρον πως ένας σημαντικός αριθμός γονίδιων – σχετιζόμενων με τη βιογένεση λιπιδίων και χοληστερόλης – παρουσίασε αύξηση στην έκφραση και έπειτα από τη παρεμπόδιση της αυτοφαγίας αλλά και από τη γενετική αποσιώπηση της ApoA-I. Η συνδυαστική επίδραση οδήγησε σε μια αξιοσημείωτη αύξηση της γονιδιακής έκφρασης των μεταβολικών οδών σε σχέση με τις μεμονωμένες επιδράσεις. Οι παρατηρήσεις αυτές είναι σε συμφωνία με τη συσσώρευση λιπιδικών σταγόνων που προκύπτει από αυτές τις επιδράσεις, και υποστηρίζουν ότι η ενδοκυττάρια ApoA-I και η αυτοφαγία συγκλίνουν στο μεταγραφικό έλεγχο της *de novo* βιοσύνθεσης λιπιδίων και χοληστερόλης. Επιβεβαιωτικά πειράματα ελέγχου της γονιδιακής έκφρασης που πραγματοποιήθηκαν υπό τις ίδιες συνθήκες επιβεβαίωσαν ότι η μείωση των επιπέδων της ApoA-I σχετίζεται με την υπερέκφραση των γονιδίων βιοσύνθεσης λιπιδίων και χοληστερόλης. Η σημασία αυτών των ευρημάτων για τον άνθρωπο αναδεικνύεται από το γεγονός ότι η ανάλυση δεδομένων αλληλούχισης του μεταγραφώματος ιστών ασθενών με ηπατοκυτταρικό καρκίνο αποκάλυψε την ίδια συσχέτιση- δηλαδή ότι η έκφραση της ApoA-I είναι αντιστρόφως ανάλογη της έκφραση γονιδίων που εμπλέκονται στη βιοσύνθεση λιπιδίων και χοληστερόλης όπως τα *HMGCR, HMGCS1, FASN, LPIN1* and *ACACA*.

Ανάλυση της έκφρασης βασικών μεταγραφικών ρυθμιστών των γονιδίων που σχετίζονται με βιοσυνθετικά μονοπάτια λιπιδίων και χοληστερόλης υπό συνθήκες γενετικής αποσιώπησης της ApoA-I ή/και αυτοφαγικής παρεμπόδισης κατέδειξε ότι η παρεμπόδιση της αυτοφαγίας επηρεάζει την ωρίμανση του SREBP2 και όχι τη φωσφορυλίωση ή έκφραση του FOXO1/3. Αντίστροφα, η γενετική αποσιώπηση της ApoA-I οδήγησε σε αύξηση της φωσφορυλιωσης του FOXO1/3 αλλά δεν επιδρά στα επίπεδα και την πρωτεολυτική εκτομή του SREBP2. Αυτά τα ευρήματα είναι σε συμφωνία με την επίδραση της ApoA-I και της αυτοφαγίας στην αλλαγή των επιπέδων έκφρασης των μεταβολικών γονιδίων αλλά και στην ενίσχυση των δράσεων τους όταν συνυπάρχουν. Καθώς η φωσφορυλίωση του FOXO1/3 καθοδηγείται από την ενεργοποίηση της Akt, σε συνέχεια εξετάσαμε την επίδραση της γενετικής αποσιώπησης της ApoA-I στο μονοπάτι

σηματοδότησης της Akt. Παρατηρήσαμε ότι η γενετική αποσιώπηση της ApoA-I οδηγεί σε εξαρτώμενη από mTORC2 φωσφορυλίωση της Akt στη σερίνη 473 και καταστολή του άξονα mTORC2/Akt μειώνει την επίδραση της αποσιώπησης της ApoA-I στην έκφραση των *HMGCR* και *HMGCS1*. Τα προκαταρκτικά αποτελέσματα καταδεικνύουν ότι η ApoA-I είναι σε φυσική αλληλεπίδραση τόσο με την Akt1 όσο και με την Akt2, τουλάχιστον όταν αυτά τα μόρια βρίσκονται σε συνθήκες υπερέκφρασης στη κυτταρική σειρά HEK293T. Επιπρόσθετες μελέτες χρειάζονται για τη διερεύνηση του μηχανισμού με τον οποίο η ApoA-I καθοδηγεί την ενεργοποίηση της Akt. Πέρα από την αύξηση της έκφρασης των γονιδίων που σχετίζονται με βιοσύνθεση λιπιδίων και χοληστερόλης, το μεταγράφωμα κυττάρων, τα οποία έχουν υποστεί ταυτόχρονα γενετική αποσιώπηση του γονίδιου της ApoA-I και παρεμπόδιση της αυτοφαγίας, είναι εμπλουτισμένα σε υποεκφραζόμενα γονίδια σχετιζόμενα με λειτουργίες ελέγχου του κυτταρικού κύκλου και με νεοπλασματικές ασθένειες. Τα αποτελέσματα αυτά υποδεικνύουν ότι η μείωση της ApoA-I σε συνδυασμό με την παρεμπόδιση της αυτοφαγίας μπορεί να διαμορφώσει ένα κυτταρικό περιβάλλον αυξημένου λιπιδικού φορτίου και ένα δυναμικό ανεξέλεγκτου κυτταρικού πολλαπλασιασμού το οποίο θα μπορούσε να οδηγήσει σε κακοήθεις φαινοτύπους του ήπατος. Σε συμφωνία με αυτή τη θεωρία παρατηρήσαμε ότι η γενετική αποσιώπηση της *ApoA1* σε HepG2 κύτταρα προστατεύει από την λιποτοξικότητα και την τοξικότητα από γενωμικό stress, ενώ παράλληλα παρέχει αντίσταση στο stress του ενδοπλασματικού δικτύου, όπως διαφαίνεται από την καταστολή της μεταγραφής των σχετικών γονιδίων. Εν κατακλείδι, τα προκαταρκτικά *in vivo* δεδομένα είναι σε συμφωνία με τα *in vitro* αποτελέσματα μας που καταδεικνύουν ότι η γενετική απαλοιφή της ApoA-I σε ποντίκια τα οποία έχουν ιστοειδική απαλοιφή του ATG5 στο ήπαρ οδηγεί σε επιδείνωση της παθολογίας στεάτωσης και μπορεί να καθοδηγήσει κακοήθεις φαινοτύπους του ήπατος.

Συμπερασματικά, η ερευνά μας ρίχνει φως στη ρύθμιση της ApoA-I στο ήπαρ καθορίζοντας ένα κύριο μετα-μεταγραφικό μονοπάτι υπεύθυνο για τον έλεγχο των ενδοκυττάριων επιπέδων της. Κάτω από συνθήκες πλούσιων σε θρεπτικά η έκφραση της ApoA-I διατηρείται από την ισορροπιστική δράση της αυτοφαγίας και της εξαρτώμενης από mTORC1 *de novo* πρωτεϊνικής σύνθεσης. Επιπρόσθετα, αποκαλύψαμε ένα καινούριο ρόλο της ApoA-I στη ρύθμιση της

λιπιδικής ομοιόστασης στο ήπαρ. Η ApoA-I φαίνεται να λειτουργεί ως φρένο στην αμετροεπή συσσώρευση λιπιδίων που προκύπτει από την αυτοφαγική παρεμπόδιση. Παρατηρήσαμε ότι η αυτοφαγική παρεμπόδιση, πέραν της γνωστής επίδρασης της μέσω της λιποφαγίας και της ρύθμισης λιπολυτικών μηχανισμών, επιδρά και στην επαγωγή της έκφρασης μεταβολικών γονιδίων στον καθορισμό του ενδοκυττάριου λιπιδικού φορτίου μέσω της ωρίμανσης του SREBP2. Η επίδραση της αυτοφαγικής παρεμπόδισης στη γονιδιακή έκφραση ενισχύεται από την γενετική αποσιώπηση της ApoA-I, η οποία διαμεσολαβείται από την εξαρτώμενη από την mTORC2 αύξηση της φωσφορυλίωσης της Akt και της συνεπακόλουθης φωσφορυλίωσης και απενεργοποίησης του μεταγραφικού παράγοντα FOXO1/3 που δρα ως καταστολέας της μεταγραφής μεταβολικών γονιδίων.

Οι νέες λειτουργίες της ApoA-I που περιγράφονται στην παρούσα διδακτορική διατριβή είναι πιθανό να επαναδιαμορφώσουν την κατανόηση του μεταβολισμού των λιπιδίων και της χοληστερόλης αλλά και τον ρόλο της ίδιας της ApoA-I. Η διαφαινόμενη φυσική και λειτουργική αλληλεπίδραση της ApoA-I με την Akt, που διαμορφώνει το δυναμικό ενεργοποίησης της κινάσης και τη συνεπακόλουθη ρύθμιση των επιπέδων έκφρασης των γονιδίων που σχετιζονται με το μεταβολισμό λιπιδίων, χρειάζεται περαιτέρω διερεύνηση. Εν κατακλείδι, η παρούσα μελέτη καταδεικνύει ότι τα ελαττωμένα επίπεδα της ApoA-I υπό συνθήκες παρεμπόδισης της αυτοφαγίας, όπως αυτές επικρατούν και στο ηπατοκυτταρικο καρκίνο, σχετίζονται με ενισχυμένη έκφραση γονιδίων σχετικά με τη βιοσύνθεση των λιπιδίων και της χοληστερόλης, με τη συσσώρευση λιπιδικών σταγόνων, με αυξημένη επιβίωσή *in vitro*, και με επιδείνωση καρκινογένεσης *in vivo*. Μελλοντικές έρευνες θα μπορούσαν να στοχεύσουν στην αποσαφήνιση του μηχανισμού με τον οποίο η ApoA-I φοσφωρυλιώνει την Akt, καθοδηγώντας και καθορίζοντας επιπρόσθετες κυτταρικές δράσεις, αλλά και στη συμμετοχή της ApoA-I στην αιτιοπαθολογία νόσων του ήπατος που σχετιζονται με αυξημένο λιπιδικό φορτίο και κακοήθεια.

ABSTRACT

Apolipoprotein A-I (ApoA-I) is involved in reverse cholesterol transport as a major component of HDL, but also conveys anti-thrombotic, anti-oxidative, anti-inflammatory and immune-regulatory properties that are pertinent to its protective roles in cardiovascular, inflammatory and malignant pathologies.

The aim of this PhD Thesis is to define post-transcriptional mechanisms responsible for the regulation of intracellular ApoA-I levels and decipher putative intracellular functions of ApoA-I, questions which remain poorly explored.

Data presented in chapter 1 address the role of proteolytic pathways, autophagy and the ubiquitin-proteasome system (UPS) in ApoA-I regulation in hepatocytes and hepatoma cells as *in vitro* models to study the impact of genetic and chemical inhibitors of autophagy and the proteasome on ApoA-I by immunoblot, immunofluorescence and electron microscopy. Different growth conditions were implemented in conjunction with mTOR inhibitors to model the influence of nutrient scarcity *versus* sufficiency on ApoA-I regulation. Hepatic ApoA-I expression was also evaluated in high fat diet-fed mice displaying blockade in autophagy.

The results documented that under nutrient-rich conditions, basal ApoA-I levels are sustained by the balancing act of autophagy and of mTORC1-dependent *de novo* protein synthesis. Pharmacologic inhibition of autophagy and not the proteasome resulted in the accumulation of ApoA-I in hepatocytes. To dissect the molecular pathway that governs ApoA-I degradation by autophagy we used genetic silencing of key modulator of autophagic machinery and monitored ApoA-I levels. We found that ApoA-I proteolysis occurs via a canonical autophagic pathway involving Beclin1 and ULK1 and the receptor protein p62/SQSTM1 that targets ApoA-I to autophagosomes. We next analyzed ApoA-I levels, under conditions of starvation that induce autophagy and in parallel block anabolic processes as translation through mTOR pathway. We found that upon aminoacid insufficiency, suppression of ApoA-I synthesis prevails, rendering mTORC1 inactivation dispensable for autophagy-mediated ApoA-I proteolysis.

Collectively, the data presented in chapter 1 underscore the major contribution of post-transcriptional mechanisms to ApoA-I levels which differentially involve mTORC1-dependent signaling to protein synthesis and autophagy, depending on nutrient availability. Given the established role of ApoA-I in HDL-mediated reverse cholesterol transport, this mode of ApoA-I regulation may reflect a hepatocellular response to the organismal requirement for maintenance of cholesterol and lipid reserves under conditions of nutrient scarcity.

As hepatic expression of ApoA-I responds to nutrient availability, we were interested to explore whether ApoA-I may act as a mediator for specific cellular energetic requirements and as modulator of intracellular lipid metabolism under conditions of autophagic blockade and/or increased lipid load. Data presented in chapter 2 delineate the putative intracellular function of ApoA-I in the regulation of lipid metabolism. Intrigued by published evidence that, (1) suppression of autophagy leads to accumulation of large size lipid droplet (LD) *in vitro* and steatosis *in vivo*; (2) ApoA-I ablation in HFD-fed mice results in steatosis; and (3) ApoA-I accumulates in response to inhibition of autophagy, we hypothesized that intracellular ApoA-I may physiologically function to suppress lipid and cholesterol overload under conditions of autophagy blockade. Indeed, the knock-down of *ApoA1* in the hepatoma cell line HepG2 resulted in the accumulation of large size lipid droplets, an effect that was amplified upon simultaneous inhibition of autophagy. This ApoA-I function was independent of autophagy, as ApoA-I depletion did not significantly affect autophagic flux. To provide mechanistic insights into the modulation of intracellular lipid stores by ApoA-I, we used a hypothesis-free approach that entails the unbiased interrogation of the transcriptome of ApoA-I depleted HepG2 cells. We identified enrichment of biological processes linked to lipid and cholesterol metabolism and an association with fatty liver and metabolic diseases. Interestingly, a significant number of genes related to cholesterol and lipid biosynthesis were commonly up-regulated by autophagy blockade and ApoA-I depletion which, when combined, led to a marked increase in metabolic gene expression compared to either treatment alone. These observations align with the LD accumulation ensued by these treatments and indicate that intracellular ApoA-I and autophagy converge to transcriptionally control *de novo* lipid and cholesterol biosynthesis. The significance

of these findings in human disease is highlighted by our mining of hepatocellular carcinoma RNAseq data which confirmed that *ApoA1* expression levels are inversely correlated with genes implicates in lipid and cholesterol biosynthesis, such as *HMGCR, HMGCS, FASN, LPIN1* and *ACACA*.

Expression analysis of key transcriptional modulators of lipid and cholesterol biosynthetic genes upon *ApoA1* knock-down and/or autophagic inhibition revealed that inhibition of autophagy affects SREBP2 maturation but not FOXO1/3, whereas the RNAi-mediated depletion of *ApoA1* leads to marked phosphorylation of FOXO1/3 but does not impact SREBP2 cleavage which is required to generate the transcriptionally active SREBP2. These findings align both with the impact of *ApoA1* depletion and autophagy inhibition on inducing the expression of a common set of cholesterol and lipid biosynthesis genes and their amplifying effects on gene expression when combined.

As FOXO1/3 phosphorylation is mediated by Akt activation, the effect of ApoA-I depletion on the Akt signaling pathway was examined. It was found that the knock-down of *ApoA1* leads to mTORC2-dependent phosphorylation of Akt at Ser^{473} and that suppression of the mTORC2/Akt axis diminishes the effect of ApoA-I depletion on *HMGCR* and *HMGCS1* expression. Our preliminary data demonstrate that ApoA-I physically interacts with both Akt1 and Akt2 at least when overexpressed in HEK293T cells. Further studies exploring the mechanism by which ApoA-I physiologically functions to moderate Akt activation are warranted.

Beyond the upregulation of lipid and cholesterol biosynthesis processes, the transcriptome of dually ApoA-I depleted and autophagy-inhibited HepG2 cells is enriched in downregulated genes related to cell cycle control and an overall association with neoplastic diseases. We therefore hypothesize that the reduction in ApoA-I coupled with autophagy blockade, could provide a cellular environment of lipid overload with a pro-survival potential that could drive malignant phenotypes in the liver. In line with this notion, the knock-down of *ApoA1* in HepG2 cells protects against lipotoxicity and genotoxicity, and in parallel provides ER-stress resistance as indicated by the transcriptional suppression of genes involved in lipid overload-mediated ER stress, facilitating cell survival. Finally, our preliminary *in vivo* data, in accordance with our *in*

vitro results, demonstrate that ApoA-I ablation in mice with liver specific ablation of ATG5 exaggerates steatosis and carcinogenic phenotypes.

Collectively, our study sheds light into the regulation of hepatic ApoA-I by defining a major post-transcriptional pathway responsible for the control of intracellular ApoA-I levels. Under nutrient-rich conditions, ApoA-I expression is sustained by the balancing acts of basal autophagy and of mTORC1-dependent *de novo* protein synthesis. In contrast, upon aminoacid insufficiency, suppression of ApoA-I synthesis prevails, rendering mTORC1 inactivation dispensable for autophagy-mediated ApoA-I proteolysis. In addition, we unveil a novel role for ApoA-I in hepatic lipid homeostasis. ApoA-I functions as a break to lipid accumulation which is particularly evident under conditions of autophagic inhibition. We also found that autophagy blockade, besides its direct involvement in the regulation of intracellular lipid stores through lipophagy and modulation of lipolytic mechanisms, acts in the transcriptional regulation of cholesterol and fatty acid biosynthetic gene expression by affecting SREBP2 maturation. The effect of autophagy inhibition on gene expression is augmented by *ApoA1* knock-down which induces mTORC2-dependent Akt phosphorylation inactivating the transcription factor FOXO1/3, a negative regulator of lipid and cholesterol biosynthesis genes.

The novel intracellular functions of ApoA-I identified in this PhD Thesis are likely to transform our understanding of lipid and cholesterol metabolism and expand our understanding of the *in vivo* physiological roles of ApoA-I. The identification of ApoA-I as a novel putative Akt-interacting protein, once consolidated with additional experiments, will also expand our knowledge of this key kinase in different tissues. Results in this PhD Thesis also demonstrate that reduced levels of ApoA-I under conditions of autophagy inhibition, as observed in hepatocellular carcinoma, are associated with amplified lipid and cholesterol biosynthetic gene expression, lipid droplet accumulation, enhanced survival *in vitro* and exaggerated hepatocarcinogenesis *in vivo*. Future studies will aim at dissection of the mechanism of ApoA-I modulation of Akt phosphorylation and provide further insights into the implication of ApoA-I regulation in liver pathologies associated with increased lipid load and carcinogenesis.

1. INTRODUCTION

1.1 Apolipoprotein A-I

1.1.1 ApoA-I as a major protein component of high-density lipoprotein

ApoA-I is the main structural protein of high-density lipoprotein (HDL) which is responsible for the transfer of unesterified cholesterol and cholesteryl esters from peripheral tissues to the liver (1). As such, the ApoA-I-containing HDL has attracted tremendous attention for its anti-atherogenic and cardioprotective effects mainly due its participation in Reverse Cholesterol Transport (RCT) (2, 3). However, the functions of ApoA-I extend beyond cholesterol transport to include a broad spectrum of anti-thrombotic, anti-oxidative, anti-inflammatory and immune-regulatory properties that are pertinent to the protective roles of ApoA-I in various pathologies related to inflammation and cancer (4).

HDLs are heterogeneous and dynamic structures exchanging lipids with cells and other lipoproteins, classified to different subcategories with pre-β1 HDL corresponding to lipid-poor ApoA-I (5, 6). ApoA-I is essential for HDL assembly as it stabilizes the ATP-binding cassette transporter 1 (ABCA1), a member of the ABC superfamily, at the cell membrane of hepatocytes and enterocytes, enabling it to mediate the efflux of cellular phospholipids and free cholesterol to nascent discoid HDL particles harboring 2-4 molecules of ApoA-I, leading to the biogenesis of HDL particles. A similar lipid efflux by ABCA1 in cells of peripheral tissues initiates the RCT (5, 7) (Figure 1.1). Also, ApoA-I activates lecithin cholesterol acyl transferase (LCAT) leading to the maturation of HDL particles (8). Interaction of lipidated ApoA-I in discoid or more mature HDL particles with another transporter of the ABC family, ATP-binding cassette sub-family G member 1 (ABCG1), contributes further to the RCT (9). HDL particles undergo additional remodeling through interaction with the cholesteryl ester transfer protein (CETP) (10). Finally, binding of HDL particles to the scavenger receptor class B type 1 (SR-BI), transfers cholesterol down a cholesterol gradient (11, 12). As a result, cholesterol mobilized at peripheral tissues can enter the liver, catabolized and excreted to the bile (12-14). ApoA-I itself is mainly catabolized in the liver (15, 16) (Figure 1.1).

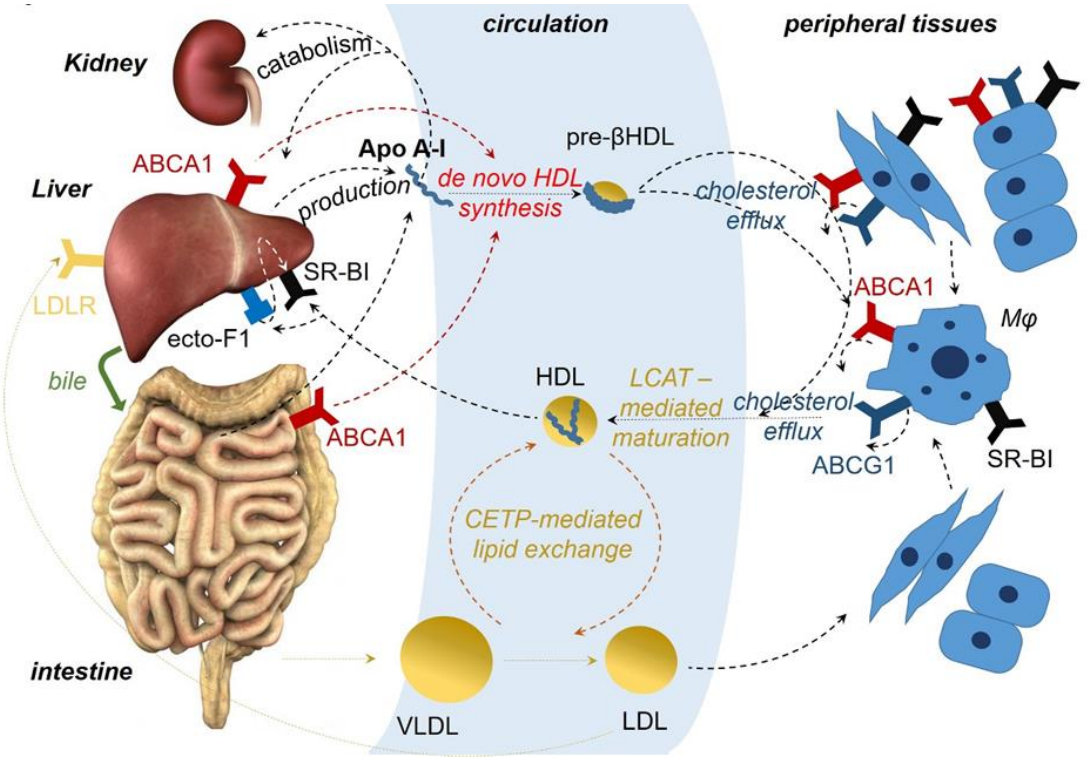

Figure 1.1. ApoA-I in relation to HDL biogenesis and the RCT. About 75% of the ApoA-I protein is produced by hepatocytes and the remaining 25% by epithelial cells of the small intestine. It has been shown that some ApoA-I is also produced by the most proximal part of the mouse colon, in line with the reported ApoA-I expression in human fetal colon. ApoA-I is mainly catabolized in the liver. In addition, ApoA-I protein unassociated with lipids can be filtered in renal glomeruli, recognized by cubulin, a protein synthesized by distal renal tubular cells, internalized and degraded by renal epithelial cells. Binding of ApoA-I to ABCA1 at the cell membrane of hepatocytes and enterocytes mediates the production of nascent HDL particles. A similar efflux of lipids by ABCA1 and ABCG1 directly in various cells, or indirectly in macrophages (Mφ) of peripheral tissues contributes to the RCT. LCAT, which catalyzes the esterification of free cholesterol and interaction through CETP transferring cholesterol esters to very low density lipoproteins (VLDL) and low density lipoproteins (LDL) and the phospholipid transfer protein (PLTP) transferring phospholipids from VLDL lipoproteins to HDL, leads to maturation and remodeling of HDL particles. Binding of HDL particles to SR-BI, expressed in hepatocytes, transfers cholesterol esters and other lipids, so that excess cholesterol can be accepted by the liver, catabolized and excreted via the bile to the intestine. Also, binding of HDL remnants produced after the action of endothelial lipase, or lipid-poor ApoA-I to the beta chain of ATP F1 synthase, expressed at the cell membrane of hepatocytes and other cells (called, also, ecto-F1F0-ATPase that is similar to the F1F0 inner mitochondrial membrane protein complex) promotes cell internalization of HDL particles bound to SR-BI. Abbreviations for various receptors and enzymes are explained in the main text.

1.1.2 ApoA-I regulation

The ApoA-I gene is regarded to have the same evolutionary origin with the genes of apolipoproteins A-II, A-IV, C-I, C-III and E, by virtue of duplication and diversification of a basic genetic motif encoding for a 11/22 amino acid sequence with a characteristic α-amphipathic

helix signature (17-20). Homologous ApoA-I-encoding genes have been described in mammals, birds and teleost fish (21).

The regulation of human ApoA-I gene expression is complex and is controlled at multiple levels. The transcription of human *ApoA1* largely depends on two Hormone Response Elements (HREs) proximal to the transcription start site that bind members of the hormone nuclear receptor superfamily. Among them, peroxisome proliferator-activated receptor-γ (PPARγ) appears to have a prominent role in *ApoA1* transactivation by interacting with HREs as heterodimer with RXRα (22). In the same line, liver tissue from mice lacking RXRα *ApoA1* expression was increased more than three- and six fold (23). *ApoA1* levels were also elevated in PPARα-deficient mice (24), consistent with RXRα being the principal PPARα heterodimeric partner in hepatocytes.

Other transcription factors implicated in the regulation of *ApoA1* promoter include hepatocyte nuclear factor 4 (HNF4), Liver Receptor Homologue 1 (LRH1) and the ApoA-I Regulatory Protein 1 (ARP1/NR2F2) which activate and repress the *ApoA1* promoter, respectively (25, 26). In addition, Kruppel-like factor 14 (KLF14) have been reported to stimulate *ApoA1* transactivation as treatment with pharmacological KLF14 activator increased of *ApoA1* gene expression in mice (27). However it is noteworthy that mice with liver-specific inactivation of the HNF4, LRH-1 or KLF14 genes display physiological or near-physiological levels of hepatic ApoA-I (26-28).

ApoA-I expression is also controlled by a long noncoding RNA, ApoA1-AS, which is transcribed in the apolipoprotein gene cluster on chromosome 11q23.3 and modulates suppressive epigenetic marks leading to *ApoA1* transcriptional repression (29). Interestingly, the liver, small intestine, and colon where ApoA-I is predominantly detected, show approximately 100-fold higher expression levels of *ApoA1* mRNA compared to *ApoA1*-AS, whereas the *ApoA1*/*ApoA1*-AS ratios are less than one in most other tissues (29).

The majority of studies were examining the transcriptional level of regulation, yet further insight into the regulation of ApoA-I expression is required to better understand how changes in intracellular ApoA-I levels occur and may impact on disease pathogenesis and therapy. In this

context, the nature and relative contribution of proteolytic pathways to ApoA-I expression remain unexplored.

1.1.3 ApoA-I in liver pathologies

To date the main focus of numerous studies is the impact of ApoA-I expression on plasma lipid levels and atherosclerosis, without investigating its possible involvement in lipid deposition to the liver. However recent studies highlight a significant association between ApoA-I levels and liver pathologies that are characterized by excess lipid load in liver, like steatosis, and malignant phenotypes, like hepatocellular carcinoma (HCC).

Accumulating evidence suggests that regulation of the ApoA-I / HDL axis is derailed in cancer. Our mining of transcriptome microarray data registered in the Oncomine database (https://www.oncomine.org) and of recently published RNAseq data (30) uncovers reduced *ApoA1* mRNA levels in HCC compared to normal liver tissue, the main source of ApoA-I. The transcriptional repression of *ApoA1* in HCC remains mechanistically unexplored but it is in line with the reported reduction in protein levels of ApoA-I in both cancerous liver tissue of HCC patients (31). In the same line in a comparative proteomic analysis ApoA-I was found down-regulated in HCC tissues with portal vein tumor thrombus (PVTT) compared to tissues without PVTT, proposing a putative association of ApoA-I expression with vascular invasion of HCC (32).

Similarly, protein profiling studies revealed a strong suppression of ApoA-I serum levels (33, 34) in hepatocellular carcinoma (HCC) patients compared to the healthy controls. A serum proteomic analysis of patients with chronic liver disease associated with hepatitis C virus (HCV) infection showed that the development of HCC was associated with lower levels of ApoA-I (35). Furthermore, a detailed study by Ma et al. found that ApoA-I serum levels were significantly down-regulated in HCC patients with recurrent disease, compared with patients without recurrence- while serum ApoA-I was identified as an independent predictor for recurrence and survival in HCC patients post-surgery in two independent cohorts. Furthermore, a significant negative correlation between serum ApoA-I levels and circulating tumor cell (CTC) levels was observed, potentially reflecting the survival of tumor cells during their hematogenous

dissemination (36). ApoA-I serum levels were reported to be significantly decreased in HCC patients with recurrent disease, as compared to patients in remission (36). In the same line, ApoA-I was found downregulated in the serum of HCC patients with metastasis compared to the relative levels of patients without HCC metastasis proposing a potent role of ApoA-I in cancer progression and response to therapy (37). A putative prognostic value of ApoA-I in HCC is further supported by a retrospective analysis that introduced a novel score based on serum ApoA-I and C-reactive protein as a prognostic biomarker in HCC- evident by the significantly poor overall survival (OS) and disease-free survival (DFS) that accompany patients with decreased ApoA-I levels and increased CRP levels (38).

In vitro studies by Ma et al. aimed to delineate the mechanism that ApoA-I may affect the proliferative, survival and migratory behavior of HCC cells. They found that HCC cells that were treated with recombinant ApoA-I undergo G0/1 cell cycle arrest and apoptosis, associated with down-regulation of mitogen-activated protein kinases 1 and 3 (MAPK1, MAPK3), known for their anti-apoptotic function, and up-regulation of pro-apoptotic genes including caspase 5 (casp5), tumor necrosis factor receptor superfamily 10B (TNFRSF10B) and apoptosis protease activating factor 1 (APAF-1) (36). ApoA-I also induced downregulation of vascular growth factor (VEGF) and matrix metalloproteinases 2 and 9 (MMP2, MMP9) genes, suggesting that ApoA-I may decrease the angiogenetic potential and the ability of HCC cells to remodel extracellular matrix, inhibiting in this way their metastatic potential (36). The attributed anti-proliferative and pro-apoptotic role of ApoA-I may account for the high recurrence rate and poor prognosis observed in HCC patients with a low serum ApoA-I level (36).

The association between decreased ApoA-I levels and overall survival by cancer was further highlighted by a recent meta-analysis identified pre-treatment serum ApoA-I as a biomarker with prognostic significance as low ApoA-I level might be an unfavorable prognostic factor in multiple malignancies including HCC (39). In the same line, a meta-analysis in Chinese cancer patients concluded that elevated level of pre-treatment serum ApoA-I was significantly associated with longer survival in patients with solid tumors (40). Collectively, the reduction in *ApoA1*

transcription, intracellular and secreted ApoA-I in HCC, hint to a putative tumor suppressor role of this pathway.

ApoA-I levels have also been found to associate with liver pathologies that predispose for cancer initiation such as liver steatosis, non-alcoholic liver disease (NALD) and cirrhosis. For instance, ApoA-I levels and ApoB/ApoA1 ratio in the serum of NAFLD patients (41-44). Additionally, a study that enrolled 30 cirrhotic alcoholics patients and 83 healthy control subjects concluded that there is a significant decrease in serum ApoA-I levels of the patients (45). Finally, comparative proteomic analysis of rat livers that were subjected to pharmacologically-induced steatosis and fibrosis showed altered expression of ApoA-I in liver tissue and serum (46). Karavia et al., performed a functional study that demonstrated that APOA1-/- mice exposed to high-fat diet displayed increased levels of steatosis, elevated number of lipid droplets and reduced hepatic cholesterol content. Interestingly, the increased deposition of triglycerides (TGs) in the livers of ApoA1-/- mice was not attributed to increased *de novo* biogenesis of TGs. Although researchers failed to provide a mechanistic interpretation to these findings, it is clear that ApoA-I deficiency severely increased liver lipid load and exaggerated steatotic phenotype (47).

1.2 The autophagic pathway

1.2.1 Types of autophagy

Autophagy is a cellular 'self-eating' degradation process in which proteins or whole organelles are degraded and recycled in lysosomes to meet the anabolic and bioenergetic needs of the cell (48).

Depending on the mechanism of delivery of the cargo to the lysosomes, three main types of autophagy are recognized: micro-autophagy that involves the direct delivery of cargo to lysosomes through lysosomal membrane invaginations. In endosomal microautophagy, cargo is sequestered 'in bulk' or selectively through a chaperone cargo protein interaction and small vesicles forming on the surface of late endosomes or lysosomes are pinched off into the lumen to be degraded by the proteases inside lysosomes (49). The second form of autophagy, namely

chaperone mediated autophagy (CMA) is typified by the lysosomal import of proteins through their interaction with specialized chaperones responsible for their delivery to the lysosomal membrane, where they undergo internalization into the lumen through a membrane translocation complex instead of being delivered by vesicles (50, 51); and macro-autophagy which is the most widely studied mechanism of autophagy. In macro-autophagy (hereafter termed autophagy), the cargo is sequestered in double membrane vesicles known as autophagosomes, which are progressively formed by the finely interconnected activities of around 15 autophagy-related (ATG) proteins (52, 53). Autophagosomes can engulf cytoplasmic material, protein aggregates, organelles including mitochondria (mitophagy), peroxisomes (pexophagy) and lipid droplets (lipophagy), as well as ribosomes (ribophagy) and parts of the nucleus (nucleophagy) (54).

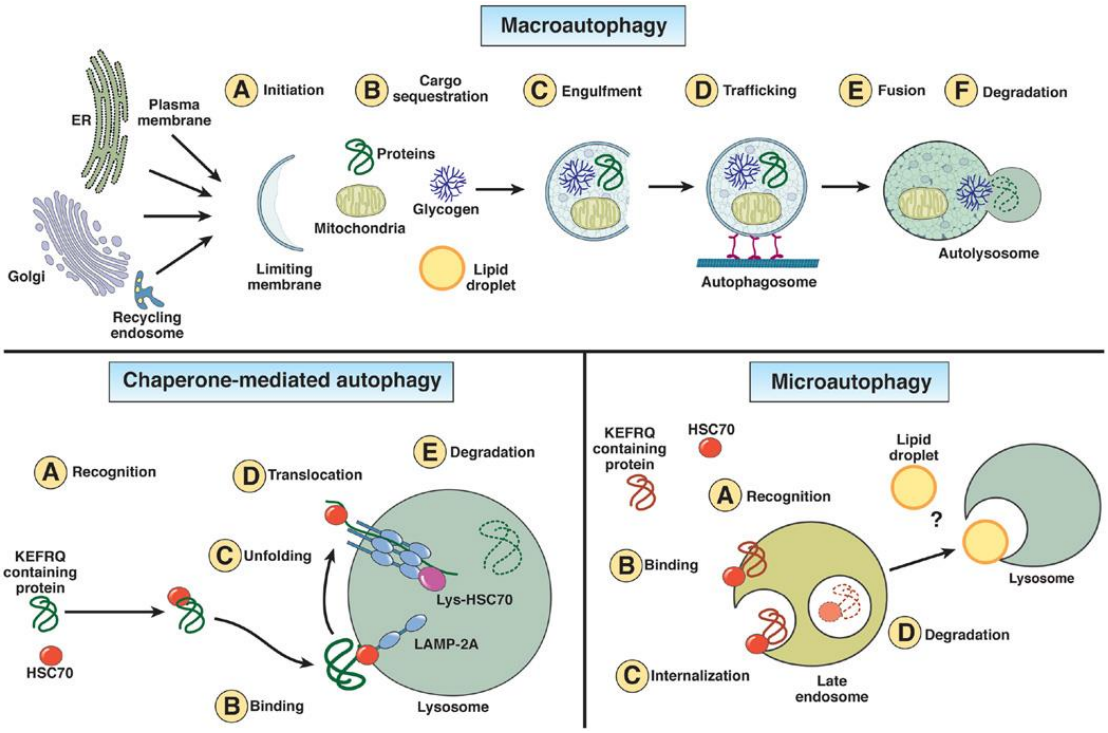

Figure 1.2. Autophagy pathways in the liver. Types of Autophagy. (Adapted from Madrigal-Matute and Cuervo, 2016)

1.2.2 The molecular pathway of autophagy

Autophagy entails the sequestration of cargo into double membrane vesicles, the autophagosomes, which deliver unwanted or damaged proteins or organelles to the lysosome (54). Autophagosome biogenesis is controlled by autophagy-related (ATG) proteins (54) and is initiated by the formation of a double-membrane structure called the phagophore, through the activation of the ULK complex comprising ULK1, ATG13, FIP200 and ATG101 and the participation of the activated phosphatidylinositol 3-kinase class III complex involving Beclin-1, Vps34, Vps15 and ATG14. The closure of the autophagosomal membrane is mediated by ATG5 and ATG7-coordinated ubiquitin-like conjugation systems responsible for the conjugation of phosphatidylethanolamine (PE) to MAP1LC3B/LC3 (hereafter: LC3). PE-conjugated ("lipidated") LC3, known as LC3-II, decorates mature autophagosomes. Thus, the relative changes in LC3-II levels that occur in a lysosome-dependent manner and the expression of specific autophagic substrates such as the LC3-II-interacting p62/SQSTM1 protein (hereafter: p62) are indicative of autophagic activity, known as "autophagic flux" (55).

Constitutive (i.e. basal) autophagy has a housekeeping role and participates in fundamental cellular and organismal functions that include survival, development, immune and metabolic regulation (56, 57). Autophagy can be further activated in response to various stress-inducing factors, such as nutrient deprivation and DNA damage, as a defense mechanism against the accumulation of damaged macromolecules and organelles, in parallel to providing energy and biological building blocks for biosynthetic and repair processes (54).

1.2.3 The mTOR pathway

Thus, nutrient sensing and autophagy pathways are intertwined and share common regulatory nodes that ensure effective crosstalk (54). Among them, mTOR pathway plays a prominent role by coupling amino-acid availability to protein synthesis and suppression of autophagy. mTOR is a serine/threonine protein kinase in the PI3K-related kinase (PIKK) family that forms the catalytic subunit of two distinct protein complexes, known as mTOR Complex 1 (mTORC1) and 2 (mTORC2). mTORC1 consists of three core components: mTOR, regulatory protein associated with mTOR (Raptor), mammalian lethal with Sec13 protein 8 (mLST8), and

two inhibitory subunits: proline-rich Akt substrate of 40 kDa (PRAS40), DEP domain containing mTOR interacting protein (Deptor)(58-61) . Among them, mTOR is the catalytic subunit of the entire complex. Raptor is a mTOR regulatory related protein that binds to the mTOR signaling motif to promote substrate recruitment of mTORC1. mLST8 is associated with the mTORC1 catalytic domain and stabilizes kinase activation (62, 63). PRAS40 and Deptor are the two negative regulatory subunits of mTORC1 activation (62-65). mTORC2 also contains mTOR and mLST8. Instead of Raptor, however, mTORC2 contains rapamycin insensitive companion of mTOR (Rictor), an unrelated protein that likely serves an analogous function (66, 67) mTORC2 also contains Deptor (Peterson et al., 2009), as well as the regulatory subunits mammalian stress-activated protein kinase interacting protein (mSIN1) (68, 69) and protein observed with rictor1 and 2 (Protor1/2) (70-72).

The TOR complex 1 (TORC1) integrates signals that sense the availability of amino acids, oxygen, growth factors as well as the cellular energy or stress levels and through it downstream effectors promotes cell growth by modulating of protein biosynthesis, cell cycle and cellular metabolism as well as autophagy. mTORC1 promotes protein synthesis largely through the phosphorylation of two key effectors, p70S6 Kinase 1 (S6K1) and eIF4E Binding Protein (4EBP) (73). mTORC1 directly phosphorylates S6K1 on its hydrophobic motif site, Thr389, enabling its subsequent phosphorylation and activation by PDK1. S6K1 phosphorylates and activates several substrates that promote mRNA translation initiation, including eIF4B, a positive regulator of the 50 cap binding eIF4F complex (74). S6K1 also phosphorylates and promotes the degradation of PDCD4, an inhibitor of eIF4B (75), and enhances the translation efficiency of spliced mRNAs via its interaction with SKAR, a component of exon-junction complexes (76). The mTORC1 substrate 4EBP is unrelated to S6K1 and inhibits translation by binding and sequestering eIF4E to prevent assembly of the eIF4F complex. mTORC1 phosphorylates 4EBP at multiple sites to trigger its dissociation from eIF4E (77, 78), allowing 50 cap-dependent mRNA translation to occur.

Growing cells require sufficient lipids for new membrane formation and expansion. mTORC1 promotes *de novo* lipid synthesis through the sterol responsive element binding protein (SREBP)

transcription factors, which control the expression of metabolic genes involved in fatty acid and cholesterol biosynthesis (79). While SREBP is canonically activated in response to low sterol levels, mTORC1 signaling can also activate SREBP independently through both an S6K1-dependent mechanism (80) as well as through the phosphorylation of an additional substrate, Lipin1 (LPN1), which inhibits SREBP in the absence of mTORC1 signaling (81, 82). Finally, mTORC1-mediated phosphorylation of CREB-regulated transcription coactivator 2 (CRTC2) facilitates translocation of SREBP1 from the ER to the Golgi by releasing inhibitory SEC31 for formation of the SEC23–SEC24 complex to maintain COPII vesicle function (83).

In addition to the various anabolic processes outlined above, mTORC1 also promotes cell growth by suppressing protein catabolism, most notably autophagy. This is mediated by posttranslational modification of autophagy key factors required for the formation of the autophagosome. ULK1 and ATG13 are early acting factors that are required for the initiation of autophagy and which are therefore phosphorylated and inhibited by TORC1 (84, 85). ULK1, for instance, is phosphorylated by TORC1 under conditions when enough nutrients are available. This inhibiting phosphorylation prevents the binding of ULK1 to and the activation by AMPK (84). TORC1 inhibits autophagy also via transcription control. Under nutrient replete conditions, TORC1 phosphorylates the transcription factor EB (TFEB) and thereby blocks its nuclear translocation and therefore inhibits expression of genes for lysosomal and autophagosomal biogenesis (86-88).

While mTORC1 regulates cell growth and metabolism, mTORC2 instead controls proliferation and survival primarily by phosphorylating several members of the AGC (PKA/PKG/PKC) family of protein kinases. The first mTORC2 substrate to be identified was PKCa, a regulator of the actin cytoskeleton (66, 67). More recently, mTORC2 has also been shown to phosphorylate several other members of the PKC family that regulate various aspects of cytoskeletal remodeling and cell migration. The most important role of mTORC2, however, is likely the phosphorylation and activation of Akt, a key effector of insulin/ PI3K signaling (89). Once active, Akt promotes cell survival, proliferation, and growth through the phosphorylation

and inhibition of several key substrates, including the FOXO1/3a transcription factors, the metabolic regulator GSK3b, and the mTORC1 inhibitor TSC2 (69, 90, 91).

1.3 Mechanism regulating lipid metabolism in the liver

1.3.1 De novo lipid synthesis and cholesterol biogenesis

Cellular lipids, especially cholesterol and fatty acids, comprise the basic structural components of cell membranes and as metabolic intermediates and act as signaling intermediates in various biological processes. Cells maintain a steady state level of membrane cholesterol by controlling its biosynthesis and uptake to maintain membrane fluidity and metabolic homeostasis. Cholesterol synthesis and uptake pathways are regulated at the transcriptional level through classic end product feedback inhibition of 3-hydroxy-3-methylglutaryl (HMG) CoA reductase (HMGCR), the rate-limiting enzyme for cholesterol biosynthesis, and via LDLR, which mediates endocytosis of cholesterol-rich LDLs. The promoter regions of these genes contain a DNA element called the sterol regulatory element (SRE), which is responsible for sterol-dependent regulation of expression. Using double-stranded DNA fragments containing the SRE sequence (5´-ATCACCCCAC-3´), DNA-bound proteins were purified from nuclear extracts of cultured cells and named SRE-binding protein 1 and 2 (SREBP1 and SREBP2, respectively)(92). These proteins are synthesized as 110-amino acid inactive precursors; then, they are inserted into the endoplasmic reticulum (ER) membrane (93). In the ER, SREBPs interact with a sterol sensor, the SREBP-cleavage activating protein (Scap) (94). The SREBP/Scap complex moves to the Golgi apparatus, where the mature or nuclear forms of SREBP are generated by two proteases, the site 1 protease and the site 2 protease, and an anchoring protein. The insulin-induced gene (Insig)-1/2 also contributes (94). Then, the nuclear SREBPs translocate to the nucleus and bind to the target gene promoters, such as those of lipid metabolism-related genes (95). The expressions of these transcriptional genes regulated by feed-forward and feedback mechanisms, such as increased intracellular cholesterol levels, inhibit the proteolytic activation of SREBPs and decrease expression of SREBP target genes (96).

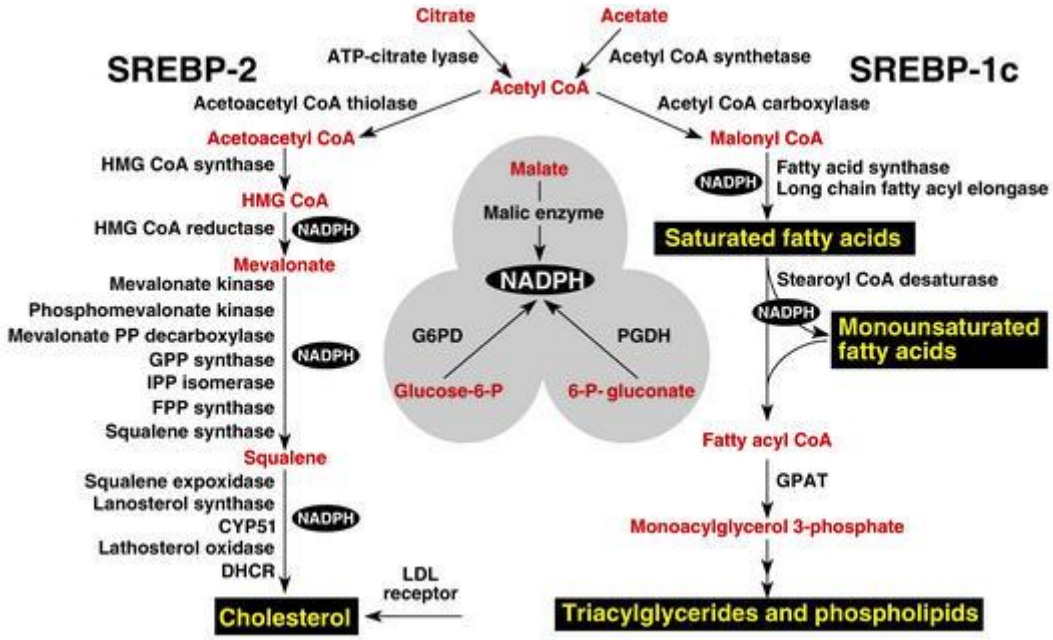

Figure 1.3. Genes regulated by SREBPs. The diagram shows the major metabolic intermediates in the pathways for synthesis of cholesterol, fatty acids, and triglycerides. In vivo, SREBP-2 preferentially activates genes of cholesterol metabolism, whereas SREBP-1c preferentially activates genes of fatty acid and triglyceride metabolism. DHCR, 7-dehydrocholesterol reductase; FPP, farnesyl diphosphate; GPP, geranylgeranyl pyrophosphate synthase; CYP51, lanosterol 14α-demethylase; G6PD, glucose-6-phosphate dehydrogenase; PGDH, 6-phosphogluconate dehydrogenase; GPAT, glycerol-3-phosphate acyltransferase (Adapted from Horton et al., 2002).

The SREBP family consists of three members: SREBP-1a; SREBP-1c, from the SREBF-1 protein coding gene; and, SREBP-2, from the SREBF-2 protein coding gene. SREBP-1c is mainly expressed in the liver, white adipose tissue, adrenal gland, skeletal muscle and brain of mice and humans;7. but SREBP-1a is expressed in cell lines, spleen and intestinal tissues (96-98).

A series of animal studies utilizing transgenic and knockout mice for each SREBP gene and iso-form demonstrated that SREBP1c primarily controls lipogenic gene expression, whereas SREBP2 regulates the transcription of genes related to cholesterol metabolism and uptake (96-98). Physiologically, SREBP1a strongly activates global lipid synthesis in rapidly growing cells, whereas SREBP1c has a role in the nutritional regulation of fatty acids and TGs in lipogenic organs such as the liver. Conversely, SREBP2 mediates sterol regulation in every tissue (96, 99).

SREBPs are controlled at multiple levels, such as the regulation of mRNA expression, cellular localization or post-transcriptional modification by nutrient-dependent signaling pathways (e.g., insulin), as well as end-product feedback mechanisms by cholesterol and other lipids (100). Aberrant SREBP activity can contribute to elevated circulating cholesterol and triglycerides TGs, and increased lipid accumulation in tissues such as liver and adipose; thus, SREBP-dependent physiological changes are key to pathologies associated with metabolic syndrome such as obesity, NAFLD, insulin resistance and cardiovascular disease (101, 102). Further to these measurements of the products of *de novo* lipogenesis in NAFLD, quantification of transcriptional data for SREBP1c, (Fatty Acid Synthase) *FASN* and (Acetyl-CoA carboxylase) *ACACA* shows elevation in these crucial regulators and enzymes of *de novo* lipogenesis in patients with NAFLD (103). The role of SREBP1c in the pathogenesis of NAFLD is further supported by mouse studies where the transcriptionally active form of SREBP1c is expressed in a liver-specific manner and leads to a consequent accumulation of hepatic lipid droplets (LDs) (104). Additionally, deletion of SREBP1c decreases the TG accumulation by ~50% in *ob/ob* mice (105), a mouse model which is hyperphagic and develops severe hepatic steatosis (106). Moreover, deletion of SCAP (the escort protein for immature SREBP1c) appeared effectively to prevent TG accumulation in *ob/ob* mice despite maintained hyperphagia and elevated body masses (105, 107).

In addition to its roles in metabolic pathways, increased SREBP activity has been linked to cancer development, as increased production is required for unlimited growth. Li *et al* .demonstrated that overexpression of SREBP-1 is associated with large tumor size, high histological grade and advanced tumor-node-metastasis stage in HCC patients, and that SREBP-1 downregulation suppressed cell proliferation and apoptosis in both HepG2 and MHCC97L cells (108). Thus, the cholesterogenic and lipogenic functions of SREBPs can contribute to multiple disease states, and therapeutic tools for modulating SREBP activities could impact not just metabolic disorders, but also cancers. One of the effects of SREBP-2 in cell proliferation is mediated by regulation of farnesyldiphosphate synthase gene transcription (109). Moreover, SREBP pathway blocking by L-Scap-/- and L-gp78-/- mice led to reduced

SREBP1c, SREBP1a and SREBP2 expression and to decrease in related enzymes, such as *FASN*, *ACACA*, *LDLR* and *HMGCs*, improving HCC tumor progression (110). Increased lipogenesis, with upregulation of *FASN* gene was induced by AKT-mTORC1-RPS6 signaling and promoted the development of HCC in mice (111).

Numerous studies have explored the molecular mechanisms by which insulin signaling leads to SREBP modulation. The Akt kinase respond to upstream signals from the insulin receptor or other growth factor-responsive pathways and phosphorylate multiple targets that act together to promote lipogenesis and energy storage. Akt-mediated phosphorylation and inhibition of glycogen synthase kinase 3 beta (GSK3β) results in the accumulation of nuclear SREBP proteins, which is mediated by reduction of SREBP degradation by the ubiquitin proteasome system (112). Akt also phosphorylates and inhibits the hepatic insulin-suppressive INSIG isoform INSIG2A, which liberates the SREBP–SCAP complex to the Golgi (113, 114). mTORC1 also responds to stimulation from Akt via phosphorylation of TSC2 and PRAS40 and regulates SREBPs activity in multiple modes, detail of this axis are described above. mTORC2 signaling was found to have a profound effect on SREBP1 as liver-specific Rictor knock-out displayed loss of Akt Ser473 that was accompanied by impaired glycolysis and lipogenesis (115). Similarly, mice with liver specific ablation of Rictor fail to develop hepatic steatosis on a high fat diet and possessed low cholesterol serum levels. This is accompanied by lower levels of expression of SREBP-1c and SREBP-2 and genes of fatty acid and cholesterol biosynthesis (116).

The downstream targets of Akt, FOXOs have been found to suppress the SREBPs at the transcriptional level. Hepatic FOXO1 ablation in mice resulted in increased VLDL secretion, increased cholesterol, and increased plasma free fatty acids, three hallmarks of the diabetic state and expressed increased levels of SREBP-2 (117). A study by Deng *et al*. indicated that FOXO1 was associated with the SREBP-1c promoter and negatively regulated *SREBP1* gene expression via multiple mechanisms including modification of the promoter binding sites of Sp1 and SREBP-1c itself (118). Recently, a long non-coding RNA HCV regulated 1 (lncHR1) was found to inhibits SREBP-1c levels through the phosphorylation of the PDK1/AKT/FOXO1 axis and by impacting on the cellular localization of FOXO1 (119). FOXO1 represses LXRα-mediated

transcriptional activity of SREBP-1c promoter in HepG2 cells (120). Additionally, combined deletion of FOXO1 and FOXO3 decreased blood glucose levels, elevated serum TG and cholesterol concentrations, and increased hepatic lipid secretion and caused hepatosteatosis. Analysis of the liver transcripts established a prominent role of FOXO1 in regulating gene expression of gluconeogenic enzymes and FOXO3 in the expression of lipogenic enzymes (121, 122).

1.3.2 Autophagy-Lipophagy

Autophagy as a regulator of lipid metabolism in the liver

Fatty acids are essential to all organisms — as substrates for energy production, as precursors of membrane lipids and as signalling molecules that control various cellular processes, including gene expression. Free fatty acids (FFAs) are taken up by hepatocytes and converted into TGs for storage with cholesterol in LDs (123). Upon nutrient deprivation TG hydrolysis is upregulates to supply FFAs for oxidation to meet cellular energy demands are re-released by the process of lipolysis. According to the classical view of lipolysis, that was described in early years cytoplasmic hydrolytic enzymes called neutral lipases, like hormone-sensitive lipase HSL and adipose-triglyceride lipase (ATGL) mediate lipid catabolism with the participation of accessory proteins like perilipins (124). However, recent studies have revealed a role for autophagy in LD breakdown. The initial observation of the pioneer study that that determined that autophagy regulates lipid metabolism, via selective autophagy of LDs, termed lipophagy, was that hepatocytes depleted for *ATG5*, one of the genes essential for the formation of autophagosomes, are characterized by increased lipid load (125). In addition, oleic challenge resulted in a marked increase in the number and size of LD in cells with compromised macroautophagy. In accordance, knock-out of *ATG7* in the liver led to an accelerated development of liver steatosis (fatty liver) in the autophagy compromised animals, when compared to control animals. Detailed biochemical and functional analyses determined that the observed lipid accumulation did not result from increased formation of LD or reduced lipid secretion from hepatocytes, but that, instead, it ensued by reduced lipolysis (125).

Cross-talk of lipolysis and lipophagy

Recent studies have shed light into the crosstalk between the lipolytic and lipophagic pathways. Specifically, Martinez-Lopez et al., found that lipase-driven LD breakdown is dependent on autophagy as they showed that cold exposure in the mediobasal hypothalamus was observed to drive lipophagy in the liver. The induction of hepatic lipophagy is coupled to lipolysis as the key cytoplasmic lipases ATGL and hormone-sensitive lipase were shown to LC3 interacting motifs and mutation of these critical motifs was sufficient to ablate ATGL-driven lipolysis (126). Conversely, ATGL activity may also modulate regulation of lipophagy, as it was found that overexpression of ATGL increases hepatic lipophagy, possibly through a mechanism involving Sirtuin-1 (127). Further evidence for a functional link between autophagy and lipolysis came from the discovery that CMA degrades LD-associated proteins and thereby regulates neutral lipolysis. Perilipin 2 and perilipin 3, which are abundant LD-associated proteins that shield LDs from lipases and lipolysis were found to be CMA targets. Consequently, the removal of perilipin 2 and perilipin 3 by CMA enables ATGL to efficiently access the LD surface, thereby increasing lipolytic rates (128, 129).

Autophagy in liver disease

The dynamic cross-talk between liver autophagic function and lipid metabolism has been reported to play a rather important role in liver diseases associated with aberrant intracellular lipid load, such as NAFLD. The first step in the pathogenesis of NAFLD is the development of a fatty liver or hepatic steatosis, where the characteristic accumulation of lipids may be due to increased lipid influx in this organ, enhanced *de novo* synthesis of lipids and decreased mobilization and utilization of hepatic lipid stores (130). The late consequences of metabolic malfunction is development of hepatocarcinomas, and pertubations of the in autophagy activity were also found to impact on hepatic lipid load and promote tumorogenesis. The fast development of steatosis and fatty liver observed in mice defective for autophagy in this organ (125) strongly supported the contribution of altered autophagy to the pathogenesis of this common disease. Furthermore, mice with defective hepatic CMA, have profound lypolytic defects and develop hepatocellular adenomas spontaneously by middle age. This enhanced

tumorogenesis could ensue by a combination of the hepatosteatosis, poor quality control, and increased oxidative damage associated with chronic CMA deficiency (128, 129). Hepatic macroautophagy exerts an anti-oncogenic function, demonstrated by the fact that lowering ATG5 or ATG7 levels triggers occurrence of multiple liver tumors. Accordingly, human HCC show reduced levels of autophagic proteins and activity which is associated with malignancy and bad prognosis (131). Accumulation of the autophagy adaptor protein p62 that occurs upon autophagy failure is in part responsible for the observed increase in liver tumors, since deletion of p62 in autophagy-deficient livers counteracts tumorogenesis (132). Interestingly, liver tumors in autophagy deficient mice lack the malignant phenotype indicating the requirement of other genetic changes coupled to macroautophagy malfunction for hepatic carcinogenesis. Growing evidence support that macroautophagy can also be utilized by hepatic cancer cells for tumor progression and, in fact, increased levels of macroautophagy markers such as LC3 in HCC has been associated with bad prognosis and higher rates of recurrence after surgery. Hence, it might possible that, at least in mice, deficient autophagy only promotes the development of benign tumors but halts their progression into cancer. While short-term incubation of hepatocytes with FFAs activates autophagy, prolonged exposure suppresses autophagy and lipophagy, as indicated by decreased interaction between LDs and LC3 (133). It has also been reported that chronic challenge with high fat diet reduces both macroautophagy and CMA due to changes in intracellular membrane composition that affects the fusion between autophagosomes and lysosomes (134), indicating that over-nutrition affects various stages of autophagy and lipophagy (135). In the same direction, high dietary lipids was found to alter the lysosomal stability of the CMA receptor leading to compromised activity of this pathway (136). Studies in obese mice and NALD patients have also demonstrated that fatty liver decreases lysosome activity through inhibition of cathepsin expression which reduces lysosomal degradation of cargo delivered by all types of autophagy and endocytosis (137). Consistent with this concept is the finding that inhibition or activation of autophagy increased or decreased respectively, methionine choline diet-induced steatosis in mice (138). Induction of autophagy was found to ameliorate fatty liver disease as administration of autophagy activator resveratrol, or overexpression of *Atg7*

or *Atg14* reversed liver steatosis in obese mice (139-141). This reduced clearance of autophagosomes could explain the accumulation in LC3-II and p62 observed in patients diagnosed with non-alcoholic steatosis (NAS) and NASH and that positively correlate with the severity of the disease (142). A compromise in hepatic autophagy has been proposed to underline also the basis for the accumulation of LDs upon exposure to toxic concentrations of ethanol (143), while pharmacological upregulation of autophagy reduces hepatotoxicity and steatosis in an alcohol-induced model of fatty liver (143). Given the above-described essential role of the different types of autophagy in liver metabolism, their dysregulation during dietary challenges or abnormal metabolic conditions can further aggravate the metabolic malfunction, thus creating a deleterious vicious cycle. This continuous negative feedback makes it often difficult to determine if the autophagic failure is primary cause or secondary consequence.

2. MATERIALS AND METHODS

2.1 Reagents and antibodies

The following primary antibodies were used: Rabbit anti-Mouse ApoA-I (Meridian, Life science, Inc, Memphis, TN, USA; Guinea Pig anti-Adipophilin (ADRP) (PROGEN Biotechnik GmbH, Heidelberg, Germany); Goat anti-human ApoA-I (Chemicon International, Billerica, MA, USA); Rabbit anti-LC3B (Novus Biologicals, Centennial, CO, USA; immunoblotting); Mouse anti-LAMP-1 and Mouse anti-p62 (BD Biosciences, Franklin Lakes, NJ, USA) for western blot and SQSTM1 monoclonal antibody (M01) clone 2C11 (Abnova, Taipei City, Taiwan) for immunofluorescence; Mouse anti-GAPDH (Sigma-Aldrich, St. Louis, MO, USA); Mouse anti-p53, HSP90, SREBP2 and SP1 (Santa Cruz Biotechnology, CA, USA; Rabbit anti-LC3B for immunofluorescence, Beclin-1, ULK1 4E-BP1, phospho-4E-BP1 ($Thr^{37/46}$), phospho-Akt (Ser^{473}), phospho-Akt (Thr^{308}), Phospho p44/42 MAPK (Erk1/2) (Thr^{202}/Tyr^{204}), P44/42 MAPK (Erk1/2), pSAPK/JNK (T^{183}/Y^{185}), phosphor- FOXO1/3, FOXO1, Raptor, Rictor (Cell Signaling Technology Inc. Danvers, MA, USA); Mouse anti-actin and rabbit anti-Akt1 antibodies (Millipore, Billerica, MA, USA). The following secondary antibodies were used for western blot detection with enhanced chemiluminescence (ECL, Western Lightning™ Chemiluminescence Reagent Plus was purchased from PerkinElmer): HRP-linked anti-mouse IgG and anti-rabbit IgG (Cell Signaling Technology Inc. Danvers, MA, USA), as well as HRP-linked anti-goat antibody (Thermo Scientific, Waltham, MA USA). Secondary antibodies for immunofluorescence donkey anti–goat, anti–mouse Alexa Fluor 488, anti–goat Alexa Fluor 568 and goat anti–rabbit Alexa Fluor 594–conjugated antibodies and ProLong® Gold Antifade Reagent with DAPI were purchased from (Thermo Fisher Scientific, Waltham, MA USA). Cells were treated with 50 nM bafilomycin A1 for 8 hrs unless noted otherwise, 10 μM chloroquine diphosphate, 10 μM CHX, metformin hydrochloride, 500 nM oleic acid, palmitic acid, 5-Fluorouracil and gentanamycin (all from Sigma-Aldrich, St. Louis, MO, USA), 250 nM Torin2 (Cayman Chemical, Ann Arbor, MI, USA), 100 nM human insulin (Eli Lilly, Indianapolis, IN, USA), 15 μg/ml APOA1 (APOAI) Recombinant Human Protein (Thermo Scientific, Waltham, MA USA), 50 ng/ml TNF-α R&D

Systems (Minneapolis, MI, USA), 10 μM MG132 (Millipore, Billerica, MA, USA). All culture media, aminoacids solutions, penicillin/streptomycin for cell culture, fetal bovine serum were purchased from Life Technologies, Carlsbad, CA, USA. The SigmaFAST Protease Inhibitor Tablets used for protein extraction purposes were purchased from Sigma-Aldrich (St. Louis, MO, USA).

2.2 Cell culture and transfection assays

HepG2 (human hepatocellular liver carcinoma) cells were grown in DMEM low glucose (1 g/L) GlutaMAX™ medium, HEK293T (human embryonic kidney 293T) cells were grown in DMEM high glucose (4.5 g/L) GlutaMAX™ medium (Life Technologies, Carlsbad, CA, USA) and both were supplemented with 100 U/ml penicillin, 100 mg/ml streptomycin and 10% FBS; referred as standard media or SM. Cells were cultured at 37 °C in a humidified atmosphere with 5% CO2.

Plasmid DNA transfection

For DNA transfection, HEK293T cells were seeded in 24-well plates and transfected with a total of 0.1 μg of pEGFP-C2 (Clontech, Heidelberg, Germany) or pAdTrack-CMV-*APOA1* (a gift from Professor D. Kardassis, University of Crete) using the Lipofectamine 2000 (Thermo Fisher Scientific, Waltham, MA USA). For co-transfection experiments (followed by immunoprecipitation) with HA-Akt1 or HA-Akt2 and plasmid pAdTrack-CMV-*APOA1* plasmid HEK293T cells were seeded in two 6 well/condition and transfected with a total of 0.5 μg of plasmid per well using the Lipofectamine 2000 (Thermo Fisher Scientific, Waltham, MA USA) according to manufacturer's instructions.

siRNA transfection

For siRNA transfections, HepG2 cells were seeded in 24-well plate ($0.6x10^5$ cells per well) and cells were transiently transfected with 10 pmol of siRNA in the presence of Lipofectamine RNAimax reagent (Thermo Fisher Scientific, Waltham, MA USA), according to the procedure provided by the manufacturer with some modifications. Briefly, 24 hrs after seeding, 1.5 μl of RNAiMAX reagent was diluted in 25 μl of OptiMEM (Thermo Fisher Scientific, Waltham, MA

USA) (tube A). Also, 10 pmol of siRNA was diluted in 25 μl of OptiMEM (tube B). Then, tube B was added to tube A and was mixed by pippetting followed by 5 min incubation at RT. In the meantime, cells was washed with OptiMEM. The transfection solution was added in the cells dropwise. Then, 200μl of serum free medium were added in the cells and afterwards the cells were incubated at 37ºC in a CO2 incubator. After 6-8 hrs of incubation, 700 μl of complete medium was added in the cells and the cells were incubated further. Next day, we performed a second round of transfection. 24h after the second round of transfection, the complete medium was renewed and the cells were further treated as indicated. The Silencer® Select siRNAs for *ULK1* (ID: s15963 and s15965), *MAP1LC3B* (ID s196887 and s37748), *BECN1* (ID: s16537 and s16538), *RAPTOR* (ID s33216 and s33215), *RICTOR* (ID s48408 and s226000) and the unrelated Luciferase (AM16204) gene that was used as negative control for sequence independent effect were purchased from Life Technologies (Carlsbad, CA, USA). The silencing efficiency was confirmed by western blot and qPCR analysis in all cases.

2.3 Primary mouse hepatocytes isolation and mouse liver samples

Hepatocytes were isolated by a single two step collagenase perfusion. Briefly 9–14 weeks-old male mice were anesthetized with ketamine/xylazine and livers were perfused via cannulation of the inferior vena cava, clumping of the suprahepatic inferior vena cava and incision of the mesenteric vein, first with Liver Perfusion medium, followed by perfusion with Liver Digest medium (Life Technologies, Carlsbad, CA, USA). Subsequently, livers were minced on a Petri dish and filtered through a sterile 100 μm nylon mesh. Isolated hepatocytes were washed three times with Hepatocyte Wash medium and centrifuged at 50 × g for 5 min. Purification of hepatocytes was made with Percoll (Sigma-Aldrich, St. Louis, MO, USA) density gradient separation. After washing of purified hepatocytes, cell pellet was resuspended in Plating medium, supplemented with 10% FBS and penicillin, steptomycin and gentanamycin. Viability was determined by trypan blue exclusion and hepatocytes were seeded for further treatments in Maintenance medium.

Modeling of steatosis was performed in 8-week-old male C57BL/6 mice fed a high-fat diet (HFD; 60% energy from lipids) or a normal standard diet (ND) (both purchased from Mucedola, Italy) for 10 weeks under SPF conditions and a 12 hour light-dark cycle. The mouse livers were provided by Professor Tsatsanis. All procedures were conducted in compliance with protocols approved by the Animal Care Committee of the University of Crete, School of Medicine (Heraklion, Crete, Greece) and from the Veterinary Department of the Region of Crete (Heraklion, Crete, Greece).

2.4 Immunoblotting and densinometric analysis

Cells were washed once with cold PBS and then lysed with RIPA buffer (50 mM Tris-Cl pH 7.4, 150 mM Nacl, 1% NP-40, 0.5% sodium deoxycholate, 0.1% SDS, 1 mM EDTA and 1X protease inhibitor solution supplemented with SigmaFAST Protease Inhibitor mixture tablets. Gentle agitation at 4° C was applied for 15 min and lysates were then centrifuged for 20 min at 13,200 rpm in a 4°C pre-cooled centrifuge. The supernatant was transferred to a new tube and protein contents in protein lysates were quantified using Pierce™ BCA Protein Assay Kit (Thermo Fisher Scientific, Waltham, MA USA) according to the manufacturer's instructions. Subcellular fractionation of proteins was performed with Subcellular Protein Fractionation Kit for Cultured Cells according to manufacturer's instructions (Thermo Fisher Scientific, Waltham, MA USA). For electrophoresis, samples were prepared by mixing 3X SDS loading buffer (150 mM Tris HCl, pH 6.8, 6% SDS, 30% glycerol, 9% β-mercaptoethanol, 0.3% bromophenol blue) with 15–30 μg of cell lysates. Equal protein amounts were loaded onto polyacrylamide gels. Separated by SDS-PAGE proteins (120V,~ 2h30) were transferred (280mA, 1h40) to nitrocellulose membranes (Amersham Protran 0.2μm, GE Healthcare Life Sciences, Chicago, Illinois, USA). Nitrocellulose membranes were blocked with 5% non-fat milk containing 1% BSA in TBS-T (Sigma-Aldrich, St. Louis, MO, USA) for 30 min and then incubated with primary antibody with gentle agitation overnight at 4°C or for 1 h at RT. After 3 washes (10 min each) with TBS-T (20 mM Tris HCl, pH 7.6, 150 mM NaCl, 0.1% Tween-20), membrane was incubated and gently agitated for 1 h in secondary antibody in 1% non-fat milk with 0.2% BSA in TBS-T.

Nitrocellulose membranes were then incubated for 1 minute with chemiluminescent substrate (PerkinElmer, Woodbridge, ON, Canada) and developed with Molecular Imager ® Gel Doc™ XR System (Bio-Rad, Hercules, CA, USA). Protein signal intensities (densitometric values of protein bands) were normalized against a GAPDH or β-actin loading control for each sample at non-saturating exposures using the Image J Software.

2.5 Immunoprecipitation

HepG2 or HEK293T transfected cells were rinsed twice with ice-cold PBS prior to lysis in NP-40 lysis buffer (50mM Tris-HCl, pH 7.4, 250mM NaCl, 5mM EDTA, 1% Nonidet P-40 (v/v), supplemented with SigmaFAST Protease Inhibitor mixture tablets (Sigma). Lysates were cleared by centrifugation for 20 min at 13,200 rpm at a 4°C. The indicated proteins were immunoprecipitated from 0.5 mg cleared lysates that were incubated with the indicated primary antibodies overnight at 4 °C. The complexes were then bound to protein G sepharose beads (BD Biosciences, Oxford, UK) for 8 hrs at 4 °C with gentle mixing. After washing with IP lysis buffer (50 mM Tris-Cl pH 7.4, 250 mM NaCl, 5 mM EDTA, 1% NP-40), bead-bound protein complexes were retrieved using Laemmli buffer and boiling. Samples were then analyzed on polyacrylamide gels.

2.6 Meausurement of secreted ApoA-I levels (ELISA)

The measurement of human secreted ApoA-I ELISA was performed at cell culture supernatants with Human Apolipoprotein AI ELISA Kit (Abcam, Cambridge, United Kingdom) according to the manufacturer's protocol. Secreted ApoA-I levels were normalized to total protein content, and expressed as % percentage relative to untreated control.

The levels of serum ApoA-I in mouse samples were measured by using mouse ELISA Kit for Apolipoprotein A1 (APOA1) (Cloud-Clone Corp., Texas, USA) according to the manufacturer's protocol.

2.7 MTT Cell Proliferation Assay

For MTT assay we seeded 8.000 cells per well in a 96-well plate and cultured in the presence of various concentrations of 5-FU or palmitic acid for 72 hrs. Each treatment was performed in

triplicates and the final culture volume was 200µl. After 72h of treatment, we added 20 µl of freshly –prepared and filtered MTT [Thiazolyl Blue Tetrazolium Bromide (Sigma-Aldrich, St. Louis, MO, USA)] in PBS at working concentration of 10mg/ml and incubated for 3-4 hrs at 37°C, until intracellular purple formazan crystals are visible under microscope. We next removed MTT and media with syringe with a thin needle to achieve minimal disruption of crystals and dissolved crystals by adding 200 µl of DMSO. We measured OD at 570 nm with reference at 630-690 nm.

2.8 Immunofluorescence staining

To analyze co-localization of ApoA-I with autophagic markers, HepG2 cells were fixed with 4% paraformaldehyde (PFA) for 15 min at RT (further fixation with methanol for 10 min at -20^{O}C, in the case of LC3 staining). Cells were washed twice with PBS before permeabilization and blocking with 0.3% Triton X-100 (Sigma-Aldrich), 5% horse serum in PBS for 60 min. Primary antibody incubation (1:200 LC3B, 1:100 ApoA-I, 1:200 p62, 1/100: LAMP-1) in 1% BSA, 0.3% Triton X-100 (in PBS) was performed overnight at 4^{o}C. After secondary antibody incubation in 1% BSA, 0.3% Triton X-100 (in PBS) for 1 h at RT, cells were washed and mounted on microscope slides using Prolong® Gold AntiFade Reagent with DAPI from Cell Signaling Technology (Thermo Scientific, Waltham, MA USA).

For lipid droplet monitoring we used the fluorescence stain BODIPY® 493/503 (Thermo Scientific, Waltham, MA USA) that specifically stains neutral lipids. We incubated PFA-fixed cells with 5 µg/ml Bodipy for 1 h at RT, we next washed twice and mounted the coverslipes on microscope slides using Prolong® Gold AntiFade Reagent with DAPI from Cell Signaling Technology (Thermo Scientific, Waltham, MA USA).

For image acquisition, the AxioObserver Z1 inverted fluorescence microscope equipped with ApoTome.2 (all by Carl Zeiss Microscopy GmbH, Hamburg, Germany) was used. Zen lite software and Image J were used to generated z stack images. The same settings of light source intensity and exposure time were used between samples in order to compare the intensity of fluorescent signals. For the measurement of LD size (diameter) we used Zen 2 (blue edition)

Zeiss. The size of LDs from at least 10 cells per condition per experiment was measured and three independent experiments were analyzed.

2.9 Electron Microscopy

HepG2 cells were fixed in 3% formaldehyde and 0.5% glutaraldehyde in 0.1 M phosphate buffer, pH 7.4, for 30 min at RT, harvested using scraper and centrifuged at 800 g for 5 min at RT. The supernatant was aspirated and the cells were resuspended in 4% gelatin aqueous solution, centrifuged at 800 g for 5 min at RT and the gelatin with the cell pellet was cooled on ice. Under stereoscope the solidified cell pellet with gelatin was cut into small fragments (1-2mm^3). The cell-gelatin fragments were then dehydrated, infiltrated and finally embedded in Lowicryl HM20 acrylic resin at -50 ^{o}C according to the Progressive Lowering of Temperature method (144), using a Leica EM AFS apparatus. Ultrathin acrylic sections (60-70nm thickness) were cut on a Leica Ultracut R ultramicrotome equipped with a Diatome diamond knife and mounted onto 200-mesh formvar-coated nickel grids for immunolabeling. For ApoA-I immunogold labeling Ultrathin acrylic sections of cells were first incubated on drops of 0.1 M glycine for 30 min at RT to block free aldehyde groups. After washing with 0.05 M Tris/HCl buffer, pH 7.4, the sections were placed on drops of blocking buffer containing 5% normal donkey serum, 0.1% Tween-20, 0.1% fish gelatin and 1% chicken serum albumin (CSA) in 0.05 M Tris/HCl buffer, pH 7.4 for 30 min at RT, and then transferred on drops of the primary antibody (1:100) diluted in 0.05 M Tris/HCl buffer, pH 8.0, containing 0.1% Tween-20, 0.1% fish gelatin and 1% CSA overnight at 4 ^{o} C. Control sections were incubated in the absence of primary antibody. The grids were rinsed (x10; 1 min each) with 0.05 M Tris/HCl, pH 7.4 containing 0.1% Tween-20 (solution I), with three changes (1min each) of 0.05M Tris/HCl, pH 7.2 containing 0.2% CSA and 0.1% Tween-20 (solution II) and finally, one change for 5min of 0.05 M Tris/HCl, pH 8.2 containing 1% CSA and 0.1% Tween-20 (solution III). The grids were drained and incubated for 1 h at RT with secondary antibody conjugated to 10 nm gold particles (1:40) diluted in solution III and they were washed with agitation in three changes (1min each) of solution II, five changes (1min each) of solution I and five changes of distilled water. Finally, ultrathin

sections were counterstained with ethanolic uranyl acetate followed by lead citrate and observed in a FEI Morgagni 268 transmission electron microscope and micrographs were taken with an Olympus Morada digital camera.

2.10 Proteasome Activity Assay

Proteasome CT-L activity was assayed based on the hydrolysis of the fluorogenic peptide LLVY-AMC (Enzo Life Sciences, Farmingdale, NY, USA). Chymotrypsin-Like Activity (CT-L) was measured in freshly-prepared protein lysates extracted in proteasome activity buffer (20 mM Tris pH 7.6, 20 mM KCl, 1 mM EDTA, 1 mM DTT, 10 mM PMSF, 0,1% NP-40, 10 µg/ml aprotinin, 10% glycerol and 5mM ATP). 10 µg of total protein were incubated with 25 µM LLVY-AMC substrate in a flat bottom black plate in triplicates per sample. Fluorescence was measured at 380/460 with VICTOR Multilabel Plate Reader (PerkinElmer, Woodbridge, ON, Canada) at 37°C for at least 30min, with measurements every 5min. Results were analyzed by linear regression via Prism Graph Pad Software, and CT-L activity was expressed as the slope of afu/min.

2.11 RNA extraction, cDNA synthesis and q-PCR, RNAseq

Total RNA was isolated using NucleoSpin RNA Kit (Macherey-Nagel, Duren, Germany) according to the manufacturer's protocol. RNA concentrations was measured spectrophotometrically and total RNA (300ng) was reverse transcribed with High-Capacity cDNA Reverse Transcription Kit (Thermo Scientific, Waltham, MA USA). q-PCR was performed by using TaqMan™ Universal Master Mix II, with UNG (Thermo Scientific, Waltham, MA USA) according to manufacturer's instructions as previously described (145). The human *APOA1* (Hs00985000_g1), *APOC3* (Hs00163644_m1), *ACTB* (Hs99999903_m1), *APOA4* (Hs00166636_m1), *APOA5* (Hs00983449_m1), *HMGCR* (Hs00168352_m1), *HMGCS1* (Hs00266810_m1), *MVD* (Hs00964563_g1), *LDLR* (Hs00181192 m1), *LPIN1* (Hs00299515_m1), *FASN* (Hs01005622_m1), *SCD* (Hs01682761_m1), *ACACA* (Hs01046047_m1), *CIDEC* (Hs00535723_m1), *PCK1* (Hs00159918_m1), *DDIT3* (Hs00358796_g1), *HSPA5* (Hs00607129_gH), *DNAJC3* (Hs00405320_g1) and the mouse

APOA1 (Mm00437568), *DDIT3* (Mm01135937_g1), *HSPA5* (Mm00517691_m1) TaqMan Gene Expression Assays (Applied Biosystems, Foster City, CA, USA) were used in an ViiA™ 7 Real-Time PCR System (Thermo Scientific, Waltham, MA USA). The relative gene expression was calculated using the comparative CT method. RNA seq and analysis was performed by BSRC Alexander Fleming Genomics Facility.

2.12 Statistical analysis

Statistical analysis was performed using PRISM (Graphpad Software Inc. La Jolla, CA, USA). Results are expressed as mean± SD. Statistical significance either with Student's t-test or with the non- parametric Mann-Whitney test.For comparisons involving more than two groups, one-way analysis of variance (ANOVA) with a post-hoc Tukey multiple comparison test being used to assess the differences between the groups. Statistical significance was defined as the conventional p value of < 0.05.

3. AIM OF THE STUDY

In this study we aim to:

1. Identify the key anabolic and catabolic pathways responsible for regulation of ApoA-I levels in hepatocytes and characterize its mechanistic components. The implication of the main degradation mechanisms, such as the proteasome and autophagy were evaluated. The contribution of transcriptional and post-transcriptional dynamics to the regulation of basal intracellular ApoA-I levels were examined under different cellular energetic requirements. We also investigated the involvement of central molecular hubs that play pivotal roles in nutrient sensing and control in ApoA-I regulation. *Results relevant to aim 1 are presented at chapter 1.*

2. Define intracellular functions of ApoA-I linked to autophagy that could influence tissue responses to metabolic stress. Given the role of serum ApoA-I in the regulation of lipid via RCT, we examined putative functions of intracellular ApoA-I in the regulation of lipid homeostasis under normal conditions or conditions of lipid overload- as those triggered by autophagy inhibition. In parallel we aimed to investigate the putative involvement of ApoA-I in the regulation of lipid catabolism processes such as autophagy and of lipid anabolic processes such as *de novo* lipogenesis, in the liver. We aimed to characterize the molecular pathways and events that mediate ApoA-I actions on lipid and cholesterol homeostasis and examine the relevance of this observation to liver pathologies, such as steatosis and hepatocellular carcinoma. *Results relevant to aim 2 are presented at chapter 2*

4. RESULTS

4.1 Chapter 1

4.1.1 Steatosis is associated with elevated levels of ApoA-I.

Extensive evidence suggests that suppression of hepatic autophagy is causally linked to the development of steatosis (reviewed in (146, 147)). In line with this evidence, long-term feeding of mice with high fat diet results in both hepatic accumulation of p62, an established autophagy substrate, and of adipophilin (ADRP), a marker of lipid accumulation (148) but not in elevated mTORC1 activity (Fig. 4.1A). Interestingly, the intracellular hepatic levels of ApoA-I were found elevated in the livers of HFD-fed mice (Fig. 4.1A), whereas *APOA1* transcription remained unaffected (Fig. 4.1B). A significant increase in the serum levels of mice fed with high fat diet was also observed (Fig. 4.1C). We further modeled this association by culturing primary mouse hepatocytes with oleic acid for 12 hours, in the presence or absence of NH_4Cl which blocks the fusion of autophagosomes with lysosomes and the lysosomal protease inhibitor leupeptin. The results (Fig. 4.1D) showed that treatment with NH_4Cl and leupeptin leads to accumulation of intracellular ApoA-I, implicating autophagy in ApoA-I regulation.

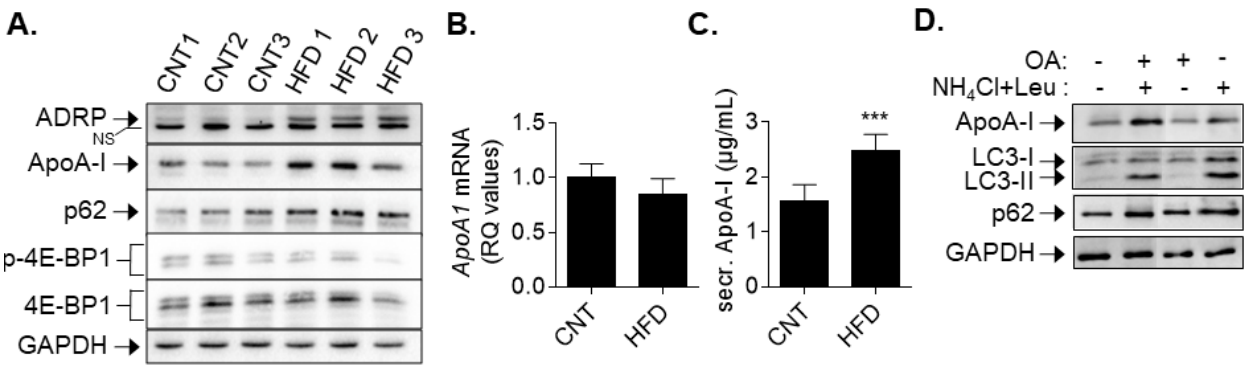

Figure 4.1. Steatosis is associated with autophagy inhibition and elevated levels of ApoA-I. (A) Representative immunoblot analysis of protein lysates from livers of mice fed high-fat diet (HFD) for 12 weeks and their respective control animals (CNT) fed normal chow. ADRP, ApoA-I, total and phosphorylated levels of 4E-BP1 are shown. *NS; non-specific.* (B) APOA-I serum levels of mice described in (*A*) (data are expressed as the mean ± SD of 5 mice of each group; ***$p < 0.001$). (C) *APOA1* mRNA expression in the same liver tissues described in (*A*). *APOA1* mRNA was normalized to the housekeeping β-actin gene (data are expressed as the mean ± SD of 3 mice of each group). (D) Representative immunoblot analysis of protein lysates from primary mouse hepatocytes modeling steatosis. Cells were exposed to 500 μM oleic acid (OA) in the presence or absence of the autophagic inhibitors NH_4Cl+leupeptin for 12 hrs and analyzed for ApoA-I. Immunoblots against anti-LC3-II and anti- p62 were used as markers of autophagic flux. GAPDH was used as loading control.

4.1.2 Autophagy but not proteasomal inhibitors lead to intracellular ApoA-I accumulation.

We explored the relative contribution of the major proteolytic pathways, autophagy and proteasome, to the regulation of basal ApoA-I levels. To this end, HepG2 hepatoma cells which represent an established model to study ApoA-I biosynthesis and secretion (149-151), were cultured in the presence of bafilomycin A1 (BAF) which inhibits the late steps in the autophagic process (152). Immunoblot analysis of lysates showed that BAF caused a time-dependent increase in ApoA-I levels in parallel to the accumulation of the lipidated form of LC3-II and of p62 (Fig. 4.2A).

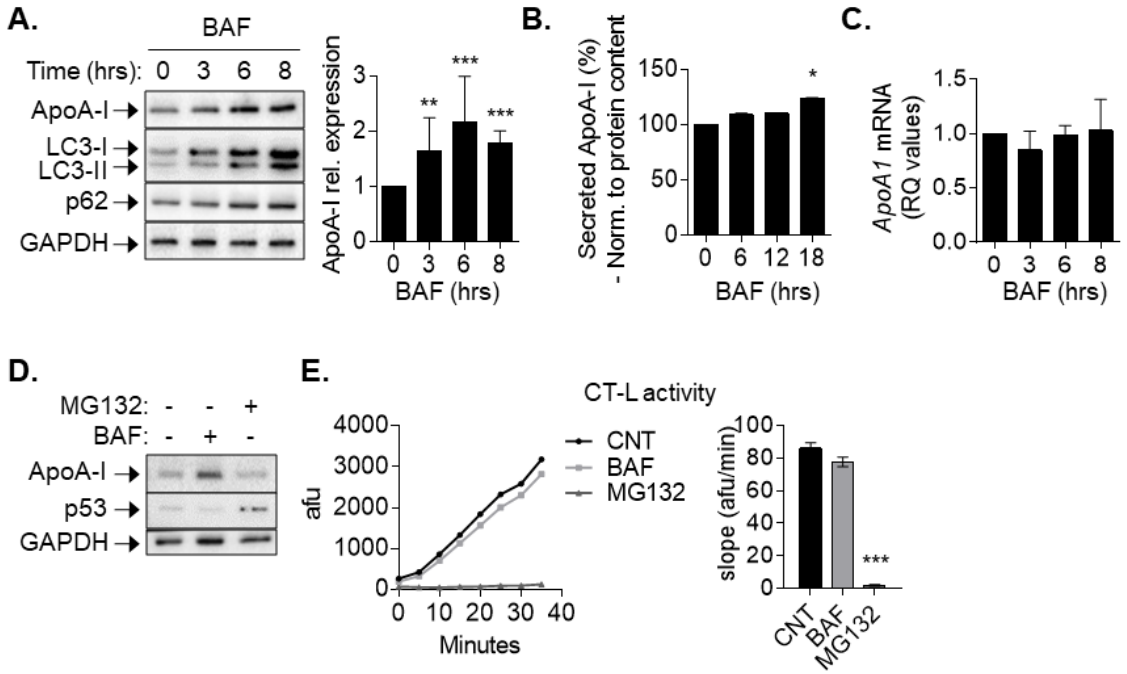

Figure 4.2. Inhibition of autophagy, but not the proteasome, leads to ApoA-I accumulation.
(A) Representative immunoblot analysis of protein lysates from HepG2 cells exposed to the autophagic inhibitor BAF for 3, 6 and 8 hrs for the indicated proteins. LC3-II and p62 levels are indicative of autophagic inhibition by BAF. The levels of ApoA-I normalized to GAPDH were quantified from 5 independent experiments and shown in the graph. Values are expressed relative to those of untreated control cells that were given the arbitrary value of 1 (**$p < 0.01$, ***$p < 0.001$). (B) Analysis of secreted ApoA-I levels measured by ELISA in HepG2 cells exposed to the autophagic inhibitor BAF for 6, 12 and 18 hrs. Secreted ApoA-I levels are expressed as % percentage relative to untreated cells that were given an arbitrary value of 100% and are normalized to total protein content of cell lysate (data are expressed as the mean ± SD of 2 experiments; *$p < 0.05$). (C) *APOA1* mRNA expression levels in HepG2 cells exposed to BAF for 3, 6 and 8 hrs relative to untreated controls which were given the arbitrary value of 1. *APOA1* mRNA was normalized to the housekeeping β-actin gene (data are expressed as the mean ± SD of at least 3 experiments). (D) Representative immunoblot analysis of protein lysates from HepG2 cells exposed to BAF or the proteasomal inhibitor MG132 for the indicated proteins. p53 immunoblot was used as positive control for the effect of the proteasomal inhibitor and GAPDH was used as loading control. (E) Proteasome

activity in HepG2 exposed to BAF or proteasome inhibitor MG132 for 6 hrs. Protein extracts were incubated with fluorogenic substrate, as described in 'Materials & Methods'. Cleaved substrate as arbitrary fluorescence units (AFU) representative of active proteasomes was measured at 5-min intervals for 35 min (data are expressed as the mean ± SD of 3 experiments; ***$p < 0.001$).

In addition, we observed a small increase of secreted ApoA-I upon BAF treatment, that became significant during prolong treatment (Fig 4.2B). Accumulation of ApoA-I occurred in the absence of an effect on transcription as indicated by the unaffected mRNA levels assessed by q-PCR (Fig. 4.2C). Unlike BAF, treatment of HepG2 cells with the proteasomal inhibitor MG132 did not affect ApoA-I protein expression levels but caused the accumulation of p53, a known target of the ubiquitin-proteasome pathway (Fig. 4.2D), and abrogation of chymotrypsin-like activity associated with the 20S proteasome (Fig. 4.2E). These data indicate that autophagy, rather than the proteasome, is the main proteolytic pathway responsible for ApoA-I proteolysis. The generality of this observation was confirmed in ApoA-I-negative HEK293 cells upon heterologous expression of *APOA1*, followed by exposure to BAF (Fig. 4.3A) or CHQ, an inhibitor of autophagosome fusion with lysosomes (153) (Fig. 4.3B). Exposure to BAF or CHQ significantly inhibited autophagic pathway, as documented by the increase of LC3-II expression levels and increased ApoA-I intracellular levels. In addition, treatment of primary mouse hepatocytes isolated from wild type animals with either NH_4Cl + leupeptin (Fig. 4.1C) or CHQ (Fig. 4.3C) also resulted in ApoA-I accumulation.

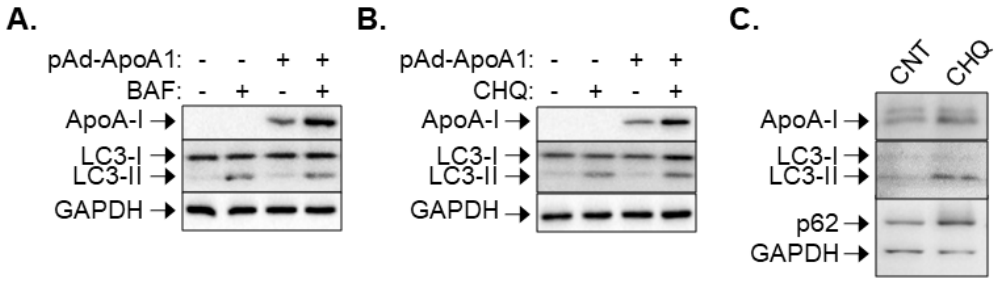

Figure 4.3. Autophagic inhibition in a different hepatic cell models causes ApoA-I accumulation. (A-B) Representative immunoblot analysis of protein lysates from HEK293T cells transfected with ApoA-I expression vector (pAd-ApoA1) or empty vector as control and exposed to BAF (A) or CHQ (B). LC3-II levels are indicative of autophagic inhibition. (C) Representative immunoblot analysis of protein lysates from primary mouse hepatocytes cultured in the presence or absence of CHQ. Immunoblots against anti-LC3-II and anti- p62 were used as markers of autophagic flux. GAPDH was used as loading control.

4.1.3 Autophagic pathway components associate with ApoA-I.

In order to further characterize the intracellular localization of ApoA-I upon autophagy inhibition we initially isolated protein extracts from different cellular compartments. Subcellular protein fractionation followed by immunoblot analysis showed that upon standard culture conditions ApoA-I is predominantly localized in the membrane fraction and, to a lesser degree the cytosol, whereas lipidated LC3 was found exclusively in the membrane fraction (Fig. 4.4A). Upon cell treatment with BAF, a significant increase in LC3-II levels was noted in the membrane fraction where ApoA-I was also predominantly detected (Fig. 4.4A). This observation prompted us to evaluate the association of ApoA-I with autophagic pathway components as well as its localization in autophagosomes. To provide additional data, regarding ApoA-I localization we next performed double immunofluorescence microscopy to monitor co-localization of ApoA-I with lipidated LC3 (LC3-II) which resides on the autophagosomal membranes [23]. At standard growth conditions, ApoA-I showed a staining pattern consistent with predominant expression in ER and Golgi, in line with previous reports (154, 155). However, upon treatment with BAF, the ApoA-I specific fluorescence increased and the protein progressively co-localized with LC3-II (Fig. 4B). The association of ApoA-I with autophagosomes was further investigated by electron microscopy. Inhibition of autophagy led to an increase in both the size and the number of autophagosomes (data not shown) while immunogold labelling of ApoA-I revealed the presence of ApoA-I molecules on autophagic vesicles at steady state, which was dramatically enhanced upon BAF treatment (Fig 4.4C).

The accumulation of ApoA-I in autophagic vesicles upon autophagy inhibition was supported by the increased co-localization of ApoA-I with the autophagic cargo receptor p62, following treatment with BAF (Fig. 4.4D). To address whether ApoA-I directly interacts with p62, we performed co-immunoprecipitations of endogenous ApoA-I with p62 using lysates from the membrane fraction of HepG2 cells treated with BAF where LC3-II is predominantly detected (Fig. 4.4A). The results showed that ApoA-I co-precipitates with p62 upon autophagy inhibition (Fig. 4.4E).

Finally, we tested whether ApoA-I accumulation was associated with endolysosomal membranes by immunofluorescence monitoring of ApoA-I co-localization and the lysosome marker LAMP1. As shown in figure 4.4F, treatment of HepG2 cells with BAF led to largely co-localized ApoA-I with enlarged perinuclear LAMP1 compartments.

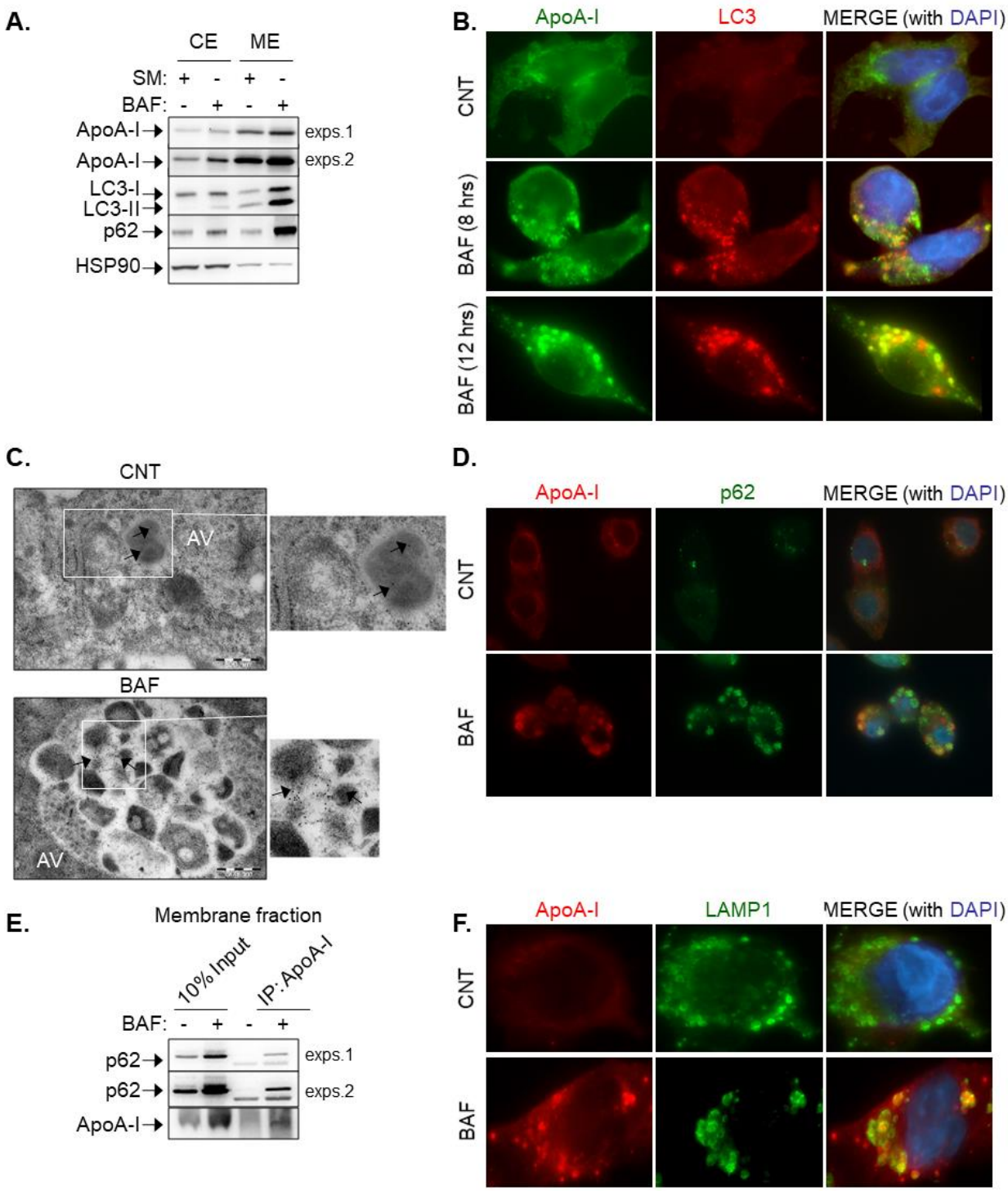

Figure 4.4. ApoA-I co-localizes with autophagosomes
(A) Representative immunoblot analysis of cytoplasmic (CE) and membrane (ME) extracts of HepG2 cells exposed to autophagic inhibitor bafilomycin (BAF) or left untreated. ApoA-I, LC3 and p62 levels are showed. The heat shock protein 90 (HSP90) was used as loading control and marker of the purity of the extracts. Two different exposures (exps) are shown for the anti-ApoA-I immunoblot. (B) Representative immunofluorescence images showing co-localization of ApoA-I (green) and LC3 (red) in HepG2 cells exposed to BAF for 8 and 12 hrs or left untreated. Nuclei are highlighted with DAPI (blue). For image acquisition 100X lens magnification was used. (C) Electron micrographs of HepG2 cells stained with ApoA-I immunogold. Cells were cultured in the presence or the absence of BAF. *AV*; autophagic vacuoles. Arrows indicate gold particles (black dots). Scale bar: 500nm. Insets show higher magnification. (D) Representative immunofluorescence images showing co-localization of ApoA-I (red) and p62 (green) in HepG2 cells exposed to BAF or left untreated. Nuclei are highlighted with DAPI (blue). For image acquisition 63X lens magnification was used. (E) ApoA-I was immunoprecipitated (IP) from lysates from the membrane fraction of HepG2 cells treated with BAF or left untreated. ApoA-I-bound p62 was detected by immunoblotting with anti-p62. Ten percent of membrane protein lysate (input) was also immunoblotted. Two different exposures (exps) are shown for the anti-p62 immunoblot. (F) Representative immunofluorescence images showing co-localization of ApoA-I (red) and the lysosomal protein LAMP-1 (green) in HepG2 cells exposed to BAF or left untreated. Nuclei are highlighted with DAPI (blue). For image acquisition 100X lens magnification was used.

4.1.4 Genetic inhibition of autophagic pathway components leads to impaired ApoA-I proteolysis.

Autophagy may occur through canonical and non-canonical pathways, the latter being mediated in ULK1 and Beclin1-independent manner (156). In order to mechanistically explore the autophagic pathway responsible for ApoA-I regulation, we performed gene silencing of Beclin1 and ULK1 that are involved in the early stages of canonical autophagy and, as control, the late pathway component LC3. As expected, the RNAi-mediated knock-down of either Beclin1 or ULK1 led to reduced LC3-II vs LC3-I with concomitant increase in p62 (Fig. 4.5A-B). ApoA-I levels also accumulated, suggesting that ULK1 and Beclin1 are involved in the autophagic pathway regulating ApoA-I degradation. The knockdown of LC3 also led to ApoA-I accumulation (Fig. 4.5C) which aligns with the co-localization of ApoA-I with LC3-II upon BAF treatment (Fig. 4.4B). We also found that knock-down of either Beclin1 or LC3, but not Mitogen-Activated Protein Kinase Kinase 8 (MAP3K8/ TPL2) also impact on ApoA-I secreted levels, as a small but significant increase in the extracellular ApoA-I levels was detected in these supernatants with ELISA (Fig. 4.5D).

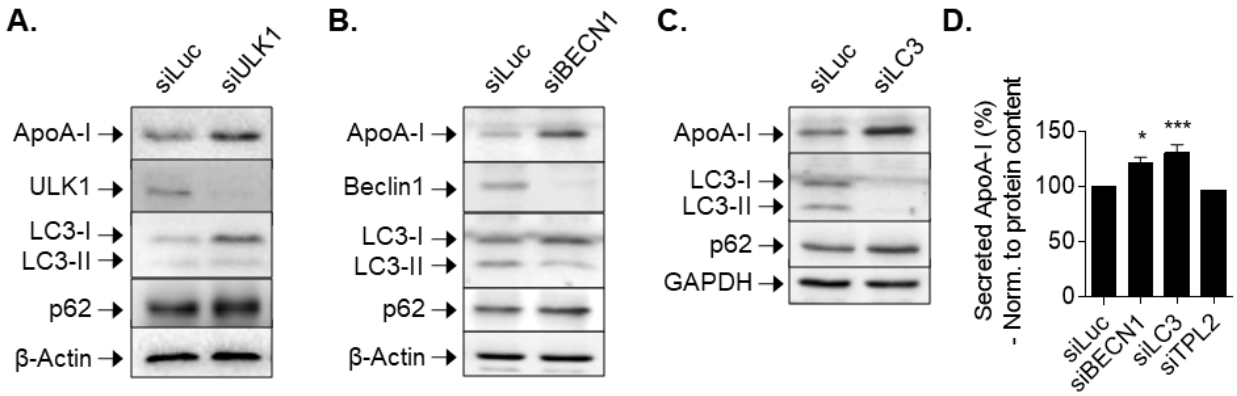

Figure 4.5. Autophagic degradation of ApoA-I is Beclin1 and ULK-1 dependent
Representative immunoblot analysis of lysates from HepG2 cells transiently transfected with siRNA targeting (A) ULK1 (siULK1), (B) Beclin1 (siBECN1) and (C) MAP1LC3B (siLC3) or control siRNA targeting the unrelated Luciferase gene (siLuc). The knock-down efficiency was evaluated by ULK1, Beclin1 and LC3 immunoblotting. p62 and LC3-II levels were used as markers of autophagic flux. GAPDH and β-actin were used as loading controls. (D) Analysis of secreted ApoA-I levels measured by ELISA in HepG2 cells transiently transfected with siRNA targeting Beclin1 (siBECN1), MAP1LC3B (siLC3) or control siRNAs targeting the unrelated Luciferase (siLuc) or MAP3K8 (siTPL2) gene. Secreted ApoA-I levels are expressed as % percentage relative to siLuc-transfected cells that were given an arbitrary value of 100% and are normalized to total protein content of cell lysate (data are expressed as the mean ± SD of 3 experiments; *$p < 0.05$, ***$p < 0.001$).

4.1.5 Starvation leads to inhibition of *de novo* synthesis of ApoA-I rather than autophagy-mediated ApoA-I degradation.

The aforementioned results demonstrate that basal autophagy impacts on ApoA-I turnover. We next sought to determine if induction of autophagy could respectively reduce ApoA-I expression. To this end, HepG2 cells were cultured under conditions of amino-acid and serum depletion in EBSS, a process known to result in the activation of autophagy (55, 157). In comparison to cells cultured in standard conditions, EBSS led to dramatic reduction in ApoA-I levels both in total and fractionated (cytoplasmic and membrane) protein lysates (Fig. 4.6A-B). This reduction was paralleled by rapid loss of phosphorylated 4E-BP1, a major component of CAP-dependent translational initiation, but not of p62 which showed a slower kinetics of reduction (Fig. 4.6A). Notably, whereas ApoA-I protein levels rapidly declined upon starvation, *APOA1* mRNA expression remained unaffected (Fig. 4.6C).

These observations prompted us to combine EBSS with BAF. We reasoned that if the EBSS-mediated reduction in ApoA-I is due to autophagy induction, treatment with BAF should result in

ApoA-I accumulation. Surprisingly, BAF did not reverse the EBSS-mediated reduction in ApoA-I (Fig. 4.6D). We found that these changes occurred in the absence of an effect on *APOA1* transcription (Fig. 4.6E) and we have excluded the possibility that the reduced intracellular levels of ApoA-I, imposed by starvation, could be attributed to exaggerated secretion; in fact, HepG2 cells cultured in EBSS displayed significant loss of ApoA-I secretion (Fig. 4.6F).

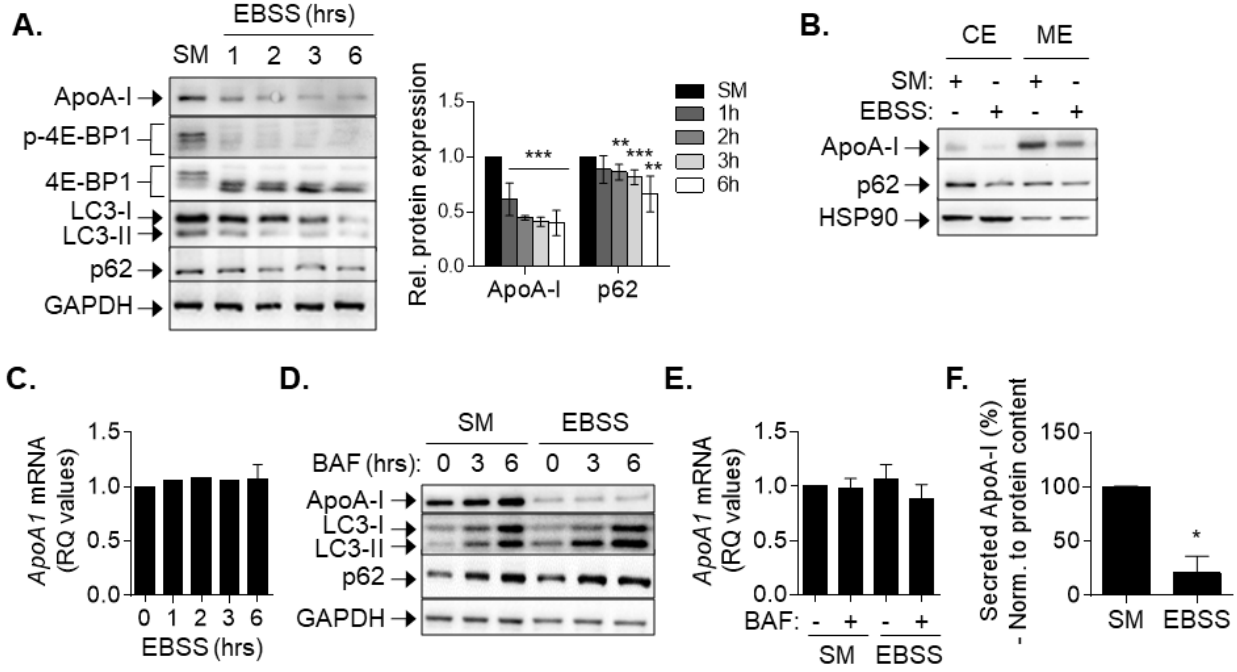

Figure 4.6. Reduced ApoA-I levels by EBSS-induced starvation are not completely restored by autophagy inhibition. (A) Immunoblot analysis for the indicated proteins of lysates from HepG2 cells cultured in standard medium (SM) or amino acid deficient medium (EBSS) for 1, 2, 3 and 6 hrs. Quantification of ApoA-I and p62 levels normalized to GAPDH are shown in the graph of the right panel. Values are expressed relative to those in untreated control cells that were given an arbitrary value of 1 and are expressed as the mean ± SD of at least 3 experiments; $^{**}p < 0.01$ and $^{***}p < 0.001$. The levels of 4E-BP1 phosphorylation were used as surrogates for mTORC1 activity, and p62 and LC3-II were used as markers of autophagic flux. (B) Immunoblot analysis of cytoplasmic (CE) and membrane (ME) protein extracts of HepG2 cells exposed to EBSS for 6 hrs. ApoA-I and p62 levels are showed. HSP90 was used as loading control and marker of the purity of the extracts. (C) Relative *APOA1* mRNA expression levels of HepG2 cells cultured in SM or EBSS to induce autophagy for 1, 2, 3 and 6 hrs. *APOA1* mRNA was normalized to the housekeeping β-actin gene and expressed as RQ values relative to untreated controls, which was given the arbitrary value of 1 (data are expressed as the mean ± SD of at least 3 experiments). (D) Representative immunoblot analysis of protein lysates of HepG2 cells cultured in SM or EBSS in the presence or absence of BAF for the indicated time periods. ApoA-I levels are shown, LC3 and p62 levels are indicative of autophagic flux and GAPDH was used as loading control. (E) Relative *APOA1* mRNA expression levels of HepG2 cells cultured in SM or EBSS in the presence or absence of BAF. *ApoA1* levels are normalized to the housekeeping β-actin gene and expressed as RQ values relative to untreated controls, which was given the arbitrary value of 1 (data are expressed as the mean ± SD of at least 2 experiments). (F) Analysis of secreted ApoA-I levels measured by ELISA in HepG2 cells cultured in SM or EBSS for 8 hrs. Secreted ApoA-I levels are expressed as % percentage relative to cells cultured in SM that were given an arbitrary value of 100% and are normalized to total protein content of cell lysate (data are expressed as the mean ± SD of 2 experiments; $^{*}p < 0.05$).

The inability of BAF to reverse the effect of EBSS on intracellular ApoA-I levels suggests that mechanisms triggered by starvation other than autophagy may dominate the regulation of ApoA-I expression in this setting. We thus embarked on studies aiming to identify factors that are present in standard culture media and could recover both the basal levels of ApoA-I in starved cells and the response to autophagy inhibition. Such putative molecules are lipids and aminoacids. We first cultured cells with EBSS supplemented with BSA-conjugated oleic acid or, as a control BSA alone, in the presence or absence of BAF. In comparison to EBSS, addition of oleic acid failed to recover ApoA-I to the levels of standard culture conditions and its response to BAF (Fig. 4.7A). Autophagy inhibition by BAF was otherwise functional, as evidenced by the relative accumulation of LC3-II and of the autophagy marker p62 (Fig. 4.7A). In contrast, addition of aminoacids to EBSS enabled expression of ApoA-I to near control culture levels which further accumulated upon treatment with BAF (Fig. 4.7B). To determine whether there is a specific requirement of aminoacid for standard ApoA-I expression we supplemented EBSS medium with either essential or non /and aminoacid and determined ApoA-I levels. The results showed that both essential and non-essential aminoacids are required for maintaining standard ApoA-I levels (Fig. 4.7C).

During these studies we also noted a correlation between levels of ApoA-I expression and phosphorylation of 4E-BP1: addition of oleic acid to EBSS failed to phosphorylate 4E-BP1 and to recover ApoA-I expression whereas aminoacids engaged 4E-BP1 phosphorylation, and recovered both basal levels of ApoA-I and its response to autophagy (Fig. 4.7A-C). This observation indicated that ApoA-I has a high turnover and that protein synthesis is required to maintain its intracellular levels. This hypothesis was tested by addition of cycloheximide (CHX), an inhibitor of *de novo* protein synthesis, to HepG2 cultures growing in complete, standard growth media. Immunoblot analysis of lysates demonstrated a half-life for ApoA-I of approximately 30 min, confirming that active protein synthesis is required to maintain intracellular ApoA-I levels (Fig. 4.7D). In contrast, the levels of LC3 and p62 remained unaffected during this course of CHX treatment. Finally addition of CHX in starved EBSS-cultured cells failed to further reduce ApoA-I (Fig. 4.7E), supporting that blockade of protein

synthesis is the critical mechanism that mediates the significant reduction of ApoA-I levels upon starvation (Fig 4.7E).

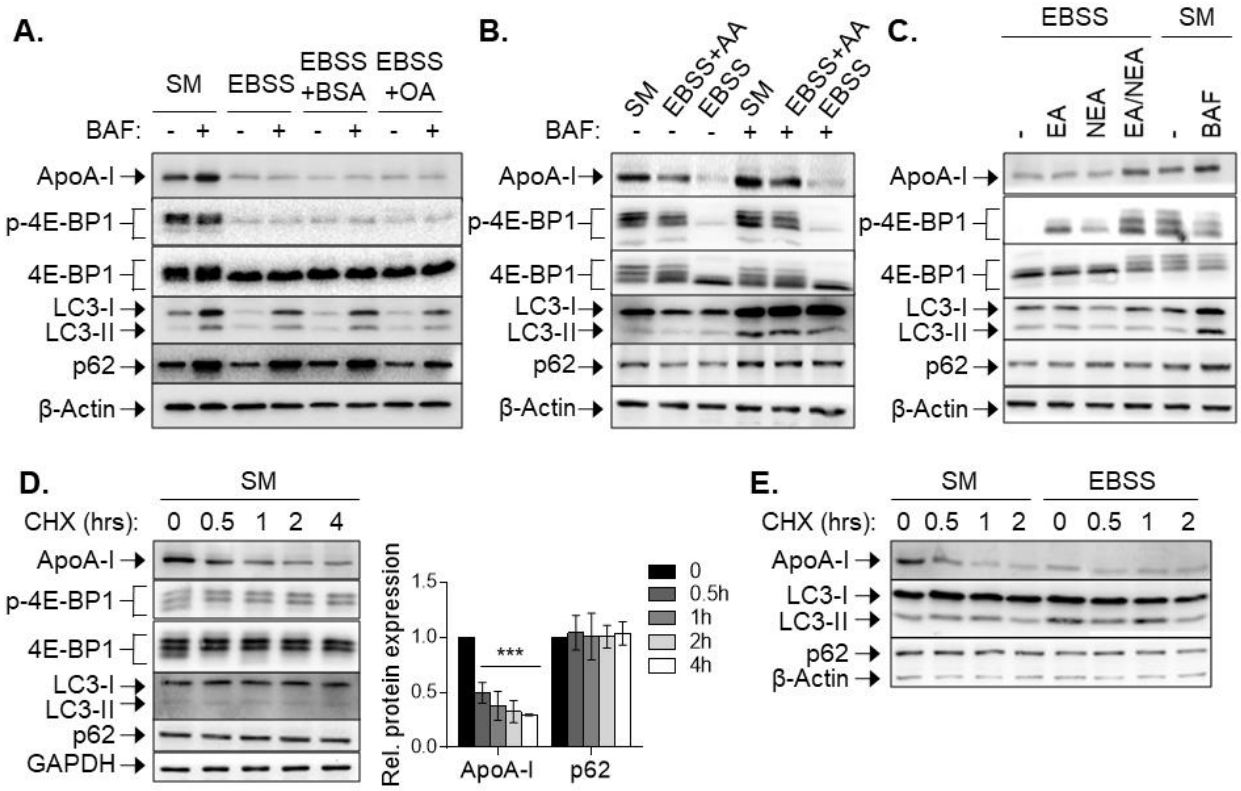

Figure 4.7. ApoA-I levels critically depend on aminoacid availability and *de novo* protein synthesis. (A) Representative immunoblot analysis of lysates from HepG2 cells cultured in EBSS in the presence or absence of BAF, with or without 500 nM BSA-conjugated oleic acid (OA) supplementation. BSA supplementation served as control. (B) Representative immunoblot analysis for the indicated proteins of lysates from HepG2 cells cultured in EBSS in the presence or absence of BAF with or without amino acid (AA) supplementation. (C) Representative immunoblot analysis of lysates from HepG2 cells cultured in EBSS or EBSS supplemented with essential amino acids (EA) or/and non-essential amino acids (NEA). Lanes 5 and 6 represent lysates from cells cultured in standard medium (SM) in the presence or absence of BAF, respectively, and serve as controls. 4E-BP1 phosphorylation was used as surrogate for mTORC1 activity and p62 and LC3-II levels were used as markers of autophagic flux. β-actin was used as loading control. (D) Representative immunoblot analysis of lysates from HepG2 cells treated with 10μM CHX for 0.5, 1, 2, 3, 4 hrs. Quantification of ApoA-I and p62 levels normalized to GAPDH was performed from at least 3 experiments and shown in the right panel graph. Values are expressed relative to those in untreated control cells that were given an arbitrary value of 1 and are expressed as the mean ± SD; ***$p < 0.001$. (E) Representative immunoblot analysis of lysates from HepG2 cells cultured for 6 hrs in either SM or EBSS prior to the addition of CHX to the culture media for the indicated time periods. β-actin was used as loading control.

4.1.6 mTORC1 signaling is required for basal ApoA-I expression.

The mTOR complexes mTORC1 and mTORC2 are master regulators of cell metabolism and growth in response to nutrient availability (158). mTORC1 responds to aminoacid availability to control biosynthetic and catabolic pathways, including translation and autophagy, respectively. mTORC2 controls proliferation and survival primarily by phosphorylating several members of the AGC (PKA/PKG/PKC) family of protein kinases, including Akt (159).

Prompted by the aforementioned effect of aminoacid availability on ApoA-I expression levels, we investigated the impact of mTORC1/2 on ApoA-I regulation. We exposed HepG2 cells to Torin2, a small molecule inhibitor of mTORC1/2 (160), under standard (Fig. 4.8A) or EBSS culture conditions (Fig. 4.8C). As previously reported in other cell types (160), treatment of HepG2 cells with Torin2 efficiently abolished mTORC1 and mTORC2 activities, evidenced by the reduced phosphorylation of 4E-BP1 at $Thr^{37/46}$ and of Akt at Ser^{473}, respectively (Fig. 4.8C). In line with the prominent role of mTORC1 inactivation in autophagy induction, treatment of HepG2 cells with Torin2 also increased autophagic flux as documented by the changes in the expression of lipidated LC3 (LC3-II) and p62 (Fig. 4.8A-C).

Similar to the effect of EBSS on ApoA-I (Fig. 4.6A-E), Torin2 reduced ApoA-I protein levels without having an effect on *APOA1* mRNA expression, and co-treatment with BAF did not significantly affect ApoA-I expression at protein or mRNA level (Fig. 4.8A-B). When Torin2 was applied in HepG2 cells cultured in EBSS medium, no further change in ApoA-I expression was observed, whereas switching culture media from EBSS to standard culture conditions recovered ApoA-I expression levels and sensitivity to Torin2 (Fig. 4.8C).

Starvation or treatment with Torin2 impacts on both mTORC1 and mTORC2 activities, documented by decreased phosphorylation of 4E-BP1 and Akt (Fig. 4.8A and C). To clarify which of mTORC1 or mTORC2 is implicated in ApoA-I regulation, we cultured HepG2 cells in the presence of insulin that is known to activate mTORC2 but not mTORC1 (161). We found that insulin induced a time-dependent increase in the Ser^{473} phosphorylated Akt that was not accompanied by changes in mTORC1-dependent phosphorylation of 4E-BP1 or ApoA-I (Fig. 4.9A). Moreover, whereas EBSS inhibited mTORC1-mediated 4E-BP1 phosphorylation and

reduced ApoA-I levels, neither was affected by insulin treatment (Fig. 4.9A). These observations suggest that mTORC2 is not involved in the regulation of ApoA-I.

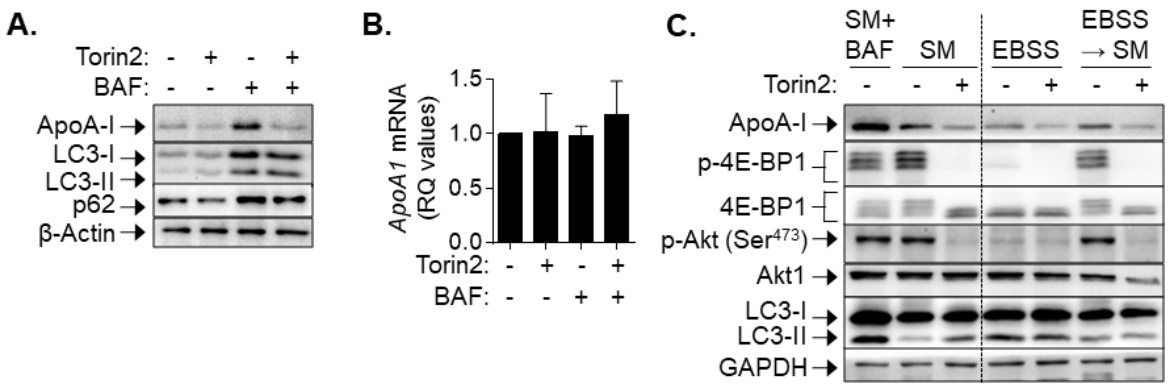

Figure 4.8. ApoA-I expression levels are dependent on mTOR activity.
(A) Representative immunoblot analysis and (B) relative mRNA expression levels of *APOA1* in HepG2 cells treated with 250 nM Torin2 and/or BAF for 6 hrs, or left untreated. *APOA1* mRNA expression levels were normalized to the housekeeping β-actin gene and expressed as RQ values relative to untreated controls, which was given the arbitrary value of 1 (data are expressed as the mean ± SD of at least 3 experiments). (C) Immunoblot analysis of lysates from HepG2 cells cultured in standard medium (SM) or in amino acid deficient medium (EBSS) or exposed to EBSS for 3 hrs and subsequently switched to SM for 6 hrs, in the presence or absence of 250 nm Torin2. Treatment of cells with BAF in lane 1 serves as positive control for ApoA-I accumulation. 4E-BP1 and Akt phosphorylation were used as surrogates for mTORC1 and mTORC2 activity respectively, and p62 and LC3-II were used as markers of autophagic flux. GAPDH and β-actin serve as loading controls.

Along these lines, co-treatment of starved (EBSS) cells with insulin and Torin2 did not affect ApoA-I (Fig. 4.9B). In contrast, Torin2 reduced intracellular ApoA-I levels in the presence of aminoacids irrespectively of insulin addition, suggesting that mTORC1 is responsible for ApoA-I regulation (Fig. 4.9B).

To provide direct evidence of ApoA-I regulation by mTORC1, we performed siRNA-mediated knock-down of Raptor and Rictor, the main protein subunits of mTORC1 and mTORC2 complexes, respectively (158). Knock-down of Raptor, but not Rictor, resulted in significant decrease in ApoA-I protein levels, providing conclusive support for the regulation of ApoA-I by mTORC1 (Fig. 4.9C).

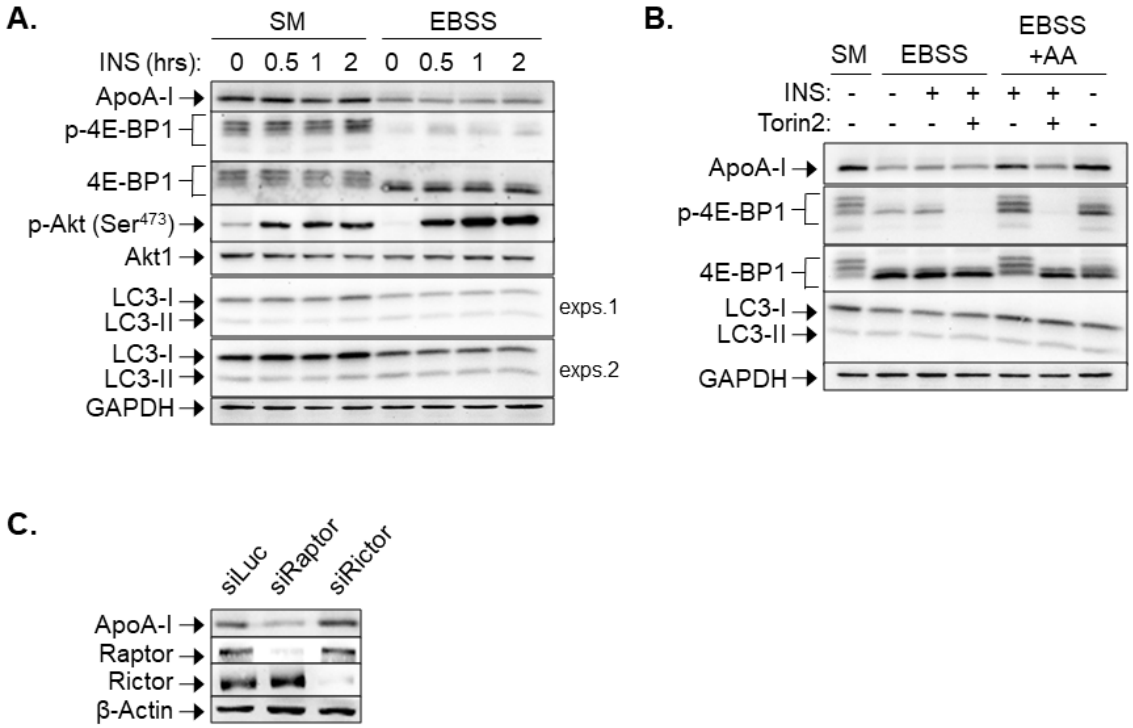

Figure 4.9. ApoA-I turnover is regulated by mTORC1 signaling pathway.
(A) Immunoblot analysis of lysates from HepG2 cells cultured in SM or in EBSS in the presence or the absence of 100 nM insulin (INS). Insulin was added during the last 0.5, 1, or 2 hrs of incubation with EBSS or SM. (B) Immunoblot analysis of lysates from HepG2 cells cultured in EBSS or EBSS supplemented with amino acids (AA) and treated with 100 nM INS and/or 250 nM Torin2. Analysed lysates from cells cultured in SM served as control. 4E-BP1 and Akt phosphorylation were used as surrogates for mTORC1 and mTORC2 activity respectively, and p62 and LC3-II were used as markers of autophagic flux. GAPDH was used as loading control. (C) Immunoblot analysis of lysates from HepG2 cells transiently transfected with siRNA targeting mTORC1 subunit Raptor (siRaptor), mTORC2 subunit Rictor (siRictor) or control siRNA (siLuc). The knock-down efficiency was evaluated by Raptor and Rictor immunoblotting, and β-actin was used as loading control.

4.1.7 Metformin reduces ApoA-I levels by downregulating apolipoprotein gene expression.

Metformin is the first-line medication for the treatment of type 2 diabetes, by controlling blood glucose levels. At a cellular level it has been shown to induce autophagy in hepatocytes. We thus examined the effects of metformin treatment on ApoA-I levels in HepG2 cells. We noted a time-dependent reduction in ApoA-I protein levels (Fig. 4.10A). However, unlike EBSS, we found that metformin also had a profound effect on ApoAI mRNA levels measured by q-PCR (Fig. 4.10 B). By examining the expression levels of various apolipoproteins such as *ApoC3*, *ApoA4* and *ApoA5*, that cluster in the same chromosomal region, we observed a common effect on metformin in the dowregulation of gene expression of these apolipoproteins (Fig 4.10C). To

further investigate the apolipoprotein transcriptional regulation by metformin we next assessed the expression levels of long non-coding natural antisense transcript (APOA1-AS), which was recently found to act as a negative transcriptional regulator of *ApoA1* and to control mRNA apolipoprotein expression levels (29). We found that the levels of ApoA1-AS were not affected by metformin, suggesting that other transcriptional modulators are implicated in the control of *ApoA1* levels upon metformin treatment (Fig.4.10). We concluded that the dominant mechanism of metformin effect on *ApoA1* is transcriptional repression. Further investigation should aim at the delineation on the mechanism of apolipoprotein transcriptional modulation by metformin and how this regulation may be involved in beneficial effects of the drug in hepatocytes.

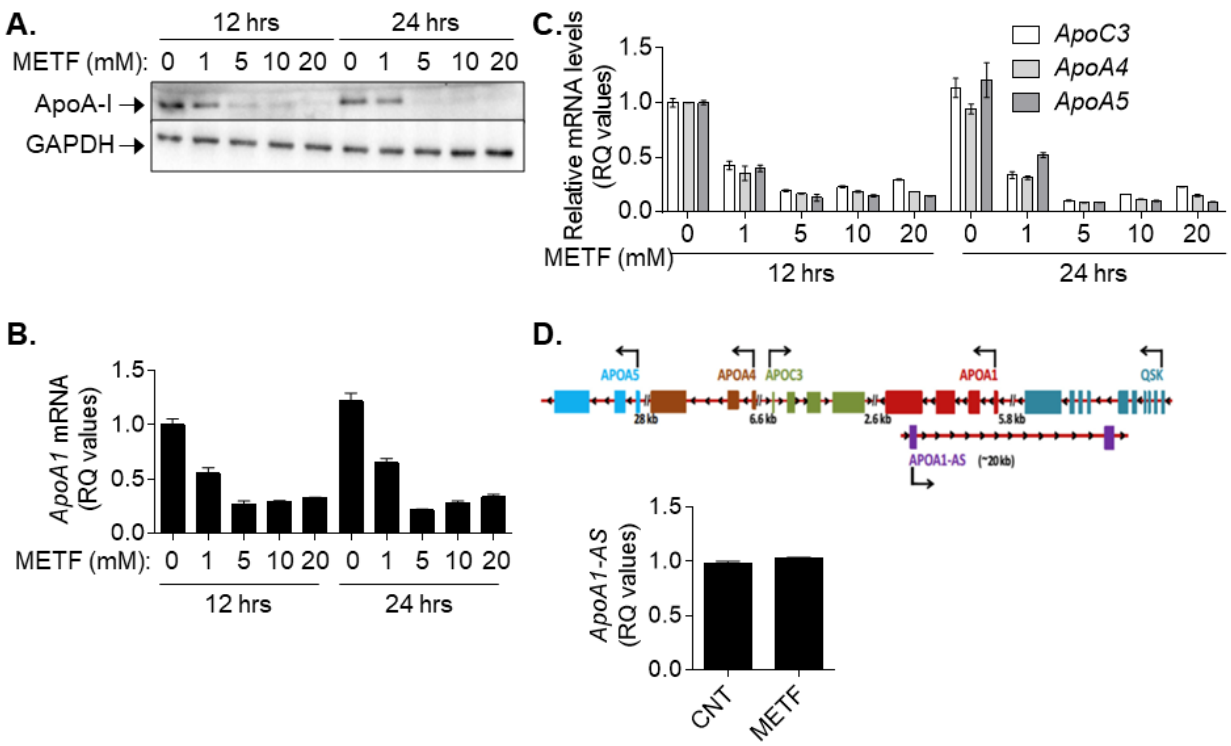

Figure 4.10. Metformin reduces ApoA-I levels by impacting on apolipoprotein transcriptional expression.
(A) Representative immunoblot analysis of ApoA-I protein levels and (B-C) representative graph of relative mRNA expression levels of *APOA1* (B), *ApoC3, ApoA4* and *ApoA5* (C) in HepG2 cells treated with the indicated concentrations of metformin for 12 and 24 hrs. (C) Representative graph of relative expression of long non-coding natural antisense transcript (*APOA1-AS*) in HepG2 cells treated with 20mM metformin for 12 hrs. mRNA expression levels were normalized to the housekeeping β-actin gene and expressed as RQ values relative to untreated control. APO gene cluster and APOA1-AS NAT organization on human chromosome 11 are depicted in the figure (adapted from Halley et al., 2014).

4.1.8 Discussion (Chapter 1)

ApoA-I is predominantly expressed in hepatocytes and represents approximately 70% of the protein content of HDL. Recent studies have expanded the role of ApoA-I beyond the HDL-mediated reverse cholesterol transport to include a broad spectrum of anti-thrombotic, anti-oxidative, anti-inflammatory and immune-regulatory properties that are pertinent to the protective roles of ApoA-I in cardiovascular, inflammatory and malignant diseases (4). ApoA-I expression differs among individuals and low ApoA-I levels correlate with increased risk of development of several colon and liver pathologies (162, 163). Despite the emergence of a multitude of ApoA-I functions, little is known about the mechanisms responsible for its regulation.

Data presented herein underscore the major contribution of post-transcriptional mechanisms to the regulation of basal ApoA-I expression. Using the hepatoma cell line HepG2 which retains the ability to synthesize and secrete ApoA-I in a manner similar to normal hepatocytes (149, 155, 164) , we show that intracellular ApoA-I protein levels may significantly vary in the absence of changes in mRNA expression. Thus, whereas ApoA-I protein levels are exquisitely sensitive to aminoacid depletion, *APOA1* transcription remains intact (Fig. 4.6). In line with this observation, inhibition of *de novo* protein synthesis by CHX revealed rapid turnover of ApoA-I with an estimated protein half-life of approximately 30 min (Fig. 4.7D). We further report that ApoA-I proteolysis occurs through autophagy rather than the proteasome pathway. Indeed, exposure of HepG2 cells or of primary mouse hepatocytes to autophagy inhibitors led to accumulation of intracellular ApoA-I in the absence of an effect on *APOA1* transcription, whereas both ApoA-I protein and mRNA levels remained unaffected by the proteasome inhibitor MG132 (Fig. 4.2). The aforementioned findings challenge the traditional view of the proteasome and autophagy pathways targeting short-lived and long-lived proteins for degradation, respectively, and align with recent reports showing that autophagy may also target short-lived proteins, including Cyclin D1 (165), the gap junction protein Connexin 43 (166), and TRIM5α (Tripartite motif-containing protein 5α), an effector of cellular anti-viral response (167).

Our results also implicate the canonical autophagic pathway, mediated through ULK1 and Beclin-1, and SQSTM1/p62 in the regulation of ApoA-I (Fig. 4.5). SQSTM1/p62 is an adaptor

protein that links cargo material to the nascent phagophore via its capacity to interact directly with LC3. Herein we showed that ApoA-I co-localizes and co-precipitates with p62, suggesting that it is a p62 cargo in autophagy.

SQSTM1/p62 is itself degraded upon induction of autophagy. Surprisingly, we observed that starvation of HepG2 cells from growth factors and essential biological building blocks triggers autophagy and p62 degradation with slower kinetics compared to the reduction in ApoA-I levels under the same conditions. Instead, the reduction in ApoA-I was paralleled by the loss of 4E-BP1 phosphorylation, a process known to depend on the nutrient sensor mTORC1.

Mammalian TORC1 activates anabolic processes, including protein synthesis by phosphorylating several targets, including p70S6 kinase and 4E-BP1 (168), and lipid synthesis by phosphorylating and sequestering Lipin-1 to the cytoplasm thereby allowing activation of sterol- and lipogenic gene transcription through the transcription factor SREBP (81). Under nutrient sufficiency, activated mTORC1 also inhibits the catabolic process of autophagy through various routes, including the phosphorylation of ULK1 at Ser^{757} which disrupts the interaction between ULK1 and AMPK and their coordinated effects on autophagy induction. Conversely, inhibition of mTORC1 triggers autophagy. Our data suggest that mTORC1-dependent regulation of protein synthesis and autophagy uncouple in the regulation of ApoA-I expression. We show that the reduction in intracellular ApoA-I imposed by starvation cannot be reversed upon inhibition of autophagy (Fig. 4.6D), whereas supplementation with aminoacids restores mTORC1 activity, basal ApoA-I expression levels and its responsiveness to autophagy inhibitors (Fig. 4.7E).

We note that whereas EBSS, mTORC1 inhibitors and CHX have a profound effect on intracellular and secreted ApoA-I levels, there is a residual ApoA-I that remains unaffected by these treatments. Indeed, CHX chase of HepG2 cells cultured in EBSS failed to further reduce ApoA-I (Fig. 4.7E). Collectively, these observations indicate the existence of two intracellular ApoA-I pools; a labile one that is modulated by mTORC1 signaling and autophagy-mediated turnover and is largely destined for secretion, and a stable pool that is not subject to autophagy

and mTORC1 regulation. The precise nature and function of the latter are subject to ongoing investigation.

Overall, the data presented herein define major post-transcriptional pathways responsible for regulation of intracellular ApoA-I levels. They demonstrate that under nutrient-rich conditions, ApoA-I expression is sustained by the balancing acts of basal autophagy and of mTORC1-dependent *de novo* protein synthesis (Fig. 4.11). Accordingly, ApoA-I accumulates in steatosis-like conditions (Fig. 4.1), associated with autophagy blockade. In contrast, upon aminoacid insufficiency, suppression of ApoA-I synthesis prevails, rendering mTORC1 inactivation dispensable for autophagy-mediated ApoA-I proteolysis (Fig. 4.11). Given the established role of ApoA-I in HDL-mediated reverse cholesterol transport, this mode of regulation of intracellular ApoA-I levels may reflect a hepatocellular response to the organismal requirement for maintenance of cholesterol and lipid reserves under conditions of nutrient scarcity. In line with this notion, a reduction in circulating ApoA-I has been noted in adults undergoing a very low calorie diet (169, 170) and in children suffering of kwashiorkor, a severe form of protein malnutrition (171, 172). Moreover, reduced HDL has been reported in rodents following severe caloric restriction (173)and in a mouse model of alcoholic liver disease (174) which is characterized by reduced mTOR activity despite autophagy suppression (171).

Emerging evidence suggests that various autophagy pathway components possess functions beyond autophagy regulation. For example, p62 expression influences mTORC1, NF-κB and Nrf2 activities and impacts on metabolic, inflammatory and malignant pathologies in the liver (172). Whether the interaction of p62 with ApoA-I under conditions of autophagy blockade may also influence the anti-inflammatory, anti-thrombotic or anti-oxidative properties of ApoA-I remains to be addressed.

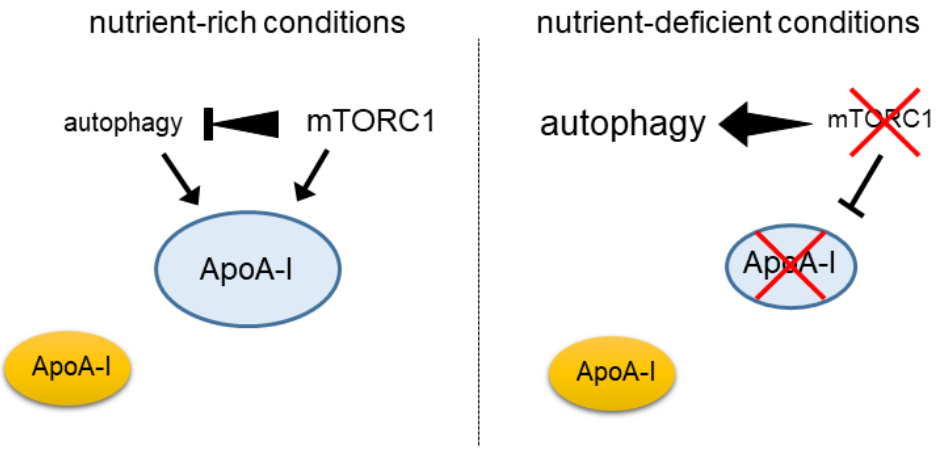

Figure 4.11. Graphical representation of regulation of intracellular ApoA-I levels under nutrient-rich and nutrient-deficient conditions. The former is associated with basal mTORC1 signaling and autophagy. Based on the findings reported herein, we propose that ApoA-I levels are balanced by basal autophagy *versus* mTORC1 signaling controlling *de novo* ApoA-I synthesis (A). Under nutrient-deficient conditions mTORC1 activity is suppressed and autophagy is activated. However, suppression of ApoA-I synthesis as a result of diminished mTORC1 signals prevails rendering mTORC1 inactivation dispensable for autophagy-mediated ApoA-I proteolysis (B). A small ApoA-I pool in HepG2 cells remains unaffected by the aforementioned mechanism.

4.2 Chapter 2

4.2.1 ApoA-I physiologically acts to suppress intracellular lipid overload by affecting LD homeostasis.

Whereas the role of extracellular of ApoA-I in the regulation of lipid metabolism is well characterized, its intracellular function, if any, remains elusive.

A previous report, published by Karavia et al., documented increased steatosis in the liver of ApoA-I –deficient (ApoA-I$^{-/-}$) mice after diet-induced hepatic triglyceride deposition, histologically manifested by accumulation of fat cells (47). As shown in chapter 1, mice fed high fat diet display hepatic autophagy blockade and elevated levels of ApoA-I. *In vitro,* inhibition of autophagy in HepG2 cells also led to accumulation of ApoA-I. Moreover, autophagy blockade is known to result in LD accumulation and increased lipid load in hepatocytes (125).

We therefore hypothesized that the accumulation of ApoA-I ensued by BAF treatment could function as a protective mechanism against the lipid overload driven by autophagic inhibition. We tested this hypothesis by assessing the size and the number of LD in HepG2 cells transiently transfected with siRNA targeting *ApoA1* (siApoA1) or control siRNA targeting the unrelated Luciferase gene (siLuc), cultured in the presence or absence of BAF. We found that either *ApoA1* knock-down or BAF treatment alone increased the percentage of intermediate and large size LD, indicative of elevated intracellular lipid load. Combinatory treatment further enhanced the size of LDs, suggesting that ApoA-I functions as a barrier to LD accumulation both at standard culture conditions and upon autophagy blockade (Fig. 4.12A).

The amplifying effect of BAF on *ApoA-1* knocked-down cells also indicates that ApoA-I may function in a pathway other than autophagy in the regulation of intracellular lipid metabolism. This hypothesis was tested by analyzing the expression levels of LC3 and p62 as marker of autophagic flux of lysates from HepG2 cells transiently transfected with siApoA1 or control siLuc cultured in the presence or absence of BAF. The knock-down of *ApoA1* led to a reduction in both LC3-I and LC3-II; however the autophagic flux did not appear to change (Fig.4.12B). In addition, the protein levels of the autophagic substrate p62 remained unaffected by the knock-

down of *ApoA1*, further supporting that ApoA-I does not significantly impact on autophagic activity. Thus, our results do not support an effect of ApoA-I on macroautophagy; however further investigation is required to define the impact of ApoA-I on LC3 –I and –II expression.

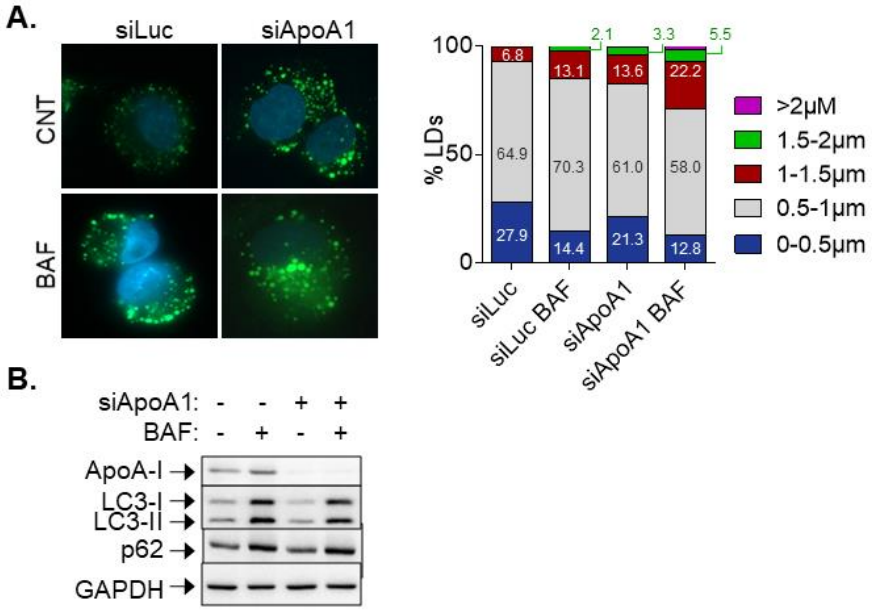

Figure 4.12. Intracellular ApoA-I impacts on hepatic lipid load, without affecting autophagic flux. HepG2 cells were transiently transfected with siRNA targeting ApoA1 (siApoA1) or control siRNA targeting the unrelated Luciferase gene (siLuc) cultured in the presence or absence of BAF. (A) Representative immunofluorescence images of cells stained with BODIPY 493/503 (indicative of lipid droplets). Analysis of % LDs with indicative LD size (diameter in µm). (B) Representative immunoblot analysis of protein lysates. Immunoblot against anti-LC3-II and anti- p62 was used as markers of autophagic flux. The efficiency of *ApoA1* knock-down was evaluated by ApoA-I immunoblotting and GAPDH was used as loading control**.**

4.2.2 The transcriptome of HepG2 hepatoma cells depleted for ApoA-I is enriched for upregulated genes related to lipid and cholesterol metabolism.

Against this background we performed RNA sequencing (RNAseq) to quantify changes in gene expression caused by the knock-down of *ApoA1* and to identify biological processes and molecular pathways linked to the observed accumulation of LD. To this end, we tested RNA extracted from HepG2 cells transiently transfected with siApoA1 or siLuc, cultured in the presence or absence of BAF.

Knock-down of *ApoA1* led to the upregulation of 483 genes with a statistical threshold of p≤0.05. Using the WebGestalt (WEB-based GEne SeT AnaLysis Toolkit) bioinformatics

platform, we found that the transcriptome of HepG2 hepatoma cells deficient of *ApoA1* is enriched for up-regulated genes related to lipid and cholesterol metabolism. This is documented by the functional enrichment analysis of gene ontology biological processes (FDR<$5x10^{-11}$) (Fig. 4.13A) and their inter-relationships (Fig. 4.13B). It is noteworthy, that in a representative enrichment analysis of 380 mapped input transcripts, 24 are annotated to cholesterol metabolic process (GO: 0008203). The annotated processes where found to cluster around cholesterol/lipid and flavonoid metabolic processes (dotted boxes). The same bioinformatics platform was explored to identify diseases predicted to be associated with the upregulated gene expression profile of HepG2 cells depleted of ApoA-I. As shown in Figure 4.13C, *ApoA1* depletion is predicted to associate with hepatic steatosis, fatty liver disease, hyperlipidemia and metabolic syndrome disorders. Therefore, a hypothesis-free, RNAseq-based approach, suggests that *ApoA1* depletion is associated with lipid and cholesterol overload pathologies. This important observation aligns well with our *in vitro* data shown in Fig. 4.12A that document increased lipid load upon *ApoA1* knock-down.

Treatment with BAF led to the upregulation of 484 genes ($p \leq 0.05$) while knock-down of *ApoA1* followed by BAF treatment resulted in the upregulation of 770 genes ($p \leq 0.05$). We combined this information to construct a Venn diagram shown in Fig. 4.14A, and we focused on those genes that are commonly upregulated in all three conditions, namely, ***i***. BAF treatment (BAF), ***ii***. ApoA1 knock-down (siApoA1), ***iii***. *ApoA1* knock-down and BAF treatment (siApoA1+ BAF). We reasoned that this intersection is most relevant to LD accumulation associated with the combined effect of ApoA-I depletion and autophagy inhibition. This intersection is represented by 164 upregulated genes, linked to biological functions related to metabolic processes and inflammatory response (Fig. 4.14B) and predicted associated pathologies such as hepatic steatosis and fatty liver disease (Fig 4.14C).

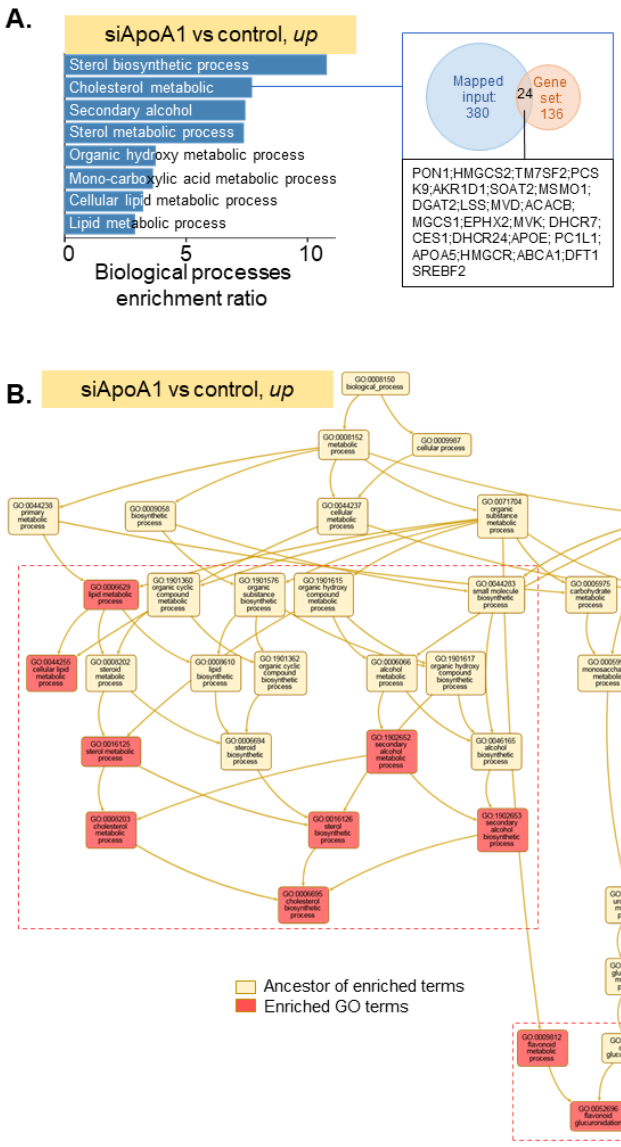

Figure 4.13. The transcriptome of HepG2 hepatoma cells depleted of ApoA-I is enriched for upregulated genes related to lipid and cholesterol metabolism. (A) Functional enrichment analysis of gene ontology biological processes (FDR<5x10^{-11}) in *ApoA1* siRNA-transfected *versus* control HepG2 cells. A representative example of enrichment is shown where out of 380 mapped input transcripts, 24 are annotated to cholesterol metabolic process (GO: 0008203).(B) The inter-relationships of GO biological processes derived from the transcriptome of HepG2 hepatoma cells depleted of ApoA-I. Each enriched Gene Ontology (GO) is shown as red-colored rectangular and their ancestors as yellow. Processes are clustered around cholesterol/lipid and flavonoid metabolic processes (dotted boxes) and they share GO:0008152 (Metabolic process) as their common ancestor term. (C) Volcano plot displaying diseases predicted to be associated with the profile of upregulated genes.

A.

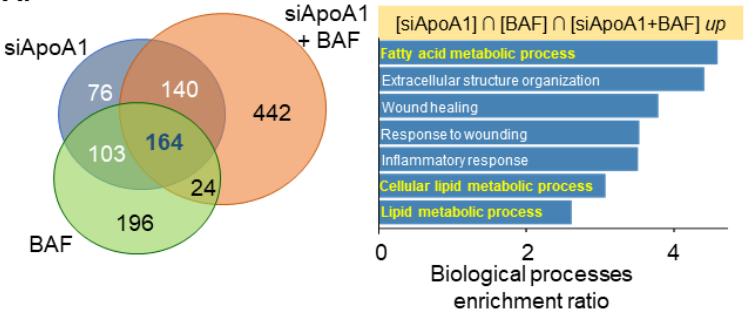

B. [siApoA1] ∩ [BAF] ∩ [siApoA1+BAF] *up*

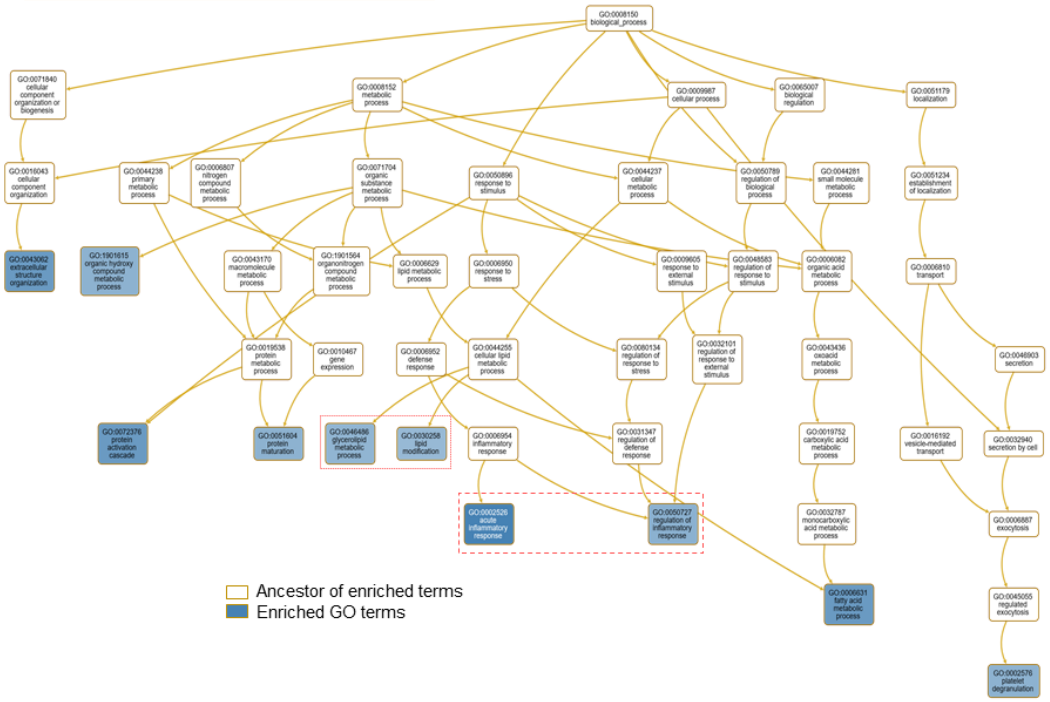

C. [siApoA1] ∩ [BAF] ∩ [siApoA1+BAF] *up*

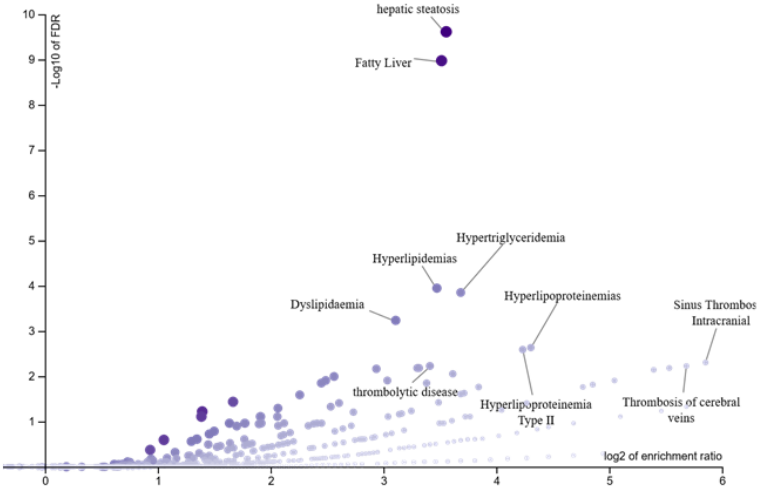

Figure 4.14. The intersection of transcriptomes of transcriptomes of ApoA-I-depleted, autophagy-inhibited and dually ApoA-I-depleted and autophagy-inhibited HepG2 cells is enriched for upregulated genes related to lipid metabolic processes and inflammatory responses.
(A) Venn diagram denoting upregulated genes upon ApoA-I-depletion (siApoA1), autophagy-inhibition (BAF) and dually ApoA-I depleted and autophagy-inhibited (siApoA1+BAF) HepG2 cells and functional enrichment analysis of gene ontology biological processes (FDR<$5x10^{-11}$) of their intersection. (B) Inter-relationship of GO processes associated with upregulated genes that intersect transcriptomes of ApoA1-depletedt (siApoA1), autophagy-inhibited (BAF) and dually ApoAI-depleted and autophagy-inhibited (siApoA1+BAF) HepG2 cells. Note that the biological processes associated with this condition cluster around cellular lipid metabolic processes and inflammatory response (dotted boxes). (C) Volcano plot displaying diseases predicted to be associated with the profile of upregulated genes of the aforementioned intersection.

4.2.3 The transcriptome of HepG2 hepatoma cells depleted for ApoA-I is enriched for downregulated genes related to cell cycle and survival processes.

Analysis of the 426 genes that were found downregulated upon *ApoA1* knock-down were associated with biological processes linked to cell cycle and rRNA processing. (FDR<$5x10^{-11}$)(Fig. 4.15 A), with their inter-relationships clustering around ribosome metabolism and the control of cell cycle (Fig.4.15B). Volcano plot representation of diseases predicted to be associated with this expression profile suggested an enrichment pertinent to *cancer* and *shock* (Fig. 4.15C).

The intersection of commonly downregulated genes in all three conditions, namely, ***i.*** BAF treatment (BAF), ***ii.*** *ApoA1* knock-down (siApoA1), ***iii.*** *ApoA1* knock-down and BAF treatment (siApoA1+ BAF) identified 172 genes, while enrichment analysis revealed associations with GO biological processes linked to cell cycle control (Fig. 4.16A). The inter-relationship of GO processes associated with downregulated genes that intersect transcriptomes of ApoA-I-depleted, autophagy-inhibited and dually ApoA-I depleted and autophagy-inhibited HepG2 cells cluster around *modulation of cell cycle* and *nucleic acid metabolism* (Fig. 4.16B). The diseases predicted to be associated with the profile of the intersection of downregulated genes are neoplastic diseases, cancer and shock (Fig. 4.16C).

Collectively, these data underscore a major intracellular role of ApoA-I in the regulation of lipid metabolism and a putative protective function in liver diseases associated with increased lipid load, such as steatosis and fatty liver disease. Interestingly, these metabolic conditions often predispose to malignant conditions like HCC, as the increased lipid load fosters tumor growth. Indeed, ApoA-I depletion is not only associated with upregulated lipid and cholesterol metabolism genes but also with perturbed cancer-associated gene expression profile.

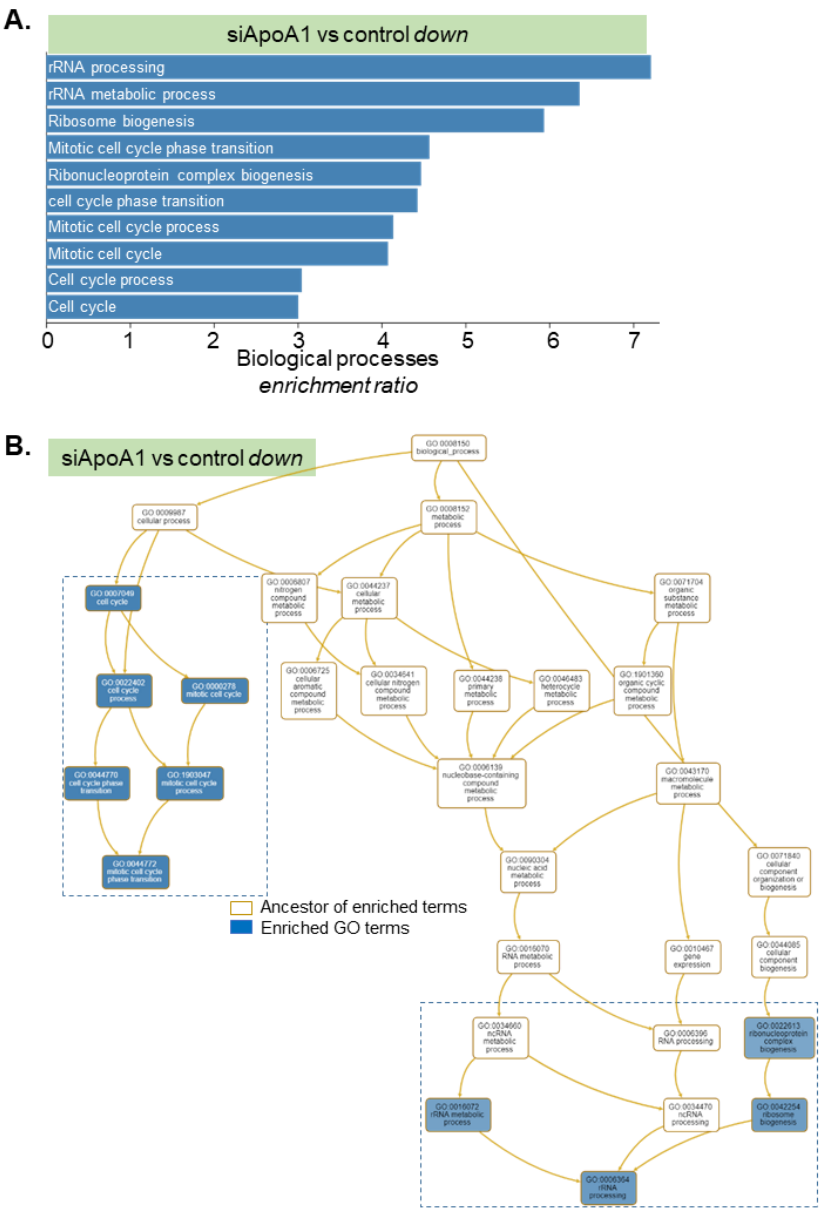

Fig 4.15. The transcriptome of HepG2 hepatoma cells depleted of ApoA-I is enriched for downregulated genes related to cell cycle and rRNA processes.
(A) Functional enrichment analysis of gene ontology biological processes (FDR<5x10^{-11}) in *ApoA1* siRNA-transfected *versus* control HepG2 cells. (B) The inter-relationships of GO biological processes derived from the transcriptome of HepG2 hepatoma cells depleted of ApoA-I. Each enriched Gene Ontology (GO) is shown as blue-colored rectangular and their ancestors as white. Note that the biological processes associated with this condition cluster around cell cycle ans rRNA processes (dotted boxes). (C) Volcano plot displaying diseases predicted to be associated with the profile of downregulated genes.

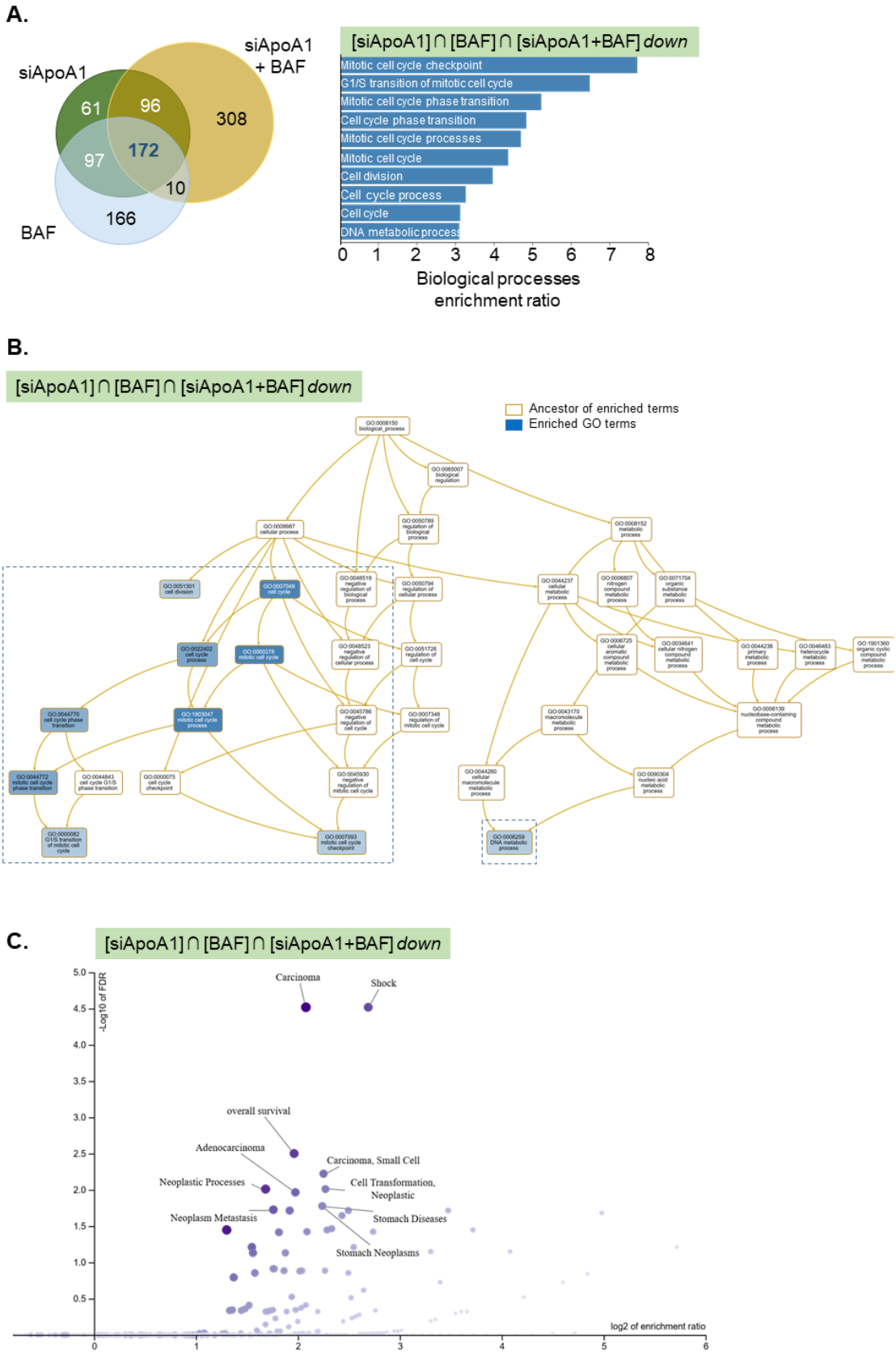

Figure 4.16. The intersection of transcriptomes of transcriptomes of ApoA-I-depleted, autophagy-inhibited and dually ApoA-I-depleted and autophagy-inhibited HepG2 cells is enriched for downregulated genes related to cell cycle and nucleic acid metabolism. (A) Venn diagram denoting

downregulated genes upon ApoA-I-depletion (siApoA1), autophagy-inhibition (BAF) and dually *ApoA-I-depleted* and autophagy-inhibited (siApoA1+BAF) HepG2 cells and functional enrichment analysis of gene ontology biological processes (FDR<$5x10^{-11}$) of their intersection. (B)The inter-relationship of GO processes associated with downregulated genes that intersect transcriptomes of ApoA-I-depleted (siApoA1), autophagy-inhibited (BAF) and dually *ApoA-I-depleted* and autophagy-inhibited (siApoA1+BAF) HepG2 cells. Each enriched Gene Ontology (GO) is shown as blue-colored rectangular and their ancestors as white. Note that the biological processes associated with this condition cluster around modulation of cell cycle and nucleic acid metabolism (dotted boxes).(C) Volcano plot displaying diseases predicted to be associated with the profile of the downregulated genes of the aforementioned intersection.

4.2.4 ApoA-I impacts on lipid metabolism by regulating cholesterol and lipid synthesis gene expression upon autophagic inhibition.

Prompted by the results of the bioinformatic analysis we proceeded to validate initially the transcriptional expression of genes related to cholesterol and lipid biosynthesis. We tested the mRNA levels of 3-hydroxy-3-methylglutaryl-CoA reductase (*HMGCR*), 3-hydroxy-3-methylglutaryl-CoA synthase 1 (*HMGCS1*), low density lipoprotein receptor (*LDLR*) and mevalonate diphosphate decarboxylase (*MVD*) which are linked to cholesterol synthesis, and of lipin 1 (*LPN1*), fatty acid synthase (*FASN*), acetyl-CoA carboxylase alpha (*ACACA*) and stearoyl-CoA desaturase (*SCD*) genes which are associated with fatty acid and lipid synthesis using HepG2 cells transiently transfected with siApoA1 or control siLuc, cultured in the presence or absence of BAF. We found that whereas the knock-down of *ApoA1* (siApoA1) or treatment with BAF alone partially increased their expression, the combination of *ApoA1* knock-down and BAF led to a dramatic increase in their mRNA levels (Fig. 4.17A). We also validated the expression of cell death-inducing DNA fragmentation factor alpha-like effector c (*CIDEC*; also known as FSP27 or fat-specific protein 27). Several studies have showed that CIDEC is highly induced in steatotic liver where its expression correlates with increased lipid load, while its overexpression promotes both the accumulation and an increase in the size of LDs in multiple cell types (175-180). We found that *CIDEC* expression is highly induced (>4 folds) by *ApoA1* knock-down but not with BAF treatment, supporting a role of ApoA-I in the modulation of LD homeostasis and lipid metabolism (Fig. 4.17A). We also assayed phosphoenolpyruvate carboxykinase 1 (*PCK1*)

mRNA expression, a glyconeogenesis-related gene, as a control, and found that its expression remained unaffected by *ApoA1* knock-down and/or BAF treatment (Fig. 4.17A).

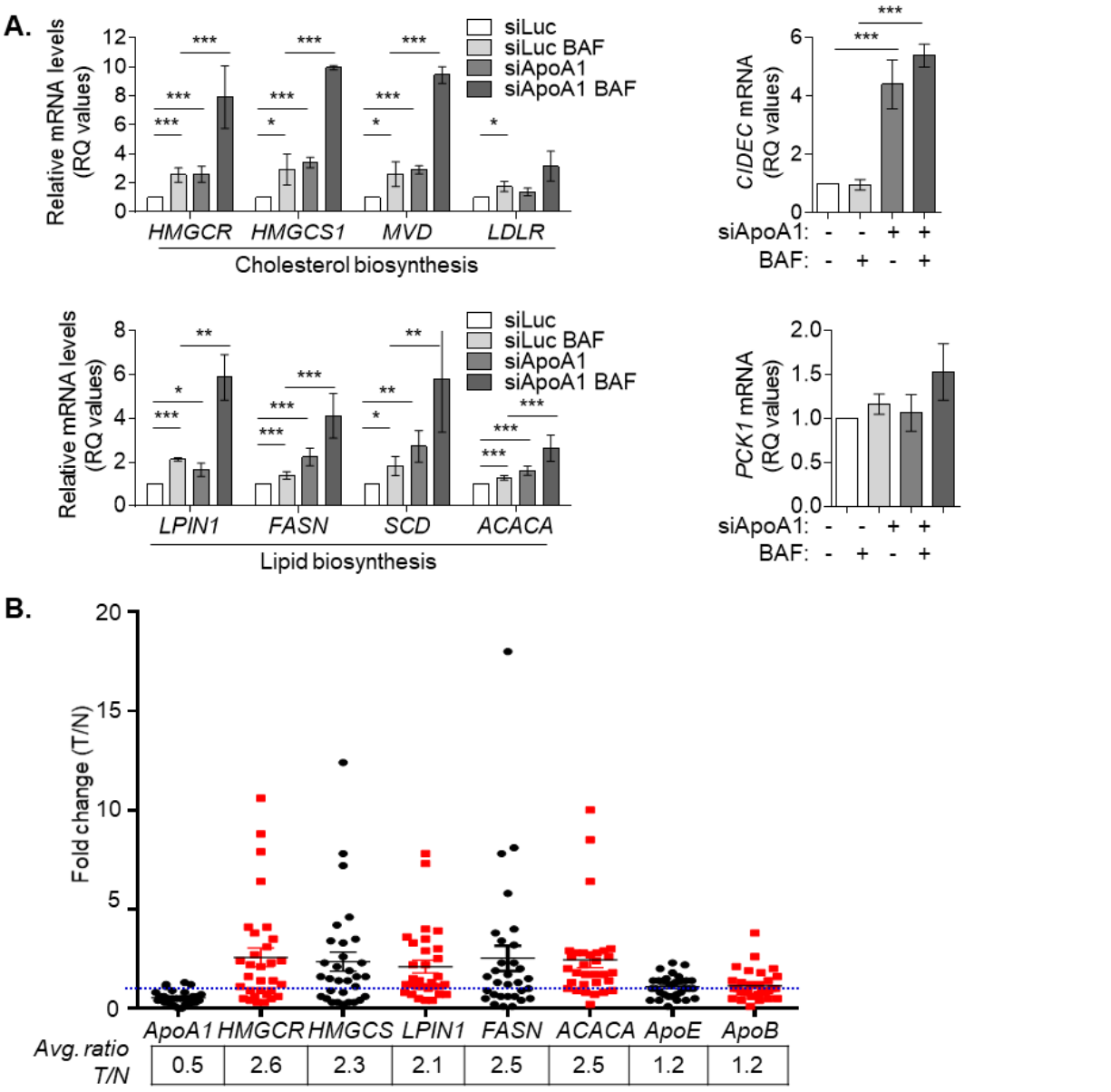

Figure 4.17. ApoA-I inversely correlates with cholesterol and lipid synthesis gene expression. (A) Relative mRNA expression levels of the indicated genes assessed by q-PCR analysis of HepG2 cells transfected with siRNA targeting *ApoA1* (siApoA1) or control siRNA against Luciferase (siLuc) cultured in the presence or absence of BAF. RQ values are expressed relative to untreated control HepG2 cells (siLuc) which were given the arbitrary value of 1. mRNA expression levels were normalized to the housekeeping β-actin gene (data are expressed as the mean ± SD of at least 3 experiments, **p*<0.05, ***p*<0.01, ****p*<0.001). (B) Mining of RNAseq data comparing 31 HCC and normal liver tissue from the same patients, registered in the ChNPP database, demonstrates reverse correlation between ApoA1 (but not ApoE or ApoB), and lipid/cholesterol biosynthesis gene mRNA expression. The average fold change of gene expression is shown below the graph.

Next, we addressed the relevance of these *in vitro* observations to human HCC, by performing mining of RNAseq data deposited in the ChNPP database. This database contains whole genome mRNA transcriptome data from malignant *versus* normal liver tissue from the same patients. Our *in silico* analysis showed significant reduction in the expression of *ApoA1* in the tumors by approximately 50%, whereas *ApoB* or *ApoE* levels did not differ between normal and tumor tissue (Fig. 4.17B). Therefore, HCC, a malignancy associated with deregulated autophagy and lipid accumulation, also displays reduced *ApoA1* mRNA levels.

Conversely, the expression of *HMGCR*, *HMGCS1*, *LPIN1, FASN* and *ACACA* genes were found increased by more than 2-fold in the malignant *versus* normal tissue (Fig. 4.17B). We conclude that *ApoA1* expression reversely correlates with the expression of cholesterol and lipid synthesis-related genes, similar to our *in vitro* observations in HepG2 cells. This finding supports the validity of our experimental cellular model in which *ApoA1* expression is modulated by RNAi, and its suitability in mimicking physiological and pathogenic human liver conditions. Importantly, the inverse correlation between the expression of *ApoA1* and that of lipid and cholesterol biosynthetic genes in HCC further suggests that intracellular ApoA-I may serve as a barrier to lipid overload and concomitant cancer progression.

4.2.5 Autophagy inhibition modulates lipid synthesis gene expression through SREBP2.

To identify transcriptional factors that may mediate the effect of ApoA-I and BAF on these genes, we initially examined the protein expression and cellular localization of the master transcription factor SREBP2. More specifically, we transiently transfected HepG2 with siApoA1 or control siLuc followed by culture in the presence or absence of BAF, and isolated the membrane (ME: membrane extract) and nuclear (NE: nuclear extract) protein fractions. ME and NE were next immunoblotted for SREBP2, as well as HSP90 and SP1 that served as controls of purity and equal loading. We found that autophagy inhibition with BAF impacts on the cleavage of SREBP2 in the membrane compartment, documented by the increased levels of the cleaved form of the protein (C) in both the membrane and the nuclear extract (Fig. 4.18A). As expected, SREBP2 was not detected in the cytoplasmic soluble protein extract (Fig. 4.18B) in control condition or following BAF treatment. *ApoA1* knock-down did not modify the precursor

(P) or cleaved (C) SREBP2 protein levels in the membrane or nuclear fraction and the combination treatment did not alter SREBP2 expression more that BAF alone, suggesting that the effect of ApoA-I on lipid and cholesterol gene expression is mediated by a mechanism that does not involve SREBP2 (FIG. 4.18A).

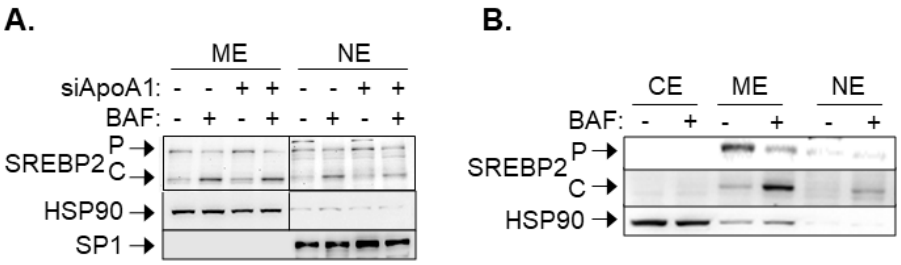

Figure 4.18. Autophagy inhibition but not ApoA-I regulates SREBP2 transcriptional activity on lipogenic genes by affecting its proteolytic cleavage.
Representative immunoblot analysis of (A) membrane (ME) and nuclear (NE) protein extracts of HepG2 cells transfected with siRNA targeting *ApoA1* (siApoA1) or control siRNA against Luciferase (siLuc) cultured in the presence or the absence of BAF and (B) cytoplasmic (CE), membrane (ME) and nuclear (NE) protein extracts of HepG2 cells cultured in the presence or the absence of BAF.P and N designate the precursor and nuclear/active form of SREBP2 respectively. The HSP90 and transcription factor SP1 were used as markers for the purity and the equal loading of the membrane and nuclear extracts, respectively.

4.2.6 Intracellular ApoA-I regulates lipid synthesis gene expression by impacting on FOXO activity through Akt phosphorylation.

We next assessed the phosphorylation of FOXO1/3 upon the same conditions. We observed a slight reduction of phosphorylated FOXO1/3 (p FOXO1/3) levels upon BAF treatment which was associated with ApoA-I accumulation (Fig.4.19A). Interestingly, knock-down of *ApoA1* lead to a dramatic increase in FOXO1/3 phosphorylation. As FOXOs transcription factors are phosphorylated by activated Akt, we next examined Serine 473 (Ser^{473}) and Threonine 308 (Thr^{308}) phosphorylation of Akt using immunoblot of cell lysates isolated under the same conditions. *ApoA1* knock-down resulted in a significant increase of Akt phosphorylation at Ser^{473} but not of Thr^{308} (Fig. 4.19A-B), and this increase was not affected by autophagy inhibition (Fig. 4.19A). We next examined cytoplasmic (CE) *versus* membrane extracts (ME) for Akt phosphorylation in HepG2 cells transiently transfected with siApoA1 or control siLuc cultured in the presence or absence of BAF. Autophagic inhibition by BAF, which associates with elevated

ApoA-I levels, caused reduction in phosphorylated Akt (pAkt) at Ser^{473}in both cytoplasmic and membrane extracts. Knock-down of *ApoA1* lead to a dramatic increase in Akt phosphorylation at Ser^{473} in the membrane fraction (Fig. 4.19C). However significant differences were also observed in p-Akt (Ser^{473}) levels at the cytoplasmic fraction, where total Akt1 is predominantly expressed (Fig. 4.19C). *ApoA1* knock-down did not significantly affect the expression levels of total Akt1 in the cytoplasmic or membrane fraction. As expected, total Akt1 was found predominantly in the cytoplasmic fraction, but low levels of the protein were also detected at the membrane fraction. HSP90 and GAPDH were used as loading controls and markers of the isolation purity of the fractions (Fig. 4.19C).

A number of control experiments were performed to validate Akt phosphorylation by *ApoA1* knock-down; First, we transiently transfected HepG2 cells with two independent siRNAs targeting different regions of *ApoA1* gene and found that the levels of pAkt increased in both cases and independently of the targeted sequence (Fig. 4.19D). Second, we transfected HEK293T cells - which do not express endogenous *ApoA1*- with siApoA1 and assayed by immunoblot protein lysates for pAkt. The results showed absence of an effect on pAkt (Fig. 4.19E). Third, we observed that unlike Akt phosphorylation, *ApoA1* knock-down in HepG2 did not affect JNK or ERK1/2 phosphorylation, supporting the specificity of the effect on Akt (Fig. 4.19F). Finally, we tested the possibility that Akt phosphorylation may be caused by soluble factors released by knock-down of *ApoA1*, rather that by the ApoA1 knock-down itself. To test this possibility we exposed HepG2 cells transfected with control siRNA (siLuc) to supernatant from cells that were transiently transfected with siApoA1. We did not observe any pAkt induction in control cell cultures cultured with supernatant isolated from siApoA1-transfected cultures (Fig. 4.19G). Conversely, treatment of HepG2 cells with recombinant ApoA-I (rApoA-I) did not affect Akt or FOXO1/3 phosphorylation (Fig. 4.19H), further supporting that is an intracellular signaling event that triggers Akt phosphorylation by *ApoA1* knock-down. Next we were interested to examine whether *ApoA1* knock-down-induced Akt phosphorylation has a generalized effect and could potentially act by enhancing signals derived from independent pathways that converge to Akt phosphorylation and are implicated in survival and inflammation. To this end we treated

HepG2 cells transiently transfected with siApoA1 with insulin (INS) or Tumor necrosis factor alpha (TNF-α). We found that knock-down of *ApoA1* augments INS and TNF-induced Akt phosphorylation at Ser^{473} (Fig. 4.19H-I). The fact that ApoA-1 knock-down amplifies Akt signaling after insulin or TNF-a stimuli support that may also affect metabolic and inflammatory pathways in an autonomous manner.

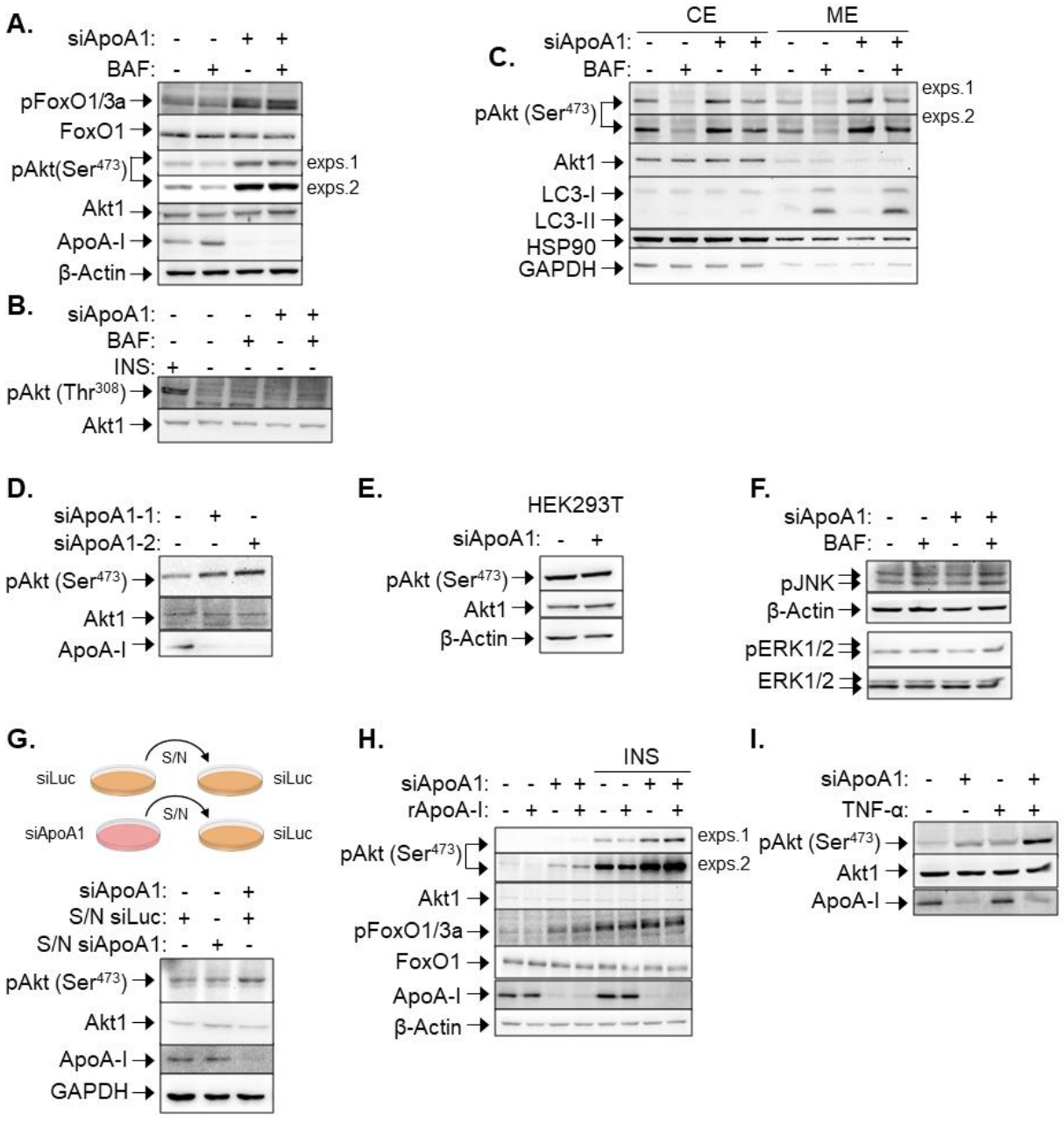

Figure 4.19. Intracellular ApoA-I regulates FOXO1/3 activity by modulation of Akt phosphorylation. (A-B) Representative immunoblot analysis of protein lysates of HepG2 cells transiently transfected with siRNA targeting *ApoA1* (siApoA1) or control siRNA against Luciferase (siLuc) cultured in the presence or the absence of BAF. (A) Total (Akt1) and phosphorylated levels of Akt at Serine 473 [pAkt (Ser^{473})] and FOXO1/3 are shown. (B) Total (Akt1) and phosphorylated levels of Akt at Threonine 308 (Thr^{308}) are

shown. Lysate of HepG2 cells exposed to 100mM insulin (INS) for 1h was used as positive control for Akt phosphorylation. (C) Immunoblot analysis of cytoplasmic (CE) and membrane (ME) extracts of HepG2 cells transiently transfected with siRNA targeting *ApoA1* (siApoA1) or control siRNA against Luciferase (siLuc) cultured in the presence or the absence of BAF. Total and phosphorylated levels of Akt at Ser^{473} are represented. Changes in LC3-II levels are indicative of autophagic inhibition by BAF. HSP90 and GAPDH were used as loading controls and markers of the purity of the extracts. (D) Representative immunoblot analysis for total (Akt1) and phosphorylated Akt at Ser^{473} [pAkt (Ser^{473})] of protein lysates of HepG2 cells with two independent siRNAs targeting different regions of *ApoA1* gene. (E) Representative immunoblot analysis for total (Akt1) and phosphorylated Akt [pAkt (Ser^{473})] at Ser^{473} of protein lysates from HEK293T cells transiently transfected with with siRNA targeting *ApoA1* (siApoA1) or control siRNA against Luciferase (siLuc). (F) Representative immunoblot analysis for phosphorylated levels of Junk (pJNK) and ERK1/2 (pERK1/2) of protein lysates of HepG2 cells transiently transfected with siRNA targeting *ApoA1* (siApoA1) or control siRNA against Luciferase (siLuc) cultured in the presence or the absence of BAF. Total levels of ERK1/2 were used as loading control of pErk1/2. (G) Representative immunoblot analysis for total (Akt1) and phosphorylated Akt at Ser^{473} [pAkt (Ser^{473})] of protein lysates of HepG2 cells transfected with control siRNA (siLuc) and exposed to supernatant from cells that were transiently transfected with siApoA1 or control siLuc. Lysates of HepG2 cells transfected with siApoA1 and cultured in siLuc supernatant were used as positive control of pAkt (Ser^{473}). The procedure is depicted by graphical representation. (H) Representative immunoblot analysis of protein lysates of HepG2 cells transiently transfected with siRNA targeting *ApoA1* (siApoA1) or control siRNA against Luciferase (siLuc) cultured in the presence or the absence of 15 μg/ml recombinant ApoA-I (rApoA-I) for 6 hrs and/or treated with 100 mM insulin (INS) for the last 1 h of culture. Total (Akt1) and phosphorylated levels of Akt at Serine 473 [pAkt (Ser^{473})] and FOXO1/3 (p FOXO1/3) are showned. (I) Representative immunoblot analysis for total and phosphorylated Akt at Ser^{473} of protein lysates of HepG2 cells transiently transfected with siRNA targeting *ApoA1* (siApoA1) or control siRNA against Luciferase (siLuc) cultured in the presence or the absence of 50ng/ml TNF-α for 15 minutes. The efficiency of *ApoA1* knock-down was evaluated by ApoA-I immunoblotting. β-Actin and GAPDH were used as loading controls. A high and a low exposure (exps) were selected to be presented for best representation is some cases.

4.2.7 ApoA-I physiologically functions to suppress Akt phosphorylation and activity by mTORC2 signaling modulation.

Akt phosphorylation at Ser^{473} is regulated by mTORC2. TNF and INS, which amplify siApoA1-driven Akt phosphorylation, also induce mTORC2 activation. We thus proceeded to assess the involvement of mTORC2 in siApoA1-induced Akt phosphorylation. To this end, we knocked-down Rictor which is an essential component of mTORC2, in the presence or absence of *ApoA1* knock-down. Lysates were analyzed by immunoblot for the expression of pAkt and p FOXO1/3, and for RICTOR to verify the efficiency of the knock-down. The results showed that knock-down of Rictor efficiently abolished siApoA1-induced FOXO1/3 and Akt phosphorylation (Fig. 4.20A). Similarly, treatment of HepG2 cells that were knocked-down for *ApoA1* with Torin2 also led to amelioration of Akt phosphorylation at Ser^{473} (Fig. 4.20B). To verify the functional role of mTORC2-Akt- FOXO pathway in the regulation of cholesterol-related gene expression we

transfected HepG2 cells with siApoA1 or control siRNA followed by Torin2 treatment and assayed with q-PCR the mRNA levels of cholesterol synthesis-related genes. The siApoA1-mediated increase in *HMGCR* and *HMGCS1* gene expression was suppressed by blockade of mTORC2 activity. We conclude that ApoA-I physiologically functions to suppress Akt phosphorylation and activity by mTORC2 signaling modulation (Fig. 4.20C).

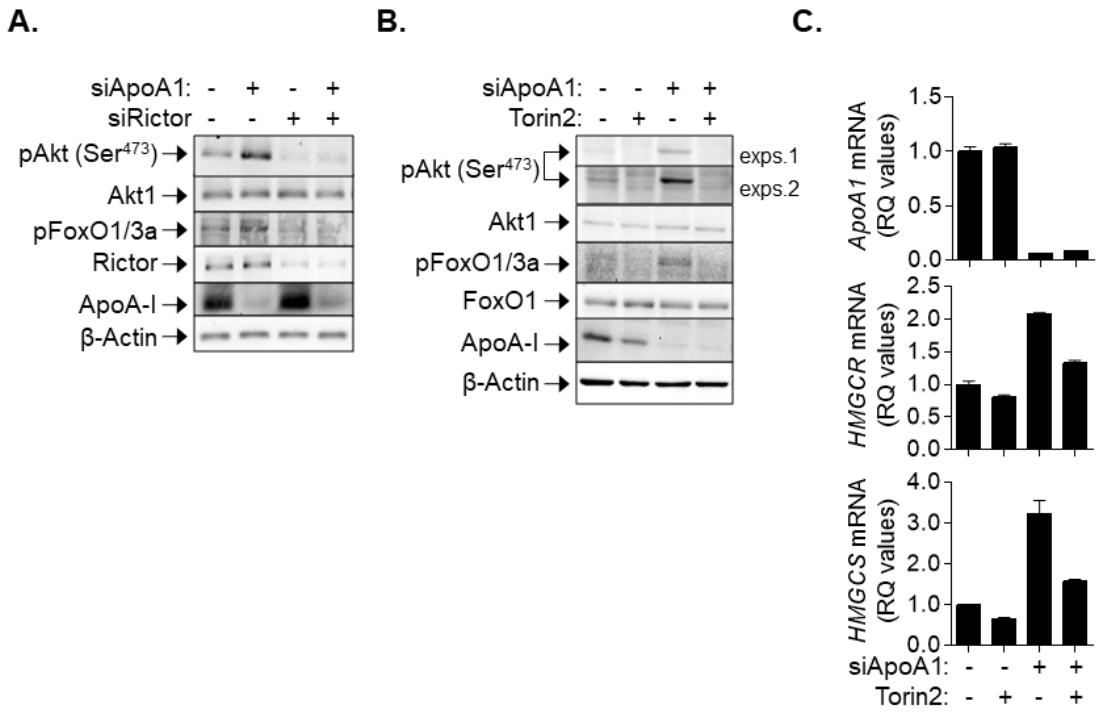

Figure 4.20. *ApoA1* knock down-induced Akt phosphorylation and regulation of cholesterol synthesis gene expression is mediated by mTORC2 signaling.
(A) Representative immunoblot analysis of lysates from HepG2 cells transiently transfected with siRNA targeting *ApoA1* (siApoA1) and/or mTORC2 subunit Rictor (siRictor) and/or control siRNA (siLuc).
(B) Representative immunoblot analysis of protein lysates of HepG2 cells transiently transfected with siRNA targeting *ApoA1* (siApoA1) or control siRNA against Luciferase (siLuc) cultured in the presence or the absence of 250 nm Torin2 for 6 hrs. Total (Akt1 and FOXO1 respectively) and phosphorylated levels of Akt at Serine 473 [pAkt (Ser^{473})] and FOXO1/3 (p FOXO1/3) are represented. Two different exposures (exps) are shown for the pAkt (Ser^{473}) immunoblot. The efficiency of *ApoA1* and *Rictor* knock-down was evaluated by ApoA-I and Rictor immunoblotting, respectively. β-Actin was used as loading control. (C) Representative graph of mRNA expression levels of the *ApoA1*, *HMGCR* and *HMGCS1* genes as revealed by q-PCR analysis of HepG2 cells transfected with siRNA targeting *ApoA1* (siApoA1) or control siRNA against Luciferase (siLuc) cultured in the presence or absence of Torin2. RQ values are expressed relative to untreated control HepG2 cells (siLuc) which were given the arbitrary value of 1. mRNA expression levels were normalized to the housekeeping β-actin gene.

4.2.8 ApoA-I physically interact with Akt.

On the basis of the aforementioned functional studies we examined whether ApoA-I physically interacts with the Akt signaling complex by co-immunoprecipition experiments following ectopic expression of the proteins in HEK293T cells. In detail, we initially transfected HEK293T cells with ApoA-I expression vector (pAd-ApoA1) or/and HA-tagged Akt1 or Akt2. HA antibody (α-HA) was used to precipitate Akt1 or Akt2 from total protein cell lysates and putative interaction was evaluated with immunoblot against ApoA-I. We found that HA-Akt1 and Akt2 were co- immunoprecipitated from total protein lysates with ApoA-I, supporting a putative direct physical and functional interaction of ApoA-I with Akt (FIG. 4.21). Future experiments are aiming to examine putative physical interaction of endogenous proteins and to identify the Akt domain that interacts with ApoA-I. We hypothesize that ApoA1-Akt interaction may interrupt Akt-mTORC2 interaction and may function antagonistically with mTORC2 for Akt binding. To address this hypothesis we aim to use Akt deletion mutants and perform a series of co-immunoprecipitation experiment in different conditions in order to determine interactions of Akt-ApoA-I with key protein interactors of the mTORC2 complex such as RICTOR or SIN1.

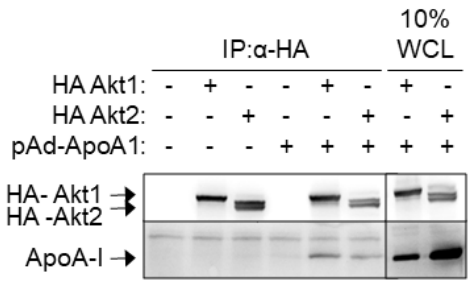

Figure 4.21. ApoA-I physically interacts with Akt. Representative immunoblot analysis of lysates from HEK293T cells transfected with ApoA-I expression vector (pAd-ApoA1) and/or HA-taggedAkt1 and Akt2. HA was immunoprecipitated (IP) from total protein lysates and HA-bound ApoA-I was detected by immunoblotting with anti-ApoA-I. Akt immunoblot confirmed transfection and IP efficiency. Ten percent of membrane protein lysate (input) was also immunoblotted.

4.2.9 ApoA-I impacts cell death.

Activation of Akt has been involved in protection from cell death. As ApoA-I negatively regulates Akt phosphorylation, we surmised that intracellular ApoA-I may impact apoptotic processes beyond its effects on lipid and cholesterol metabolism. In line with this notion, the knock-down of *ApoA1* in HepG2 cells led to a transcriptional signature enriched for genes involved in ribosome biogenesis-related processes (Fig. 4.15A). Impairment of ribosomal

biogenesis can activate p53 and cell death independently of DNA damage. We thus tested the effect of 5-fluorouracil (5-FU), an inhibitor of ribosome biogenesis, on HepG2 cell survival following *ApoA1* knock-down. As shown in Figure 4.22, *ApoA1*-depleted HepG2 cells displayed increased survival following exposure to 5-FU compared to control cultures, with an IC50 of 140 *versus* 803 µM in siApoA1 and siLuc-transfected HepG2 cells, respectively.

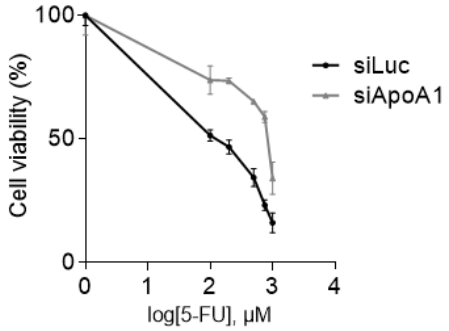

Figure 4.22. *ApoA1* knock-down confers resistance to 5-FU induced toxicity.
Cell viability measured by the MTT assay of HepG2 cells transiently transfected with siRNA targeting *ApoA1* (siApoA1) or control siRNA against Luciferase (siLuc) exposed to various concentration of 5-FU for 72h. Cell viability is expressed % relative to untreated controls and 5-FU concentrations as log values.

4.2.10 ApoA1 depletion confers resistance to lipotoxicity and attenuates ER-stress gene expression.

Excessive accumulation of lipids may also trigger cell death, a process termed lipotoxicity. In light of the increased accumulation of LDs in ApoA-I-depleted HepG2 cells, we asked if ApoA-I may also impact lipotoxicity. To this end, siApoA1 and siLuc-transfected HepG2 cells were cultured in the presence of BSA-conjugated palmitic acid (PA) or BSA as control. MTT assays were used to assess cell survival. The results (Fig. 4.23A), showed that the knock-down of *ApoA1* provided a survival advantage to HepG2 cells exposed to high concentrations of PA.

Lipotoxicity is causally linked to ER stress. Exposure of HepG2 hepatoma cells to PA has been shown to reduce viability through exaggerated ER stress and, conversely, attenuation of ER stress was found to suppress PA-induced cell death. On the basis of these observations, we examined the impact of ApoA-I ablation on PA-induced ER stress by quantifying the mRNA levels of *HSPA5* (also known as *BiP* or *GRP78*) and *DDIT3* (also known as *GADD153* or *CHOP*), which are involved in the apoptotic response to ER stress. As shown in Figure 4.23B, the expression of both ER markers was elevated upon exposure to high concentrations of PA.

Whereas *ApoA1* knock-down did not significantly affect basal *HSPA5* and *DDIT3* mRNA levels, it markedly reduced the PA-triggered induction of their expression (Fig. 4.23B).

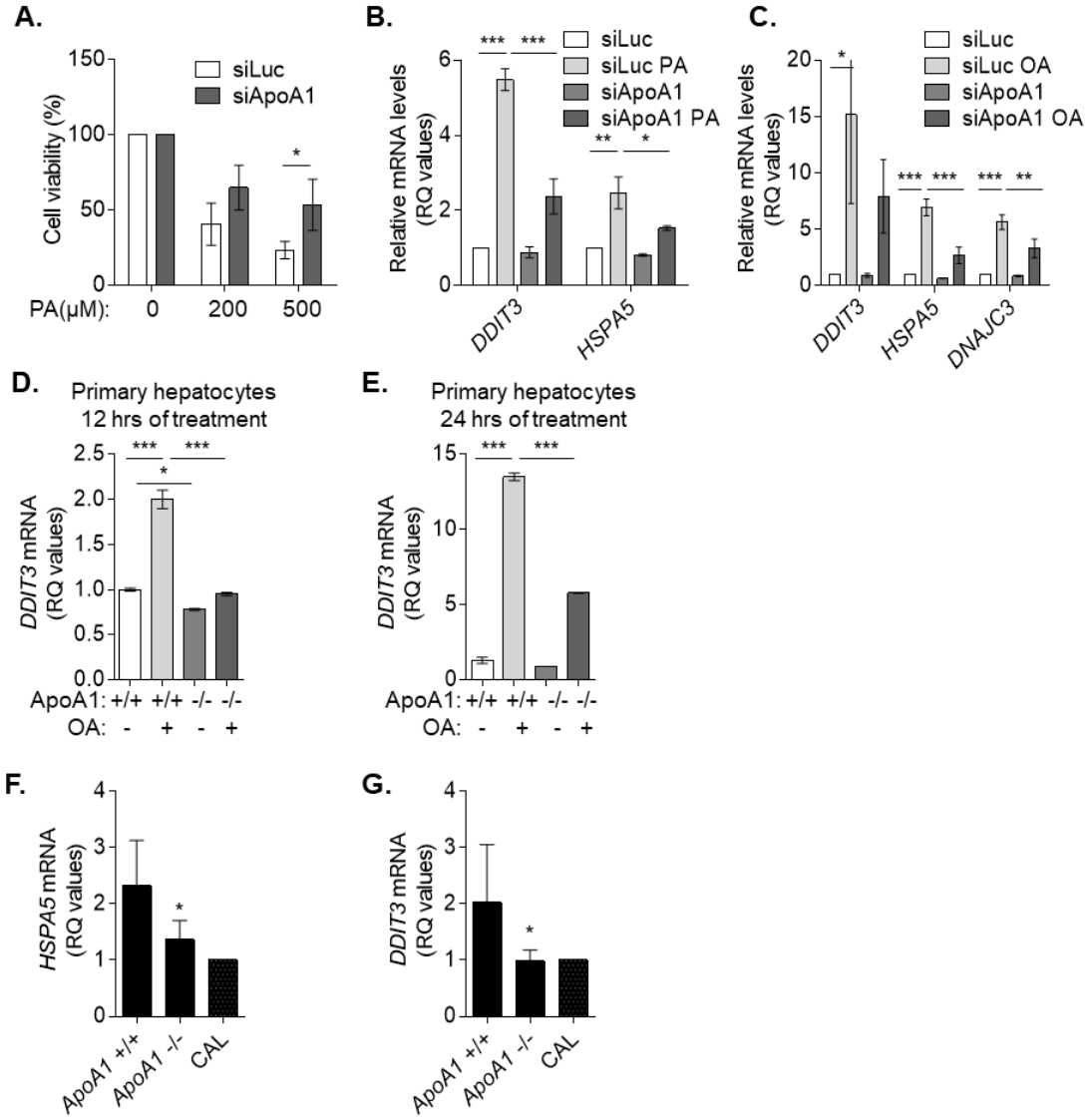

Figure 4.23. ApoA1 depletion confers resistance to lipotoxicity and attenuates ER-stress gene expression.

(A) Cell viability measured by the MTT assay of HepG2 cells transiently transfected with siRNA targeting *ApoA1* (siApoA1) or control siRNA against Luciferase (siLuc) exposed to 200 or 500 μM palmitic acid (PA) or remained untreated for 72h. Cell viability is expressed % relative to untreated controls (data are expressed as the mean ± SD of at least 3 experiments, **p*<0.05). (B-C) Relative mRNA expression levels of the indicated genes as assessed by q-PCR analysis of HepG2 cells transfected with siRNA targeting *ApoA1* (siApoA1) or control siRNA against Luciferase (siLuc) cultured in the presence or absence of (A) 250 μM palmitic acid (PA) and (B) 500 μM oleic acid (OA) for 24 hrs. RQ values are expressed relative to untreated control HepG2 cells (siLuc) which were given the arbitrary value of 1. mRNA expression levels were normalized to the housekeeping β-actin gene (data are expressed as the mean ± SD of at least 3 experiments, **p*<0.05, ***p*<0.01, ****p*<0.001). (D-E) Relative mRNA expression levels of *DDIT3* as revealed by qPCR analysis of mouse primary hepatocytes isolated by wild type (+/+) or ApoA1 deficient (ApoA-I -/-) animals that were cultured in the presence or absence of 500 μM OA for (D) 12 hrs or (E) 24 hrs. RQ values are expressed relative to an independent control that was used as calibrator (CAL) which

was given the arbitrary value of 1. mRNA expression levels were normalized to the housekeeping β-actin gene (data are expressed as the mean ± SD of 2 experiments, *p<0.05, ***p<0.001). (F-G) Relative mRNA expression levels of *HSPA5* and *DDIT3* as revealed by qPCR analysis of liver lysates isolated by wild type (+/+) or *ApoA1* deficient (ApoA-I -/-). RQ values are expressed relative to an independent control that was used as calibrator (CAL) which was given the arbitrary value of 1. mRNA expression levels were normalized to the housekeeping β-actin gene (data are expressed as the mean ± SD of 7 mice of each group, *p<0.05).

We also tested the ApoA-I effect on ER stress induced by high concentrations of the unsaturated fatty acid, oleic acid (OA). Similar to PA, exposure of HepG2 cells to OA up-regulated the expression of *DDIT3*, *HSPA5* and *DNAJC3* but knock-down of *ApoA1* reduced this effect by more than 50% (Fig. 4.23C). Similar results were obtained when hepatocytes from *APOA1*$^{+/+}$ and *APOA1*$^{-/-}$ mice were cultured for 12 or 24 hrs in the presence of OA; hepatocytes lacking ApoA-I displayed a marked reduction in OA-induced up-regulation of *DDIT3* (Fig. 4.23D-E). We note, however, that unlike *ApoA1* knock-down in HepG2 hepatoma cells, both *ex vivo* cultured normal hepatocytes (Fig. 4.23D-E) and liver tissue (FIG. 4.23F-G) from *APOA1*$^{-/-}$ mice were found to express reduced basal levels of *DDIT3* and *HSPA5*.

4.2.11 Discussion (chapter 2)

ApoA-I has attracted significant attention ever since it was identified as a major protein component of HDL. As such, ApoA-I has been extensively studied in the context of HDL-mediated reverse cholesterol transfer. Recent studies have expanded the extracellular roles of ApoA-I and HDL to include a broad spectrum of anti-thrombotic, antioxidative, anti-inflammatory and immune-regulatory properties. However, putative intracellular functions of ApoA-I remain unknown. We have herein addressed this unanswered question and disclosed important cellular and molecular pathways and processes influenced by endogenous ApoA-I in hepatocytes.

We were intrigued by the observations that, (1) suppression of autophagy leads to accumulation of large size LD *in vitro* and steatosis *in vivo*; (2) ApoA-I ablation in HFD-fed mice results in steatosis; and (3) ApoA-I accumulates in response to inhibition of autophagy, and hypothesized that intracellular ApoA-I may physiologically function to suppress lipid and cholesterol overload under conditions of autophagy blockade. Indeed, we found that the knock-down of *ApoA1* in the hepatoma cell line HepG2 resulted in the accumulation of large size LDs,

an effect that was amplified upon simultaneous inhibition of autophagy by BAF. Thus, *in vitro* ApoA-I depletion under conditions of autophagy blockade leads to marked accumulation of large size LDs, compared to either treatment alone. However, although autophagy inhibition leads to ApoA-I accumulation, we have found that *ApoA1* depletion does not influence autophagic flux. This finding suggests that ApoA-I functions independently of autophagy to suppress intracellular lipid and cholesterol levels (Fig. 4.12).

Using a hypothesis-free approach that entails the unbiased interrogation of the transcriptome of ApoA-I depleted HepG2 cells, we identified enrichment of biological processes linked to lipid and cholesterol metabolism and an association with fatty liver and metabolic diseases. Interestingly, a significant number of genes related to cholesterol and lipid biosynthesis were commonly up-regulated by autophagy blockade and ApoA-I depletion which, when combined, led to a marked increase in metabolic gene expression compared to either treatment alone (Fig. 4.13-4.14). These observations align with the LD accumulation (Fig.4.12A) ensued by these treatments and indicate that intracellular ApoA-I and autophagy converge to transcriptionally control *de novo* lipid and cholesterol biosynthesis.

Are these findings relevant to human disease? We addressed this question by performing mining of HCC RNAseq data deposited in the ChNPP database. The strength of this database is that it compares expression between normal and malignant liver tissue for each individual. Our analyses showed that *ApoA1* but not *ApoB* or *ApoE* mRNA levels are markedly reduced in HCC whereas expression of *HMGCR, HMGCS, FASN, LPIN1* and *ACACA* was up-regulated by more than 2-fold. Therefore, similar to the results in HepG2 cells, the down-regulation of *ApoA1* is associated with over-expression of lipid and cholesterol biosynthesis genes (Fig4.17).

SREBP2 and FOXO1/3 are major regulators of cholesterol and lipid biosynthesis gene expression. We have found that inhibition of autophagy by BAF affects SREBP2 but not FOXO1/3, whereas the RNAi-mediated depletion of *ApoA1* leads to marked phosphorylation of FOXO1/3 but does not impact SREBP2 cleavage which is required to generate the transcriptional active SREBP2 (Fig 4.18 and 4.19 A). These findings align both with the impact of *ApoA1* depletion and autophagy inhibition on inducing the expression of a common set of

cholesterol and lipid biosynthesis genes and their amplifying effects on gene expression when combined.

As FOXO1/3 phosphorylation is mediated by Akt activation, we explored the impact of endogenous ApoA-I on the Akt signaling pathway. We have found that the RNAi-mediated depletion of *ApoA1* leads to mTORC2-dependent phosphorylation of Akt at Ser^{473} but does not affect PDK1-mediated Thr^{308} phosphorylation beyond basal levels. In line with these findings, suppression of the mTORC2/Akt axis diminishes the effect of *ApoA1* depletion on *HMGCR* and *HMGCS1* expression (Fig4.20 and 4.21). Although additional studies are required to characterize the mechanism by which ApoA-I physiologically functions to moderate Akt activation, our preliminary data demonstrate that ApoA-I physically interacts with both Akt1 and Akt2 (Fig 4.22). We could thus envisage a scenario in which ApoA-I may compete with the mTORC2 complex in interacting with Akt or may modify Akt subcellular localization and activation.

Beyond the up-regulation of lipid and cholesterol biosynthesis processes, the transcriptome of dually *ApoA1* depleted and autophagy-inhibited HepG2 cells is enriched for downregulated genes related to cell cycle control and an overall association with neoplastic diseases (Fig 4.15 and 4.16). We therefore hypothesize that the reduction in ApoA-I coupled with autophagy blockade, a dual characteristic of HCC, may drive malignancy in the liver. In line with this notion, the knock-down of *ApoA1* in HepG2 cells protects against lipotoxicity and genotoxicity (Fig 4.23) and our preliminary data using *APOA1*-knockout mice carrying liver-specific ablation of *ATG5* show dramatic enhancement of liver pathologies, including carcinoma.

Overall, the data presented in this Chapter uncover novel functions of ApoA-I which are likely to transform our understanding of lipid and cholesterol metabolism and the role of ApoA-I thereof. We show that intracellular ApoA-I physically and functionally interacts with Akt to moderate its activation and thus reduce lipid and cholesterol biosynthetic gene expression. Conversely, reduced levels of ApoA-I under conditions of autophagy inhibition, as observed in HCC, are associated with amplified lipid and cholesterol biosynthetic gene expression, LD accumulation, enhanced survival *in vitro* and exaggerated hepatocarcinogenesis *in vivo*.

5. DISCUSSION

ApoA-I has attracted significant attention ever since it was identified as a major protein component of HDL. As such, ApoA-I has been extensively studied in the context of HDL-mediated reverse cholesterol transfer. Recent studies have expanded the extracellular roles of ApoA-I to include a broad spectrum of anti-thrombotic, antioxidative, anti-inflammatory and immune-regulatory properties, largely as a component of HDL. However, the intracellular fate and function of ApoA-I has been widely unexplored.

This PhD Thesis aimed to address major questions concerning the regulation and function of intracellular ApoA-I. In particular, we aimed to (1) examine post-transcriptional mechanisms responsible for ApoA-I regulation, and, (2) identify intracellular functions of ApoA-I, which remain unknown.

ApoA-I expression differs among individuals. Low circulating ApoA-I levels correlate with increased risk of development of several colon and liver pathologies (162, 163), as well as the clinical response to chemo- - (181) and immuno-therapy (182, 183). Therefore, the detailed characterization of the mechanisms regulating ApoA-I expression is important as it may provide novel information pertinent to clinically-relevant problems.

In this PhD Thesis we disclosed major post-transcriptional pathways responsible for the regulation of intracellular ApoA-I levels. We showed that under nutrient-rich conditions, ApoA-I expression is sustained by the balancing acts of basal autophagy and of mTORC1-dependent *de novo* protein synthesis (Fig. 5) This observation may explain the accumulation of intracellular ApoA-I in steatosis-like pathologies which are characterized by autophagy blockade.

In contrast, upon aminoacid insufficiency, suppression of ApoA-I synthesis prevails, rendering mTORC1 inactivation dispensable for autophagy-mediated ApoA-I proteolysis. Given the established role of ApoA-I in HDL-mediated reverse cholesterol transport, this mode of regulation of intracellular ApoA-I levels may reflect a hepatocellular response to the organismal requirement for maintenance of cholesterol and lipid reserves under conditions of nutrient scarcity. In line with this notion, a reduction in circulating ApoA-I has been noted in adults

undergoing a very low calorie diet (169, 170) and in African children suffering of kwashiorkor, a severe form of protein malnutrition (171, 172). Reduced HDL, presumably linked to lower synthesis of ApoA-I, has been reported in rodents following severe caloric restriction (173) and in a mouse model of alcoholic liver disease (174) which is characterized by reduced mTOR activity despite autophagy suppression (171). Therefore, the data presented in this Thesis provide important mechanistic insights pertinent to biological phenomena and clinical observations that remained poorly understood.

Intracellular functions of ApoA-I remain unknown. We have herein addressed this unanswered question and disclosed, for the first time, important cellular and molecular pathways and processes influenced by endogenous ApoA-I in hepatocytes, the main source of ApoA-I. We showed that endogenous ApoA-I physically interacts with Akt and moderates the mTORC2 – Akt – FOXO1/3 pathway to disable *de novo* cholesterol and lipid biosynthetic gene expression. These data uncover intracellular ApoA-I as a novel regulator of the Akt pathway and intracellular moderator of *de novo* lipogenesis. As the mTORC2 – Akt dyad has additional functions, including regulation of apoptosis, it is likely that intracellular ApoA-I may simultaneously affect various hallmarks of cancer. Indeed, we have found that the knock-down of *ApoA1* in HepG2 cells leads to partial protection from lipotoxicity and genotoxicity, in addition to the upregulation of cholesterol and lipid biosynthetic gene expression. This observation provides a biological explanation for the reported correlation between low ApoA-I levels and higher recurrence rates and shorter survival times in HCC patients (36).

Autophagy is a major catabolic pathway, targeting organelles and macromolecules for lysosomal degradation. Autophagy is involved in lipid droplet (LD) degradation and, therefore, may be crucial to avoid lipid accumulation. Conversely, genetic or chemical-induced inhibition of autophagy results in LD accumulation *in vitro* and *in vivo*. Our data indicate that inhibition of autophagy by bafilomycin may not only lead to LD accumulation by suppressing LD degradation but may also transcriptionally elevate the expression of several lipid and cholesterol biosynthesis genes. This observation provides novel insight into the role of autophagy in lipid and cholesterol

overload that is pertinent to several human steatotic liver diseases and HCC which are typified by autophagy blockade.

In this Thesis we have shown that autophagy blockade and reduced expression of ApoA-I intersect in the transcriptional regulation of cholesterol and lipid biosynthetic gene expression. Indeed, the knock-down of *ApoA1* exaggerates the effects of autophagy inhibition on intracellular lipid and cholesterol accumulation *in vitro*, concomitant to the amplified induction of genes involved in cholesterol and lipid biosynthesis. Therefore, intracellular ApoA-I may physiologically function to suppress lipid and cholesterol overload under conditions of autophagy blockade (Fig. 5).

On the basis of the data presented in this Thesis, we propose that ApoA-I accumulation ensued by autophagy blockade likely serves as a protective mechanism against exaggerated accumulation of lipids and cholesterol in hepatocytes. Low circulating levels of ApoA-I represent a feature of a subset of a HCC patients which is associated with poor prognosis (34, 36). In this Thesis we have shown that reduced expression of ApoA-I *in vitro*, is associated with elevated expression of several lipid and cholesterol biosynthesis genes in hepatocytes which is amplified under conditions of autophagy blockade. Therefore, we propose that intracellular ApoA-I may function as a suppressor of hepatocarcinogenesis by lowering the activation of mTORC2 – Akt signaling. Our hypothesis aligns with recent evidence demonstrating that constitutive engagement of the mTORC2 pathway drives hepatosteatosis and liver cancer in mice via fatty acid and lipid synthesis (184).

Overall, the data presented in this PhD Thesis uncover novel functions of ApoA-I which are likely to transform our understanding of lipid and cholesterol metabolism and the role of ApoA-I thereof.

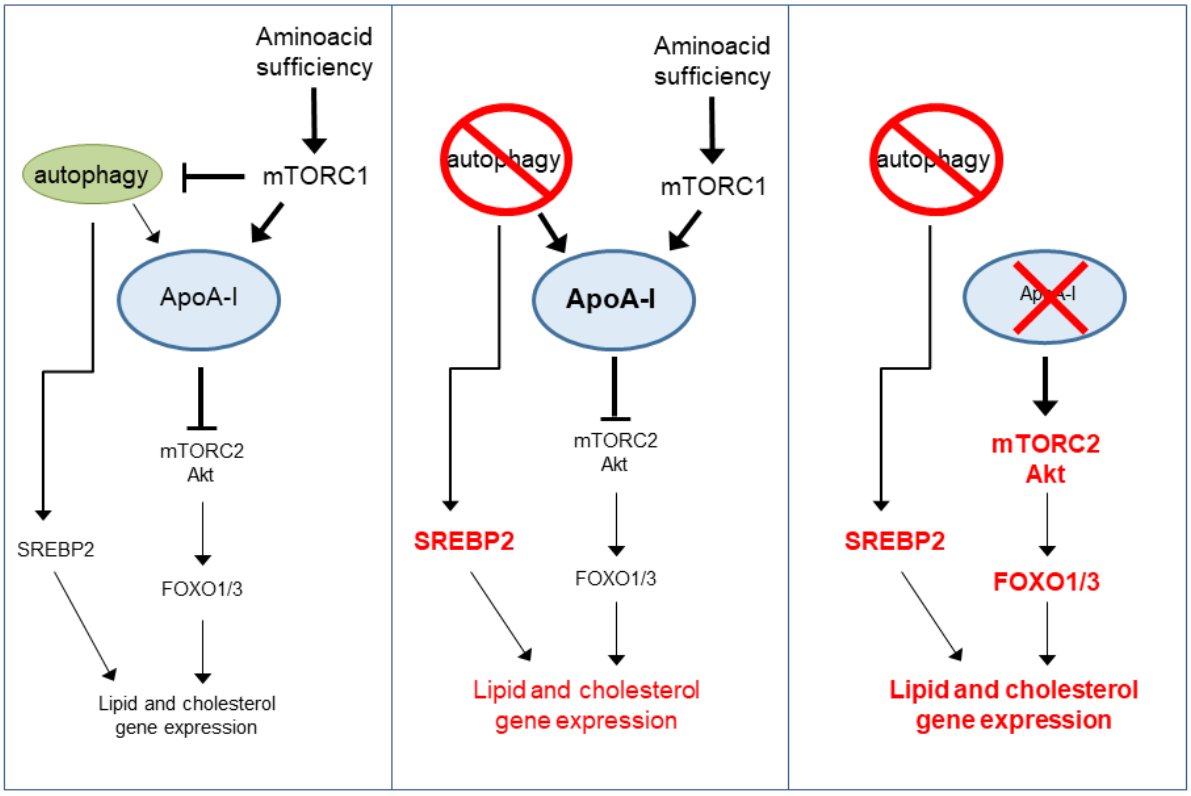

Figure 5. A summary of the findings generated in this PhD Thesis. The cross-talk between autophagy and ApoA-I affects intracellular metabolic pathways. Under normal conditions (left panel), aminoacid sufficiency maintains mTORC1 signaling and basal autophagy. ApoA-I functions to moderate Akt signals to FOXO1/3 and lipid and cholesterol gene expression. When autophagy is inhibited (middle panel), SREBP2 is activated to transactivate lipid and cholesterol gene expression; however, ApoA-I also accumulates and negatively controls metabolic gene expression. When both autophagy is inhibited and ApoA-I levels are reduced, SREBP2 and mTORC2-dependent engagement of Akt – FOXO1/3 pathway converge to amplify transcriptional activation of genes involved in lipid and cholesterol biosynthesis.

Future studies

Further studies are warranted to define the *in vivo* role of ApoA-I in hepatosteatosis and HCC using appropriate mouse models. Of particular interest is the effect of ApoA-I ablation on liver pathologies ensued by liver-specific autophagy blockade. Thus, ablation of ATG5 in mouse hepatocytes is known to cause hepatosteatosis and growth of non-malignant tumors. Our preliminary results demonstrate that ablation of ApoA-I on this background exaggerates steatosis and inflammation and, interestingly, leads to the development of HCC. This model provides a platform for in depth *in vivo* analyses of the cross-talk between autophagy and ApoA-I that is relevant to the human disease.

The observation that aminoacids are required for continuous synthesis of ApoA-I raises the possibility that diet poor in protein but rich in fat may exaggerate liver pathologies. Indeed, early-life protein restriction in mice, followed by high carbohydrate and high fat feeding, results in non-alcoholic fatty liver disease (185), albeit the role of ApoA-I in this effect remains unknown.

The physical and functional interaction between ApoA-I and Akt identified herein, is an additional important area that warrants further investigations. Akt is a major signaling pathway involved in several key cellular functions. It has been suggested that the topology of Akt phosphorylation by mTORC2 may dictate which of these functions are engaged (186). It would thus be of interest to both dissect the intracellular localization of the ApoA-I / Akt interaction and its impact on Akt-dependent outputs. In addition, the mechanism by which ApoA-I impinges on Akt phosphorylation should be defined. We hypothesize that ApoA-I may antagonize mTORC2 components for their binding to Akt. Delineation of this hypothesis requires detailed mapping of the Akt domain responsible for ApoA-I *versus* mTORC2 (i.e. Sin1) interaction by immunoprecipitation or pull-down assays.

Beyond Akt, ApoA-I may functionally interact with additional intracellular pathways that need to be defined. A proteomic and/or yeast-2-hybrid approach is thus warranted to identify novel ApoA-I interactors which may shed light into the pleiotropic activities of this fascinating molecule.

6. REFERENCES

1. Gordon SM, Hofmann S, Askew DS, Davidson WS. High density lipoprotein: it's not just about lipid transport anymore. Trends in endocrinology and metabolism: TEM. 2011;22(1):9-15.
2. Rosenson RS, Brewer HB, Jr., Ansell BJ, Barter P, Chapman MJ, Heinecke JW, et al. Dysfunctional HDL and atherosclerotic cardiovascular disease. Nature reviews Cardiology. 2016;13(1):48-60.
3. Schwertani A, Choi HY, Genest J. HDLs and the pathogenesis of atherosclerosis. Current opinion in cardiology. 2018;33(3):311-6.
4. Georgila K, Vyrla D, Drakos E. Apolipoprotein A-I (ApoA-I), Immunity, Inflammation and Cancer. Cancers. 2019;11(8).
5. Duong PT, Weibel GL, Lund-Katz S, Rothblat GH, Phillips MC. Characterization and properties of pre beta-HDL particles formed by ABCA1-mediated cellular lipid efflux to apoA-I. Journal of lipid research. 2008;49(5):1006-14.
6. Rosenson RS, Brewer HB, Jr., Chapman MJ, Fazio S, Hussain MM, Kontush A, et al. HDL measures, particle heterogeneity, proposed nomenclature, and relation to atherosclerotic cardiovascular events. Clinical chemistry. 2011;57(3):392-410.
7. Wang N, Silver DL, Costet P, Tall AR. Specific binding of ApoA-I, enhanced cholesterol efflux, and altered plasma membrane morphology in cells expressing ABC1. The Journal of biological chemistry. 2000;275(42):33053-8.
8. Liang HQ, Rye KA, Barter PJ. Cycling of apolipoprotein A-I between lipid-associated and lipid-free pools. Biochim Biophys Acta. 1995;1257(1):31-7.
9. Sankaranarayanan S, Oram JF, Asztalos BF, Vaughan AM, Lund-Katz S, Adorni MP, et al. Effects of acceptor composition and mechanism of ABCG1-mediated cellular free cholesterol efflux. Journal of lipid research. 2009;50(2):275-84.
10. Rye KA, Hime NJ, Barter PJ. Evidence that cholesteryl ester transfer protein-mediated reductions in reconstituted high density lipoprotein size involve particle fusion. The Journal of biological chemistry. 1997;272(7):3953-60.
11. Acton S, Rigotti A, Landschulz KT, Xu S, Hobbs HH, Krieger M. Identification of scavenger receptor SR-BI as a high density lipoprotein receptor. Science (New York, NY). 1996;271(5248):518-20.
12. Kozarsky KF, Donahee MH, Rigotti A, Iqbal SN, Edelman ER, Krieger M. Overexpression of the HDL receptor SR-BI alters plasma HDL and bile cholesterol levels. Nature. 1997;387(6631):414-7.
13. Martinez LO, Jacquet S, Esteve JP, Rolland C, Cabezon E, Champagne E, et al. Ectopic beta-chain of ATP synthase is an apolipoprotein A-I receptor in hepatic HDL endocytosis. Nature. 2003;421(6918):75-9.
14. Martinez LO, Najib S, Perret B, Cabou C, Lichtenstein L. Ecto-F1-ATPase/P2Y pathways in metabolic and vascular functions of high density lipoproteins. Atherosclerosis. 2015;238(1):89-100.
15. Christensen EI, Gburek J. Protein reabsorption in renal proximal tubule-function and dysfunction in kidney pathophysiology. Pediatric nephrology (Berlin, Germany). 2004;19(7):714-21.
16. Glass C, Pittman RC, Weinstein DB, Steinberg D. Dissociation of tissue uptake of cholesterol ester from that of apoprotein A-I of rat plasma high density lipoprotein: selective delivery of cholesterol ester to liver, adrenal, and gonad. Proceedings of the National Academy of Sciences of the United States of America. 1983;80(17):5435-9.
17. Barker WC, Dayhoff MO. Evolution of lipoproteins deduced from protein sequence data. Comparative biochemistry and physiology B, Comparative biochemistry. 1977;57(4):309-15.
18. Fitch WM. Phylogenies constrained by the crossover process as illustrated by human hemoglobins and a thirteen-cycle, eleven-amino-acid repeat in human apolipoprotein A-I. Genetics. 1977;86(3):623-44.
19. Li WH, Tanimura M, Luo CC, Datta S, Chan L. The apolipoprotein multigene family: biosynthesis, structure, structure-function relationships, and evolution. Journal of lipid research. 1988;29(3):245-71.

20. McLachlan AD. Repeated helical pattern in apolipoprotein-A-I. Nature. 1977;267(5610):465-6.
21. Bashtovyy D, Jones MK, Anantharamaiah GM, Segrest JP. Sequence conservation of apolipoprotein A-I affords novel insights into HDL structure-function. Journal of lipid research. 2011;52(3):435-50.
22. Staels B, Auwerx J. Regulation of apo A-I gene expression by fibrates. Atherosclerosis. 1998;137 Suppl:S19-23.
23. Wan YJ, Cai Y, Lungo W, Fu P, Locker J, French S, et al. Peroxisome proliferator-activated receptor alpha-mediated pathways are altered in hepatocyte-specific retinoid X receptor alpha-deficient mice. The Journal of biological chemistry. 2000;275(36):28285-90.
24. Peters JM, Hennuyer N, Staels B, Fruchart JC, Fievet C, Gonzalez FJ, et al. Alterations in lipoprotein metabolism in peroxisome proliferator-activated receptor alpha-deficient mice. The Journal of biological chemistry. 1997;272(43):27307-12.
25. Kardassis D, Mosialou I, Kanaki M, Tiniakou I, Thymiakou E. Metabolism of HDL and its regulation. Current medicinal chemistry. 2014;21(25):2864-80.
26. Hayhurst GP, Lee YH, Lambert G, Ward JM, Gonzalez FJ. Hepatocyte nuclear factor 4alpha (nuclear receptor 2A1) is essential for maintenance of hepatic gene expression and lipid homeostasis. Mol Cell Biol. 2001;21(4):1393-403.
27. Guo Y, Fan Y, Zhang J, Lomberk GA, Zhou Z, Sun L, et al. Perhexiline activates KLF14 and reduces atherosclerosis by modulating ApoA-I production. J Clin Invest. 2015;125(10):3819-30.
28. Mataki C, Magnier BC, Houten SM, Annicotte JS, Argmann C, Thomas C, et al. Compromised intestinal lipid absorption in mice with a liver-specific deficiency of liver receptor homolog 1. Mol Cell Biol. 2007;27(23):8330-9.
29. Halley P, Kadakkuzha BM, Faghihi MA, Magistri M, Zeier Z, Khorkova O, et al. Regulation of the apolipoprotein gene cluster by a long noncoding RNA. Cell Rep. 2014;6(1):222-30.
30. Jiang Y, Sun A, Zhao Y, Ying W, Sun H, Yang X, et al. Proteomics identifies new therapeutic targets of early-stage hepatocellular carcinoma. Nature. 2019;567(7747):257-61.
31. Ai J, Tan Y, Ying W, Hong Y, Liu S, Wu M, et al. Proteome analysis of hepatocellular carcinoma by laser capture microdissection. Proteomics. 2006;6(2):538-46.
32. Xu X, Wei X, Ling Q, Cheng J, Zhou B, Xie H, et al. Identification of two portal vein tumor thrombosis associated proteins in hepatocellular carcinoma: protein disulfide-isomerase A6 and apolipoprotein A-I. Journal of gastroenterology and hepatology. 2011;26(12):1787-94.
33. Fye HK, Wright-Drakesmith C, Kramer HB, Camey S, Nogueira da Costa A, Jeng A, et al. Protein profiling in hepatocellular carcinoma by label-free quantitative proteomics in two west African populations. PloS one. 2013;8(7):e68381.
34. Steel LF, Shumpert D, Trotter M, Seeholzer SH, Evans AA, London WT, et al. A strategy for the comparative analysis of serum proteomes for the discovery of biomarkers for hepatocellular carcinoma. Proteomics. 2003;3(5):601-9.
35. Mustafa MG, Petersen JR, Ju H, Cicalese L, Snyder N, Haidacher SJ, et al. Biomarker discovery for early detection of hepatocellular carcinoma in hepatitis C-infected patients. Molecular & cellular proteomics : MCP. 2013;12(12):3640-52.
36. Ma XL, Gao XH, Gong ZJ, Wu J, Tian L, Zhang CY, et al. Apolipoprotein A1: a novel serum biomarker for predicting the prognosis of hepatocellular carcinoma after curative resection. Oncotarget. 2016;7(43):70654-68.
37. Qin X, Chen Q, Sun C, Wang C, Peng Q, Xie L, et al. High-throughput screening of tumor metastatic-related differential glycoprotein in hepatocellular carcinoma by iTRAQ combines lectin-related techniques. Medical oncology (Northwood, London, England). 2013;30(1):420.
38. Mao M, Wang X, Sheng H, Liu Y, Zhang L, Dai S, et al. A novel score based on serum apolipoprotein A-1 and C-reactive protein is a prognostic biomarker in hepatocellular carcinoma patients. BMC cancer. 2018;18(1):1178.
39. Zhang Y, Yang X. Prognostic Significance of Pretreatment Apolipoprotein A-I as a Noninvasive Biomarker in Cancer Survivors: A Meta-Analysis. Disease markers. 2018;2018:1034037.

40. Wu J, Zhang C, Zhang G, Wang Y, Zhang Z, Su W, et al. Association Between Pretreatment Serum Apolipoprotein A1 and Prognosis of Solid Tumors in Chinese Population: A Systematic Review and Meta-Analysis. Cellular physiology and biochemistry : international journal of experimental cellular physiology, biochemistry, and pharmacology. 2018;51(2):575-88.
41. Choe YG, Jin W, Cho YK, Chung WG, Kim HJ, Jeon WK, et al. Apolipoprotein B/AI ratio is independently associated with non-alcoholic fatty liver disease in nondiabetic subjects. Journal of gastroenterology and hepatology. 2013;28(4):678-83.
42. Bril F, Sninsky JJ, Baca AM, Superko HR, Portillo Sanchez P, Biernacki D, et al. Hepatic Steatosis and Insulin Resistance, But Not Steatohepatitis, Promote Atherogenic Dyslipidemia in NAFLD. The Journal of clinical endocrinology and metabolism. 2016;101(2):644-52.
43. Fadaei R, Poustchi H, Meshkani R, Moradi N, Golmohammadi T, Merat S. Impaired HDL cholesterol efflux capacity in patients with non-alcoholic fatty liver disease is associated with subclinical atherosclerosis. Scientific reports. 2018;8(1):11691.
44. Yang MH, Sung J, Gwak GY. The associations between apolipoprotein B, A1, and the B/A1 ratio and nonalcoholic fatty liver disease in both normal-weight and overweight Korean population. Journal of clinical lipidology. 2016;10(2):289-98.
45. Lemberg A, Schreier L, Romay S, Fernandez MA, Rosello D, Gonzales S, et al. Involvement of serum apolipoprotein AI and B100 and lecithin cholesterol acyl transferase in alcoholic cirrhotics. Annals of hepatology. 2007;6(4):227-32.
46. McDyre BC, AbdulHameed MDM, Permenter MG, Dennis WE, Baer CE, Koontz JM, et al. Comparative Proteomic Analysis of Liver Steatosis and Fibrosis after Oral Hepatotoxicant Administration in Sprague-Dawley Rats. Toxicologic pathology. 2018;46(2):202-23.
47. Karavia EA, Papachristou DJ, Liopeta K, Triantaphyllidou IE, Dimitrakopoulos O, Kypreos KE. Apolipoprotein A-I modulates processes associated with diet-induced nonalcoholic fatty liver disease in mice. Mol Med. 2012;18:901-12.
48. Mizushima N, Komatsu M. Autophagy: renovation of cells and tissues. Cell. 2011;147(4):728-41.
49. Li WW, Li J, Bao JK. Microautophagy: lesser-known self-eating. Cellular and molecular life sciences : CMLS. 2012;69(7):1125-36.
50. Cuervo AM, Wong E. Chaperone-mediated autophagy: roles in disease and aging. Cell research. 2014;24(1):92-104.
51. Kaushik S, Cuervo AM. The coming of age of chaperone-mediated autophagy. Nature reviews Molecular cell biology. 2018;19(6):365-81.
52. Wirth M, Joachim J, Tooze SA. Autophagosome formation--the role of ULK1 and Beclin1-PI3KC3 complexes in setting the stage. Seminars in cancer biology. 2013;23(5):301-9.
53. Rubinsztein DC, Shpilka T, Elazar Z. Mechanisms of autophagosome biogenesis. Current biology : CB. 2012;22(1):R29-34.
54. Eliopoulos AG, Havaki S, Gorgoulis VG. DNA Damage Response and Autophagy: A Meaningful Partnership. Frontiers in genetics. 2016;7:204.
55. Klionsky DJ, Abdalla FC, Abeliovich H, Abraham RT, Acevedo-Arozena A, Adeli K, et al. Guidelines for the use and interpretation of assays for monitoring autophagy. Autophagy. 2012;8(4):445-544.
56. Kuma A, Hatano M, Matsui M, Yamamoto A, Nakaya H, Yoshimori T, et al. The role of autophagy during the early neonatal starvation period. Nature. 2004;432(7020):1032-6.
57. Madrigal-Matute J, Cuervo AM. Regulation of Liver Metabolism by Autophagy. Gastroenterology. 2016;150(2):328-39.
58. Sancak Y, Thoreen CC, Peterson TR, Lindquist RA, Kang SA, Spooner E, et al. PRAS40 is an insulin-regulated inhibitor of the mTORC1 protein kinase. Molecular cell. 2007;25(6):903-15.
59. Kim DH, Sarbassov DD, Ali SM, Latek RR, Guntur KV, Erdjument-Bromage H, et al. GbetaL, a positive regulator of the rapamycin-sensitive pathway required for the nutrient-sensitive interaction between raptor and mTOR. Molecular cell. 2003;11(4):895-904.
60. Hara K, Maruki Y, Long X, Yoshino K, Oshiro N, Hidayat S, et al. Raptor, a binding partner of target of rapamycin (TOR), mediates TOR action. Cell. 2002;110(2):177-89.

61. Kim DH, Sarbassov DD, Ali SM, King JE, Latek RR, Erdjument-Bromage H, et al. mTOR interacts with raptor to form a nutrient-sensitive complex that signals to the cell growth machinery. Cell. 2002;110(2):163-75.
62. Yang H, Rudge DG, Koos JD, Vaidialingam B, Yang HJ, Pavletich NP. mTOR kinase structure, mechanism and regulation. Nature. 2013;497(7448):217-23.
63. Wang L, Harris TE, Roth RA, Lawrence JC, Jr. PRAS40 regulates mTORC1 kinase activity by functioning as a direct inhibitor of substrate binding. The Journal of biological chemistry. 2007;282(27):20036-44.
64. Peterson TR, Laplante M, Thoreen CC, Sancak Y, Kang SA, Kuehl WM, et al. DEPTOR is an mTOR inhibitor frequently overexpressed in multiple myeloma cells and required for their survival. Cell. 2009;137(5):873-86.
65. Gao D, Inuzuka H, Tan MK, Fukushima H, Locasale JW, Liu P, et al. mTOR drives its own activation via SCF(betaTrCP)-dependent degradation of the mTOR inhibitor DEPTOR. Molecular cell. 2011;44(2):290-303.
66. Sarbassov DD, Ali SM, Kim DH, Guertin DA, Latek RR, Erdjument-Bromage H, et al. Rictor, a novel binding partner of mTOR, defines a rapamycin-insensitive and raptor-independent pathway that regulates the cytoskeleton. Current biology : CB. 2004;14(14):1296-302.
67. Jacinto E, Loewith R, Schmidt A, Lin S, Ruegg MA, Hall A, et al. Mammalian TOR complex 2 controls the actin cytoskeleton and is rapamycin insensitive. Nature cell biology. 2004;6(11):1122-8.
68. Frias MA, Thoreen CC, Jaffe JD, Schroder W, Sculley T, Carr SA, et al. mSin1 is necessary for Akt/PKB phosphorylation, and its isoforms define three distinct mTORC2s. Current biology : CB. 2006;16(18):1865-70.
69. Jacinto E, Facchinetti V, Liu D, Soto N, Wei S, Jung SY, et al. SIN1/MIP1 maintains rictor-mTOR complex integrity and regulates Akt phosphorylation and substrate specificity. Cell. 2006;127(1):125-37.
70. Pearce LR, Sommer EM, Sakamoto K, Wullschleger S, Alessi DR. Protor-1 is required for efficient mTORC2-mediated activation of SGK1 in the kidney. The Biochemical journal. 2011;436(1):169-79.
71. Thedieck K, Polak P, Kim ML, Molle KD, Cohen A, Jeno P, et al. PRAS40 and PRR5-like protein are new mTOR interactors that regulate apoptosis. PloS one. 2007;2(11):e1217.
72. Pearce LR, Huang X, Boudeau J, Pawlowski R, Wullschleger S, Deak M, et al. Identification of Protor as a novel Rictor-binding component of mTOR complex-2. The Biochemical journal. 2007;405(3):513-22.
73. Ma XM, Blenis J. Molecular mechanisms of mTOR-mediated translational control. Nature reviews Molecular cell biology. 2009;10(5):307-18.
74. Holz MK, Ballif BA, Gygi SP, Blenis J. mTOR and S6K1 mediate assembly of the translation preinitiation complex through dynamic protein interchange and ordered phosphorylation events. Cell. 2005;123(4):569-80.
75. Dorrello NV, Peschiaroli A, Guardavaccaro D, Colburn NH, Sherman NE, Pagano M. S6K1- and betaTRCP-mediated degradation of PDCD4 promotes protein translation and cell growth. Science (New York, NY). 2006;314(5798):467-71.
76. Ma XM, Yoon SO, Richardson CJ, Julich K, Blenis J. SKAR links pre-mRNA splicing to mTOR/S6K1-mediated enhanced translation efficiency of spliced mRNAs. Cell. 2008;133(2):303-13.
77. Gingras AC, Gygi SP, Raught B, Polakiewicz RD, Abraham RT, Hoekstra MF, et al. Regulation of 4E-BP1 phosphorylation: a novel two-step mechanism. Genes & development. 1999;13(11):1422-37.
78. Brunn GJ, Hudson CC, Sekulic A, Williams JM, Hosoi H, Houghton PJ, et al. Phosphorylation of the translational repressor PHAS-I by the mammalian target of rapamycin. Science (New York, NY). 1997;277(5322):99-101.
79. Porstmann T, Santos CR, Griffiths B, Cully M, Wu M, Leevers S, et al. SREBP activity is regulated by mTORC1 and contributes to Akt-dependent cell growth. Cell metabolism. 2008;8(3):224-36.

80. Duvel K, Yecies JL, Menon S, Raman P, Lipovsky AI, Souza AL, et al. Activation of a metabolic gene regulatory network downstream of mTOR complex 1. Molecular cell. 2010;39(2):171-83.
81. Peterson TR, Sengupta SS, Harris TE, Carmack AE, Kang SA, Balderas E, et al. mTOR complex 1 regulates lipin 1 localization to control the SREBP pathway. Cell. 2011;146(3):408-20.
82. Laplante M, Sabatini DM. An emerging role of mTOR in lipid biosynthesis. Current biology : CB. 2009;19(22):R1046-52.
83. Han J, Li E, Chen L, Zhang Y, Wei F, Liu J, et al. The CREB coactivator CRTC2 controls hepatic lipid metabolism by regulating SREBP1. Nature. 2015;524(7564):243-6.
84. Kim J, Kundu M, Viollet B, Guan KL. AMPK and mTOR regulate autophagy through direct phosphorylation of Ulk1. Nature cell biology. 2011;13(2):132-41.
85. Alers S, Wesselborg S, Stork B. ATG13: just a companion, or an executor of the autophagic program? Autophagy. 2014;10(6):944-56.
86. Settembre C, Zoncu R, Medina DL, Vetrini F, Erdin S, Erdin S, et al. A lysosome-to-nucleus signalling mechanism senses and regulates the lysosome via mTOR and TFEB. The EMBO journal. 2012;31(5):1095-108.
87. Roczniak-Ferguson A, Petit CS, Froehlich F, Qian S, Ky J, Angarola B, et al. The transcription factor TFEB links mTORC1 signaling to transcriptional control of lysosome homeostasis. Science signaling. 2012;5(228):ra42.
88. Martina JA, Chen Y, Gucek M, Puertollano R. MTORC1 functions as a transcriptional regulator of autophagy by preventing nuclear transport of TFEB. Autophagy. 2012;8(6):903-14.
89. Sarbassov DD, Guertin DA, Ali SM, Sabatini DM. Phosphorylation and regulation of Akt/PKB by the rictor-mTOR complex. Science (New York, NY). 2005;307(5712):1098-101.
90. Guertin DA, Stevens DM, Thoreen CC, Burds AA, Kalaany NY, Moffat J, et al. Ablation in mice of the mTORC components raptor, rictor, or mLST8 reveals that mTORC2 is required for signaling to Akt-FOXO and PKCalpha, but not S6K1. Developmental cell. 2006;11(6):859-71.
91. Boutouja F, Stiehm CM, Platta HW. mTOR: A Cellular Regulator Interface in Health and Disease. Cells. 2019;8(1).
92. Brown MS, Goldstein JL. The SREBP pathway: regulation of cholesterol metabolism by proteolysis of a membrane-bound transcription factor. Cell. 1997;89(3):331-40.
93. Eberle D, Hegarty B, Bossard P, Ferre P, Foufelle F. SREBP transcription factors: master regulators of lipid homeostasis. Biochimie. 2004;86(11):839-48.
94. Gong Y, Lee JN, Lee PC, Goldstein JL, Brown MS, Ye J. Sterol-regulated ubiquitination and degradation of Insig-1 creates a convergent mechanism for feedback control of cholesterol synthesis and uptake. Cell metabolism. 2006;3(1):15-24.
95. Bengoechea-Alonso MT, Ericsson J. SREBP in signal transduction: cholesterol metabolism and beyond. Current opinion in cell biology. 2007;19(2):215-22.
96. Horton JD, Goldstein JL, Brown MS. SREBPs: activators of the complete program of cholesterol and fatty acid synthesis in the liver. J Clin Invest. 2002;109(9):1125-31.
97. Shimano H, Horton JD, Hammer RE, Shimomura I, Brown MS, Goldstein JL. Overproduction of cholesterol and fatty acids causes massive liver enlargement in transgenic mice expressing truncated SREBP-1a. J Clin Invest. 1996;98(7):1575-84.
98. Shimano H, Horton JD, Shimomura I, Hammer RE, Brown MS, Goldstein JL. Isoform 1c of sterol regulatory element binding protein is less active than isoform 1a in livers of transgenic mice and in cultured cells. J Clin Invest. 1997;99(5):846-54.
99. Shimano H, Sato R. SREBP-regulated lipid metabolism: convergent physiology - divergent pathophysiology. Nature reviews Endocrinology. 2017;13(12):710-30.
100. Osborne TF, Espenshade PJ. Evolutionary conservation and adaptation in the mechanism that regulates SREBP action: what a long, strange tRIP it's been. Genes & development. 2009;23(22):2578-91.
101. Moslehi A, Hamidi-Zad Z. Role of SREBPs in Liver Diseases: A Mini-review. J Clin Transl Hepatol. 2018;6(3):332-8.
102. Horton JD, Shimomura I, Ikemoto S, Bashmakov Y, Hammer RE. Overexpression of sterol regulatory element-binding protein-1a in mouse adipose tissue produces adipocyte hypertrophy,

increased fatty acid secretion, and fatty liver. The Journal of biological chemistry. 2003;278(38):36652-60.
103. Higuchi N, Kato M, Shundo Y, Tajiri H, Tanaka M, Yamashita N, et al. Liver X receptor in cooperation with SREBP-1c is a major lipid synthesis regulator in nonalcoholic fatty liver disease. Hepatology research : the official journal of the Japan Society of Hepatology. 2008;38(11):1122-9.
104. Knebel B, Haas J, Hartwig S, Jacob S, Kollmer C, Nitzgen U, et al. Liver-specific expression of transcriptionally active SREBP-1c is associated with fatty liver and increased visceral fat mass. PloS one. 2012;7(2):e31812.
105. Moon YA, Liang G, Xie X, Frank-Kamenetsky M, Fitzgerald K, Koteliansky V, et al. The Scap/SREBP pathway is essential for developing diabetic fatty liver and carbohydrate-induced hypertriglyceridemia in animals. Cell metabolism. 2012;15(2):240-6.
106. Zhang Y, Proenca R, Maffei M, Barone M, Leopold L, Friedman JM. Positional cloning of the mouse obese gene and its human homologue. Nature. 1994;372(6505):425-32.
107. Yahagi N, Shimano H, Hasty AH, Matsuzaka T, Ide T, Yoshikawa T, et al. Absence of sterol regulatory element-binding protein-1 (SREBP-1) ameliorates fatty livers but not obesity or insulin resistance in Lep(ob)/Lep(ob) mice. The Journal of biological chemistry. 2002;277(22):19353-7.
108. Li C, Yang W, Zhang J, Zheng X, Yao Y, Tu K, et al. SREBP-1 has a prognostic role and contributes to invasion and metastasis in human hepatocellular carcinoma. International journal of molecular sciences. 2014;15(5):7124-38.
109. Ishimoto K, Tachibana K, Hanano I, Yamasaki D, Nakamura H, Kawai M, et al. Sterol-regulatory-element-binding protein 2 and nuclear factor Y control human farnesyl diphosphate synthase expression and affect cell proliferation in hepatoblastoma cells. The Biochemical journal. 2010;429(2):347-57.
110. Li N, Zhou ZS, Shen Y, Xu J, Miao HH, Xiong Y, et al. Inhibition of the sterol regulatory element-binding protein pathway suppresses hepatocellular carcinoma by repressing inflammation in mice. Hepatology (Baltimore, Md). 2017;65(6):1936-47.
111. Calvisi DF, Wang C, Ho C, Ladu S, Lee SA, Mattu S, et al. Increased lipogenesis, induced by AKT-mTORC1-RPS6 signaling, promotes development of human hepatocellular carcinoma. Gastroenterology. 2011;140(3):1071-83.
112. Sundqvist A, Bengoechea-Alonso MT, Ye X, Lukiyanchuk V, Jin J, Harper JW, et al. Control of lipid metabolism by phosphorylation-dependent degradation of the SREBP family of transcription factors by SCF(Fbw7). Cell metabolism. 2005;1(6):379-91.
113. Yecies JL, Zhang HH, Menon S, Liu S, Yecies D, Lipovsky AI, et al. Akt stimulates hepatic SREBP1c and lipogenesis through parallel mTORC1-dependent and independent pathways. Cell metabolism. 2011;14(1):21-32.
114. Yabe D, Komuro R, Liang G, Goldstein JL, Brown MS. Liver-specific mRNA for Insig-2 down-regulated by insulin: implications for fatty acid synthesis. Proceedings of the National Academy of Sciences of the United States of America. 2003;100(6):3155-60.
115. Hagiwara A, Cornu M, Cybulski N, Polak P, Betz C, Trapani F, et al. Hepatic mTORC2 activates glycolysis and lipogenesis through Akt, glucokinase, and SREBP1c. Cell metabolism. 2012;15(5):725-38.
116. Yuan M, Pino E, Wu L, Kacergis M, Soukas AA. Identification of Akt-independent regulation of hepatic lipogenesis by mammalian target of rapamycin (mTOR) complex 2. The Journal of biological chemistry. 2012;287(35):29579-88.
117. Haeusler RA, Han S, Accili D. Hepatic FoxO1 ablation exacerbates lipid abnormalities during hyperglycemia. The Journal of biological chemistry. 2010;285(35):26861-8.
118. Deng X, Zhang W, I OS, Williams JB, Dong Q, Park EA, et al. FoxO1 inhibits sterol regulatory element-binding protein-1c (SREBP-1c) gene expression via transcription factors Sp1 and SREBP-1c. The Journal of biological chemistry. 2012;287(24):20132-43.
119. Li D, Guo L, Deng B, Li M, Yang T, Yang F, et al. Long noncoding RNA HR1 participates in the expression of SREBP1c through phosphorylation of the PDK1/AKT/FoxO1 pathway. Mol Med Rep. 2018;18(3):2850-6.

120. Liu X, Qiao A, Ke Y, Kong X, Liang J, Wang R, et al. FoxO1 represses LXRalpha-mediated transcriptional activity of SREBP-1c promoter in HepG2 cells. FEBS Lett. 2010;584(20):4330-4.
121. Tao R, Wei D, Gao H, Liu Y, DePinho RA, Dong XC. Hepatic FoxOs regulate lipid metabolism via modulation of expression of the nicotinamide phosphoribosyltransferase gene. The Journal of biological chemistry. 2011;286(16):14681-90.
122. Zhang K, Li L, Qi Y, Zhu X, Gan B, DePinho RA, et al. Hepatic suppression of Foxo1 and Foxo3 causes hypoglycemia and hyperlipidemia in mice. Endocrinology. 2012;153(2):631-46.
123. Martin S, Parton RG. Lipid droplets: a unified view of a dynamic organelle. Nature reviews Molecular cell biology. 2006;7(5):373-8.
124. Finn PF, Dice JF. Proteolytic and lipolytic responses to starvation. Nutrition (Burbank, Los Angeles County, Calif). 2006;22(7-8):830-44.
125. Singh R, Kaushik S, Wang Y, Xiang Y, Novak I, Komatsu M, et al. Autophagy regulates lipid metabolism. Nature. 2009;458(7242):1131-5.
126. Martinez-Lopez N, Garcia-Macia M, Sahu S, Athonvarangkul D, Liebling E, Merlo P, et al. Autophagy in the CNS and Periphery Coordinate Lipophagy and Lipolysis in the Brown Adipose Tissue and Liver. Cell metabolism. 2016;23(1):113-27.
127. Sathyanarayan A, Mashek MT, Mashek DG. ATGL Promotes Autophagy/Lipophagy via SIRT1 to Control Hepatic Lipid Droplet Catabolism. Cell Rep. 2017;19(1):1-9.
128. Kaushik S, Cuervo AM. Degradation of lipid droplet-associated proteins by chaperone-mediated autophagy facilitates lipolysis. Nature cell biology. 2015;17(6):759-70.
129. Schneider JL, Suh Y, Cuervo AM. Deficient chaperone-mediated autophagy in liver leads to metabolic dysregulation. Cell metabolism. 2014;20(3):417-32.
130. Greenberg AS, Coleman RA, Kraemer FB, McManaman JL, Obin MS, Puri V, et al. The role of lipid droplets in metabolic disease in rodents and humans. J Clin Invest. 2011;121(6):2102-10.
131. Ding ZB, Shi YH, Zhou J, Qiu SJ, Xu Y, Dai Z, et al. Association of autophagy defect with a malignant phenotype and poor prognosis of hepatocellular carcinoma. Cancer Res. 2008;68(22):9167-75.
132. Takamura A, Komatsu M, Hara T, Sakamoto A, Kishi C, Waguri S, et al. Autophagy-deficient mice develop multiple liver tumors. Genes & development. 2011;25(8):795-800.
133. Rodriguez A, Duran A, Selloum M, Champy MF, Diez-Guerra FJ, Flores JM, et al. Mature-onset obesity and insulin resistance in mice deficient in the signaling adapter p62. Cell metabolism. 2006;3(3):211-22.
134. Koga H, Kaushik S, Cuervo AM. Altered lipid content inhibits autophagic vesicular fusion. Faseb j. 2010;24(8):3052-65.
135. Flores-Toro JA, Go KL, Leeuwenburgh C, Kim JS. Autophagy in the liver: cell's cannibalism and beyond. Archives of pharmacal research. 2016;39(8):1050-61.
136. Rodriguez-Navarro JA, Kaushik S, Koga H, Dall'Armi C, Shui G, Wenk MR, et al. Inhibitory effect of dietary lipids on chaperone-mediated autophagy. Proceedings of the National Academy of Sciences of the United States of America. 2012;109(12):E705-14.
137. Inami Y, Yamashina S, Izumi K, Ueno T, Tanida I, Ikejima K, et al. Hepatic steatosis inhibits autophagic proteolysis via impairment of autophagosomal acidification and cathepsin expression. Biochemical and biophysical research communications. 2011;412(4):618-25.
138. Chen R, Wang Q, Song S, Liu F, He B, Gao X. Protective role of autophagy in methionine-choline deficient diet-induced advanced nonalcoholic steatohepatitis in mice. European journal of pharmacology. 2016;770:126-33.
139. Xiong X, Tao R, DePinho RA, Dong XC. The autophagy-related gene 14 (Atg14) is regulated by forkhead box O transcription factors and circadian rhythms and plays a critical role in hepatic autophagy and lipid metabolism. The Journal of biological chemistry. 2012;287(46):39107-14.
140. Yang L, Li P, Fu S, Calay ES, Hotamisligil GS. Defective hepatic autophagy in obesity promotes ER stress and causes insulin resistance. Cell metabolism. 2010;11(6):467-78.
141. Ji G, Wang Y, Deng Y, Li X, Jiang Z. Resveratrol ameliorates hepatic steatosis and inflammation in methionine/choline-deficient diet-induced steatohepatitis through regulating autophagy. Lipids in health and disease. 2015;14:134.

142. Gonzalez-Rodriguez A, Mayoral R, Agra N, Valdecantos MP, Pardo V, Miquilena-Colina ME, et al. Impaired autophagic flux is associated with increased endoplasmic reticulum stress during the development of NAFLD. Cell Death Dis. 2014;5:e1179.
143. Ding WX, Li M, Chen X, Ni HM, Lin CW, Gao W, et al. Autophagy reduces acute ethanol-induced hepatotoxicity and steatosis in mice. Gastroenterology. 2010;139(5):1740-52.
144. Robertson D, Monaghan P, Clarke C, Atherton AJ. An appraisal of low-temperature embedding by progressive lowering of temperature into Lowicryl HM20 for immunocytochemical studies. Journal of microscopy. 1992;168(Pt 1):85-100.
145. Gkirtzimanaki K, Gkouskou KK, Oleksiewicz U, Nikolaidis G, Vyrla D, Liontos M, et al. TPL2 kinase is a suppressor of lung carcinogenesis. Proceedings of the National Academy of Sciences of the United States of America. 2013;110(16):E1470-9.
146. Wang K. Molecular mechanism of hepatic steatosis: pathophysiological role of autophagy. Expert reviews in molecular medicine. 2016;18:e14.
147. Czaja MJ. Function of Autophagy in Nonalcoholic Fatty Liver Disease. Digestive diseases and sciences. 2016;61(5):1304-13.
148. Heid HW, Moll R, Schwetlick I, Rackwitz HR, Keenan TW. Adipophilin is a specific marker of lipid accumulation in diverse cell types and diseases. Cell and tissue research. 1998;294(2):309-21.
149. Chisholm JW, Burleson ER, Shelness GS, Parks JS. ApoA-I secretion from HepG2 cells: evidence for the secretion of both lipid-poor apoA-I and intracellularly assembled nascent HDL. Journal of lipid research. 2002;43(1):36-44.
150. Bhat S, Zabalawi M, Willingham MC, Shelness GS, Thomas MJ, Sorci-Thomas MG. Quality control in the apoA-I secretory pathway: deletion of apoA-I helix 6 leads to the formation of cytosolic phospholipid inclusions. Journal of lipid research. 2004;45(7):1207-20.
151. Miles RR, Perry W, Haas JV, Mosior MK, N'Cho M, Wang JW, et al. Genome-wide screen for modulation of hepatic apolipoprotein A-I (ApoA-I) secretion. The Journal of biological chemistry. 2013;288(9):6386-96.
152. Mauvezin C, Neufeld TP. Bafilomycin A1 disrupts autophagic flux by inhibiting both V-ATPase-dependent acidification and Ca-P60A/SERCA-dependent autophagosome-lysosome fusion. Autophagy. 2015;11(8):1437-8.
153. Mauthe M, Orhon I, Rocchi C, Zhou X, Luhr M, Hijlkema KJ, et al. Chloroquine inhibits autophagic flux by decreasing autophagosome-lysosome fusion. Autophagy. 2018;14(8):1435-55.
154. Hamilton RL, Wong JS, Guo LS, Krisans S, Havel RJ. Apolipoprotein E localization in rat hepatocytes by immunogold labeling of cryothin sections. Journal of lipid research. 1990;31(9):1589-603.
155. Maric J, Kiss RS, Franklin V, Marcel YL. Intracellular lipidation of newly synthesized apolipoprotein A-I in primary murine hepatocytes. The Journal of biological chemistry. 2005;280(48):39942-9.
156. Corona Velazquez AF, Jackson WT. So Many Roads: the Multifaceted Regulation of Autophagy Induction. Mol Cell Biol. 2018;38(21).
157. Martinet W, De Meyer GR, Andries L, Herman AG, Kockx MM. In situ detection of starvation-induced autophagy. The journal of histochemistry and cytochemistry : official journal of the Histochemistry Society. 2006;54(1):85-96.
158. Saxton RA, Sabatini DM. mTOR Signaling in Growth, Metabolism, and Disease. Cell. 2017;169(2):361-71.
159. Kim J, Guan KL. mTOR as a central hub of nutrient signalling and cell growth. Nature cell biology. 2019;21(1):63-71.
160. Liu Q, Xu C, Kirubakaran S, Zhang X, Hur W, Liu Y, et al. Characterization of Torin2, an ATP-competitive inhibitor of mTOR, ATM, and ATR. Cancer Res. 2013;73(8):2574-86.
161. Liu P, Gan W, Chin YR, Ogura K, Guo J, Zhang J, et al. PtdIns(3,4,5)P3-Dependent Activation of the mTORC2 Kinase Complex. Cancer discovery. 2015;5(11):1194-209.
162. Borgquist S, Butt T, Almgren P, Shiffman D, Stocks T, Orho-Melander M, et al. Apolipoproteins, lipids and risk of cancer. International journal of cancer. 2016;138(11):2648-56.

163. van Duijnhoven FJ, Bueno-De-Mesquita HB, Calligaro M, Jenab M, Pischon T, Jansen EH, et al. Blood lipid and lipoprotein concentrations and colorectal cancer risk in the European Prospective Investigation into Cancer and Nutrition. Gut. 2011;60(8):1094-102.
164. Zannis VI, Breslow JL, SanGiacomo TR, Aden DP, Knowles BB. Characterization of the major apolipoproteins secreted by two human hepatoma cell lines. Biochemistry. 1981;20(25):7089-96.
165. Chen G, Ding XF, Bouamar H, Pressley K, Sun LZ. Everolimus induces G1 cell cycle arrest through autophagy-mediated protein degradation of cyclin D1 in breast cancer cells. Am J Physiol Cell Physiol. 2019;317(2):C244-c52.
166. Bejarano E, Girao H, Yuste A, Patel B, Marques C, Spray DC, et al. Autophagy modulates dynamics of connexins at the plasma membrane in a ubiquitin-dependent manner. Molecular biology of the cell. 2012;23(11):2156-69.
167. Imam S, Talley S, Nelson RS, Dharan A, O'Connor C, Hope TJ, et al. TRIM5alpha Degradation via Autophagy Is Not Required for Retroviral Restriction. Journal of virology. 2016;90(7):3400-10.
168. Zoncu R, Bar-Peled L, Efeyan A, Wang S, Sancak Y, Sabatini DM. mTORC1 senses lysosomal amino acids through an inside-out mechanism that requires the vacuolar H(+)-ATPase. Science (New York, NY). 2011;334(6056):678-83.
169. Asztalos B, Lefevre M, Wong L, Foster TA, Tulley R, Windhauser M, et al. Differential response to low-fat diet between low and normal HDL-cholesterol subjects. Journal of lipid research. 2000;41(3):321-8.
170. Shoji T, Nishizawa Y, Koyama H, Hagiwara S, Aratani H, Izumotani-Sasao K, et al. Lipoprotein metabolism in normolipidemic obese women during very low calorie diet: changes in high density lipoprotein. Journal of nutritional science and vitaminology. 1991;37 Suppl:S57-64.
171. Babuta M, Furi I, Bala S, Bukong TN, Lowe P, Catalano D, et al. Dysregulated Autophagy and Lysosome Function Are Linked to Exosome Production by Micro-RNA 155 in Alcoholic Liver Disease. Hepatology (Baltimore, Md). 2019.
172. Manley S, Williams JA, Ding WX. Role of p62/SQSTM1 in liver physiology and pathogenesis. Experimental biology and medicine (Maywood, NJ). 2013;238(5):525-38.
173. Duarte FO, Sene-Fiorese M, Manzoni MS, de Freitas LF, Cheik NC, Garcia de Oliveira Duarte AC, et al. Caloric restriction and refeeding promoted different metabolic effects in fat depots and impaired dyslipidemic profile in rats. Nutrition (Burbank, Los Angeles County, Calif). 2008;24(2):177-86.
174. Tan P, Liang H, Nie J, Diao Y, He Q, Hou B, et al. Establishment of an alcoholic fatty liver disease model in mice. The American journal of drug and alcohol abuse. 2017;43(1):61-8.
175. Langhi C, Baldan A. CIDEC/FSP27 is regulated by peroxisome proliferator-activated receptor alpha and plays a critical role in fasting- and diet-induced hepatosteatosis. Hepatology (Baltimore, Md). 2015;61(4):1227-38.
176. Xu L, Zhou L, Li P. CIDE proteins and lipid metabolism. Arteriosclerosis, thrombosis, and vascular biology. 2012;32(5):1094-8.
177. Xu X, Park JG, So JS, Lee AH. Transcriptional activation of Fsp27 by the liver-enriched transcription factor CREBH promotes lipid droplet growth and hepatic steatosis. Hepatology (Baltimore, Md). 2015;61(3):857-69.
178. Matsusue K, Kusakabe T, Noguchi T, Takiguchi S, Suzuki T, Yamano S, et al. Hepatic steatosis in leptin-deficient mice is promoted by the PPARgamma target gene Fsp27. Cell metabolism. 2008;7(4):302-11.
179. Yu S, Matsusue K, Kashireddy P, Cao WQ, Yeldandi V, Yeldandi AV, et al. Adipocyte-specific gene expression and adipogenic steatosis in the mouse liver due to peroxisome proliferator-activated receptor gamma1 (PPARgamma1) overexpression. The Journal of biological chemistry. 2003;278(1):498-505.
180. Gong J, Sun Z, Wu L, Xu W, Schieber N, Xu D, et al. Fsp27 promotes lipid droplet growth by lipid exchange and transfer at lipid droplet contact sites. J Cell Biol. 2011;195(6):953-63.

181. Cheng T, Dai X, Zhou DL, Lv Y, Miao LY. Correlation of apolipoprotein A-I kinetics with survival and response to first-line platinum-based chemotherapy in advanced non-small cell lung cancer. Medical oncology (Northwood, London, England). 2015;32(1):407.
182. Gazouli M, Anagnostopoulos AK, Papadopoulou A, Vaiopoulou A, Papamichael K, Mantzaris G, et al. Serum protein profile of Crohn's disease treated with infliximab. Journal of Crohn's & colitis. 2013;7(10):e461-70.
183. Walter S, Weinschenk T, Stenzl A, Zdrojowy R, Pluzanska A, Szczylik C, et al. Multipeptide immune response to cancer vaccine IMA901 after single-dose cyclophosphamide associates with longer patient survival. Nature medicine. 2012;18(8):1254-61.
184. Guri Y, Colombi M, Dazert E, Hindupur SK, Roszik J, Moes S, et al. mTORC2 Promotes Tumorigenesis via Lipid Synthesis. Cancer cell. 2017;32(6):807-23 e12.
185. Dalvi PS, Yang S, Swain N, Kim J, Saha S, Bourdon C, et al. Long-term metabolic effects of malnutrition: Liver steatosis and insulin resistance following early-life protein restriction. PloS one. 2018;13(7):e0199916.
186. Ebner M, Sinkovics B, Szczygiel M, Ribeiro DW, Yudushkin I. Localization of mTORC2 activity inside cells. J Cell Biol. 2017;216(2):343-53.

Metabolism Clinical and Experimental 105 (2020) 154186

Contents lists available at ScienceDirect

Metabolism Clinical and Experimental

journal homepage: www.metabolismjournal.com

mTORC1-dependent protein synthesis and autophagy uncouple in the regulation of Apolipoprotein A-I expression

Konstantina Georgila [a,b], Michalis Gounis [a], Sophia Havaki [c], Vassilis G. Gorgoulis [c,d,e], Aristides G. Eliopoulos [b,d,*]

[a] Laboratory of Molecular and Cellular Biology, University of Crete Medical School, Heraklion, Crete, Greece
[b] Department of Biology, School of Medicine, National and Kapodistrian University of Athens, Athens, Greece
[c] Molecular Carcinogenesis Group, Department of Histology and Embryology, School of Medicine, National and Kapodistrian University of Athens, Athens, Greece
[d] Centre of Basic Research, Biomedical Research Foundation of the Academy of Athens (BRFAA), Athens, Greece
[e] Faculty Institute for Cancer Sciences, Manchester Academic Health Sciences Centre, University of Manchester, Manchester, UK

ARTICLE INFO

Article history:
Received 18 December 2019
Accepted 16 February 2020
Available online xxxx

Keywords:
ApoA-I
Autophagy
mTORC1

ABSTRACT

Background: Apolipoprotein A-I (ApoA-I) is involved in reverse cholesterol transport as a major component of HDL, but also conveys anti-thrombotic, anti-oxidative, anti-inflammatory and immune-regulatory properties that are pertinent to its protective roles in cardiovascular, inflammatory and malignant pathologies. Despite the pleiotropy in ApoA-I functions, the regulation of intracellular ApoA-I levels remains poorly explored.
Methods: HepG2 hepatoma cells and primary mouse hepatocytes were used as *in vitro* models to study the impact of genetic and chemical inhibitors of autophagy and the proteasome on ApoA-I by immunoblot, immunofluorescence and electron microscopy. Different growth conditions were implemented in conjunction with mTORC inhibitors to model the influence of nutrient scarcity *versus* sufficiency on ApoA-I regulation. Hepatic ApoA-I expression was also evaluated in high fat diet-fed mice displaying blockade in autophagy.
Results: Under nutrient-rich conditions, basal ApoA-I levels in liver cells are sustained by the balancing act of autophagy and of mTORC1-dependent *de novo* protein synthesis. ApoA-I proteolysis occurs through a canonical autophagic pathway involving Beclin1 and ULK1 and the receptor protein p62/SQSTM1 that targets ApoA-I to autophagosomes. However, upon aminoacid insufficiency, suppression of ApoA-I synthesis prevails, rendering mTORC1 inactivation dispensable for autophagy-mediated ApoA-I proteolysis.
Conclusion: These data underscore the major contribution of post-transcriptional mechanisms to ApoA-I levels which differentially involve mTORC1-dependent signaling to protein synthesis and autophagy, depending on nutrient availability. Given the established role of ApoA-I in HDL-mediated reverse cholesterol transport, this mode of ApoA-I regulation may reflect a hepatocellular response to the organismal requirement for maintenance of cholesterol and lipid reserves under conditions of nutrient scarcity.

© 2020 Elsevier Inc. All rights reserved.

1. Introduction

ApoA-I is the main structural protein of HDL which is responsible for the transfer of unesterified cholesterol and cholesteryl esters from peripheral tissues to the liver [1]. As such, the ApoA-I-containing HDL has attracted tremendous attention for its anti-atherogenic and cardioprotective effects [2,3]. However, the functions of ApoA-I extend beyond cholesterol transport to include a broad spectrum of anti-thrombotic, anti-oxidative, anti-inflammatory and immune-regulatory properties that are pertinent to the protective roles of ApoA-I in inflammation and cancer [4]. Indeed, we and others have shown that ApoA-I and ApoA-I mimetic peptides protect against experimental colitis in the mouse [5,6] and suppress malignant growth *in vitro* and *in vivo* [5,7]. In line with these experimental findings, reduced circulating levels of ApoA-I are associated with increased risk of several human pathologies, including atherosclerotic cardiovascular disease [8], diabetes [9], inflammatory bowel disease [10] and various types of malignancy [11,12], as well as with the clinical response to chemo- [13] and immuno-therapy [14,15].

Despite the pleiotropy in ApoA-I functions, the mechanisms controlling ApoA-I expression remain nebulous. KLF14 and several nuclear hormone receptors, including HNF4 and LRH1, have been reported to stimulate *APOA1* transactivation [16,17]. However, mice with liver-specific inactivation of the HNF4, LRH-1 or KLF14 genes display physiological or near-physiological levels of hepatic ApoA-I [18–20]. Suppressive epigenetic marks conferred by a long non-coding RNA transcribed in the apolipoprotein gene cluster on chromosome 11q23.3 have been incriminated for the absence of *APOA1* transcription in tissues other than the liver and colon where ApoA-I is exclusively detected [21]; yet, further insight into the regulation of ApoA-I expression is required to better understand how changes in intracellular ApoA-I levels occur and may impact disease pathogenesis and therapy. In this context, the

https://doi.org/10.1016/j.metabol.2020.154186
0026-0495/© 2020 Elsevier Inc. All rights reserved.

nature and relative contribution of proteolytic pathways to ApoA-I expression also remain unexplored.

The main pathways responsible for protein degradation are the ubiquitin-proteasome system and (macro)autophagy. Autophagy entails the sequestration of cargo into double membrane vesicles, the autophagosomes, which deliver unwanted or damaged proteins or organelles to the lysosome [22]. Autophagosome biogenesis is controlled by autophagy-related (ATG) proteins [22] and is initiated by the formation of a double-membrane structure called the phagophore, through the activation of the ULK complex comprising ULK1, ATG13, FIP200 and ATG101 and the participation of the activated phosphatidylinositol 3-kinase class III complex involving Beclin-1, Vps34, Vps15 and ATG14. The closure of the autophagosomal membrane is mediated by ATG5 and ATG7-coordinated ubiquitin-like conjugation systems responsible for the conjugation of phosphatidylethanolamine (PE) to MAP1LC3B/LC3 (hereafter: LC3). PE-conjugated ("lipidated") LC3, known as LC3-II, decorates mature autophagosomes. Thus, the relative changes in LC3-II levels that occur in a lysosome-dependent manner and the expression of specific autophagic substrates such as the LC3-II-interacting p62/SQSTM1 protein (hereafter: p62) are indicative of autophagic activity, known as "autophagic flux" [23].

Constitutive (*i.e.* basal) autophagy has a housekeeping role and participates in fundamental cellular and organismal functions that include survival, development, immune and metabolic regulation [24,25]. Autophagy can be further activated in response to various stress-inducing factors, such as nutrient deprivation and DNA damage, as a defense mechanism against the accumulation of damaged macromolecules and organelles, in parallel to providing energy and biological building blocks for biosynthetic and repair processes [22]. Thus, nutrient sensing and autophagy pathways are intertwined and share common regulatory nodes that ensure effective crosstalk [22]. Among them, mTORC1 plays a prominent role by coupling amino-acid availability to protein synthesis and suppression of autophagy. Thus, mTORC1 phosphorylates various kinases and effector molecules involved in protein synthesis, such as the translation suppressor protein 4E-BP1 causing its dissociation from the translation initiation factor eIF4E, and inhibits autophagy through phosphorylation of ULK1 resulting in its inactivation [26].

Perturbations of autophagic activity have been directly linked to several metabolic diseases of the liver, including fatty liver disease and hepatocellular carcinoma [25], conditions in which hepatic ApoA-I levels are found deregulated [27,28]. These findings provided a theoretical link between autophagy and ApoA-I, and prompted us to investigate the role of autophagic and mTORC pathways in the regulation of ApoA-I expression.

2. Materials and methods

2.1. Reagents and antibodies

The following antibodies were used: Rabbit anti-Mouse ApoA-I (Meridian, Life science, Inc., Memphis, TN, USA); Guinea Pig anti-Adipophilin (ADRP) (PROGEN Biotechnik GmbH, Heidelberg, Germany); Goat anti-human ApoA-I (Chemicon International, Billerica, MA, USA); rabbit anti-LC3B (Novus Biologicals, Centennial, CO, USA; immunoblotting); mouse anti-p62 (BD Biosciences, Franklin Lakes, NJ, USA); mouse anti-GAPDH (*Sigma*-Aldrich, St. Louis, MO, *USA*); p53 and HSP90 (*Santa Cruz Biotechnology*, CA, USA); rabbit anti-LC3B for immunofluorescence, Beclin-1, ULK1 4E-BP1, phospho-4E-BP1 ($Thr^{37/46}$), p-Akt (Ser^{473}), Raptor, Rictor (Cell Signaling Technology Inc. Danvers, MA, USA); mouse anti-actin and rabbit anti-Akt1 antibodies (*Millipore*, Billerica, MA, USA). Secondary donkey anti–goat, anti–mouse Alexa Fluor 488, anti–goat Alexa Fluor 568 and goat anti–rabbit Alexa Fluor 594–conjugated antibodies were purchased from *Sigma*-Aldrich and ProLong® Gold Antifade Reagent with DAPI from Cell Signaling Technology Inc. Cells were treated with 50 nM bafilomycin A1, 10 μM chloroquine diphosphate, 10 μM CHX, 500 nM oleic acid (all from *Sigma*-Aldrich), 250 nM Torin2 (Cayman Chemical, Ann Arbor, MI, USA), 100 nM human insulin (Eli Lilly, Indianapolis, IN, USA) or 10 μM MG132 (*Millipore*, Billerica, MA, USA). All culture media and aminoacids were purchased from Life Technologies, Carlsbad, CA, *USA*.

2.2. Cell culture and transfection assays

HepG2 and HEK293T cells were cultured in low glucose DMEM (Life Technologies), supplemented with 10% FBS and antibiotics (100 U/ml penicillin, 100 mg/ml streptomycin); referred as standard media or SM. For DNA transfection, HEK293T cells were seeded in 24-well plates and transfected with a total of 0.1 μg of pEGFP-C2 (Clontech, Heidelberg, Germany) or pAdTrack-CMV-*APOA1* (a gift from Professor D. Kardassis, University of Crete) using the Lipofectamine 2000 (Life Technologies). RNAi was performed using 10 pmol of siRNAs as previously described [29]. The Silencer® Select siRNAs for *ULK1* (ID: s15963 and s15965), *MAP1LC3B* (ID s196887 and s37748), *BECN1* (ID: s16537 and s16538), *RAPTOR* (ID s33216 and s33215), *RICTOR* (ID s48408 and s226000) and the unrelated Luciferase (AM16204) gene that was used as negative control for sequence independent effect [29] were purchased from Life Technologies.

2.3. Primary mouse hepatocytes and liver lysates

Hepatocytes were isolated by a single two step collagenase perfusion. Briefly 9–14 weeks-old male mice were anesthetized with ketamine/xylazine and livers were perfused *via* cannulation of the inferior vena cava, clumping of the suprahepatic inferior vena cava and incision of the mesenteric vein, first with Liver Perfusion medium, followed by perfusion with Liver Digest medium (Life Technologies). Subsequently, livers were minced on a Petri dish and filtered through a sterile 100 μm nylon mesh. Isolated hepatocytes were washed three times with Hepatocyte Wash medium and centrifuged at 50 ×*g* for 5 min. Purification of hepatocytes was made with Percoll (*Sigma*-Aldrich) density gradient separation. After washing of purified hepatocytes, cell pellet was resuspended in Plating medium, supplemented with 10% FBS and penicillin, steptomycin and gentanamycin. Viability was determined by trypan blue exclusion and hepatocytes were seeded for further treatments in Maintenance medium. Modeling of steatosis was performed in 8-week-old male C57BL/6 mice fed a high-fat diet (HFD; 60% energy from lipids) or a normal standard diet (ND) (both purchased from Mucedola, Italy) for 10 weeks under SPF conditions and a 12 h light-dark cycle. All procedures were conducted in compliance with protocols approved by the Animal Care Committee of the University of Crete, School of Medicine (Heraklion, Crete, Greece) and from the Veterinary Department of the Region of Crete (Heraklion, Crete, Greece).

2.4. Immunoprecipitation and immunoblotting

Cells lysis and immunoblotting were performed as previously described [29]. Fractionation of cytoplasmic and membrane proteins was performed with Subcellular Protein Fractionation Kit for Cultured Cells according to manufacturer's instructions (Thermo Scientific, San Jose, CA, USA). Protein signal intensities (densitometric values of protein bands) were normalized to GAPDH or β-actin loading control for each sample at non-saturating exposures using the Image J Software. ApoA-I was immunoprecipitated from 0.5 mg cleared lysates overnight at 4 °C. The complexes were then bound to protein G sepharose beads (BD Biosciences, Oxford, UK) for 8 h at 4 °C with gentle mixing. After washing with IP lysis buffer (50 mM Tris-Cl pH 7.4, 250 mM NaCl, 5 mM EDTA, 1% NP-40), bead-bound protein complexes were retrieved using Laemmli buffer and boiling. Samples were then analyzed on polyacrylamide gels.

2.5. Immunofluorescence staining

To analyze co-localization of ApoA-I with autophagic markers, HepG2 cells were fixed with 4% paraformaldehyde for 15 min at RT (further fixation with methanol for 10 min at −20 °C, in the case of LC3 staining). Cells were washed twice with PBS before permeabilization and blocking with 0.3% Triton X-100 (Sigma-Aldrich), 5% horse serum in PBS for 60 min. Primary antibody incubation (1:200 LC3B, 1:100 ApoA-I, 1:200 p62) in 1% BSA, 0.3% Triton X-100 (in PBS) was performed overnight at 4 °C. After secondary antibody incubation in 1% BSA, 0.3% Triton X-100 (in PBS) for 1 h at RT, cells were washed and mounted on microscope slides using Prolong® Gold AntiFade Reagent with DAPI from Cell Signaling Technology. For image acquisition, the AxioObserver Z1 inverted fluorescence microscope equipped with ApoTome.2, an EC Plan-Neofluar objective (100×/1.30 oil lens) and the Zen lite software (all by Carl Zeiss Microscopy GmbH, Hamburg, Germany) were used and z stack images were generated using Image J. The same settings of light source intensity and exposure time were used between samples in order to compare the intensity of fluorescent signals.

2.6. Electron microscopy

HepG2 cells were fixed in 3% formaldehyde and 0.5% glutaraldehyde in 0.1 M phosphate buffer, pH 7.4, for 30 min at RT, harvested using scraper and centrifuged at 800*g* for 5 min at RT. The supernatant was aspirated and the cells were resuspended in 4% gelatin aqueous solution, centrifuged at 800 *g* for 5 min at RT and the gelatin with the cell pellet was cooled on ice. Under stereoscope the solidified cell pellet with gelatin was cut into small fragments (1–2 mm^3). The cell-gelatin fragments were then dehydrated, infiltrated and finally embedded in Lowicryl HM20 acrylic resin at −50 °C according to the Progressive Lowering of Temperature method [30], using a Leica EM AFS apparatus. Ultrathin acrylic sections (60–70 nm thickness) were cut on a Leica Ultracut R ultramicrotome equipped with a Diatome diamond knife and mounted onto 200-mesh formvar-coated nickel grids for immunolabeling. For ApoA-I immunogold labeling Ultrathin acrylic sections of cells were first incubated on drops of 0.1 M glycine for 30 min at RT to block free aldehyde groups. After washing with 0.05 M Tris/HCl buffer, pH 7.4, the sections were placed on drops of blocking buffer containing 5% normal donkey serum, 0.1% Tween-20, 0.1% fish gelatin and 1% chicken serum albumin (CSA) in 0.05 M Tris/HCl buffer, pH 7.4 for 30 min at RT, and then transferred on drops of the primary antibody (1:100) diluted in 0.05 M Tris/HCl buffer, pH 8.0, containing 0.1% Tween-20, 0.1% fish gelatin and 1% CSA overnight at 4 °C. Control sections were incubated in the absence of primary antibody. The grids were rinsed (×10; 1 min each) with 0.05 M Tris/HCl, pH 7.4 containing 0.1% Tween-20 (solution I), with three changes (1 min each) of 0.05 M Tris/HCl, pH 7.2 containing 0.2% CSA and 0.1% Tween-20 (solution II) and finally, one change for 5 min of 0.05 M Tris/HCl, pH 8.2 containing 1% CSA and 0.1% Tween-20 (solution III). The grids were drained and incubated for 1 h at RT with secondary antibody conjugated to 10 nm gold particles (1:40) diluted in solution III and they were washed with agitation in three changes (1 min each) of solution II, five changes (1 min each) of solution I and five changes of distilled water. Finally, ultrathin sections were counterstained with ethanolic uranyl acetate followed by lead citrate and observed in a FEI Morgagni 268 transmission electron microscope and micrographs were taken with an Olympus Morada digital camera.

2.7. Proteasome activity assay

Proteasome CT-L activity was assayed as previously described [31,32] based on the hydrolysis of the fluorogenic peptide LLVY-AMC (Enzo Life Sciences, Farmingdale, NY, USA), measured on VICTOR Multilabel Plate Reader (PerkinElmer, Woodbridge, ON, Canada).

2.8. RNA extraction, cDNA synthesis and qPCR

RNA isolation, cDNA synthesis and qPCR were performed as previously described [29]. The *APOA1* (Hs00985000_g1) and *ACTB* (Hs99999903_m1) TaqMan Gene Expression Assays (Applied Biosystems, Foster City, CA, USA) were used in an ViiA™ 7 Real-Time PCR engine. The relative gene expression was calculated using the comparative CT method. A second reference gene, *Beta Glucuronidase* (β-*GUSB)* (TaqMan Assay ID: Hs99999908_m1, Applied Biosystems, Foster City, CA, USA) was used to confirm quantitative differences.

2.9. Statistical analysis

Statistical analysis was performed using PRISM (Graphpad Software Inc. La Jolla, CA, USA). Results are expressed as mean ± SD. Statistical significance either with Student's *t*-test or with the non-parametric Mann-Whitney test. For comparisons involving more than two groups, one-way analysis of variance (ANOVA) with a *post hoc* Tukey multiple comparison test being used to assess the differences between the groups. Statistical significance was defined as the conventional *p* value of <0.05.

3. Results

3.1. Steatosis is associated with elevated levels of ApoA-I

Extensive evidence suggests that suppression of hepatic autophagy is causally linked to the development of steatosis (reviewed in [33,34]). In line with this evidence, long-term feeding of mice with high fat diet results in both hepatic accumulation of p62, an established autophagy substrate, and of adipophilin (ADRP), a marker of lipid accumulation [35] but not in elevated mTORC1 activity (Suppl. Fig. 1A). Interestingly, the intracellular levels of ApoA-I were also found elevated in the livers of HFD-fed mice (Fig. 1A), whereas *APOA1* transcription remained unaffected (Fig. 1B). We further modeled this association by culturing primary mouse hepatocytes with oleic acid for 12 h, in the presence or absence of NH_4Cl which blocks the fusion of autophagosomes with lysosomes and of the lysosomal protease inhibitor leupeptin. The results (Fig. 1C) showed that treatment with NH_4Cl and leupeptin leads to accumulation of ApoA-I, implicating autophagy in ApoA-I regulation.

3.2. Autophagy but not proteasomal inhibitors lead to intracellular ApoA-I accumulation

We explored the relative contribution of the major proteolytic pathways, autophagy and proteasome, to the regulation of basal ApoA-I levels. To this end, HepG2 hepatoma cells which represent an established model to study ApoA-I biosynthesis and secretion [36–38], were cultured in the presence of bafilomycin A1 (BAF) which inhibits the late steps in the autophagic process [39]. Immunoblot analysis of lysates showed that BAF caused a time-dependent increase in ApoA-I levels in parallel to the accumulation of the lipidated form of LC3-II and of p62 (Fig. 2A). Accumulation of ApoA-I occurred in the absence of an effect on transcription (Fig. 2B). Unlike BAF, treatment of HepG2 cells with the proteasomal inhibitor MG132 did not affect ApoA-I but caused the accumulation of p53, a known target of the ubiquitin-proteasome pathway (Fig. 2C), and abrogation of chymotrypsin-like activity associated with the 20S proteasome (Supplementary Fig. 1B). These data indicate that autophagy, rather than the proteasome, is the main proteolytic pathway responsible for ApoA-I proteolysis.

The generality of this observation was confirmed in ApoA-I-negative HEK293 cells upon heterologous expression of *APOA1*, followed by exposure to BAF (Fig. 2D) or CHQ, an inhibitor of autophagosome fusion with lysosomes [40] (Fig. 2E). Treatment of primary mouse hepatocytes

with either NH_4Cl + leupeptin (Fig. 1C) or CHQ (Supplementary Fig. 1B) also resulted in ApoA-I accumulation.

3.3. Autophagic pathway components associate with ApoA-I

We combined fractionation and immunofluorescence in HepG2 cells to further characterize the intracellular fate of ApoA-I upon autophagy inhibition. At standard growth conditions, ApoA-I was detected by immunoblot predominantly in the membrane fraction and, to a lesser degree the cytosol, whereas lipidated LC3 was found exclusively in the membrane fraction (Supplementary Fig. 1D). Upon cell treatment with BAF, a significant increase in LC3-II levels was noted in the membrane fraction where ApoA-I was also predominantly detected (Supplementary Fig. 1D). This observation prompted us to evaluate the association of ApoA-I with autophagic pathway components as well as its localization in autophagosomes.

We performed double immunofluorescence studies to monitor co-localization of ApoA-I with lipidated LC3 (LC3-II) which resides on the autophagosomal membranes [23]. At standard growth conditions, ApoA-I showed a staining pattern consistent with predominant expression in ER and Golgi, in line with previous reports [41,42]. However, upon treatment with BAF, the ApoA-I specific fluorescence increased and the protein progressively co-localized with LC3-II (Fig. 3A).

The association of ApoA-I with autophagosomes was further investigated by electron microscopy. Inhibition of autophagy led to an increase in both the size and the number of autophagosomes (data not shown). Immunogold labeling of ApoA-I revealed the presence of ApoA-I molecules on autophagic vesicles at steady state, which was dramatically enhanced upon BAF treatment (Fig. 3B).

The accumulation of ApoA-I in autophagic vesicles upon autophagy inhibition was supported by the increased co-localization of ApoA-I with the autophagic cargo receptor p62, following treatment with BAF (Fig. 3C). To address whether ApoA-I directly interacts with p62, we performed co-immunoprecipitations of endogenous ApoA-I with p62 using lysates from the membrane fraction of HepG2 cells treated with BAF where LC3-II is predominantly detected (see Supplementary Fig. 1D). The results showed that ApoA-I co-precipitates with p62 upon autophagy inhibition (Fig. 3D).

Finally, we tested whether ApoA-I accumulation was associated with endolysosomal membranes by imaging ApoA-I co-localization with the lysosome marker LAMP1. As shown in Supplementary Fig. 1E, treatment of HepG2 cells with BAF led to largely co-localized ApoA-I with enlarged perinuclear LAMP1 compartments.

3.4. Genetic inhibition of autophagic pathway components leads to impaired ApoA-I proteolysis

Autophagy may occur through canonical and non-canonical pathways, the latter being mediated in ULK1 and Beclin1-independent manner [43]. In order to mechanistically explore the autophagic pathway responsible for ApoA-I regulation, we performed gene silencing of Beclin1 and ULK1 that are involved in the early stages of canonical autophagy and, as control, the late pathway component LC3. As expected, the RNAi-mediated knockdown of either Beclin1 or ULK1 led to reduced LC3-II *vs* LC3-I with concomitant increase in p62 (Fig. 4A-B). ApoA-I levels also accumulated, suggesting that ULK1 and Beclin1 are involved in the autophagic pathway regulating ApoA-I degradation. The knockdown of LC3 also led to ApoA-I accumulation (Fig. 4C) in line with the co-localization of ApoA-I with LC3-II upon BAF treatment (Fig. 3A).

3.5. Starvation leads to inhibition of de novo synthesis of ApoA-I rather than autophagy-mediated ApoA-I degradation

The aforementioned results demonstrate that basal autophagy impacts on ApoA-I turnover. We next sought to determine if induction of autophagy could respectively reduce ApoA-I expression. To this end, HepG2 cells were cultured under conditions of amino-acid and serum depletion in EBSS, a process known to result in the activation of autophagy [23,44]. In comparison to cells cultured in standard conditions, EBSS led to dramatic reduction in ApoA-I levels both in total and fractionated (cytoplasmic and membrane) lysates (Fig. 5A and Supplementary Fig. 2A). This reduction was paralleled by rapid loss of phosphorylated 4E-BP1, a major component of CAP-dependent translational initiation, but not of p62 which showed a slower kinetics of reduction (Fig. 5A). Notably, whereas ApoA-I protein levels rapidly declined upon starvation, *APOA1* mRNA expression remained unaffected (Supplementary Fig. 2B and D).

These observations prompted us to combine EBSS with BAF. We reasoned that if the EBSS-mediated reduction in ApoA-I is due to autophagy induction, treatment with BAF should result in ApoA-I accumulation. Surprisingly, BAF did not reverse the EBSS-mediated reduction in ApoA-I (Fig. 5B). We found that these changes occurred in the absence of an effect on *APOA1* transcription (Supplementary Fig. 2C and D) and we have excluded the possibility that the reduced intracellular levels of ApoA-I, imposed by starvation, could be attributed to exaggerated secretion; in fact, HepG2 cells cultured in EBSS displayed significant loss of ApoA-I secretion (Fig. 5C).

The inability of BAF to reverse the effect of EBSS on intracellular ApoA-I levels suggests that mechanisms triggered by starvation other than autophagy may dominate the regulation of ApoA-I expression in this setting. We thus embarked on studies aiming to identify factors that are present in standard culture media and could recover both the basal levels of ApoA-I in starved cells and the response to autophagy inhibition. Such putative molecules are lipids and aminoacids. We first cultured cells with EBSS supplemented with BSA-conjugated oleic acid or, as a control BSA alone, in the presence or absence of BAF. In comparison to EBSS, addition of oleic acid failed to recover ApoA-I to the levels of standard culture conditions and its response to BAF (Fig. 5D).

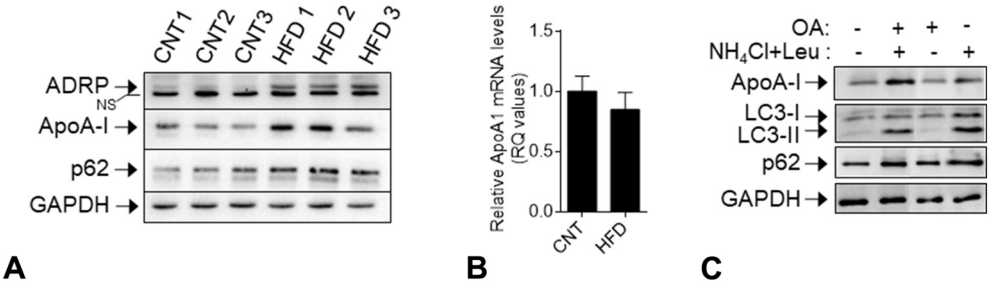

Fig. 1. Steatosis is associated with autophagy inhibition and elevated levels of ApoA-I. (A) Representative immunoblot analysis of proteins extracted from livers of mice fed high-fat diet (HFD) for 12 weeks and their respective control animals (CNT) fed normal chow. *NS; non-specific.* (B) *APOA1* mRNA expression in the same liver tissues described in (*A*). *APOA1* mRNA was normalized to the housekeeping β-actin gene (data are expressed as the mean ± SD of 3 mice of each group). (C) Representative immunoblot analysis of protein lysates from primary mouse hepatocytes modeling steatosis. Cells were exposed to 500 μM oleic acid (OA) in the presence or absence of the autophagic inhibitors NH_4Cl + leupeptin for 12 h and analyzed for the indicated proteins.

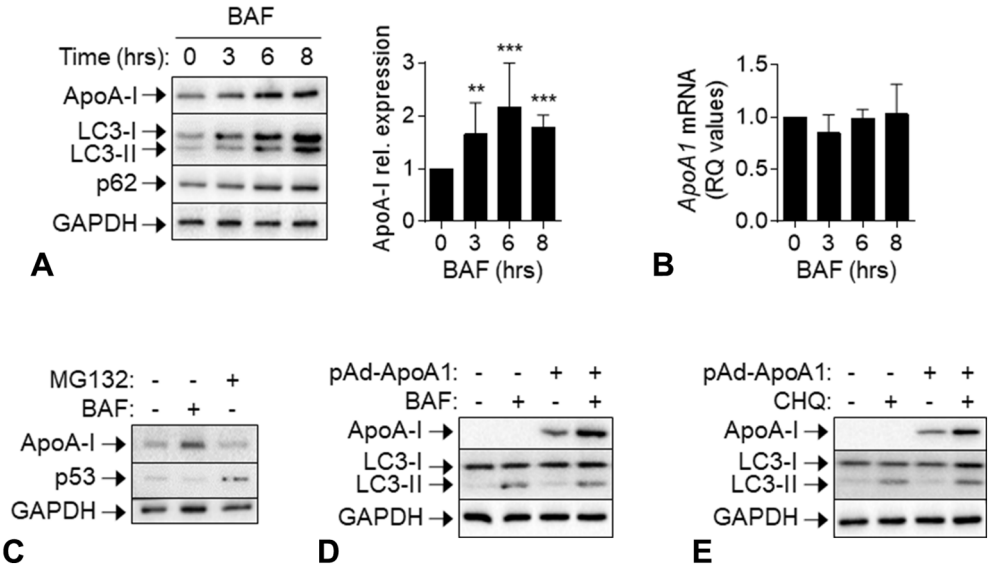

Fig. 2. Inhibition of autophagy, but not the proteasome, leads to ApoA-I accumulation. (A) Representative immunoblot analysis of protein lysates from HepG2 cells exposed to the autophagic inhibitor BAF for 3, 6 and 8 h for the indicated proteins. The levels of ApoA-I normalized to GAPDH were quantified from 5 independent experiments and shown in the graph. Values are expressed relative to those of untreated control cells that were given the arbitrary value of 1 ($^{**}p < 0.01$, $^{***}p < 0.001$). (B) *APOA1* mRNA expression levels in HepG2 cells exposed to BAF for 3, 6 and 8 h relative to untreated controls which were given the arbitrary value of 1. *APOA1* mRNA was normalized to the housekeeping β-actin gene (data are expressed as the mean ± SD of at least 3 experiments). (C) Immunoblot analysis of protein lysates from HepG2 cells exposed to BAF or the proteasomal inhibitor MG132 for the indicated proteins. p53 was used as positive control for the effect of the proteasomal inhibitor. (D & E) Immunoblot analysis of protein lysates from HEK293T cells transfected with ApoA-I expression vector (pAd-ApoA1) or empty vector as control and exposed to BAF *(D)* or CHQ *(E)*. Changes in LC3-II and p62 levels indicate the effect of the autophagy inhibitors.

Autophagy inhibition by BAF was otherwise functional, as evidenced by the relative accumulation of LC3-II and of the autophagy marker p62 (Fig. 5D). In contrast, addition of aminoacids to EBSS enabled expression of ApoA-I to near control culture levels which further accumulated upon treatment with BAF (Fig. 5E). Additional analyses showed that both essential and non-essential aminoacids are required for maintaining ApoA-I levels (Supplementary Fig. 2E).

During these studies we also noted a correlation between levels of ApoA-I expression and phosphorylation of 4E-BP1: addition of oleic acid to EBSS failed to phosphorylate 4E-BP1 and to recover ApoA-I

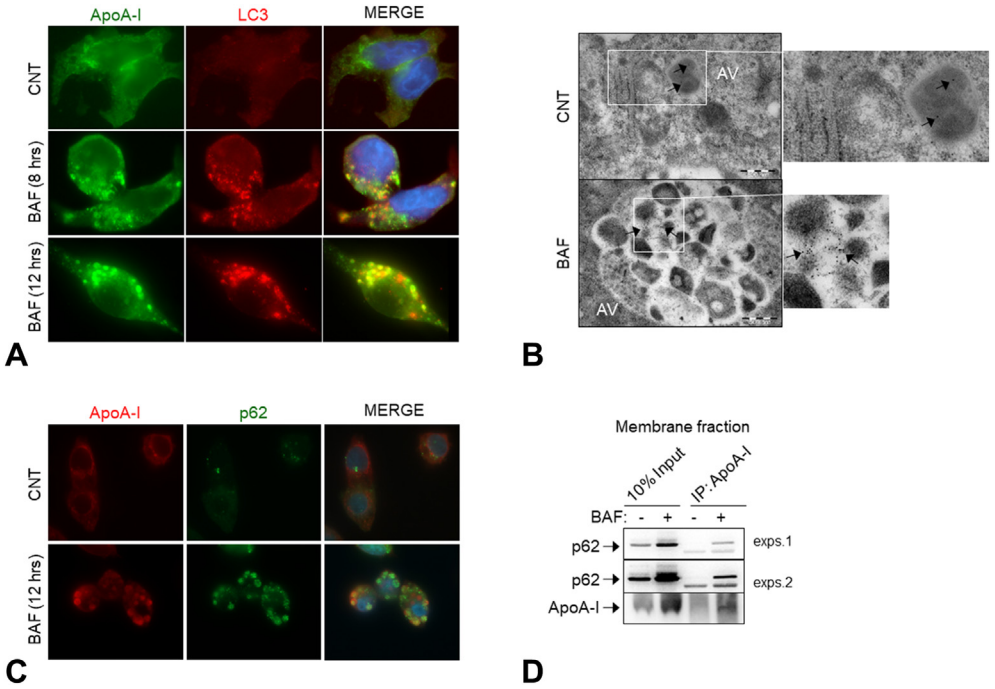

Fig. 3. ApoA-I co-localizes with autophagosomes. (A) Representative immunofluorescence images showing co-localization of ApoA-I (green) and LC3 (red) in HepG2 cells exposed to BAF. Nuclei are highlighted with DAPI (blue). For image acquisition 100× lens magnification was used. (B) Electron micrographs of HepG2 cells stained with ApoA-I immunogold. *AV*; autophagic vacuoles. Arrows indicate gold particles (black dots). Scale bar: 500 nm. Insets show higher magnification. (C) Representative immunofluorescence images showing co-localization of ApoA-I (red) and p62 (green) in HepG2 cells exposed to BAF. Nuclei are highlighted with DAPI (blue). For image acquisition 63× lens magnification was used. (D) ApoA-I was immunoprecipitated (IP) from lysates from the membrane fraction of HepG2 cells treated with BAF or left untreated. ApoA-I-bound p62 was detected by immunoblotting with anti-p62. Ten percent of membrane protein lysate (input) was also immunoblotted. Two different exposures (exps) are shown for the anti-p62 immunoblot. (For interpretation of the references to color in this figure legend, the reader is referred to the web version of this article.)

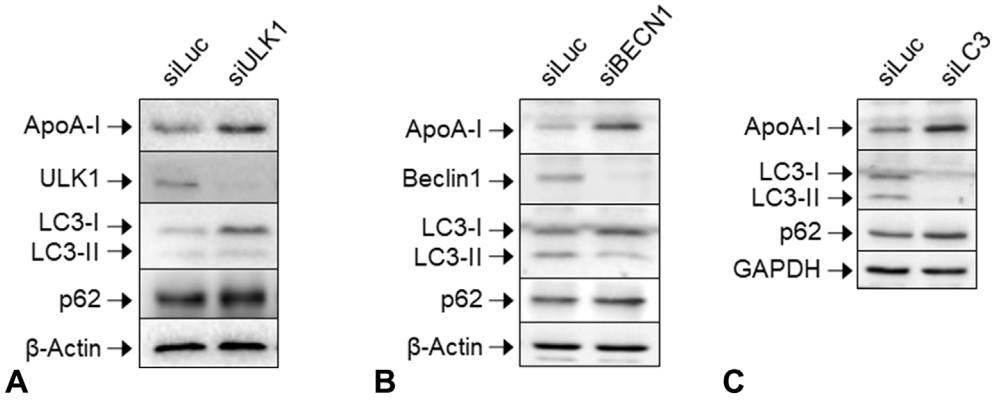

Fig. 4. Autophagic degradation of ApoA-I is Beclin1 and ULK-1 dependent. Immunoblot analysis of lysates from HepG2 cells transiently transfected with siRNA targeting (A) ULK1 (siULK1), (B) Beclin1 (siBECN1) and (C) MAP1LC3B (siLC3) or control siRNA targeting the unrelated Luciferase gene (siLuc). GAPDH and β-actin were used as loading controls. p62 and LC3-II were used as markers of autophagic flux.

expression whereas aminoacids engaged 4E-BP1 phosphorylation, and recovered both basal levels of ApoA-I and its response to autophagy (Fig. 5D-E and Supplementary Fig. 2E). This observation indicated that ApoA-I has a high turnover and that protein synthesis is required to maintain its intracellular levels. This hypothesis was tested by addition of cycloheximide (CHX), an inhibitor of *de novo* protein synthesis, to HepG2 cultures growing in complete, standard growth media. Immunoblot analysis of lysates demonstrated a half-life for ApoA-I of approximately 30 min, confirming that active protein synthesis is required to maintain intracellular ApoA-I levels (Fig. 5F). In contrast, the levels of LC3 and p62 remained unaffected during this course of CHX treatment.

3.6. mTORC1 signaling is required for basal ApoA-I expression

The mTOR complexes mTORC1 and mTORC2 are master regulators of cell metabolism and growth in response to nutrient availability [45]. mTORC1 responds to aminoacid availability to control biosynthetic and catabolic pathways, including translation and autophagy, respectively.

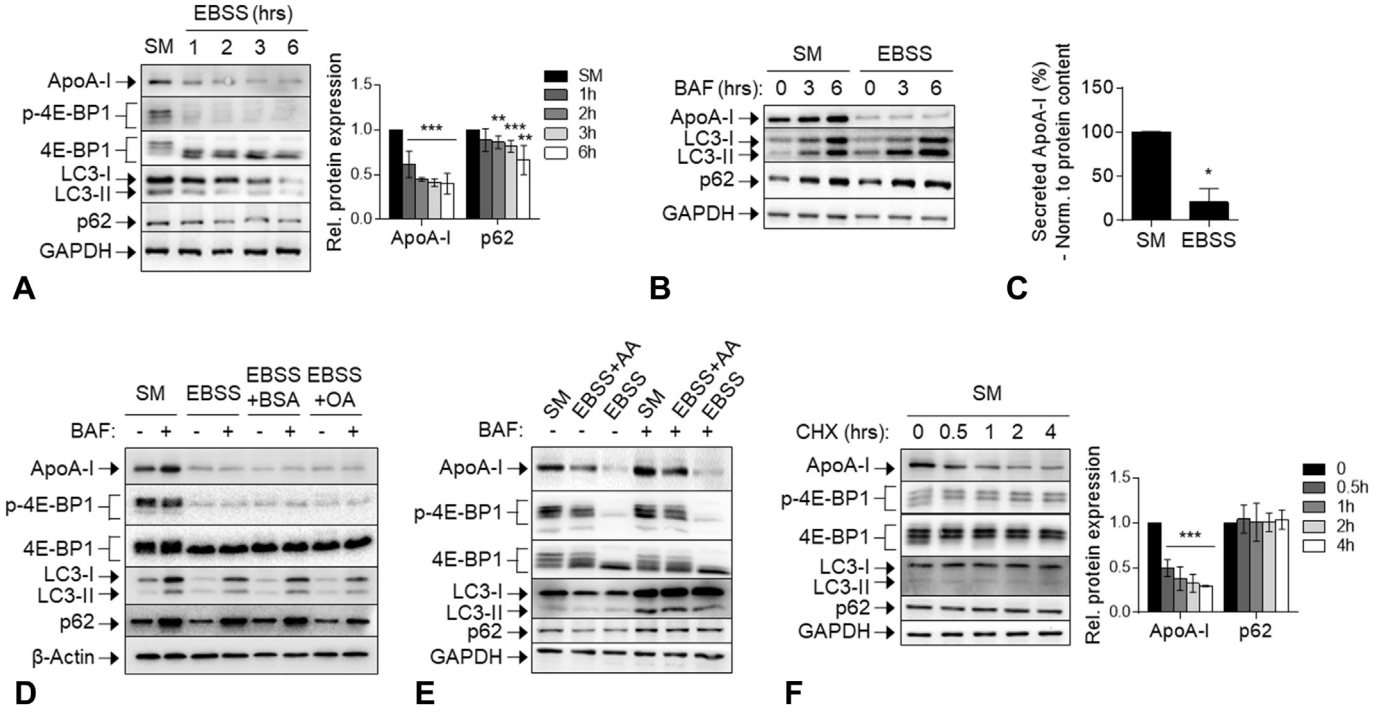

Fig. 5. ApoA-I levels critically depend on aminoacid availability and de novo protein synthesis. (A) Immunoblot analysis for the indicated proteins of lysates from HepG2 cells cultured in standard medium (SM) or amino acid deficient medium (EBSS) for 1, 2, 3 and 6 h. Quantification of ApoA-I and p62 levels normalized to GAPDH are shown in the graph of the right panel. Values are expressed relative to those in untreated control cells that were given an arbitrary value of 1 and are expressed as the mean ± SD of at least 3 experiments; $^{**}p < 0.01$ and $^{***}p < 0.001$. (B) Immunoblot analysis of lysates from HepG2 cells cultured in SM or EBSS in the presence or absence of BAF for the indicated time periods. (C) Analysis of secreted ApoA-I levels measured by ELISA in HepG2 cells cultured in SM or EBSS for 8 h. Secreted ApoA-I levels are expressed relative to cells cultured in SM that were given an arbitrary value of 100 and are normalized to total protein content of the respective cell lysate (data are expressed as the mean ± SD of 2 experiments; $^{*}p < 0.05$). (D) Immunoblot analysis of lysates from HepG2 cells cultured in EBSS in the presence or absence of BAF, with or without 500 nM BSA-conjugated oleic acid (OA) supplementation. BSA supplementation served as control. (E) Immunoblot analysis for the indicated proteins of lysates from HepG2 cells cultured in EBSS in the presence or absence of BAF with or without amino acid (AA) supplementation. (F) Immunoblot analysis for the indicated proteins of lysates from HepG2 cells treated with 10 μM CHX for 0.5, 1, 2, 3, 4 h. Quantification of ApoA-I and p62 levels normalized to GAPDH was performed from at least 3 experiments and shown in the right panel graph. Values are expressed relative to those in untreated control cells that were given an arbitrary value of 1 and are expressed as the mean ± SD; $^{***}p < 0.001$.

mTORC2 controls proliferation and survival primarily by phosphorylating several members of the AGC (PKA/PKG/PKC) family of protein kinases, including Akt [26].

Prompted by the aforementioned effect of aminoacid availability on ApoA-I expression levels, we investigated the impact of mTORC1/2 on ApoA-I regulation. We exposed HepG2 cells to Torin2, a small molecule inhibitor of mTORC1/2 [46], under standard (Fig. 6A) or EBSS culture conditions (Fig. 6C). As previously reported in other cell types [46], treatment of HepG2 cells with Torin2 efficiently abolished mTORC1 and mTORC2 activities, evidenced by the reduced phosphorylation of 4E-BP1 at $Thr^{37/46}$ and of Akt at Ser^{473}, respectively (Fig. 6C). In line with the prominent role of mTORC1 inactivation in autophagy induction, treatment of HepG2 cells with Torin2 also increased autophagic flux as documented by the changes in the expression of lipidated LC3 and p62 (Fig. 6A and C).

Similar to the effect of EBSS on ApoA-I (Fig. 5A-B), Torin2 reduced ApoA-I protein levels without having an effect on *APOA1* mRNA expression, and co-treatment with BAF did not significantly affect ApoA-I expression at protein or mRNA level (Fig. 6A-B). When Torin2 was applied in HepG2 cells cultured in EBSS medium, no further change in ApoA-I expression was observed, whereas switching culture media from EBSS to standard culture conditions recovered ApoA-I expression levels and sensitivity to Torin2 (Fig. 6C).

Starvation or treatment with Torin2 impacts on both mTORC1 and mTORC2 activities, documented by decreased phosphorylation of 4E-BP1 and Akt (Fig. 6A and C). To clarify which of mTORC1 or mTORC2 is implicated in ApoA-I regulation, we cultured HepG2 cells in the presence of insulin that is known to activate mTORC2 but not mTORC1 [47]. We found that insulin induced a time-dependent increase in the Ser^{473} phosphorylated Akt that was not accompanied by changes in mTORC1-dependent phosphorylation of 4E-BP1 or ApoA-I levels (Fig. 6D). Moreover, whereas EBSS inhibited mTORC1-mediated 4E-BP1 phosphorylation and reduced ApoA-I levels, neither was affected by insulin treatment (Fig. 6D). These observations suggest that mTORC2 is not involved in the regulation of ApoA-I.

Along these lines, co-treatment of starved (EBSS) cells with insulin and Torin2 did not affect ApoA-I (Fig. 6E). In contrast, Torin2 reduced intracellular ApoA-I levels in the presence of aminoacids irrespectively of insulin addition, suggesting that mTORC1 is responsible for ApoA-I regulation (Fig. 6E).

To provide direct evidence of ApoA-I regulation by mTORC1, we performed siRNA-mediated knock-down of Raptor and Rictor, the main protein subunits of mTORC1 and mTORC2 complexes, respectively [45]. Knock-down of Raptor, but not Rictor, resulted in significant decrease in ApoA-I protein levels, providing conclusive support for the regulation of ApoA-I by mTORC1 (Fig. 6F).

4. Discussion

ApoA-I is predominantly produced in hepatocytes and represents approximately 70% of the protein content of HDL. Recent studies have expanded the role of ApoA-I beyond the HDL-mediated reverse cholesterol transport to include a broad spectrum of anti-thrombotic, antioxidative, anti-inflammatory and immune-regulatory properties that are pertinent to the protective roles of ApoA-I in cardiovascular, inflammatory and malignant diseases [4]. ApoA-I expression differs among individuals and low ApoA-I levels correlate with increased risk of development of several colon and liver pathologies [11,12]. Despite the emergence of a multitude of ApoA-I functions, little is known about the mechanisms responsible for its regulation.

Data presented herein underscore the major contribution of post-transcriptional mechanisms to the regulation of basal ApoA-I expression. Using the hepatoma cell line HepG2 which retains the ability to synthesize and secrete ApoA-I in a manner similar to normal hepatocytes [36,42,48], we show that intracellular ApoA-I protein levels may significantly vary in the absence of changes in mRNA expression. Thus,

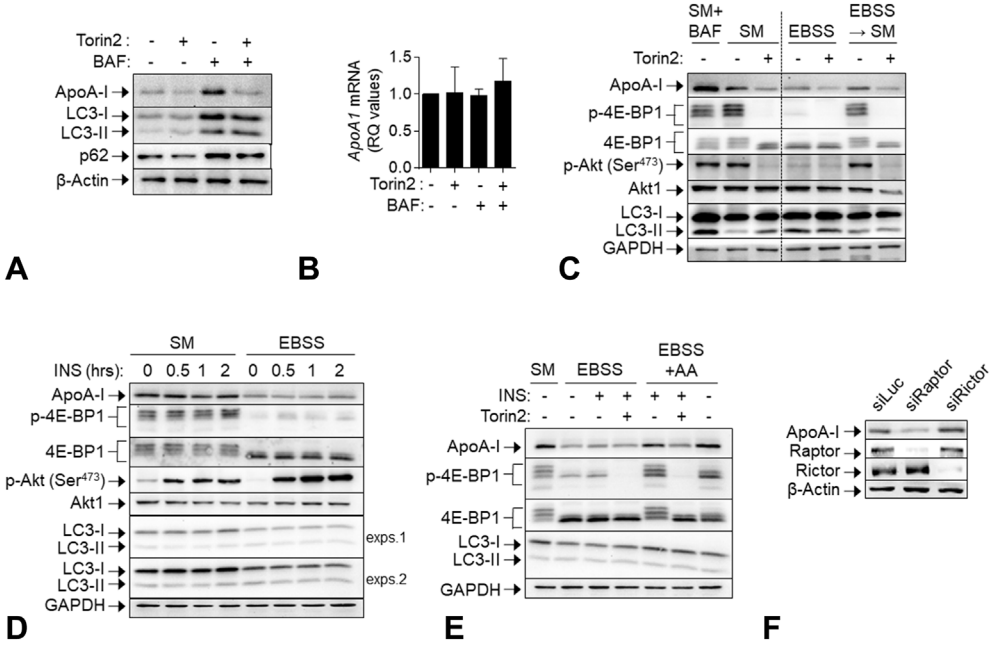

Fig. 6. ApoA-I turnover is regulated by mTORC1 signaling pathway. (A) Immunoblot analysis and (B) relative mRNA expression levels of *APOA1* in HepG2 cells treated with 250 nM Torin2 and/or BAF for 6 h, or left untreated. *APOA1* mRNA expression levels were normalized to the housekeeping β-actin gene and expressed as RQ values relative to untreated controls, which was given the arbitrary value of 1 (data are expressed as the mean ± SD of at least 3 experiments). (C) Immunoblot analysis of lysates from HepG2 cells cultured in standard medium (SM) or in amino acid deficient medium (EBSS) or exposed to EBSS for 3 h and subsequently switched to SM for 6 h (EBSS→SM), in the presence or absence of 250 nm Torin2. Treatment of cells with BAF in lane 1 serves as positive control for ApoA-I accumulation. (D) Immunoblot analysis of lysates from HepG2 cells cultured in SM or in EBSS in the presence or the absence of 100 nM insulin (INS). Insulin was added during the last 0.5, 1, or 2 h of incubation with EBSS or SM. (E) Immunoblot analysis of lysates from HepG2 cells cultured in EBSS or EBSS supplemented with amino acids (AA) and treated with 100 nM INS and/or 250 nM Torin2. Cells cultured in SM served as control. (F) Immunoblot analysis of lysates from HepG2 cells transiently transfected with siRNA targeting mTORC1 subunit Raptor (siRaptor), mTORC2 subunit Rictor (siRictor) or control siRNA (siLuc). 4E-BP1 and Akt phosphorylation were used as surrogates for mTORC1 and mTORC2 activity respectively, and p62 and LC3-II were used as markers of autophagic flux. GAPDH and β-actin serve as loading controls.

whereas ApoA-I protein levels are exquisitely sensitive to aminoacid depletion, *APOA1* transcription remains intact (Fig. 5 and Supplementary Fig. 2). In line with this observation, inhibition of *de novo* protein synthesis by CHX revealed rapid turnover of ApoA-I with an estimated protein half-life of approximately 30 min (Fig. 5F). We further report that ApoA-I proteolysis occurs through autophagy rather than the proteasome pathway. Indeed, exposure of HepG2 cells or of primary mouse hepatocytes to autophagy inhibitors led to accumulation of intracellular ApoA-I in the absence of an effect on *APOA1* transcription, whereas both ApoA-I protein and mRNA levels remained unaffected by the proteasome inhibitor MG132 (Fig. 2). The aforementioned findings challenge the traditional view of the proteasome and autophagy pathways targeting short-lived and long-lived proteins for degradation, respectively, and align with recent reports showing that autophagy may also target short-lived proteins, including Cyclin D1 [49], the gap junction protein Connexin 43 [50], and TRIM5α (Tripartite motif-containing protein 5α), an effector of cellular anti-viral response [51].

Our results also implicate the canonical autophagic pathway, mediated through ULK1 and Beclin-1, and SQSTM1/p62 in the regulation of ApoA-I (Fig. 4). SQSTM1/p62 is an adaptor protein that links cargo material to the nascent phagophore *via* its capacity to interact directly with LC3. Herein we showed that ApoA-I co-localizes and co-precipitates with p62, suggesting that it is a p62 cargo in autophagy.

SQSTM1/p62 is itself degraded upon induction of autophagy. Surprisingly, we observed that starvation of HepG2 cells from growth factors and essential biological building blocks triggers autophagy and p62 degradation with slower kinetics compared to the reduction in ApoA-I levels under the same conditions. Instead, the reduction in ApoA-I was paralleled by the loss of 4E-BP1 phosphorylation, a process known to depend on the nutrient sensor mTORC1.

Mammalian TORC1 activates anabolic processes, such as protein synthesis by phosphorylating several targets, including p70S6 kinase and 4E-BP1 [52], and lipid synthesis by phosphorylating and sequestering Lipin-1 to the cytoplasm thereby allowing activation of sterol- and lipogenic gene transcription through the transcription factor SREBP [53]. Under nutrient sufficiency, activated mTORC1 also inhibits the catabolic process of autophagy through various routes, including the phosphorylation of ULK1 at Ser^{757} which disrupts the interaction between ULK1 and AMPK and their coordinated effects on autophagy induction. Conversely, inhibition of mTORC1 triggers autophagy. Our data suggest that mTORC1-dependent regulation of protein synthesis and autophagy uncouple in the regulation of ApoA-I expression. We show that the reduction in intracellular ApoA-I imposed by starvation cannot be reversed upon inhibition of autophagy (Fig. 5C), whereas supplementation with aminoacids restores mTORC1 activity, basal ApoA-I expression levels and its responsiveness to autophagy inhibitors (Fig. 5E).

We note that whereas EBSS, mTORC1 inhibitors and CHX have a profound effect on intracellular and secreted ApoA-I levels, there is a residual ApoA-I that remains unaffected by these treatments. Indeed, CHX chase of HepG2 cells cultured in EBSS failed to further reduce ApoA-I (Supplementary Fig. 2F), yet expression is ablated by ApoA-I-specific RNAi (Supplementary Fig. 2G). Collectively, these observations indicate the existence of two intracellular ApoA-I pools; a labile one that is modulated by mTORC1 signaling and autophagy-mediated turnover and is largely destined for secretion, and a stable pool that is not subject to autophagy and mTORC1 regulation. The precise nature and function of the latter are subject to ongoing investigation.

Overall, the data presented herein define major post-transcriptional pathways responsible for regulation of intracellular ApoA-I levels. They demonstrate that under nutrient-rich conditions, ApoA-I expression is sustained by the balancing acts of basal autophagy and of mTORC1-dependent *de novo* protein synthesis (Supplementary Fig. 3). Accordingly, ApoA-I accumulates in steatosis-like conditions (Fig. 1) which are associated with autophagy blockade. In contrast, upon aminoacid insufficiency, suppression of ApoA-I synthesis prevails, rendering mTORC1 inactivation dispensable for autophagy-mediated ApoA-I proteolysis (Supplementary Fig. 3). Given the established role of ApoA-I in HDL-mediated reverse cholesterol transport, this mode of regulation of intracellular ApoA-I levels may reflect a hepatocellular response to the organismal requirement for maintenance of cholesterol and lipid reserves under conditions of nutrient scarcity. In line with this notion, a reduction in circulating ApoA-I has been noted in adults undergoing a very low calorie diet [54,55] and in children suffering of kwashiorkor, a severe form of protein malnutrition [58,59]. Moreover, reduced HDL has been reported in rodents following severe caloric restriction [56] and in a mouse model of alcoholic liver disease [57] which is characterized by reduced mTOR activity despite autophagy suppression [58].

Emerging evidence suggests that various autophagy pathway components possess functions beyond autophagy regulation. For example, p62 expression influences mTORC1, NF-κB and Nrf2 activities and impacts metabolic, inflammatory and malignant pathologies in the liver [59]. Whether the interaction of p62 with ApoA-I under conditions of autophagy blockade may also influence the anti-inflammatory, antithrombotic or anti-oxidative properties of ApoA-I remains to be addressed.

Supplementary data to this article can be found online at https://doi.org/10.1016/j.metabol.2020.154186.

CRediT authorship contribution statement

Konstantina Georgila: Investigation, Formal analysis, Visualization, Writing - original draft. **Michalis Gounis:** Investigation, Validation, Writing - original draft. **Sophia Havaki:** Investigation. **Vassilis G. Gorgoulis:** Writing - review & editing. **Aristides G. Eliopoulos:** Conceptualization, Formal analysis, Visualization, Writing - original draft, Writing - review & editing.

Acknowledgements

We are grateful to Professor Dimitris Kardassis (University of Crete Medical School) for reagents, Associate Professor George Notas (University of Crete Medical School) for guidance in isolation of primary mouse hepatocytes, and Assistant Professor Elias Drakos (University of Crete Medical School) for helpful discussions. KG acknowledges support from a University of Crete "Maria Manassaki" scholarship.

Declaration of competing interest

None to declare.

References

[1] Gordon SM, Hofmann S, Askew DS, Davidson WS. High density lipoprotein: it's not just about lipid transport anymore. Trends Endocrinol Metab 2011;22:9–15.
[2] Rosenson RS, Brewer Jr HB, Ansell BJ, Barter P, Chapman MJ, Heinecke JW, et al. Dysfunctional HDL and atherosclerotic cardiovascular disease. Nat Rev Cardiol 2016;13:48–60.
[3] Schwertani A, Choi HY, Genest J. HDLs and the pathogenesis of atherosclerosis. Curr Opin Cardiol 2018;33:311–6.
[4] Georgila K, Vyrla D, Drakos E. Apolipoprotein A-I (ApoA-I), immunity, inflammation and cancer. Cancers (Basel) 2019:11.
[5] Gkouskou KK, Ioannou M, Pavlopoulos GA, Georgila K, Siganou A, Nikolaidis G, et al. Apolipoprotein A-I inhibits experimental colitis and colitis-propelled carcinogenesis. Oncogene 2016;35:2496–505.
[6] Meriwether D, Sulaiman D, Volpe C, Dorfman A, Grijalva V, Dorreh N, et al. Apolipoprotein A-I mimetics mitigate intestinal inflammation in COX2-dependent inflammatory bowel disease model. J Clin Invest 2019;130:3670–85.
[7] Su F, Kozak KR, Imaizumi S, Gao F, Amneus MW, Grijalva V, et al. Apolipoprotein A-I (apoA-I) and apoA-I mimetic peptides inhibit tumor development in a mouse model of ovarian cancer. Proc Natl Acad Sci U S A 2010;107:19997–20002.
[8] McQueen MJ, Hawken S, Wang X, Ounpuu S, Sniderman A, Probstfield J, et al. Lipids, lipoproteins, and apolipoproteins as risk markers of myocardial infarction in 52 countries (the INTERHEART study): a case-control study. Lancet 2008;372:224–33.
[9] Feng X, Gao X, Yao Z, Low XY. apoA-I is associated with insulin resistance in patients with impaired glucose tolerance: a cross-sectional study. Lipids Health Dis 2017;16:69.

[10] Haberman Y, Tickle TL, Dexheimer PJ, Kim MO, Tang D, Karns R, et al. Pediatric Crohn disease patients exhibit specific ileal transcriptome and microbiome signature. J Clin Invest 2014;124:3617–33.
[11] Borgquist S, Butt T, Almgren P, Shiffman D, Stocks T, Orho-Melander M, et al. Apolipoproteins, lipids and risk of cancer. Int J Cancer 2016;138:2648–56.
[12] van Duijnhoven FJ, Bueno-De-Mesquita HB, Calligaro M, Jenab M, Pischon T, Jansen EH, et al. Blood lipid and lipoprotein concentrations and colorectal cancer risk in the European Prospective Investigation into Cancer and Nutrition. Gut 2011;60:1094–102.
[13] Cheng T, Dai X, Zhou DL, Lv Y, Miao LY. Correlation of apolipoprotein A-I kinetics with survival and response to first-line platinum-based chemotherapy in advanced non-small cell lung cancer. Med Oncol 2015;32:407.
[14] Gazouli M, Anagnostopoulos AK, Papadopoulou A, Vaiopoulou A, Papamichael K, Mantzaris G, et al. Serum protein profile of Crohn's disease treated with infliximab. J Crohns Colitis 2013;7:e461–70.
[15] Walter S, Weinschenk T, Stenzl A, Zdrojowy R, Pluzanska A, Szczylik C, et al. Multipeptide immune response to cancer vaccine IMA901 after single-dose cyclophosphamide associates with longer patient survival. Nat Med 2012;18:1254–61.
[16] Kardassis D, Gafencu A, Zannis VI, Davalos A. Regulation of HDL genes: transcriptional, posttranscriptional, and posttranslational. Handb Exp Pharmacol 2015;224:113–79.
[17] Zannis VI, Kan HY, Kritis A, Zanni EE, Kardassis D. Transcriptional regulatory mechanisms of the human apolipoprotein genes in vitro and in vivo. Curr Opin Lipidol 2001;12:181–207.
[18] Guo Y, Fan Y, Zhang J, Lomberk GA, Zhou Z, Sun L, et al. Perhexiline activates KLF14 and reduces atherosclerosis by modulating ApoA-I production. J Clin Invest 2015;125:3819–30.
[19] Hayhurst GP, Lee YH, Lambert G, Ward JM, Gonzalez FJ. Hepatocyte nuclear factor 4alpha (nuclear receptor 2A1) is essential for maintenance of hepatic gene expression and lipid homeostasis. Mol Cell Biol 2001;21:1393–403.
[20] Mataki C, Magnier BC, Houten SM, Annicotte JS, Argmann C, Thomas C, et al. Compromised intestinal lipid absorption in mice with a liver-specific deficiency of liver receptor homolog 1. Mol Cell Biol 2007;27:8330–9.
[21] Halley P, Kadakkuzha BM, Faghihi MA, Magistri M, Zeier Z, Khorkova O, et al. Regulation of the apolipoprotein gene cluster by a long noncoding RNA. Cell Rep 2014;6:222–30.
[22] Eliopoulos AG, Havaki S, Gorgoulis VG. DNA damage response and autophagy: a meaningful partnership. Front Genet 2016;7:204.
[23] Klionsky DJ, Abdalla FC, Abeliovich H, Abraham RT, Acevedo-Arozena A, Adeli K, et al. Guidelines for the use and interpretation of assays for monitoring autophagy. Autophagy 2012;8:445–544.
[24] Kuma A, Hatano M, Matsui M, Yamamoto A, Nakaya H, Yoshimori T, et al. The role of autophagy during the early neonatal starvation period. Nature 2004;432:1032–6.
[25] Madrigal-Matute J, Cuervo AM. Regulation of liver metabolism by autophagy. Gastroenterology 2016;150:328–39.
[26] Kim J, Guan KL. mTOR as a central hub of nutrient signalling and cell growth. Nat Cell Biol 2019;21:63–71.
[27] Fye HK, Wright-Drakesmith C, Kramer HB, Camey S, Nogueira da Costa A, Jeng A, et al. Protein profiling in hepatocellular carcinoma by label-free quantitative proteomics in two west African populations. PLoS One 2013;8:e68381.
[28] Steel LF, Shumpert D, Trotter M, Seeholzer SH, Evans AA, London WT, et al. A strategy for the comparative analysis of serum proteomes for the discovery of biomarkers for hepatocellular carcinoma. Proteomics 2003;3:601–9.
[29] Gkirtzimanaki K, Gkouskou KK, Oleksiewicz U, Nikolaidis G, Vyrla D, Liontos M, et al. TPL2 kinase is a suppressor of lung carcinogenesis. Proc Natl Acad Sci U S A 2013;110:E1470–9.
[30] Robertson D, Monaghan P, Clarke C, Atherton AJ. An appraisal of low-temperature embedding by progressive lowering of temperature into Lowicryl HM20 for immunocytochemical studies. J Microsc 1992;168:85–100.
[31] Chondrogianni N, Georgila K, Kourtis N, Tavernarakis N, Gonos ES. 20S proteasome activation promotes life span extension and resistance to proteotoxicity in Caenorhabditis elegans. FASEB J 2015;29:611–22.
[32] Georgila K, Voutetakis K, Delitsikou V, Chondrogianni N, Gonos ES. Optimization of in vitro measurement of proteasome activity in mammalian cells using fluorogenic substrates. Free Radic Biol Med 2014;75(Suppl. 1):S31.
[33] Wang K. Molecular mechanism of hepatic steatosis: pathophysiological role of autophagy. Expert Rev Mol Med 2016;18:e14.
[34] Czaja MJ. Function of autophagy in nonalcoholic fatty liver disease. Dig Dis Sci 2016;61:1304–13.
[35] Heid HW, Moll R, Schwetlick I, Rackwitz HR, Keenan TW. Adipophilin is a specific marker of lipid accumulation in diverse cell types and diseases. Cell Tissue Res 1998;294:309–21.
[36] Chisholm JW, Burleson ER, Shelness GS, Parks JS. ApoA-I secretion from HepG2 cells: evidence for the secretion of both lipid-poor apoA-I and intracellularly assembled nascent HDL. J Lipid Res 2002;43:36–44.
[37] Bhat S, Zabalawi M, Willingham MC, Shelness GS, Thomas MJ, Sorci-Thomas MG. Quality control in the apoA-I secretory pathway: deletion of apoA-I helix 6 leads to the formation of cytosolic phospholipid inclusions. J Lipid Res 2004;45:1207–20.
[38] Miles RR, Perry W, Haas JV, Mosior MK, N'Cho M, Wang JW, et al. Genome-wide screen for modulation of hepatic apolipoprotein A-I (ApoA-I) secretion. J Biol Chem 2013;288:6386–96.
[39] Mauvezin C, Neufeld TP. Bafilomycin A1 disrupts autophagic flux by inhibiting both V-ATPase-dependent acidification and Ca-P60A/SERCA-dependent autophagosome-lysosome fusion. Autophagy 2015;11:1437–8.
[40] Mauthe M, Orhon I, Rocchi C, Zhou X, Luhr M, Hijlkema KJ, et al. Chloroquine inhibits autophagic flux by decreasing autophagosome-lysosome fusion. Autophagy 2018;14:1435–55.
[41] Hamilton RL, Wong JS, Guo LS, Krisans S, Havel RJ. Apolipoprotein E localization in rat hepatocytes by immunogold labeling of cryothin sections. J Lipid Res 1990;31:1589–603.
[42] Maric J, Kiss RS, Franklin V, Marcel YL. Intracellular lipidation of newly synthesized apolipoprotein A-I in primary murine hepatocytes. J Biol Chem 2005;280:39942–9.
[43] Corona Velazquez AF, Jackson WT. So many roads: the multifaceted regulation of autophagy induction. Mol Cell Biol 2018;38.
[44] Martinet W, De Meyer GR, Andries L, Herman AG, Kockx MM. In situ detection of starvation-induced autophagy. J Histochem Cytochem 2006;54:85–96.
[45] Saxton RA, Sabatini DM. mTOR signaling in growth, metabolism, and disease. Cell 2017;169:361–71.
[46] Liu Q, Xu C, Kirubakaran S, Zhang X, Hur W, Liu Y, et al. Characterization of Torin2, an ATP-competitive inhibitor of mTOR, ATM, and ATR. Cancer Res 2013;73:2574–86.
[47] Liu P, Gan W, Chin YR, Ogura K, Guo J, Zhang J, et al. PtdIns(3,4,5)P3-dependent activation of the mTORC2 kinase complex. Cancer Discov 2015;5:1194–209.
[48] Zannis VI, Breslow JL, SanGiacomo TR, Aden DP, Knowles BB. Characterization of the major apolipoproteins secreted by two human hepatoma cell lines. Biochemistry 1981;20:7089–96.
[49] Chen G, Ding XF, Bouamar H, Pressley K, Sun LZ. Everolimus induces G1 cell cycle arrest through autophagy-mediated protein degradation of cyclin D1 in breast cancer cells. Am J Physiol Cell Physiol 2019;317:C244–c52.
[50] Bejarano E, Girao H, Yuste A, Patel B, Marques C, Spray DC, et al. Autophagy modulates dynamics of connexins at the plasma membrane in a ubiquitin-dependent manner. Mol Biol Cell 2012;23:2156–69.
[51] Imam S, Talley S, Nelson RS, Dharan A, O'Connor C, Hope TJ, et al. TRIM5alpha degradation via autophagy is not required for retroviral restriction. J Virol 2016;90:3400–10.
[52] Zoncu R, Bar-Peled L, Efeyan A, Wang S, Sancak Y, Sabatini DM. mTORC1 senses lysosomal amino acids through an inside-out mechanism that requires the vacuolar H(+)-ATPase. Science 2011;334:678–83.
[53] Peterson TR, Sengupta SS, Harris TE, Carmack AE, Kang SA, Balderas E, et al. mTOR complex 1 regulates lipin 1 localization to control the SREBP pathway. Cell 2011;146:408–20.
[54] Asztalos B, Lefevre M, Wong L, Foster TA, Tulley R, Windhauser M, et al. Differential response to low-fat diet between low and normal HDL-cholesterol subjects. J Lipid Res 2000;41:321–8.
[55] Shoji T, Nishizawa Y, Koyama H, Hagiwara S, Aratani H, Izumotani-Sasao K, et al. Lipoprotein metabolism in normolipidemic obese women during very low calorie diet: changes in high density lipoprotein. J Nutr Sci Vitaminol (Tokyo) 1991;37(Suppl:S57–64).
[56] Duarte FO, Sene-Fiorese M, Manzoni MS, de Freitas LF, Cheik NC, Garcia de Oliveira Duarte AC, et al. Caloric restriction and refeeding promoted different metabolic effects in fat depots and impaired dyslipidemic profile in rats. Nutrition 2008;24:177–86.
[57] Tan P, Liang H, Nie J, Diao Y, He Q, Hou B, et al. Establishment of an alcoholic fatty liver disease model in mice. Am J Drug Alcohol Abuse 2017;43:61–8.
[58] Babuta M, Furi I, Bala S, Bukong TN, Lowe P, Catalano D, et al. Dysregulated autophagy and lysosome function are linked to exosome production by micro-RNA 155 in alcoholic liver disease. Hepatology; 2019.
[59] Manley S, Williams JA, Ding WX. Role of p62/SQSTM1 in liver physiology and pathogenesis. Exp Biol Med (Maywood) 2013;238:525–38.

Oncogene (2016) **35,** 2496–2505
© 2016 Macmillan Publishers Limited All rights reserved 0950-9232/16
www.nature.com/onc

ORIGINAL ARTICLE

Apolipoprotein A-I inhibits experimental colitis and colitis-propelled carcinogenesis

KK Gkouskou[1], M Ioannou[2], GA Pavlopoulos[3], K Georgila[1], A Siganou[1], G Nikolaidis[1], DC Kanellis[1], S Moore[4], KA Papadakis[5,6], D Kardassis[2,7], I Iliopoulos[3], FA McDyer[4], E Drakos[8] and AG Eliopoulos[1,2]

In both humans with long-standing ulcerative colitis and mouse models of colitis-associated carcinogenesis (CAC), tumors develop predominantly in the distal part of the large intestine but the biological basis of this intriguing pathology remains unknown. Herein we report intrinsic differences in gene expression between proximal and distal colon in the mouse, which are augmented during dextran sodium sulfate (DSS)/azoxymethane (AOM)-induced CAC. Functional enrichment of differentially expressed genes identified discrete biological pathways operating in proximal vs distal intestine and revealed a cluster of genes involved in lipid metabolism to be associated with the disease-resistant proximal colon. Guided by this finding, we have further interrogated the expression and function of one of these genes, apolipoprotein A-I (ApoA-I), a major component of high-density lipoprotein. We show that ApoA-I is expressed at higher levels in the proximal compared with the distal part of the colon and its ablation in mice results in exaggerated DSS-induced colitis and disruption of epithelial architecture in larger areas of the large intestine. Conversely, treatment with an ApoA-I mimetic peptide ameliorated the phenotypic, histopathological and inflammatory manifestations of the disease. Genetic interference with ApoA-I levels *in vivo* impacted on the number, size and distribution of AOM/DSS-induced colon tumors. Mechanistically, ApoA-I was found to modulate signal transducer and activator of transcription 3 (STAT3) and nuclear factor-κB activation in response to the bacterial product lipopolysaccharide with concomitant impairment in the production of the pathogenic cytokine interleukin-6. Collectively, these data demonstrate a novel protective role for ApoA-I in colitis and CAC and unravel an unprecedented link between lipid metabolic processes and intestinal pathologies.

Oncogene (2016) **35,** 2496–2505; doi:10.1038/onc.2015.307; published online 17 August 2015

INTRODUCTION

Patients with ulcerative colitis (UC) have increased risk of developing colorectal cancer compared with the general population and this risk further increases with the extent of the inflammatory disease.[1,2] Although the precise mechanisms underlying UC and its progression to cancer remain nebulous, both genetic factors and aberrations in the host microbiome ecosystem have been implicated in the establishment of systemic inflammatory reactions leading to carcinogenesis.[3,4]

Various experimental models for UC have been developed to study the link between chronic inflammation and intestinal neoplasia, most of which involve the application of chemicals such as the polysaccharide dextran sodium sulfate (DSS). Oral administration of DSS causes colonic inflammation, which is instigated by the physical disruption of the mucosal barrier and exposure of the lamina propria immune cells to lumen bacterial products.[5,6] Mice exposed to DSS exhibit several characteristics of human UC, including weight loss, diarrhea and rectal bleeding, mucosal tissue damage, infiltration of various types of immune cells and elevated levels of local and circulating pro-inflammatory cytokines such as interleukin-1β (IL-1β), IL-1α, IL-6 and tumor necrosis factor.[7,8]

Although colitis induced by DSS rarely progresses to cancer, the combination of a single application of the carcinogen azoxymethane (AOM) with repeated cycles of DSS administration leads to tumorigenesis.[9] Interestingly, carcinomas develop exclusively in the distal part of the large intestine[10] where inflammation is also more prominent.[11] In humans with UC, low-grade dysplasia also develops predominantly in the distal colon, progresses more rapidly to neoplasia than proximal colon low-grade dysplasia[12,13] and associates with worse patient prognosis.[14] In this study, we have explored the biological basis of this intriguing pathology and identified a cluster of genes involved in lipid metabolism to be associated with the disease-resistant proximal colon. Guided by this finding, we have further interrogated the expression and function of one of these genes encoding apolipoprotein A-I (ApoA-I), which represents the major structural protein of high-density lipoprotein (HDL) complexes that are responsible for the transfer of unesterified cholesterol and cholesteryl esters from peripheral tissues and cells to the liver.[15,16] Herein, we describe a novel protective role for ApoA-I in colitis and colitis-associated carcinogenesis (CAC).

[1]Molecular and Cellular Biology Laboratory, Division of Basic Sciences, University of Crete Medical School, Heraklion, Greece; [2]Institute of Molecular Biology and Biotechnology, Foundation for Research and Technology Hellas (FORTH), Heraklion, Greece; [3]Bioinformatics and Computational Biology Laboratory, Division of Basic Sciences, University of Crete Medical School, Heraklion, Greece; [4]Almac Diagnostics, Craigavon, UK; [5]Department of Gastroenterology, University of Crete Medical School, Heraklion, Greece; [6]Division of Gastroenterology and Hepatology, Mayo Clinic, Rochester, MN, USA; [7]Laboratory of Biochemistry, Division of Basic Sciences, University of Crete Medical School, Heraklion, Greece and [8]Department of Pathology, University of Crete Medical School, Heraklion, Greece. Correspondence: Professor AG Eliopoulos, Molecular and Cellular Biology Laboratory, Division of Basic Sciences, University of Crete Medical School, Heraklion 71003, Crete, Greece.
E-mail: eliopag@med.uoc.gr
Received 18 February 2015; revised 12 July 2015; accepted 13 July 2015; published online 17 August 2015

RESULTS

Gene expression profiling identifies distinct biological processes operating in proximal vs distal colon during CAC

We explored the transcriptome of proximal vs distal colon of C57BL/6J mice using microarrays capable of assaying most protein-coding mRNAs. Approximately 420 genes were found to be differentially expressed between the two parts of the tissue (GEO accession number GSE64423). To interpret this list of genes as biological functions, gene ontology (GO) enrichment was performed and indicated that the gene expression signature of the proximal colon is associated with processes related to tissue morphogenesis and lipid metabolism, whereas the distal part of the large intestine is enriched in processes related to glycosylation (Supplementary Tables S1A and S1B).

We applied the DSS/AOM protocol shown in Figure 1a to induce CAC. Tumors were observed at end point and enumerated (Figure 1b). Histopathological evaluation showed that at the early stages of the disease (two DSS cycles; Figure 1a), only localized low-grade dysplastic lesions occur in the distal colon, whereas high-grade dysplasia and carcinomas develop at end point (Figure 1c). In contrast, no major tissue abnormalities were detected in the proximal part of the large intestine (data not shown).

We performed an unbiased interrogation of the transcriptome of proximal and distal colon following two or four DSS cycles to gain insight into biological processes involved in the regional responses to CAC. We analyzed the expression data (GEO accession number GSE64658) for genes that are differentially expressed exclusively in the proximal part of the large intestine of the early AOM/DSS treatment group as we reasoned that these genes may associate with resistance to colitis and/or CAC. In addition, we pursued the analysis of genes that are up- or downregulated in the distal colon at both early and late disease states as we hypothesized that such genes are likely to be most relevant to the initiation, progression and maintenance of CAC.

In the early treatment group, we identified 1997 genes that are differentially expressed in the distal colon of AOM/DSS-treated vs untreated animals, whereas the respective number of genes in the proximal tissue was 1684 (Figure 1d). As shown in the Venn diagram of Figure 1e (left panel), comparison of these groups identified 612 uniquely mapped genes to be differentially expressed exclusively in the proximal colon, hereafter termed the 'resistance-associated gene signature'. In the late disease group, the number of differentially expressed genes increased in the distal colon to 4326 but was reduced in the proximal tissue to 586 (Figure 1d). The two groups of genes, which were differentially expressed exclusively in the distal colon at the early and late disease stages (Figure 1e; middle panel), were compared and led to the identification of a common gene signature of 637 uniquely mapped genes (Figure 1e; right panel), hereafter termed 'the CAC signature'. GO analysis showed that the CAC signature associates with biological processes related to inflammation and cell death (Supplementary Tables S2 and S3), whereas the resistance-associated gene signature is linked to lipid metabolism pathways (Supplementary Table S4 and S5).

Prediction of transcription factors linked to 'resistance' and 'CAC'-associated gene expression signatures

To predict molecular pathways that relate to these signatures, we performed transcription regulator analysis using the Ingenuity platform. A significant overlap of transcription factors predicted to be involved in early and late stages of CAC was noted (Supplementary Table S6), including nuclear factor-κB (NF-κB) and signal transducer and activator of transcription 3 (STAT3), which have been reported to operate in both enterocytes and immune cells in the inflamed intestine to promote carcinogenesis.[17–20] In contrast, transcription factors predicted to be involved in the regulation of resistance-associated genes relate to morphogenesis, differentiation and development but not inflammation (Supplementary Table S7).

To validate the prediction that STAT3 and NF-κB are activated in distal but not proximal colon tissue of AOM/DSS-treated mice, we performed immunohistochemistry (IHC) using antibodies that recognize Tyr^{705} phosphorylated STAT3 (p-STAT3) and p65/RelA NF-κB, respectively. As shown in Supplementary Figures S1 and S2, p-STAT3 was undetectable in intestinal epithelial cells of untreated animals irrespective of tissue topology but was detected in inflammatory cells in lamina propria. Following exposure to AOM/DSS, p-STAT3 levels progressively increased in the nucleus of dysplastic epithelial cells of the distal colon, being more prominent in carcinomas developed at late stage disease. In contrast, no p-STAT3 reactivity was detected in proximal colon epithelial tissue during disease progression. Similar observations were made for NF-κB (Supplementary Figures S3 and S4).

ApoA-I expression is elevated in proximal vs distal colon

The significant representation of genes associated with lipid metabolism in the resistance-associated gene signature was unexpected. One of these genes, ApoA-I, was expressed at significantly higher levels in the proximal vs distal colon of untreated mice, an observation confirmed by reverse transcriptase–quantitative PCR (Figures 2a and b). This marked difference in expression was also observed in untreated immunodeficient NSG (NOD-*scid* IL2R$\gamma^{-/-}$) and germ-free mice (Figures 2a and b), excluding a major role for immune components and the microbiome in ApoA-I regulation.

The differential expression of ApoA-I in the colon was surprising given the prevailing view that it is exclusively produced by the liver and small intestine, a notion that stems from an early study using northern blot-based RNA analysis of different tissues.[21] In contrast, a more recent study reported expression of ApoA-I protein in human fetal colon.[22] Prompted by this ambiguity, we performed IHC to assess levels and localization of ApoA-I protein in the colon. As shown in Figure 2c and Supplementary Figure 5A, strong ApoA-I reactivity was detected in absorbent epithelial cells of the proximal colon, whereas ApoA-I was nearly undetectable in distal colon tissue. Western blot analysis of tissue lysates confirmed expression of ApoA-I in proximal colon, albeit to lower levels than the liver (Supplementary Figure S5B).

We next analyzed the relative changes in ApoA-I mRNA levels during CAC. The proximal colon responded to DSS/AOM with a 2.5-fold increase in ApoA-I expression in the early stages of the disease, which, however, subsided to control levels in the late treatment group (Figure 2d). In contrast, the low ApoA-I mRNA levels detected in the distal colon of untreated mice did not significantly change during CAC (Figure 2d).

ApoA-I ablation exacerbates DSS-induced colitis

AOM functions as mutagen by inducing DNA damage and apoptosis in epithelial cells in the colon crypts,[23,24] whereas DSS is a luminal toxin that causes intestinal inflammation required for CAC.[9] The aforementioned topology and pattern of ApoA-I expression, namely its upregulation at the early stages of AOM/DSS-induced CAC in the proximal part of the colon, coupled with the observation that tumor development is associated with inflammatory gene signatures and pathways (Supplementary Table S2) indicated a role for ApoA-I in suppressing the colitis phase of CAC. To examine this hypothesis, wild-type (WT) and *ApoA1*$^{-/-}$ mice were exposed to 3% DSS for 7 days and monitored for survival and weight loss. *ApoA1*$^{-/-}$ animals suffered excessive weight loss and succumbed within 7 days of DSS administration (Figure 3a and data not shown). Colon shortening, a clinical feature of intestinal inflammation in the DSS model,[25] was also

© 2016 Macmillan Publishers Limited

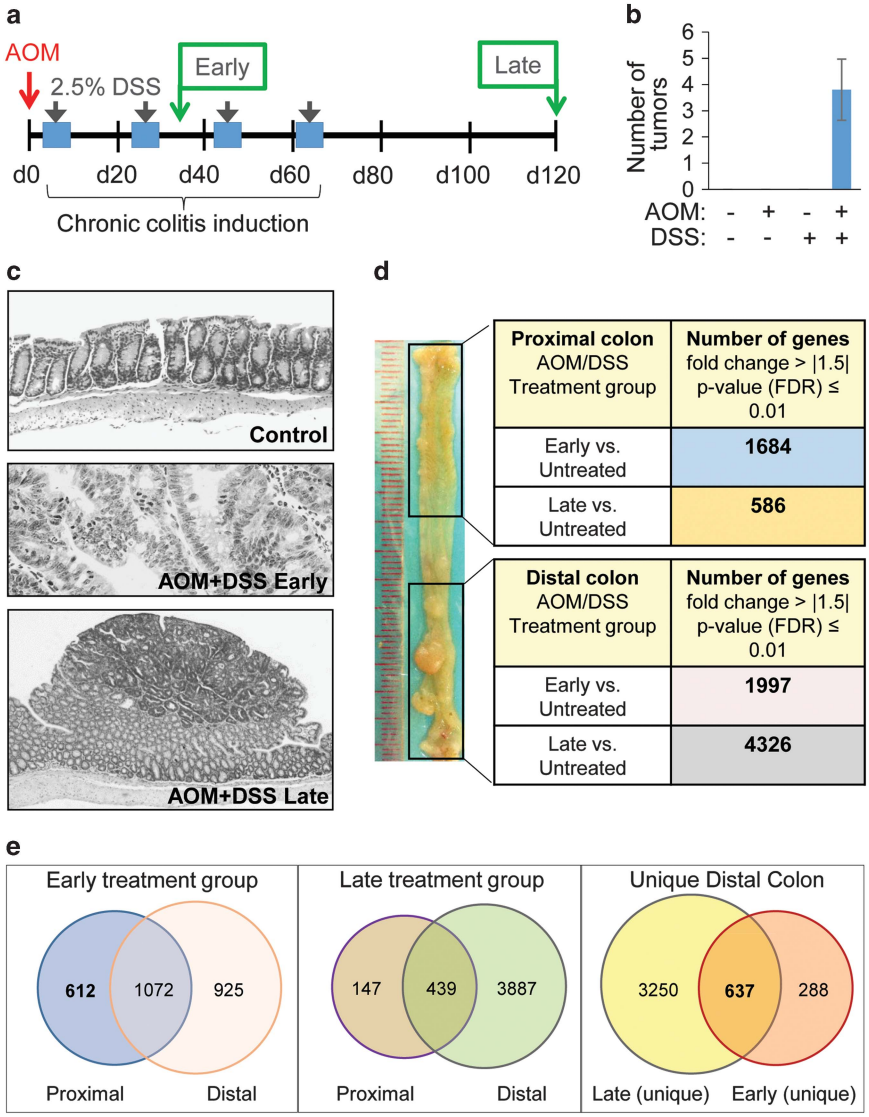

Figure 1. Genome-wide assessment of gene expression changes in proximal vs distal colon of AOM/DSS-treated mice. (**a**) Schematic representation of the AOM/DSS protocol of CAC. Female C57BL/6J mice were injected intaperitoneally with AOM and 4 days later 2.5% DSS was administered in their drinking water for 5 days (blue box), followed by 14 days of regular water. This cycle was repeated three more times, as indicated. Mice were killed 42 days (early treatment group) or 120 days (late treatment group) after the AOM injection. (**b**) Number of tumors developed on day 120 following administration of the AOM/DSS protocol described in **a**. (**c**) Hematoxylin and eosin (H&E) staining of distal colon tissue sections from untreated (upper panel) and AOM/DSS-treated mice killed 42 days (middle panel) or 120 days (bottom panel) after the AOM injection. Original magnification is x100, x200 and x40 from top to bottom. (**d**) Number of genes differentially expressed on the basis of between-group fold change differences of |1.5| or greater and false discovery rate correction of the analysis of variance *P*-values ≤ 0.01. (**e**) Venn diagrams showing comparisons of genes, which are differentially expressed at the AOM/DSS early and late time points (left and middle panel, respectively) between distal and proximal colon.

significantly more pronounced in *ApoA1*$^{-/-}$ than WT mice (Supplementary Figure S6).

Analysis of IL-6, IL-1β and tumor necrosis factor levels in *ApoA1*$^{-/-}$ mice killed on day 5 of treatment revealed markedly elevated expression of these cytokines in distal gut tissue compared with WT animals (Figure 3b and Supplementary Figure S7). Interestingly, increased IL-6 and IL-1β expression was also observed in the proximal colon of *ApoA1*$^{-/-}$ but not WT mice exposed to DSS (Figure 3c and Supplementary Figure S7). Histological assessment of the distal intestine of DSS-treated *ApoA1*$^{-/-}$ mice revealed massive destruction of epithelial architecture with complete loss of crypts and intense inflammatory cell content (Figure 3c). The distal colon of WT mice also displayed significant tissue damage and loss of epithelial integrity albeit to a lesser extent than *ApoA1*$^{-/-}$ animals (Figure 3c). Importantly, although epithelial architecture was fully preserved in the proximal intestine of DSS-treated WT animals, areas of significant tissue damage and inflammatory cell infiltrate were noted in the proximal colon of *ApoA1*$^{-/-}$ mice (Figure 3c). Indeed, the histological score of colitis severity representing the degree and extent of inflammation and crypt damage was significantly higher in the colon of *ApoA1*$^{-/-}$ vs WT mice (Figure 3d). These findings demonstrate that endogenous ApoA-I confers protective effect on DSS-induced colitis, which is required for CAC.

An ApoA-I mimetic peptide alleviates pathological manifestations of DSS-induced colitis

Short synthetic peptide mimics of ApoA-I have been developed in the context of atherosclerosis prevention and shown to confer

© 2016 Macmillan Publishers Limited

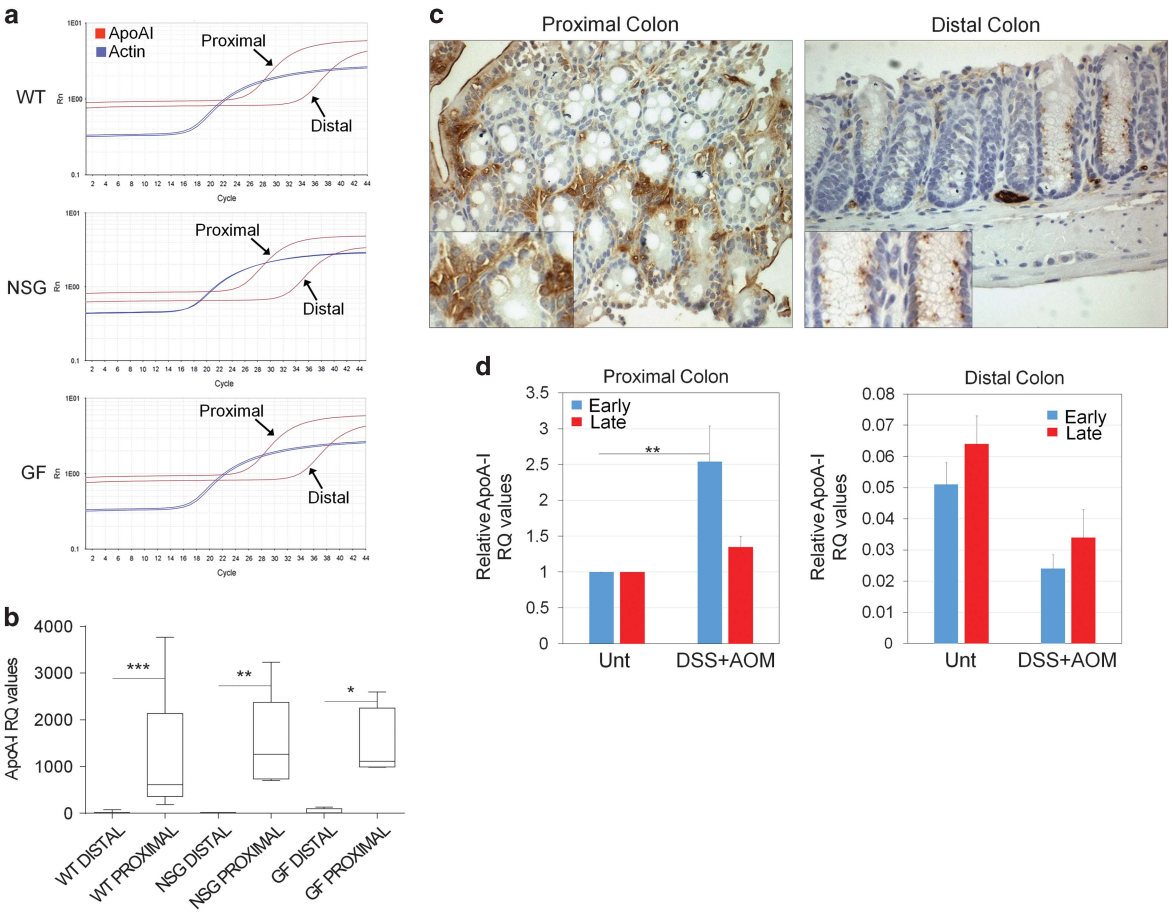

Figure 2. Expression of ApoA-I in proximal vs distal colon of untreated and AOM/DSS-treated mice. (**a**) Representative qPCR profiles of ApoA-I mRNA expression in proximal and distal colon tissue from untreated WT and immunodeficient NSG mice maintained in specific pathogen-free conditions and germ-free (GF) C57BL/6J mice. Actin was used as amplification control. (**b**) Collective ApoA-I mRNA expression data of proximal and distal colon tissue from WT ($n = 10$) and NSG ($n = 5$) mice maintained in specific pathogen-free conditions and GF mice ($n = 6$). One-way analysis of variance Bonferroni post-test suggested no statistically significant difference in ApoA-I expression between proximal groups but differences between proximal and distal tissue were statistically significant (Mann–Whitney test; $^{***}P < 0.001$; $^{**}P < 0.01$; $^{*}P < 0.05$). (**c**) IHC staining of ApoA-I in transparietal colon sections. Original magnification is x200; for insets x400. (**d**) Quantification of ApoA-I mRNA expression in proximal and distal colon of untreated and AOM/DSS-treated WT mice at early and late disease states. Results were normalized to the housekeeping β-actin gene and expressed as RQ values relative to proximal colon tissue of untreated controls, which was given the arbitrary value of '1'. Data are the means ± s.e.m. of at least five animals in each group. Among the AOM/DSS vs untreated groups only the early stage proximal colon showed statistically significant increase in ApoA-I levels ($^{**}P < 0.01$; Mann–Whitney test).

anti-oxidant and anti-inflammatory effects *in vitro* and to reduce atherosclerosis in mouse models.[26] 4F synthesized from all D-amino acids (D-4F) is the most commonly used ApoA-I mimetic peptide for *in vivo* applications.[27,28] On the basis of the aforementioned observations, we explored the effects of D-4F on experimental colitis. We performed this evaluation in WT mice because of previous work demonstrating that endogenous ApoA-I is required for maximum effectiveness of D-4F in mouse models of atherosclerosis[29,30] and this treatment is most relevant to putative future therapeutic applications in colitis patients.

Oral administration of D-4F reduced colitis-associated weight loss, colon shortening and histological score of colitis severity compared with mice treated with scramble peptide (Figures 4a and d). Moreover, the expression of *Il6* mRNA, a cytokine with a major pathogenic role in colitis and CAC[18–20] was reduced in the distal colon of D-4F compared with scramble peptide-treated animals undergoing colitis (Figure 4e).

In DSS-induced colitis, intestinal epithelial cells respond to products of pathogenic bacteria by activating Toll-like receptor (TLR) signaling leading to the production of cytokines and other inflammatory mediators, which contribute to neoplasia.[31,32] ApoA-I and 4F directly bind to the lipid-A domain of lipopolysaccharide (LPS), the prototypic Gram-negative bacterial product, reducing its TLR4-stimulating capacity in macrophages.[33,34] To determine whether 4F could also directly act on intestinal epithelial cells to modulate their response to LPS, CMT-93 mouse rectum carcinoma cell cultures were exposed to 4F or control peptide followed by treatment with LPS. As shown in Figure 4f, the LPS-induced upregulation of *il-6* mRNA was significantly attenuated in 4F-treated cells.

Stimulation of TLR4 results in nuclear translocation of RelA/p65 NF-κB enabling transactivation of the *Il6* promoter. Compared with control peptide, treatment of CMT-93 cells with 4F led to reduced nuclear accumulation of RelA and p-STAT3, an IL-6 signaling target (Figure 4g). Collectively, these data further support an anti-inflammatory role for ApoA-I in the intestine mediated at least in part through modulation of TLR4 signaling in intestinal epithelial cells.

Reduced ApoA-I levels confer susceptibility to colitis-associated colorectal carcinogenesis

As *ApoA1*$^{-/-}$ mice develop severe inflammatory response during acute colitis (Figure 3) and the degree of inflammation correlates

© 2016 Macmillan Publishers Limited

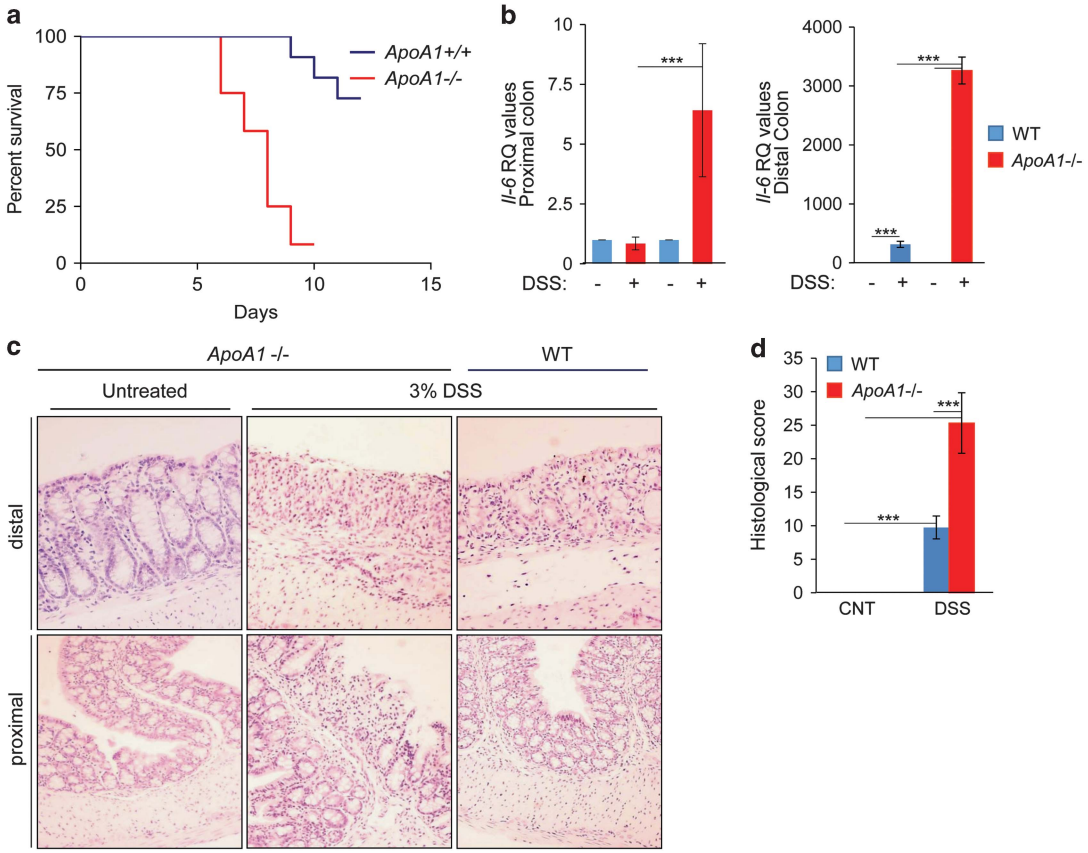

Figure 3. Ablation of ApoA-I exacerbates DSS-induced colitis in the mouse. (**a**) Kaplan–Meier survival plots of *ApoA1*$^{-/-}$ ($n=12$) and WT ($n=11$) mice exposed to 3% DSS. The difference in survival between studied groups was statistically significant ($P<0.001$; log-rank (Mantel–Cox) test). (**b**) The distal and proximal colon of ApoA-I-deficient mice exposed to DSS displays elevated expression of *Il6* mRNA compared with WT animals ($n=5$ from each group); ***$P<0.001$; Mann–Whitney test. (**c**) Histology (hematoxylin and eosin (H&E) staining) of distal and proximal colon tissue sections from untreated and DSS-treated WT and *ApoA1*$^{-/-}$ mice killed on day 5 of DSS administration. (**d**) Histological score of colitis severity in the colon (proximal and distal) of *ApoA1*$^{-/-}$ ($n=6$) vs WT ($n=5$) mice described in **c**. ***$P<0.001$; Mann–Whitney test.

with the development of dysplasia in minor lesion aberrant crypt foci,[35] we reasoned that ApoA-I levels may also influence CAC. *ApoA1*$^{-/-}$ and WT mice were thus exposed to the AOM/DSS protocol of CAC induction shown in Figure 1a. During the course of this treatment, >90% of the knock-out animals died by the fourth cycle of DSS administration. Although the remaining *ApoA1*$^{-/-}$ mice displayed marked increase in the number and size of tumors, the lethality ensued by the AOM/DSS treatment prohibited the analysis of the impact of ApoA-I ablation on CAC in a statistically meaningful manner. We thus assessed susceptibility to CAC in heterozygous (*ApoA1*$^{+/-}$) mice displaying markedly reduced circulating levels of HDL and ApoA-I (Supplementary Figure S8) and elevated IL-6 expression in their colon when exposed to the acute DSS-induced colitis model (Supplementary Figure S9).

ApoA1$^{+/-}$ mice treated with AOM/DSS developed more and larger tumors than WT mice (Figures 5a, b and e), indicating higher proliferation and/or survival of transformed cells. IHC analysis of the expression of the proliferation marker Ki67 (Figure 5c) and semiquantitation of the percentage of Ki67-positive cells in multiple tumors and animals (Figure 5d) confirmed significantly elevated proliferative index in *ApoA1*$^{+/-}$ compared with WT tumors. As STAT3 progressively becomes activated in the distal intestine of mice undergoing CAC (Supplementary Figure S1) and contributes to carcinogenesis by regulating the expression of genes necessary for enterocyte survival and proliferation,[18–20] we assessed p-STAT3 levels in *ApoA1*$^{+/-}$ vs WT tumors. *ApoA1*$^{+/-}$ tumors displayed elevated levels and harbored increased numbers of p-STAT3-positive colon cancer cells compared with those developed in WT mice (Figures 5c and d). Similar results were obtained for p65 NF-κB (Supplementary Figure 10).

Interestingly, although malignancy developed predominantly in the distal part of the colon in WT animals, tumors in *ApoA1*$^{+/-}$ mice were macroscopically visible in the distal, middle and, occasionally, proximal regions (Figure 5e). Quantification of the distribution of tumors confirmed localization in approximately the lower 30% of the colon length in WT and 55% in *ApoA1*$^{+/-}$ mice (Figure 5e). Therefore, reduced ApoA-I levels result in increased susceptibility to CAC and alterations in the distribution of tumors in the mouse colon.

DISCUSSION

Colorectal cancer represents a major complication of UC. Intriguingly, carcinoma development in colitis patients occurs with significantly higher frequency in the distal compared with proximal part of the large intestine where inflammation is also more prominent and is associated with poor prognosis.[11–14] A mouse model of CAC induced by administration of the mutagen AOM and the luminal toxin DSS phenocopies the topological manifestation of tumor development in human UC.[5,10,36] We surmised that the identification of pathways underpinning the differential susceptibility of distal vs proximal colon to CAC may not only provide insight into the pathogenesis of the disease but it

© 2016 Macmillan Publishers Limited

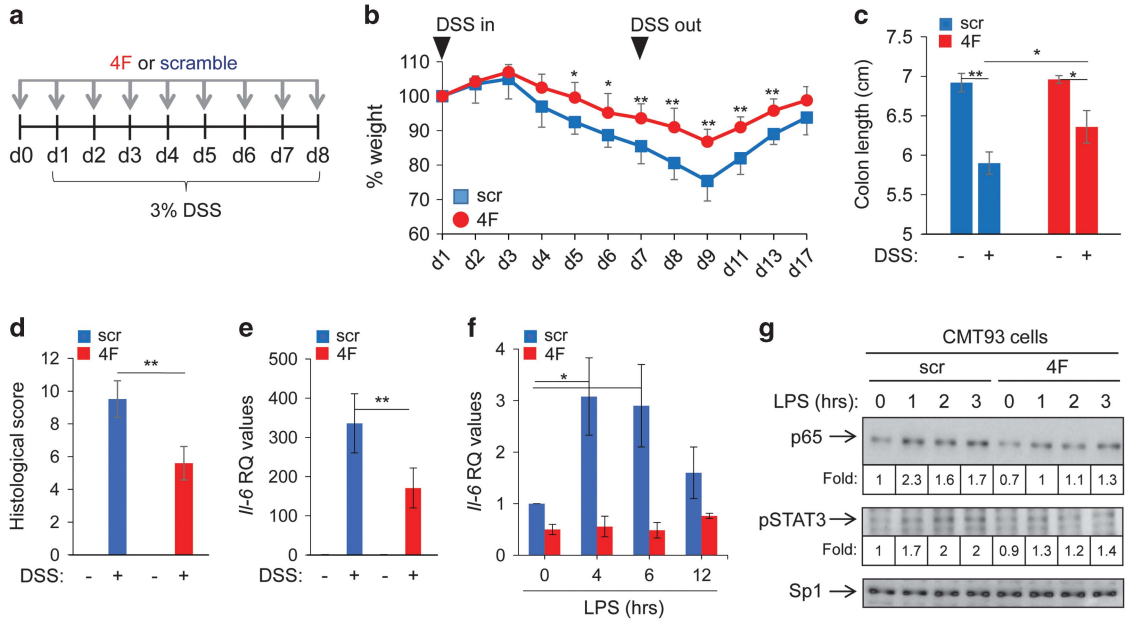

Figure 4. Administration of the ApoA-I-mimetic peptide 4F reduces the severity of DSS-induced colitis in the mouse. (**a**) Schematic representation of the protocol used to assess the effects of the ApoA-I-mimetic peptide D-4F and its scramble (scr) control on DSS-induced colitis. (**b**) Changes in the weight of mice administered D-4F or scramble peptide in the presence of 3% DSS ($n=6$ from each group); $^{**}P<0.01$; $^{*}P<0.05$; Mann–Whitney test. (**c**) Colon shortening is significantly ($^{*}P<0.05$; $n=6$) attenuated in mice receiving D-4F. (**d**) Histological score of colitis severity in the colon of D-4F vs scramble peptide-administered mice. $^{**}P<0.01$. (**e**) Relative levels of *Il6* mRNA, measured by qPCR, in the distal colon of mice exposed to DSS in the presence of D-4F or scramble peptide. $^{**}P<0.01$; Mann–Whitney test. (**f**) The ApoA-I-mimetic peptide 4F reduces LPS-induced IL-6 gene expression. CMT-93 cells were pre-treated with 50 μg/ml 4F or scramble peptides for 48 h and then exposed to 1 μg/ml LPS for various time intervals in the presence of freshly added peptides. Relative levels of *Il6* mRNA were measured by qPCR using actin as control. $^{*}P<0.05$; Mann–Whitney test. (**g**) The ApoA-I-mimetic peptide 4F reduces the LPS-induced nuclear accumulation of p65 NF − κB and Tyr^{705}-p-STAT3. CMT-93 cells were pre-treated as in **f**, followed by LPS stimulation for various time intervals as indicated. The levels of nuclear p65 and p-STAT3 levels were measured on a Biorad ChemiDoc XRS+ Imaging System (Bio-Rad Laboratories, Inc., Hercules, CA, USA) as a means of measurements of three different exposures normalized to SP1, which serves as a loading nuclear protein control. Results are expressed as fold increase relative to untreated controls, which were given the arbitrary value of 1. At least four independent experiments were performed with similar results.

could also be exploited for the development of novel therapeutic interventions.

We monitored in an unbiased manner global changes in the transcriptome of mouse proximal and distal colon during exposure to AOM/DSS with the aim to define biological pathways and processes that characterize regional responses of the large intestine to CAC. These analyses led to the identification of a gene expression signature that is uniquely associated with the disease-susceptible distal part of the intestine and typifies both the early (pre-malignant) and late (malignant) stages of CAC. Functional enrichment and transcription factor regulator analysis indicated that this expression profile is closely associated with inflammatory processes and transcription factors with major roles in inflammation and cancer, including NF-κB and STAT3. In contrast, the proximal colon, which displays resistance to CAC, is not associated with inflammatory processes, NF-κB or STAT3 activation, suggesting that inflammation is required for focal malignant transformation in the AOM/DSS model. This conclusion is corroborated by published work showing that the development of dysplasia in minor lesion aberrant crypt foci is closely associated with the degree of chronic inflammation[35] and that genetic or pharmacological suppression of inflammatory mediators, such as IL-6, ameliorates AOM/DSS-induced colorectal carcinogenesis.[18,20] Moreover, NF-κB and STAT3 have been shown to promote carcinogenesis by regulating epithelial cell survival, proliferation and production of inflammatory cytokines with tumorigenic function including IL-6.[18,19] In line with these observations in the mouse, the risk of colon cancer in colitis patients increases with the severity of inflammation[37,38] and expression of IL-6 and STAT3 is significantly elevated in the intestine of patients with active UC or colorectal cancer compared with patients with inactive disease.[39]

Which is the biological basis of the ability of the proximal colon to withstand inflammation thereby resisting colitis-associated carcinogenesis? Intrigued by the observation that the gene expression signature that typifies the proximal part of the large intestine is enriched for lipid metabolism network components, we explored the function of one of these genes, ApoA-I, which displays the largest difference in expression between proximal and distal colon. ApoA-I produced by intestinal epithelial cells is secreted into the blood and mesenteric lymph where it physiologically functions in the transport of processed dietary components.[40,41] In this context, our finding that ApoA-I is overexpressed in the proximal compared with distal part of the large intestine is intriguing and further studies are required to fully appreciate the physiological requirements for these regional differences in ApoA-I gene expression. Results presented in this study exclude a major role for immune cells and host–microbiome in this phenomenon. The involvement of lipids in ApoA-I regulation is likely and is supported by published work showing that dietary triglycerides may partly influence ApoA-I levels in the small intestine.[42,43]

Beyond its established physiological role in lipid metabolic processes in the intestine, we demonstrate herein an unprecedented protective role of ApoA-I in intestinal pathologies. A functional link between ApoA-I and CAC was inferred by the observation that the levels of ApoA-I increase in the disease-resistant proximal colon during the colitis phase of AOM/DSS treatment. Further studies demonstrated that *ApoA1*$^{-/-}$ mice display exacerbated DSS-induced pathology and elevated levels of

© 2016 Macmillan Publishers Limited

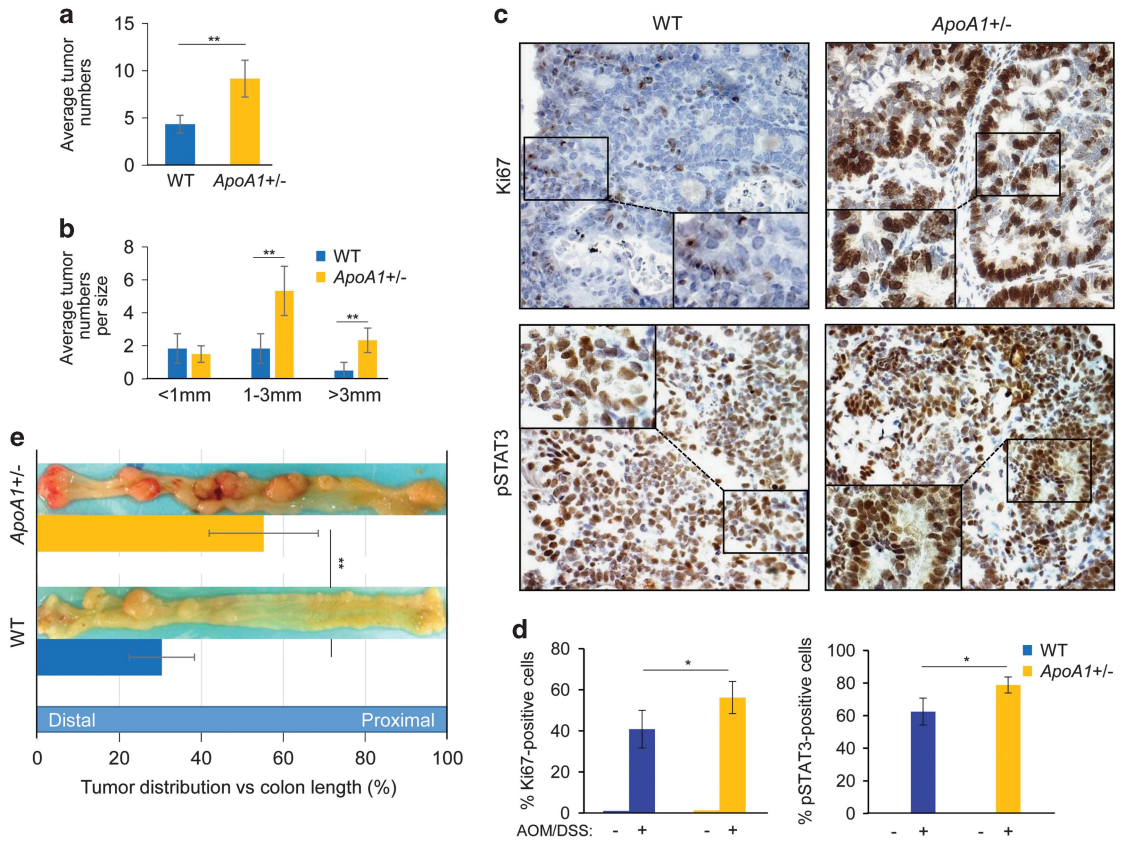

Figure 5. ApoA1$^{+/-}$ mice display increased number, size and distribution of AOM/DSS-induced colon tumors. (**a**) Average number of macroscopic tumors developed in WT ($n=10$) and *ApoA1*$^{+/-}$ ($n=11$) mice following application of the AOM/DSS protocol described in Figure 1a. Based on the mean values and the standard deviation of the WT and heterozygous groups, two-tailed test and alpha error 0.01, the statistical power for the observed difference is 1 (100%). (**b**) Size distribution of tumors developed in the colon of AOM/DSS-treated WT and *ApoA1*$^{+/-}$ mice. In both (**a, b**), mean values ± s.e.m. are shown. (**$P<0.01$; Mann–Whitney test). (**c, d**) Tumors developed in *ApoA1*$^{+/-}$ mice expressed higher levels of phosphorylated, nuclear STAT3 and of the proliferation marker Ki67. Representative IHC staining is shown for each group (**c**). Average proliferative index, assessed as the percentage (%) of Ki67-positive tumor cells, and % of cells expressing p-STAT3 were higher in tumors developed in *ApoA1*$^{+/-}$ compared with WT mice (*$P<0.05$) (**d**). The differences in Ki67 and p-STAT3 expression between AOM/DSS-treated and untreated groups were statistically significant ($P<0.001$; Mann–Whitney test). (**e**) Representative photographs of tumor-bearing colons and collective data of tumor distribution in WT ($n=9$) and *ApoA1*$^{+/-}$ ($n=11$) mice are shown. **$P<0.01$.

pro-inflammatory cytokines in both proximal and distal parts of the large intestine. Conversely, administration of the ApoA-I-mimetic peptide 4F reduces disease burden and histological manifestations of colitis in the mouse, indicating that ApoA-I could directly confer anti-inflammatory effects in the intestine. These findings support the recently reported association between low ApoA-I levels and inflammation in human IBD patients.[44]

Recent studies have underscored a crucial role for TLR signaling in inflammation and cancer in the colon. In DSS-induced colitis, intestinal epithelial and lamina propria cells respond to products of pathogenic bacteria by activating TLRs, leading to the production of a plethora of inflammatory mediators. Among them, IL-6 signaling through STAT3 is a critical regulator of LPS-driven pro-inflammatory responses[45] and malignant transformation of intestinal epithelial cells.[31,32] Thus, the establishment of a cell-autonomous TLR4-STAT3 signaling axis promotes colon tumor growth,[46] whereas ablation of TLR4 results in resistance to AOM/DSS-induced CAC.[47] The ApoA-I mimetic peptide 4F and ApoA-I directly bind to the lipid-A domain of LPS, reducing its TLR4-stimulating capacity in macrophages.[33,34] Herein we extend these observations by showing that 4F suppresses TLR4-induced NF-κB signal transduction, IL-6 synthesis and STAT3 activation in a transformed mouse intestinal epithelial cell line, underscoring putative mechanistic links between ApoA-I and protection from intestinal pathologies. In agreement with these *in vitro* findings, reduced ApoA-I levels lead to susceptibility to CAC with tumors extending to middle and proximal regions of the colon and possessing elevated levels of Ki67 and activated STAT3 compared with carcinomas developed in WT animals. This observation provides experimental support to epidemiological observations showing an inverse association between ApoA-I and colon cancer risk in a cohort of >520 000 Europeans.[48]

Although the anti-inflammatory effects of enterocyte-produced ApoA-I or exogenously administered mimetic peptide are likely to include cell types other than epithelial cells in the intestine, such as macrophages,[49] our study suggests that modulation of ApoA-I levels could be explored for the management of colitis and colon cancer.[28] In line with this notion, an ApoA-I mimetic peptide has been reported to reduce the incidence of tumors in the APC$^{min/+}$ mouse model for human familial adenomatous polyposis.[50] In addition to the protective effect of an ApoA-I-mimetic peptide on colitis described herein, statins have been reported to increase ApoA-I levels,[51] to attenuate DSS-induced colitis in the mouse[52] and to significantly reduce colorectal cancer risk in humans.[53] Statins also synergize with D-4F to upregulate ApoA-I in the intestine and reduce atherosclerotic lesions in susceptible mice.[54] Collectively, these findings expand our appreciation of the impact of lipid metabolic pathways on intestinal pathologies and suggest that induction in ApoA-I levels has the potential to minimize the severity of colitis and its comorbidities.

© 2016 Macmillan Publishers Limited

MATERIALS AND METHODS

Mice and *in vivo* treatments

Mice were maintained as previously described.[55] For the colitis and CAC model, female C57BL/6J mice (approximately 18–20 g weight) were injected intaperitoneally with 10 mg/kg body weight AOM and 4 days later 2.5% DSS was administered in their drinking water for 5 days, followed by 14 days of regular water. This cycle was repeated once or three times more before mice were killed. Power analysis, based on χ^2 statistics has been used to determine the number of animals required to allow a valid assessment of the data using appropriate statistical tests. Typically, 10–12 mice were used per treatment and genotype group and each experiment was performed at least twice. For the acute colitis model, mice (22–24 g weight) were administered 3% (w/v) DSS in water for 7 consecutive days followed by water without DSS. Typically, six mice were used per group and each experiment was performed at least twice. ApoA-I knock-out mice (ApoA-Itm1Unc, C57BL/6J background) were obtained from Jackson ImmunoResearch Laboratories (Bar Harbor, ME, USA), bred with WT mice and maintained as $ApoA1^{+/-}$ for at least eight generations. $ApoA1^{+/-}$ animals were then used to generate experimental groups of different *ApoA1* genotypes ($ApoA1^{+/+}$, $ApoA1^{+/-}$ and $ApoA1^{-/-}$), which were co-housed and maintained in identical conditions before treatment. The investigators recording mouse data (KG and MI) were blinded to the group allocation according to genotype (genotype assessed by AS). The peptide 4F and its scramble control were synthesized from all D-amino acids,[27] high-performance liquid chromatography purified to $>90\%$ (Caslo ApS, Lyngby, Denmark) and used at 300 μg/ml[56] in drinking water. Intestinal tissues from NSG mice and germ-free animals were provided by the animal facility of IMBB-FORTH (Heraklion, Greece) and by the EMMA-Axenic Service, Instituto Gulbenkian de Ciência, Oeiras, Portugal, respectively. Animal experiments were approved by the ethical committee of the University of Crete Medical School, Heraklion, Greece.

Tissue processing, histological and IHC evaluations

After killing, the large intestine of the mouse was removed, opened longitudinally, scored for number of tumors and fixed in buffered formalin for histological analyses. For each animal, two sections approximately 400 μm apart were scored and averaged by an experienced pathologist (ED) blinded to the experimental conditions using a validated scoring system developed by Cooper *et al*.[36] and Dieleman *et al*.[57] and modified by Williams *et al*.[58] in a scale of 0–40. IHC was performed as previously described[55] using the following antibodies applied overnight at 4 °C: α-mouse ApoA-I (Meridian Life Science, Memphis, TN, USA, cat no. K23500R, used at 1:2000 dilution); α-phospho-Tyr^{705} STAT3 (Cell Signaling, Danvers, MA, USA, cat no. 9145, used at 1:500 dilution); α-NFκB p65 (Cell Signaling, cat no. 8242, used at 1:500 dilution). Ki67 (Novus Biologicals, Littleton, CO, USA, cat no. NB110-89719, used at 1:100 dilution) was applied for 2 h at room temperature. Any nuclear staining of cells for p-STAT3, p65 or Ki67 was considered positive. Expression levels for p-STAT3, p65 or Ki67 were determined by counting at least 500 nuclei in each case. The percentage of Ki67-positive cells was designated as the proliferation index.

Gene expression profiling

Approximately 2.5 cm of proximal and distal colon tissue was dissected (Figure 1d) and processed for RNA isolation using homogenization in Trizol (Invitrogen, Carlsbad, CA, USA). Total RNA underwent QC using the Agilent Bioanalyzer system (Agilent Technologies, Inc., Santa Clara, CA, USA) and amplified using the NuGEN Ovation RNA Amplification System V2 (NuGEN Technologies, Inc., San Carlos, CA, USA). Six biological replicates of each untreated proximal and distal colon, three biological replicates of each early treatment proximal and distal colon (Figure 1a), four biological replicates of late treatment proximal and six biological replicates of late treatment distal colon (total 28 samples) were further processed. The appropriate amount of amplified single-stranded complementary DNA was fragmented and labeled using the FL-Ovation cDNA Biotin Module V2 (NuGEN Technologies, Inc.). Fragmented labeled complementary DNA was hybridized to the Affymetrix Mouse 430 2.0 array. The data discussed in this publication have been deposited in NCBI's Gene Expression Omnibus and are accessible through accession numbers GSE64423 (http://www.ncbi.nlm.nih.gov/geo/query/acc.cgi?acc=GSE64423) and GSE64658 (http://www.ncbi.nlm.nih.gov/geo/query/acc.cgi?acc=GSE64658).

In silico analysis of microarray data

Raw microarray profile data have been pre-processed with the Robust Multichip Average algorithm. The pre-processed data have been filtered to remove control probesets and uninformative transcripts based on probe set intensity (background *P*-value = 0.001) and variance (variance *α*-value = 0.65). A two-way analysis of variance model (time point and colon location) and post-hoc pairwise comparisons has been used identify transcripts differentially expressed in the AOM/DSS early and AOM/DSS late time points (untreated/WT as baseline), for each colon region. The impact of multiple test inflation has been reduced using false discovery rate correction of the analysis of variance *P*-values. Transcription factor relationships were established using Ingenuity Upstream Regulator Analysis in IPA. GO enrichment was performed using the DAVID functional annotation repository (http://david.abcc.ncifcrf.gov/).

Quantification of circulating HDL and ApoA-I levels in mouse blood

Mice were killed after a 4-h fast and blood was collected by cardiac puncture. Serum samples were mixed with a precipitation solution comprising 10 g/l dextran sulfate and 0.5 M $MgCl_2$ at a volume ratio of 10:1 and incubated for 10 min at room temperature. The mixture was centrifuged for 40 min at 14 000 r.p.m. at 4 °C, and the HDL-containing supernatant was collected. HDL-cholesterol was measured using a commercially available assay (Thermo Scientific, Waltham, MA, USA) according to the manufacturer's recommendations. ApoA-I levels in serum were assessed by enzyme-linked immunosorbent assay (Cloud Clone Corp., Houston, TX, USA) according to the instructions of the manufacturer.

Real-time PCR

RNA isolation, complementary DNA synthesis and quantitative PCR reactions were performed as previously described.[55] The following TaqMan gene expression assays (Applied Biosystems, Waltham, MA, USA) were used: *il-6* (ID Mm00446190_m1, FAM (6 - Carboxyfluorescein)-labeled), *tnf* (ID Mm00443259_g1, FAM), *il-1b* (ID Mm00434228_m1, FAM), *ApoA-I* (ID Mm00437568_g1, FAM) and *β-actin* (ID Mm00607939_s1, VIC-labeled) as endogenous control.

Cell lines, treatments and western blotting

CMT-93 cells (ATCC, cat no. CCL-223, Manassas, VA, USA) were used within 6 months of purchase and tested as mycoplasma negative. Exponentially growing cultures were treated with 4F or scramble control peptide at 50 μg/ml before stimulation with 1 μg/ml LPS (*E. coli* strain 055:B5, Sigma-Aldrich, St Louis, MO, USA) for various time intervals. Nuclear cell extracts were isolated and processed for immunoblotting as previously described[55] using p65/RelA (clone D14E12; Cell Signaling, cat no. 8242), p-STAT3 (clone D3A7; Cell Signaling, cat no. 9145) and SP1 (clone PEP2; Santa Cruz Biotechnology, Dallas, TX, USA, cat no. SC-59) antibodies.

Statistical analyses

Results are expressed as mean ± s.e.m. The statistical significance of differences between two groups was determined using a two-tailed non-parametric Mann–Whitney *U*-test or one-way analysis of variance for comparison of three or more groups as indicated. All analyses were performed using GraphPad PRISM version 5.00 (GraphPad Software, San Diego, CA, USA). The statistical power for the *in vivo* experiments was calculated using an online tool from Statistical Solutions (http://www.statisticalsolutions.net/pss_calc.php). Variances were similar between groups that were statistically compared.

CONFLICT OF INTEREST

The authors declare no conflict of interest.

ACKNOWLEDGEMENTS

We thank Dimitra Vyrla (University of Crete Medical School), Triantafyllos Liloglou (University of Liverpool) and Maria Denis (Biomedcode Hellas SA) for helpful discussions. This work was supported by the European Commission (EC) research program Inflammation and Cancer Research in Europe (*INFLA-CARE*; EC contract number 223151) to AGE and Almac Diagnostics and the EC REGPOT support program Translational Potential (*TransPOT;* EC contract number 285948) to AGE, KP, II and DK.

© 2016 Macmillan Publishers Limited

AUTHOR CONTRIBUTIONS

KKG and MI contributed equally to this work. KKG, MI, AS, KG, GN, DCK, DK and ED contributed to acquisition, analysis and interpretation of experimental data and critical reading of the manuscript; SM and FAM performed the gene expression profiling and contributed to *in silico* analysis of results; GAP and II contributed to bioinformatic analyses and critically reviewed the manuscript; KAP, DK and ED contributed to interpretation of experimental data and critically reviewed the manuscript; AGE contributed to conception, design, analysis and interpretation of data and drafting of the manuscript.

REFERENCES

1 Eaden JA, Abrams KR, Mayberry JF. The risk of colorectal cancer in ulcerative colitis: a meta-analysis. *Gut* 2001; **48**: 526–535.
2 Bernstein CN, Blanchard JF, Kliewer E, Wajda A. Cancer risk in patients with inflammatory bowel disease: a population-based study. *Cancer* 2001; **91**: 854–862.
3 Maloy KJ, Powrie F. Intestinal homeostasis and its breakdown in inflammatory bowel disease. *Nature* 2011; **474**: 298–306.
4 Gkouskou KK, Deligianni C, Tsatsanis C, Eliopoulos AG. The gut microbiota in mouse models of inflammatory bowel disease. *Front Cell Infect Microbiol* 2014; **4**: 28.
5 Okayasu I, Hatakeyama S, Yamada M, Ohkusa T, Inagaki Y, Nakaya R. A novel method in the induction of reliable experimental acute and chronic ulcerative colitis in mice. *Gastroenterology* 1990; **98**: 694–702.
6 Laroui H, Ingersoll SA, Liu HC, Baker MT, Ayyadurai S, Charania MA *et al.* Dextran sodium sulfate (DSS) induces colitis in mice by forming nano-lipocomplexes with medium-chain-length fatty acids in the colon. *PloS one* 2012; **7**: e32084.
7 Bersudsky M, Luski L, Fishman D, White RM, Ziv-Sokolovskaya N, Dotan S *et al.* Non-redundant properties of IL-1alpha and IL-1beta during acute colon inflammation in mice. *Gut* 2014; **63**: 598–609.
8 Mudter J, Neurath MF. Il-6 signaling in inflammatory bowel disease: pathophysiological role and clinical relevance. *Inflamm Bowel Dis* 2007; **13**: 1016–1023.
9 Yan Y, Kolachala V, Dalmasso G, Nguyen H, Laroui H, Sitaraman SV *et al.* Temporal and spatial analysis of clinical and molecular parameters in dextran sodium sulfate induced colitis. *PloS One* 2009; **4**: e6073.
10 Okayasu I, Ohkusa T, Kajiura K, Kanno J, Sakamoto S. Promotion of colorectal neoplasia in experimental murine ulcerative colitis. *Gut* 1996; **39**: 87–92.
11 Mahler M, Bristol IJ, Leiter EH, Workman AE, Birkenmeier EH, Elson CO *et al.* Differential susceptibility of inbred mouse strains to dextran sulfate sodium-induced colitis. *Am J Physiol* 1998; **274**: G544–G551.
12 Choi PM. Predominance of rectosigmoid neoplasia in ulcerative colitis and its implication on cancer surveillance. *Gastroenterology* 1993; **104**: 666–667.
13 Goldstone R, Itzkowitz S, Harpaz N, Ullman T. Dysplasia is more common in the distal than proximal colon in ulcerative colitis surveillance. *Inflamm Bowel Dis* 2012; **18**: 832–837.
14 Goldstone R, Itzkowitz S, Harpaz N, Ullman T. Progression of low-grade dysplasia in ulcerative colitis: effect of colonic location. *Gastrointest Endosc* 2011; **74**: 1087–1093.
15 Wu AL, Windmueller HG. Relative contributions by liver and intestine to individual plasma apolipoproteins in the rat. *J Biol Chem* 1979; **254**: 7316–7322.
16 Ramasamy I. Recent advances in physiological lipoprotein metabolism. *Clin Chem Lab Med* 2014; **52**: 1695–1727.
17 Bollrath J, Greten FR. IKK/NF-kappaB and STAT3 pathways: central signalling hubs in inflammation-mediated tumour promotion and metastasis. *EMBO Rep* 2009; **10**: 1314–1319.
18 Grivennikov S, Karin E, Terzic J, Mucida D, Yu GY, Vallabhapurapu S *et al.* IL-6 and Stat3 are required for survival of intestinal epithelial cells and development of colitis-associated cancer. *Cancer Cell* 2009; **15**: 103–113.
19 Bollrath J, Phesse TJ, von Burstin VA, Putoczki T, Bennecke M, Bateman T *et al.* gp130-mediated Stat3 activation in enterocytes regulates cell survival and cell-cycle progression during colitis-associated tumorigenesis. *Cancer Cell* 2009; **15**: 91–102.
20 Becker C, Fantini MC, Schramm C, Lehr HA, Wirtz S, Nikolaev A *et al.* TGF-beta suppresses tumor progression in colon cancer by inhibition of IL-6 trans-signaling. *Immunity* 2004; **21**: 491–501.
21 Miller JC, Barth RK, Shaw PH, Elliott RW, Hastie ND. Identification of a cDNA clone for mouse apoprotein A-1 (apo A-1) and its use in characterization of apo A-1 mRNA expression in liver and small intestine. *Proc Natl Acad Sci USA* 1983; **80**: 1511–1515.
22 Basque JR, Levy E, Beaulieu JF, Menard D. Apolipoproteins in human fetal colon: immunolocalization, biogenesis, and hormonal regulation. *J Cell Biochem* 1998; **70**: 354–365.
23 Toft NJ, Winton DJ, Kelly J, Howard LA, Dekker M, te Riele H *et al.* Msh2 status modulates both apoptosis and mutation frequency in the murine small intestine. *Proc Natl Acad Sci USA* 1999; **96**: 3911–3915.
24 Gupta J, del Barco Barrantes I, Igea A, Sakellariou S, Pateras IS, Gorgoulis VG *et al.* Dual function of p38alpha MAPK in colon cancer: suppression of colitis-associated tumor initiation but requirement for cancer cell survival. *Cancer Cell* 2014; **25**: 484–500.
25 Neufert C, Becker C, Neurath MF. An inducible mouse model of colon carcinogenesis for the analysis of sporadic and inflammation-driven tumor progression. *Nat Protoc* 2007; **2**: 1998–2004.
26 Navab M, Anantharamaiah GM, Reddy ST, Fogelman AM. Apolipoprotein A-I mimetic peptides and their role in atherosclerosis prevention. *Nat Clin Pract Card* 2006; **3**: 540–547.
27 Navab M, Anantharamaiah GM, Hama S, Garber DW, Chaddha M, Hough G *et al.* Oral administration of an Apo A-I mimetic peptide synthesized from D-amino acids dramatically reduces atherosclerosis in mice independent of plasma cholesterol. *Circulation* 2002; **105**: 290–292.
28 Do RQ, Nicholls SJ, Schwartz GG. Evolving targets for lipid-modifying therapy. *EMBO Mol Med* 2014; **6**: 1215–1230.
29 Ou J, Wang J, Xu H, Ou Z, Sorci-Thomas MG, Jones DW *et al.* Effects of D-4F on vasodilation and vessel wall thickness in hypercholesterolemic LDL receptor-null and LDL receptor/apolipoprotein A-I double-knockout mice on western diet. *Circ Res* 2005; **97**: 1190–1197.
30 Navab M, Anantharamaiah GM, Fogelman AM. An apolipoprotein A-I mimetic works best in the presence of apolipoprotein A-I. *Circ Res* 2005; **97**: 1085–1086.
31 Fukata M, Hernandez Y, Conduah D, Cohen J, Chen A, Breglio K *et al.* Innate immune signaling by Toll-like receptor-4 (TLR4) shapes the inflammatory microenvironment in colitis-associated tumors. *Inflamm Bowel Dis* 2009; **15**: 997–1006.
32 Gribar SC, Anand RJ, Sodhi CP, Hackam DJ. The role of epithelial Toll-like receptor signaling in the pathogenesis of intestinal inflammation. *J Leukoc Biol* 2008; **83**: 493–498.
33 Ma J, Liao XL, Lou B, Wu MP. Role of apolipoprotein A-I in protecting against endotoxin toxicity. *Acta Biochim Biophys Sin* 2004; **36**: 419–424.
34 Gupta H, Dai L, Datta G, Garber DW, Grenett H, Li Y *et al.* Inhibition of lipopolysaccharide-induced inflammatory responses by an apolipoprotein AI mimetic peptide. *Circ Res* 2005; **97**: 236–243.
35 Cooper HS, Murthy S, Kido K, Yoshitake H, Flanigan A. Dysplasia and cancer in the dextran sulfate sodium mouse colitis model. Relevance to colitis-associated neoplasia in the human: a study of histopathology *B*-catenin and p53 expression and the role of inflammation.*Carcinogenesis* 2000; **21**: 757–768.
36 Cooper HS, Murthy SN, Shah RS, Sedergran DJ. Clinicopathologic study of dextran sulfate sodium experimental murine colitis. *Lab Invest* 1993; **69**: 238–249.
37 Danese S, Mantovani A. Inflammatory bowel disease and intestinal cancer: a paradigm of the Yin-Yang interplay between inflammation and cancer. *Oncogene* 2010; **29**: 3313–3323.
38 Rubin DC, Shaker A, Levin MS. Chronic intestinal inflammation: inflammatory bowel disease and colitis-associated colon cancer. *Front Immunol* 2012; **3**: 107.
39 Li Y, de Haar C, Chen 1M, Deuring J, Gerrits MM, Smits R *et al.* Disease-related expression of the IL6/STAT3/SOCS3 signalling pathway in ulcerative colitis and ulcerative colitis-related carcinogenesis. *Gut* 2010; **59**: 227–235.
40 Haghpassand M, Bourassa PA, Francone OL, Aiello RJ. Monocyte/macrophage expression of ABCA1 has minimal contribution to plasma HDL levels. *J Clin Invest* 2001; **108**: 1315–1320.
41 Brunham LR, Kruit JK, Iqbal J, Fievet C, Timmins JM, Pape TD *et al.* Intestinal ABCA1 directly contributes to HDL biogenesis in vivo. *J Clin Invest* 2006; **116**: 1052–1062.
42 Davidson NO, Glickman RM. Apolipoprotein A-I synthesis in rat small intestine: regulation by dietary triglyceride and biliary lipid. *J Lipid Res* 1985; **26**: 368–379.
43 Rong R, Ramachandran S, Penumetcha M, Khan N, Parthasarathy S. Dietary oxidized fatty acids may enhance intestinal apolipoprotein A-I production. *J Lipid Res* 2002; **43**: 557–564.
44 Haberman Y, Tickle TL, Dexheimer PJ, Kim MO, Tang D, Karns R *et al.* Pediatric Crohn disease patients exhibit specific ileal transcriptome and microbiome signature. *J Clin Invest* 2014; **124**: 3617–3633.
45 Greenhill CJ, Rose-John S, Lissilaa R, Ferlin W, Ernst M, Hertzog PJ *et al.* IL-6 trans-signaling modulates TLR4-dependent inflammatory responses via STAT3. *J Immunol* 2011; **186**: 1199–1208.
46 Eyking A, Ey B, Runzi M, Roig AI, Reis H, Schmid KW *et al.* Toll-like receptor 4 variant D299G induces features of neoplastic progression in Caco-2 intestinal cells and is associated with advanced human colon cancer. *Gastroenterology* 2011; **141**: 2154–2165.
47 Fukata M, Chen A, Vamadevan AS, Cohen J, Breglio K, Krishnareddy S *et al.* Toll-like receptor-4 promotes the development of colitis-associated colorectal tumors. *Gastroenterology* 2007; **133**: 1869–1881.
48 van Duijnhoven FJ, Bueno-De-Mesquita HB, Calligaro M, Jenab M, Pischon T, Jansen EH *et al.* Blood lipid and lipoprotein concentrations and colorectal cancer

© 2016 Macmillan Publishers Limited

risk in the European Prospective Investigation into Cancer and Nutrition. *Gut* 2011; **60**: 1094–1102.
49 Smythies LE, White CR, Maheshwari A, Palgunachari MN, Anantharamaiah GM, Chaddha M *et al.* Apolipoprotein A-I mimetic 4F alters the function of human monocyte-derived macrophages. *Am J Physiol Cell Physiol* 2010; **298**: C1538–C1548.
50 Su F, Grijalva V, Navab K, Ganapathy E, Meriwether D, Imaizumi S *et al.* HDL mimetics inhibit tumor development in both induced and spontaneous mouse models of colon cancer. *Mol Cancer Ther* 2012; **11**: 1311–1319.
51 Bonn V, Cheung RC, Chen B, Taghibiglou C, Van Iderstine SC, Adeli K. Simvastatin, an HMG-CoA reductase inhibitor, induces the synthesis and secretion of apolipoprotein AI in HepG2 cells and primary hamster hepatocytes. *Atherosclerosis* 2002; **163**: 59–68.
52 Kanagarajan N, Nam JH, Noah ZA, Murthy S. Disease modifying effect of statins in dextran sulfate sodium model of mouse colitis. *Inflamm Res* 2008; **57**: 34–38.
53 Poynter JN, Gruber SB, Higgins PD, Almog R, Bonner JD, Rennert HS *et al.* Statins and the risk of colorectal cancer. *N Engl J Med* 2005; **352**: 2184–2192.
54 Navab M, Anantharamaiah GM, Hama S, Hough G, Reddy ST, Frank JS *et al.* D-4F and statins synergize to render HDL antiinflammatory in mice and monkeys and cause lesion regression in old apolipoprotein E-null mice. *Arterioscl Thromb Vasc Biol* 2005; **25**: 1426–1432.
55 Gkirtzimanaki K, Gkouskou KK, Oleksiewicz U, Nikolaidis G, Vyrla D, Liontos M *et al.* TPL2 kinase is a suppressor of lung carcinogenesis. *Proc Natl Acad Sci USA* 2013; **110**: E1470–E1479.
56 Su F, Kozak KR, Imaizumi S, Gao F, Amneus MW, Grijalva V *et al.* Apolipoprotein A-I (apoA-I) and apoA-I mimetic peptides inhibit tumor development in a mouse model of ovarian cancer. *Proc Natl Acad Sci USA* 2010; **107**: 19997–20002.
57 Dieleman LA, Palmen MJ, Akol H, Bloemena E, Pena AS, Meuwissen SG *et al.* Chronic experimental colitis induced by dextran sulphate sodium (DSS) is characterized by Th1 and Th2 cytokines. *Clin Exp Immunol* 1998; **114**: 385–391.
58 Williams KL, Fuller CR, Dieleman LA, DaCosta CM, Haldeman KM, Sartor RB *et al.* Enhanced survival and mucosal repair after dextran sodium sulfate-induced colitis in transgenic mice that overexpress growth hormone. *Gastroenterology* 2001; **120**: 925–937.

Supplementary Information accompanies this paper on the Oncogene website (http://www.nature.com/onc)

© 2016 Macmillan Publishers Limited

www.oncotarget.com Oncotarget, 2019, Vol. 10, (No. 41), pp: 4224-4246

Review

Constructing personalized longitudinal holo'omes of colon cancer-prone humans and their modeling in flies and mice

Myrofora Panagi[1], Konstantina Georgila[2], Aristides G. Eliopoulos[2,3] and Yiorgos Apidianakis[1]

[1] Department of Biological Sciences, University of Cyprus, Aglatzia, Nicosia, Cyprus

[2] Laboratory of Molecular and Cellular Biology, Division of Basic Sciences, University of Crete Medical School, Heraklion, Crete, Greece

[3] Institute of Molecular Biology and Biotechnology, Forth, Heraklion, Crete, Greece

Correspondence to: *Yiorgos Apidianakis,* ***email***: *apidiana@ucy.ac.cy*

Keywords: Drosophila, inflammation, cancer, microbiota

Received: *August 12, 2015* ***Accepted***: *November 26, 2015* ***Epub***: *December 04, 2015* ***Published***: *June 25, 2019*

Copyright: Panagi et al. This is an open-access article distributed under the terms of the Creative Commons Attribution License 3.0 (CC BY 3.0), which permits unrestricted use, distribution, and reproduction in any medium, provided the original author and source are credited.

ABSTRACT

Specific host genes and intestinal microbes, dysbiosis, aberrant immune responses and lifestyle may contribute to intestinal inflammation and cancer, but each of these parameters does not suffice to explain why sporadic colon cancer develops at an old age and only in some of the people with the same profile. To improve our understanding, longitudinal multi-omic and personalized studies will help to pinpoint combinations of host genetic, epigenetic, microbiota and lifestyle-shaped factors, such as blood factors and metabolites that change as we age. The intestinal holo'ome – defined as the combination of host and microbiota genomes, transcriptomes, proteomes, and metabolomes – may be imbalanced and shift to disease when the wrong host gene expression profile meets the wrong microbiota composition. These imbalances can be triggered by the dietary- or lifestyle-shaped intestinal environment. Accordingly, personalized human intestinal holo'omes will differ significantly among individuals and between two critical points in time: long before and upon the onset of disease. Detrimental combinations of factors could therefore be pinpointed computationally and validated using animal models, such as mice and flies. Finally, treatment strategies that break these harmful combinations could be tested in clinical trials. Herein we provide an overview of the literature and a roadmap to this end.

INTRODUCTION

Among cancers that affect both men and women, colorectal cancer (CRC) is the second leading cause of death in the United States and Europe. Interestingly, more than 90% of CRC cases occur in people 50 years or older. This fact is in line with the notion that sporadic cancers are diseases of old age and indicates that changes that accompany aging exert major influences on the biology and evolution of cancer. Nevertheless, the factors that change with age are not well understood. Mutations in *K-Ras, APC, p53* and other genes are well-known CRC-contributing factors and accumulate in tumors over time. However, these mutations accumulate at different rates in individuals and do not necessarily exert the same effects. One could therefore reason that additional, non-genetic risk factors may act in concert with genetic changes to drive sporadic CRC as we age.

Lifestyle is another factor contributing to CRC. The intestinal biochemical environment is shaped most prominently by dietary habits and by additional lifestyle factors [1, 2], including cigarette smoking [3], heavy use of alcohol [4], infections [5], stress [6], obesity [7] and physical inactivity [1]. These factors may induce detrimental genetic or epigenetic alterations and changes in the microbiota. Interestingly, adopting healthy lifestyle habits at an old age, including following CRC diagnosis, improves survival prospects, indicating that prior detrimental alterations can be counteracted [8].

Similarly, various intestinal microbes have been

suspected to contribute to CRC by impacting enterocyte proliferation and death, modifying host metabolism, or by disrupting immunological homeostasis. However, assigning a role for any of them as a causative agent of CRC is complicated. For example, establishing a causative relationship between *Helicobacter pylori* and gastric ulcers causing gastritis and cancer needed to satisfy most of Koch's postulates, i.e. be found and isolated from ulcers, proven to cause disease when introduced to a healthy organism (Barry Marshall, the Nobel laureate himself), and tackled through antibiotic treatment for ulcer eradication. It is even more difficult to establish Koch's postulates with a complex microbial community, especially if some microbes cannot be readily cultured.

Chronic inflammatory pathologies such as inflammatory bowel disease (IBD) provide examples of how genetic and nongenetic factors intersect to orchestrate disease pathogenesis. Accumulating evidence highlights the impact of an exaggerated immune response to intestinal microbiota and dysbiosis, or aberrant microbial community composition, in the development of IBD and potentially cancer [9]. The systemic inflammatory reactions to dysbiosis coupled with metabolic products of pathogenic bacteria establish a microenvironment rich in free radicals, DNA-damaging toxins, cytokines and growth factors that, collectively, foster tumor development [10]. While IBD preexists in only a small number of people with CRC, the role of inflammation in cancer might be broader than previously thought. A subclinical form of inflammatory signaling that contributes to heightened epithelial regeneration, as pointed by studies in flies and mice, may instead contribute to many of the CRC cases [11-13].

The complex nature of CRC integrating genetic, epigenetic, environmental and microbial cues underscores the need for a holistic perspective and suggests that assessing these factors combinatorially on a personalized basis may be the key to pinpoint them. Moreover, CRC studies necessitate the use of simple model hosts that can reduce the complexity of the disease while reflecting key aspects of the human histopathology and concomitant molecular signals [14]. Mice and fruit flies possess these two key properties and are thus widely used. Based on data from human, mouse and *Drosophila* studies, the present review points to the importance of interactions among host gene expression, the intestinal microbiome and environment and systemic factors and metabolites, which comprise the intestinal holo'ome, an integral system controlling homeostasis, inflammation and cancer. As a roadmap for future studies on intestinal holo'omes we propose: a) a synthesis of information on individual human genome, transcriptome and proteome, the microbiota metagenome and metatranscriptome, the fecal metabolome and proteome and the blood secretome at critical time points, long before and upon the development of pre-cancerous lesions; b) the identification of the co-existence of factors as potential detrimental synergisms within holo'omes linked to disease onset; c) the validation of such synergisms using model organisms, such as flies and mice; and d) the assessment of therapeutics against such detrimental synergisms in clinical trials (Figures 1 and 2).

THE INTESTINAL HOLO'OME

The host genome and epigenome in intestinal inflammation and cancer

An early step in CRC is the development of polyps. Polyps, the aberrant growth of cells within the colorectal epithelial mucosa, can be benign (non-dysplastic) or dysplastic. If dysplastic, these are referred to as premalignant adenomas. Adenomas proceed to malignancy when they invade the underlying tissues (lamina propria) and successfully form secondary tumors to distant sites (metastasis). In addition, genomic instability contributes to tumorigenesis due to defects in DNA repair systems and the concomitant increase in the rate of mutations [15, 16]. The transition from a normal to hyperplastic epithelium is frequently linked to the inactivation of the *adenomatous polyposis coli (APC)* tumor suppressor. *K-Ras* or *B-Raf* oncogene activation leads to the formation of large adenomas [17]. Late adenomas may associate with loss of *SMAD4,* a key component of the transforming growth factor beta (TGFβ) signaling pathway, which normally suppresses tumor growth [18, 19]. The progression from large adenomas to cancer may also require a mutation in the *p53* locus [20]. Loss of function of the tumor suppressor *PTEN* and subsequent upregulation of the PI3K/AKT signaling pathways, also facilitate the development of colon cancer [21]. Tumor metastasis can be further facilitated by PRL3 overexpression, a gene involved in malignant tumor cell motility and metastasis [22]. All the aforementioned genes have homologues in *Drosophila* and similarly to mammals, *Drosophila Apc* loss of function and *K-Ras/Ras1* oncogene promote disease and may synergize during intestinal tumorigenesis [23]. Interestingly, many *Drosophila* studies point to a highly conserved JNK-Hippo-JAK/STAT pathway axis that promotes tumorigenesis in many cases, for example, upon synergism between the *Ras1* oncogene and cell polarity gene mutants [24, 25]. Such a pathway axis is yet to be established in mammals.

In addition, there is a strong genetic basis for mutations and polymorphisms linked to increased inflammation in the intestine of flies, mice, and humans. For example, frame-shift mutations within the *NOD2* locus may cause IBD *via* impaired NF-κB activation in response to bacterial peptidoglycan [26]. Similarly, the Asp299Gly polymorphism in the TLR4 is associated with

IBD, due to impaired NF-κB activation by Gram-negative bacteria [27]. Mutations of the autophagy gene Atg16L1 in combination with viral infection induces intestinal pathologies in mice resembling those observed in IBD patients [28]. Polymorphisms within the pro-inflammatory cytokines IL-1, IL-6 and IL-22 and STAT3 pathway activation may boost mucosal cytokine expression and enterocyte regeneration, thereby facilitating gastrointestinal cancer [29-31]. Strikingly, STAT, Imd/NF-κB, autophagy and NADPH oxidase pathways play a pivotal role in both mammalian and *Drosophila* innate immunity and intestinal host defense [11, 32-35].

Gender itself is a genetic variation that affects inflammation and cancer in the intestine. At all ages, women are less likely than men to develop sporadic colon cancer [36], an observation that has been recapitulated in the $Apc^{Min/+}$ CRC mouse model and attributed to tumor-promoting effects of testosterone [37]. By contrast, estrogens dampen inflammation and protect from colitis and colitis-associated cancer in mice [38, 39], in line with the reduced severity of IBD in postmenopausal women receiving estrogen hormone replacement therapy [40].

In addition to genetic alterations, the transition from normal mucosa to adenomatous polyps is marked by epigenetic changes, namely DNA methylation, histone modifications and aberrant expression of non-coding RNAs[17]. These epigenetic events include hypermethylation and silencing of a number of genes with a proven contribution to CRC including genes of the Wnt signaling pathway such as *APC*, *WNT5A* and *AXIN2* and the DNA repair genes *MLH1*, *MLH2* and *MGMT* among others [41]. Importantly, high-throughput methylation profiling has indicated the existence of three epigenetic subtypes characterized by high, intermediate, and low methylation that exhibit particular clinicopathological and molecular features [41]. Thus, CpG island methylator phenotype 1 (CIMP1) tumors that are typified by high DNA methylation levels are associated with microsatellite instability (MSI) and *B-Raf* mutations. CIMP2 tumors show frequent *K-Ras* but not *B-Raf* mutations or MSI and CIMP-low/negative CRC display high frequency of p53 mutations. A recent study by Akhtar-Zaidi *et al.* has also implicated histone modifications in CRC by identifying changes in Lys4-methylated histone 3 (H3K4me1) as drivers of a transcriptional program that promotes carcinogenesis in the colon [42]. Intestinal inflammation may significantly contribute to epigenetic reprogramming affecting all stages of CRC. For example, IL-6 regulates the expression and activity of DNA methyltransferase 1 (DNMT1) leading to enhanced methylation of tumor suppressor genes [43, 44]. IL-6 also engages a STAT3 pathway that suppresses the expression of miR-34a releasing its inhibitory control over the IL-6 receptor. This epigenetic switch results in amplification of IL-6 signaling and the establishment of a feedback loop that promotes EMT, invasion and metastasis [45].

Links between the genome and epigenome in orchestrating intestinal pathologies are also beginning to emerge. Of note, an IBD susceptibility SNP variant of IL-23 receptor (IL-23R) exhibits reduced ability to bind microRNAs Let-73 and Let-7f, leading to aberrant IL-23R expression and deregulated signaling relevant to IBD pathogenesis [46]. However, the type of epigenetic modifications, the timing and causality to CRC and IBD remain poorly defined and utilization of simple models amenable to genetic manipulation such as *Drosophila* are warranted to define how genomic and epigenetic events intertwine to control intestinal pathologies.

The intestinal microbiome

The mucosal epithelium is in continuous contact with a myriad of autochthonous (resident) and allochthonous (transient in the fecal stream) microbes. In humans, the density of microbes is approximately 10^{12} bacteria per gram of dried colonic content [47]. Microbial colonization begins immediately after birth and the composition changes, over the first two years, to reach a steady community whose composition is defined by many factors, including immune responses, enterocyte turnover, intestinal motility, pH, redox status and nutrient availability [48]. For instance, during the neonatal mammalian life, the intestinal environment is characterized by a reduced oxidation potential that favors the growth of facultative anaerobes, such as streptococci and coliforms [49]. Following weaning, the microbial community becomes more dense and diverse as the high-fat milk diet is replaced by a high-carbohydrate diet. In mice, the mature microbiome is mainly defined by Firmicutes, Bacteroides and Proteobacteria [48]. The mucosal layer of the mouse large intestine is highly enriched for the phylum Firmicutes and, more specifically, for the families Lachnospiraceae and Ruminococcaceae, whereas families such as Bacteroidaceae, Enterococcaceae and Lactobacillaceae are enriched in the mouse lumen [48]. Similarly, the human colon is dominated by four phyla, namely, Firmicutes, Bacteroides, Proteobacteria and Actinobacteria [50]. Gender associations of the gut microbiome composition in healthy humans remain inconclusive, likely reflecting strong environmental influences [51]. Of note, however, specific taxa of Actinobacteria, Proteobacteria, and Firmicutes express enzymes that have the capacity to metabolize steroid hormones and influence their activity [52, 53]. Whether microbiome-derived sex steroids impact on host immunity in a manner similar to that of host-derived hormones and, indirectly, through changes in intestinal microbiome composition remains unknown. Interestingly, a bi-directional association between testosterone levels and microbial communities in the mouse gut has been noted and linked to protection from Type 1 diabetes [54].

The *Drosophila* is most frequently colonized by

Lactobacillales and Acetobacteraceae and occasionally by Enterobacteriaceae, which belong to the Firmicutes and Proteobacteria phyla, but it lacks Bacteroides and other obligate anaerobes presumably due to the presence of oxygen in the fly gut [55]. However, there is significant bacterial variation in terms of diversity and density along the gastrointestinal tract in mammals and in flies [56]. Bacteria populations are more dense in the small and large intestine than in the stomach [48] partly because ingested bacteria die in the acidic environment of the stomach. Thus, areas with approximately neutral pH in the mammalian small and large intestine or the anterior and posterior *Drosophila* midgut might offer a more conducive environment for colonization [48, 56]. Despite the similarities at the level of Firmicutes and Proteobacteria phyla between humans and mice or invertebrates, there are profound differences even among or within individuals of the same species, longitudinally over time and upon various treatments or diets as one moves towards the bacterial species level [50, 57]. This variation makes analysis of human microbiota very complicated; therefore, simple model organisms can be useful in elucidating the contributions of microbiota in inflammation and cancer. For example, NF-κB signaling in the *Drosophila* intestine directly decreases the abundance and modifies the structure of microbiota, while NAPDH oxidase/Duox signaling decreases microbiota abundance and causes oxidative stress to the midgut epithelium [58].

Benefits and problems of having intestinal microbiota

In the absence of intestinal immunological imbalances or pathogenic microbiota, intestinal microbes are largely considered beneficial or neutral. These bacteria are in constant competition for intestinal niches, which is very important for fending off *bona fide* or opportunistic enteric pathogens and operate synergistically

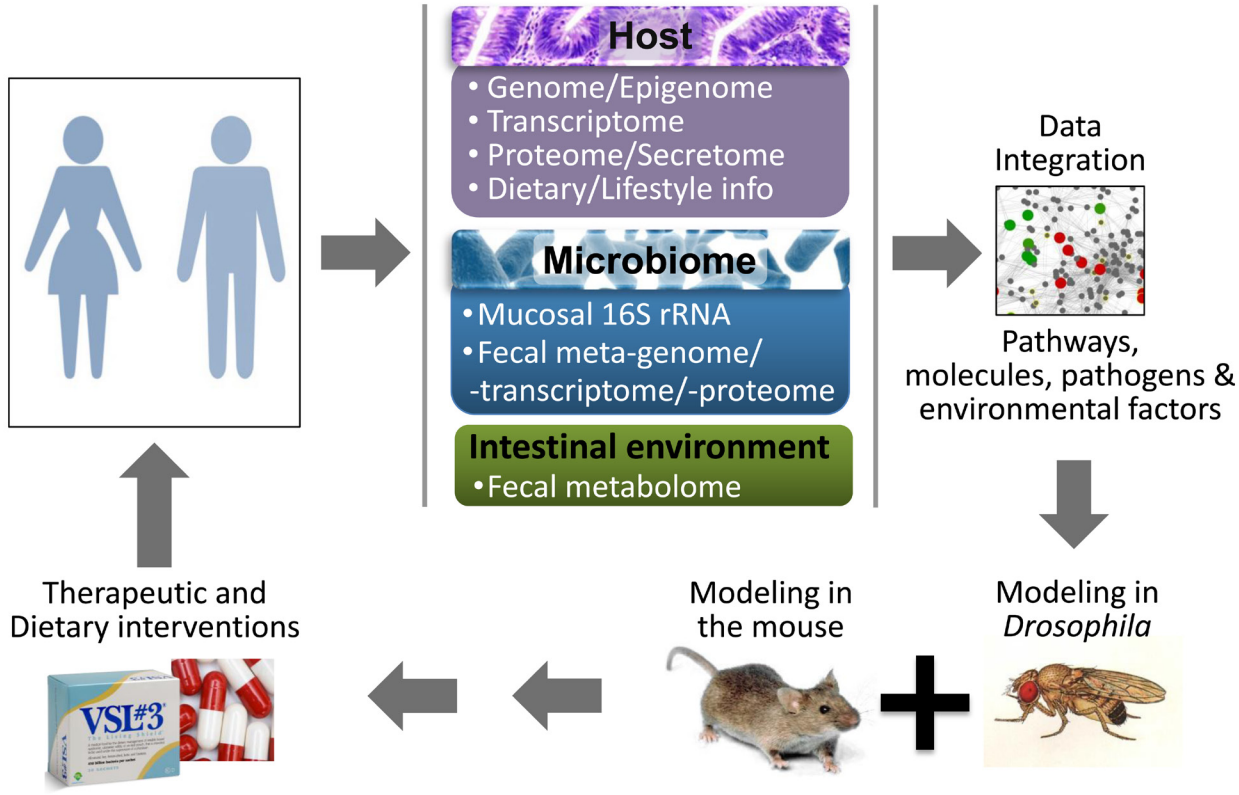

Figure 1: A roadmap to identify detrimental synergisms within human holo'omes as causal for colon cancer and develop personalized therapeutic or preventive strategies. A systems biology approach to assess shifts in intestinal holo'omes in humans and its link to colorectal pathologies will necessitate analysis of host intestine and microbial community genome, transcriptome, proteome metabolome and blood secretome. Using computational platforms, the genetic, metabolic, nutritional, microbial and immunological information accumulated, together with publicly available phenotypic and molecular function data, will be explored to obtain a 'holistic' view of key pathogenic processes and their hierarchies, to simulate the expected response to hypothetical interventions and develop new basic and translational research hypotheses. Reductionist approaches in *Drosophila* and mice - which can be genetically manipulated to express or lose the expression of specific genes in the intestine, while fed or injected with specific microbes and metabolites - could be used to assess detrimental synergisms of the intestinal holo'ome in driving inflammation and tumorigenesis, and guide the development of intervention strategies. Such therapeutic or dietary interventions could be translated to the clinic aiming to treat patients against microbial and intestinal environment imbalances as a means to alleviate intestinal inflammation and CRC.

in order to maintain the overall community function [59]. Furthermore, the metabolic by-products of one species may support the growth of other species or inhibit the colonization by other potentially harmful microbes [50, 60]. Bacteria can also affect the host metabolism while benefiting from the nutrient-rich niche of the intestine. For example, humans lack cellulases and therefore need intestinal bacteria to digest plant cellulose. The mammalian host also takes advantage of the terminal products of microbial fermentation, such as butyrate, acetate and propionate as energy sources [61, 62]. In addition, these bacterial short-chain fatty acids (SCFAs) can act as immunomodulators that contribute to immune homeostasis while suppressing the secretion of pro-inflammatory cytokines [62]. Similarly, in *Drosophila*, *Lactobacillus plantarum* and *Acetobacter pomorum* have been shown to contribute to the nutrition of the host upon nutrient-poor diet. For example, colonization of axenically reared embryos with *L. plantarum* promotes growth when nutrients are limiting by activating the TOR signaling pathway which improves viability and accelerates the developmental rate [63]. Similarly, *A. pomorum* enhances growth of larvae under nutrient scarcity *via* the alcohol dehydrogenase PQQ-ADH, which is required for acetic acid production by the bacteria and the subsequent host insulin pathway activation [64]. On the other hand, *Drosophila* infection with *Vibrio cholerae* leads to inactivation of insulin/insulin-like growth factor signaling (IIS) and lipid accumulation in enterocytes *via* intestinal acetate depletion [65].

Intestinal microbiota may also contribute to the maintenance of mucosal barrier integrity. For example,

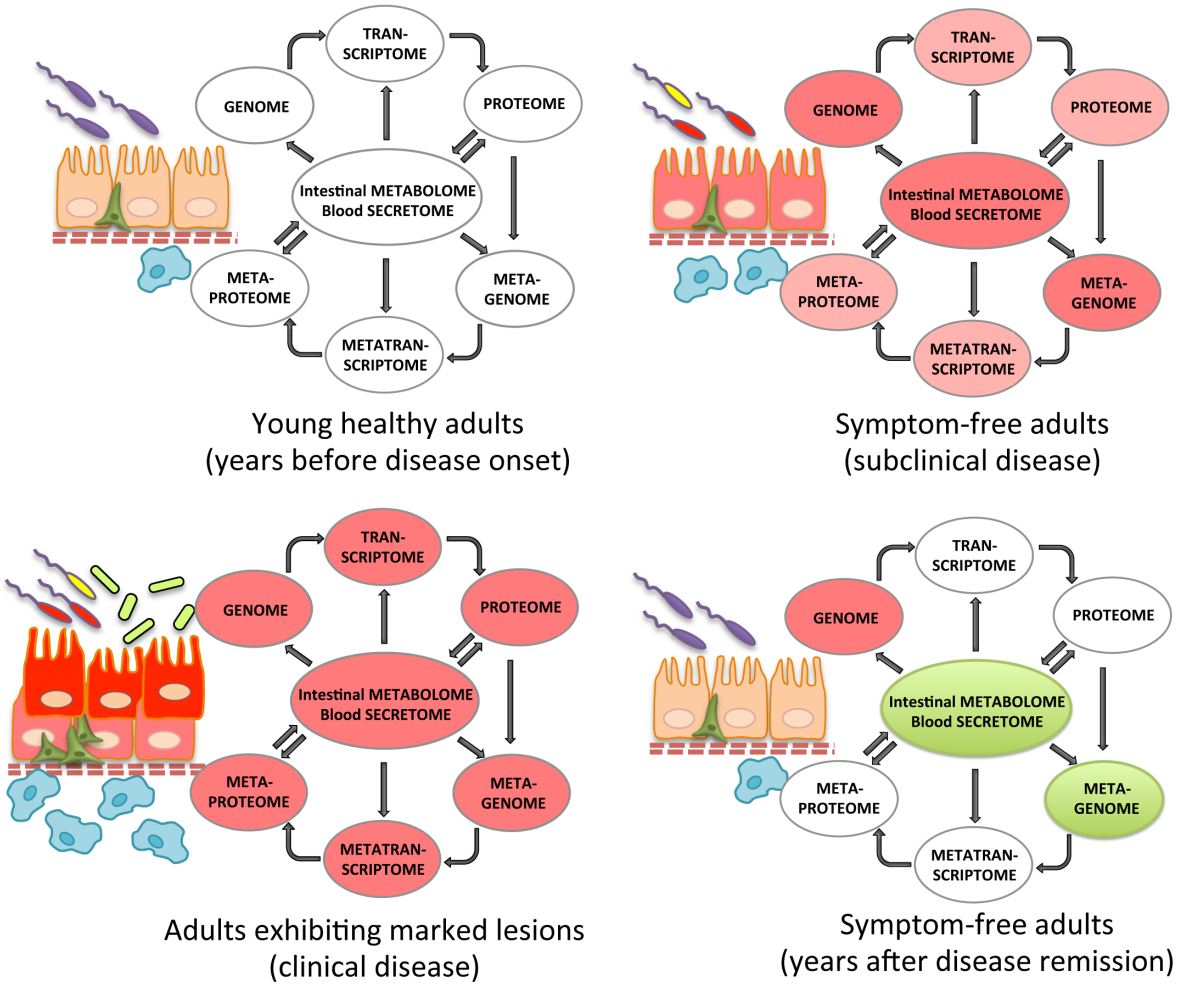

Figure 2: Recording the holo'ome longitudinally in humans. The holo'ome can be recorded via genomics, transcriptomics and proteomics of the host and the microbiota, metabolomics and proteomics of stool samples and secreted factors (e.g. cytokines and metabolites) of blood samples. To identify detrimental synergisms within the holo'ome, its parts need to be recorded around two points in time for each human individual: a**.** at a disease-free state, years before the onset of subclinical disease or long after disease remission, and b**.** upon the onset of subclinical disease. Disease remission may be facilitated by diet- or microbiota-based treatments that change the intestinal or blood environment or the microbiota.

symbiotic bacteria are capable of suppressing the activation of NF-κB pathway in intestinal epithelial cells by inhibiting the ubiquitination of IκB, the inhibitory molecule of NF-κB. Additionally, they may block NF-κB signaling by facilitating the nuclear export of NF-κB subunit, p65, *via* regulation of the peroxisome proliferator-activated receptor (PPAR)γ [66]. Considering the contribution of resident bacteria in host defense mechanisms, polysaccharide antigens produced by *B. fragilis* promote $CD4^+$ T cell expansion and cytokine production [67]. Furthermore, *Lactobacillus spp.* modulate the activation of dendritic and natural killer cells [68, 69]. Strikingly, in both flies and mice *Lactobacillus spp.* are important in maintaining a baseline of intestinal regeneration of the intestine as a mechanism of host defense *via* the induction of reactive oxygen species [33, 70].

The beneficial role of microbiota is clearly demonstrated in germ-free animal models. Animals raised in germ-free conditions have acute developmental and immunologic deficiencies e.g. altered intestinal morphology defined by a reduced muscle wall thickness and underdeveloped villus capillaries [71]. The decrease in angiogenesis is attributed to the limited expression of Angiogenin-4, a potent stimulator of new blood vessels [72] which can be specifically induced by *Bacteroides thetaiotaomicron* [73]. Host-specific commensal bacteria are required for the expansion of T cells and consequently, for the full maturation of intestinal immune system. For example, segmented filamentous bacteria are involved in intestinal T cell expansion [74], IgA activation and induction of epithelial MHC-II expression [75]. Interestingly, the differences between mouse and human microbiota appear to be functionally important because, for instance, colonization of mice with human microbiota results in an immature innate and adaptive immunity and greater susceptibility to infection, as seen in germ-free mice [74]. Germ-free animals are also characterized by impaired cytokine and antimicrobial peptide production, smaller Peyer's patches, fewer intraepithelial lymphocytes and IgA secretion and thus, they are more vulnerable to infections [76]. Germ-free mice show aberrant nutrient absorption presumably due to a decreased metabolic rate and limited digestive enzyme activity, and as a result they tend to consume more calories to maintain a normal body weight [77]. Interestingly, re-colonization of germ-free animals with an intestinal microflora is sufficient to restore many of those functions [78]. Similarly, mono-colonization of germ-free animals with the human commensal bacterium *Bacteroides fragilis* suffices to restore the $CD4^+$ T-cell development through the expression of the microbial molecule polysaccharide A (PSA) [79] . Moreover, inoculation with the single gut inhabitant *Bacteroides thetaiotaomicron* [71] or *B. fragilis* [79] can stimulate villus capillary formation and promote intestinal development. Therefore, the presence of the "right microbes" in the "right host and environment" may determine gut homeostasis.

Various conditions may lead to intestinal dysbiosis, a change in the microbiota composition that is unfavorable for the host and/or immunological imbalances, such as an exaggerated chronic response to the microbiota. Dysbiosis has been reported in a number of enteric disorders and great efforts have been made to define the microbial communities in the intestine of diseased individuals. Bacterial 16S ribosomal RNA and whole genome sequencing studies have linked numerous yet uncultured microorganisms to intestinal disease [80, 81]. Certain bacterial species are prevalent among colon cancer patients. These autochthonous bacteria include *Streptococcus gallolyticus* [82], enterotoxigenic *Bacteroides fragilis* [83], *Escherichia coli* [84] and *Fusobacterium nucleatum* [85]. Similarly, the relative abundance of *Proteobacteria*, such as *E. coli* and other *Enterobacteriaceae*, compared to other phyla is linked to IBD [86]. However, it is difficult to determine whether these alterations refer to the pre- or post-disease state. Alterations within the intestinal ecosystem secondary to pathogen invasion, chronic inflammation or antibiotic treatment may influence the availability of nutrients in the intestinal environment, deregulate the immune response and promote the colonization of opportunistic pathogens [87].

IBD studies in model systems demonstrate that the breakdown of immune tolerance towards indigenous bacteria could lead to inflammatory colitis. For example, immunocompromised mice deficient for T-bet, a transcription factor that orchestrates inflammatory genetic programs in both adaptive and innate immunity, develop IBD that largely resembles human ulcerative colitis [88]. Surprisingly, this colitic phenotype could be transmitted not only to the progeny but also to unrelated wild-type animals, indicating that the presence of an aberrant microbiota is sufficient to cause colitis. Similarly, deregulation of innate immunity against intestinal microbiota in flies *via* mutations of negative regulators of intestinal innate immune response or *via* senescence-related deregulation of innate immunity leads to intestinal dysbiosis and intestinal dysplasia-like phenotypes [60, 89].

Changes in microbiota composition have also been documented during colorectal carcinogenesis. In an established mouse model of colitis-propelled CRC induced by the combined application of the mutagen azoxymethane (AOM) and the luminal toxin dextran sodium sulfate (DSS), the progression from chronic inflammation to dysplasia and adenocarcinoma was associated with significant shifts in microbial community structure, for example of *Prevotella*, *Porphyromonadaceae* and *Bacteroides* genera [90]. Notably, the late stages of colitis-associated CRC in this model were typified by enriched populations of *Erysipelotrichaceae* of the phyllum Firmicutes and colonization of germ-free mice

with tumor-associated gut microbiome exacerbated tumorigenesis in these animals [90]. In another model of CRC induced by application of AOM to colitis-susceptible *Il10*$^{-/-}$ mice lacking the immunoregulatory cytokine IL10, commensal polyketide synthase (*pks*)-positive *E. coli* were found to accelerate progression from dysplasia to invasive carcinoma [91]. Whilst the role, if any, of microbiota perturbations in metastasis remains poorly studied, the abundance of *Fusobacterium nucleatum* in human colon tumors has been reported to associate with lymph node metastasis [85]. Together, these observations imply that changes in microbiota composition may impact on different stages of colorectal carcinogenesis. However, the identification of autochthonous bacterial members as pathobionts (inflammation-/tumor-promoting) or beneficial (inflammation-/tumor-suppressing) would require longitudinal studies in human individuals i.e. long before and upon the onset of disease and monitoring during disease progression [92, 93].

Environmental factors affecting intestinal dysbiosis

The intestinal biochemical environment plays a fundamental role in sustaining a "healthy" host-microbiota interplay. Approximately 5% of people in the United States will develop CRC and half of them will die from the disease [94]. About 75% of the diagnosed CRC cases are sporadic, that is, not evidently hereditary. Thus, beyond genetics, the environment plays a critical role in cancer [2]. Western pattern diet and lifestyle, heavily processed food, frequent use of antibiotics and apparently the improved hygiene in industrialized countries are among the key environmental factors that adversely affect microbiota composition and its interaction with the host.

Diet

Diet is a source of both gut-colonizing bacteria and nutrients that can rapidly alter microbiome structure [95]. The impact of diet has been studied in mice after they have switched from a diet low in fat and high in complex polysaccharides to a westernized diet, rich in fat and sugars. Within a day, the mice display distinct alterations in microbiota composition, gene expression and metabolic pathways, and develop significant adiposity within two weeks [96]. Moreover, diets limited in simple sugars enable mouse intestinal microbiota to outcompete pathogenic *Citrobacter rodentium* [97]. Similarly, the *Drosophila* intestinal microbiota interacts with dietary ingredients to produce vitamin B and proteins or modify the lipid/carbohydrate storage of the host [98]. Interestingly, fly studies show that diet preference and bacterial intestinal colonization level can be affected by the presence of bacterial metabolites in the fly food [99]. Such feeding behaviors and metabolites may have a profound influence on the establishment of intestinal microbiota and the shape of the intestinal biochemical environment. Moreover gender-specific effects of diet on gut microbiota composition and metabolism have been reported across different vertebrate species. For example, *Lactobacillus* and *Clostridium* are more abundant in male mice fed a high-fat rather than chow diet, whereas in females these genera are less abundant in high-fat diets [100]. In *Drosophila,* aspects of the interaction between the microbiota and the host metabolic programs, such as energy storage and protein content, are also sex specific [98].

Changes in diet that modify microbiota may affect the development of inflammatory and malignant diseases. For example, high fat diet promotes the expansion of intestinal bacterium *Bilophila wadsworthia* and colitis in IL10-deficient mice [101]. In addition, lower dietary fiber intake precedes the development of inflammatory pathologies by reducing the production of microbial immunomodulatory products, such as SCFAs [102]. SCFAs selectively expand IL10-producing regulatory T cells (T_{reg}) in the intestine, which in turn suppress inflammation [103]. Interestingly, the SCFA effects on T_{reg} are mediated in part by histone acetylation of the *FoxP3* (forkhead box P3) locus leading to elevated expression of FoxP3, a transcription factor required for the differentiation of $CD4^+$ T lymphocytes to T_{reg} [104, 105]. These findings suggest that microbial metabolic products of diet epigenetically modulate host gene expression and hint to important links between commensal microbiota and epigenetic changes in the immune system that may influence the onset of inflammation and cancer in the intestine. In line with this hypothesis, high levels of *Fusobacterium* that typify both IBD and CRC, correlate with aberrant CpG island methylation in inflamed and malignant tissue [106, 107]. However, as *Fusobacterium* is also part of the normal microbial ecosystem and is not associated with DNA methylation in cancer-free subjects, further studies are required to establish causative links between *Fusobacterium* species and epigenetic re-programming of the host and to identify putative co-factors that enable them to promote intestinal disease.

In terms of carcinogenesis, a number of studies have demonstrated a correlation between saturated fats and CRC [108, 109]. Dietary fat intake increases the production of bile acids. The primary products of bile acid metabolism are synthesized in the liver, where they get conjugated with glycine and taurine. These products get deconjugated by colonic bacteria to form secondary bile acids, namely lithocholic and deoxycholic acid. Accumulating evidence indicates that patients with CRC have elevated amounts of fecal lithocholic and deoxycholic acids compared to healthy controls [110]. Lithocholic and deoxycholic acids stimulate the production of reactive oxygen and nitrogen species, and the activation of the NF-κB signalling pathway [111, 112]. Chronic exposure to these secondary bile acids may enhance mutagenesis

and increase epithelial cell proliferation and/or survival. Taken together, lithocholic and deoxycholic acids could be considered as proinflammatory and procarcinogenic bacterial metabolites. Further understanding of the interactions between indigenous microbiota and intestinal metabolites could thus take us one step forward in elucidating the complex relationship among diet, microbiota and colorectal pathologies.

Accumulating evidence indicates that probiotics could be used as therapeutic strategies for the treatment of metabolic syndromes and chronic inflammatory diseases associated with aberrant gut microbiota [113]. Manipulation of microbiota through probiotic intervention may enhance resistance to intestinal colonization by pathogenic microbes, improve intestinal barrier function, increase the metabolism of nutrients and modulate immune responses [114]. For instance, the lactic acid bacteria *Lactobacillus plantarum* and *Lactobacillus brevis* may inhibit the secretion of pro-inflammatory cytokines and degrade bacterial glycosaminoglycan in a chemically induced colitis mouse model [115]. Inoculation of mice with *Lactobacillus acidophilus* early in life enhances host defense and prevents *Citrobacter rodentium* induced colitis [116]. Despite the lack of adaptive immune responses that may mediate the beneficial responses to *Lactobacillus* species, fly autochthonous bacteria, such as *L. plantarum,* but also pathogens, such as *Pseudomonas aeruginosa*, induce regenerative inflammatory signaling *via* the highly conserved JNK and STAT pathways, as part of the host defense response against intestinal infection [11, 117-119].

Probiotics have also been tested for their ability to prevent intestinal carcinogenesis in mouse models, with promising results [120]. Beyond the role of dysbiosis in the development of CRC, the gut microbiota impacts the therapeutic activity of anticancer agents by influencing pharmacodynamic and immunological parameters that define drug bioavailability and shape the tumor microenvironment respectively [121]. Manipulating the composition of gut microbiota through probiotics, prebiotics (that is, non-digestible agents that stimulate the growth and/or functions of specific microbiota components) and other dietary interventions may thus hold promise for the improved management of cancer patients. A better characterization of the interactions between bacterial species using axenic and gnotobiotic *Drosophila* and mouse models will facilitate this goal.

Differences in the gut microbiota are more striking between different geographic areas, presumably because they encompass both genetic e.g. race and dietary differences. For instance, the microbiota of some African children fed with a diet rich in fiber, as compared to some European children, were found to be enriched in *Bacteroidetes, Xylanibacter* and *Prevotella* species and poor in *Enterobacteriaceae* [122]. The same African children produced significantly more SCFAs in their intestinal lumen [122]. Japanese, on the other hand, despite high standards of hygiene, do not show high allergy incidence (as the hygiene hypothesis would dictate), presumably due to the high intestinal levels of SCFAs, which are produced by the gut microbiota as a byproduct of fermentation of dietary fiber [102]. Nevertheless, other environmental factors, such as differences in pharmaceutical treatments may contribute to the microbiota composition [96].

Antibiotics and other drugs

Antibiotic treatment affects the gut microbiota abundance and diversity at the level of bacterial species. Bacterial communities more vulnerable to common antibiotics are reduced or lost allowing other communities to expand. As a result, intestinal dysbiosis may develop by the expansion of opportunistic pathogens. For example, antibiotics are usually associated with the expansion of *E. coli*, an inhabitant of the mammalian and invertebrate intestine [123]. An increase in the intestinal *E. coli* population is associated with the onset of IBD [124]. Drugs may assist pathogens indirectly by reducing the competitiveness of the host and the healthy microbiota against indigenous opportunistic pathogens. For instance, patients receiving chemotherapy or antibiotics are more vulnerable to *P. aeruginosa* infections, primarily due to compromised host immunity and altered intestinal microbiota [125, 126]. Similarly, antibiotic treatment in mice reduces the resistance of animals to intestinal colonization with *P. aeruginosa* [126]. Of note, endogenous *P. aeruginosa* can cross the intestinal barrier, translocate to and infect other organs, thereby causing systemic inflammation [127].

Although most of the bacterial families manage to re-colonize the gut following an antibiotic regime, the time in between is particularly critical for the host health, because antibiotic-resistant or -tolerant microbes may expand and become established for years [50, 128]. An example of this situation is the persistence of *Staphylococcus epidermidis* following clarithromycin treatment [129]. Since most antimicrobials cannot discriminate between pathogenic and non-pathogenic bacteria, dysbiosis is a likely result of extensive antimicrobial treatments. Similarly, frequent transfer of flies on new food containing preservatives eliminates most of their intestinal bacteria [130]. Thus identifying the microbial populations that become more abundant or virulent following antimicrobial treatments should be a serious consideration.

Hygiene hypothesis

Strachan was the first to mention the role of hygiene in disease predisposition [131]. He coined the term “hygiene hypothesis” in his attempt to elucidate how the decreased exposure to infectious agents in early childhood, as a result of improved hygiene, could lead to an allergic incidence later in life. According to epidemiological studies, a dramatic increase in colon

cancer, IBD, type 1 diabetes, atopy and asthma incidence has been observed during the past 50 years, principally in industrialized countries [132-134]. Communities with low socioeconomic status do not show a similar increase in disease incidence, implying that the immune system becomes educated by experiencing a range of microbes throughout life and consequently, acquires tolerance to relatively innocuous microorganisms [135]. Notwithstanding fundamental issues of hygiene, Tanzania's hunter-gatherer Hadzabe people often consume the uncooked stomachs and colons of killed animals which may increase gut microbial diversity to the benefit of maintaining health in their ecosystem [136]. In developed countries vaccination and antimicrobial therapy must be taken into consideration to better understand and explain these population-based observations. Nevertheless, exposure to infectious agents early in life, may promote the development of regulatory T cells which in turn attenuates the inflammatory response *via* the induction of IL10 and transforming growth factor (TGF)-β1. For example, induction of IL10 following infection with enteric helminthes in mice protects against particular food allergens [137]. Further studies are warranted to address which microbes and anti-inflammatory responses are able to protect against chronic intestinal inflammation.

ANIMAL MODELS IN INFLAMMATION AND CANCER

Various organisms may be used to model aspects of pathophysiology of human intestinal inflammation and cancer [138, 139]. Among them primarily rodents and secondarily flies are the most popular because they combine feasibility and significant similarity to humans. The mouse is highly conserved in many aspects of the human disease and well streamlined for various small-scale experiments. *Drosophila* on the other hand shares surprisingly high similarity to humans regarding disease related genes and signaling pathways while being less complex, which is an advantage for studying some of the basic principles of disease biology and performing large-scale *in vivo* studies on inflammation and cancer [11, 14, 140].

Commonalities and differences between mouse and *Drosophila* intestinal anatomy and physiology

The mammalian and invertebrate gastrointestinal tracts are defined by unique compartments, each of which is responsible for the execution of distinct biological processes. The fly intestine is segregated into five main compartments; the foregut, the crop, the midgut, the malpighian tubules and the hindgut [141]. The foregut corresponds to the mammalian esophagus, whereas the crop and the acidic copper cell region in the middle of the midgut stores and helps digesting food, respectively, thus sharing similarities with the mammalian stomach. The midgut corresponds to the fast renewing mammalian small intestine where the majority of digestion and nutrient absorption takes place [142-144] and is further subdivided into various anterior and posterior regions of distinct expression profiles and stem cell regulation [145, 146]. The malpighian tubules have renal-like properties and are located at the midgut-hindgut boundary. Hindgut is the last compartment of invertebrate intestine and corresponds to the slow, damage-induced renewing property of the mammalian large intestine [144, 147]. The hindgut is the tissue where water and ions most likely get absorbed and the fecal content is promoted to the rectum for excretion [14, 148].

The *Drosophila* midgut is a linear tube that lacks the mammalian intestine crypts and villi. Nevertheless, both of these tissues are of endodermal origin, containing an epithelial monolayer of cells. Enterocytes (ECs) are the most abundant cells in the intestine and have absorptive functions, while secretory enteroendocrine cells (EE), intestinal stem cells (ISCs) and enteroblasts (EBs), account for the minor cell populations of the gut epithelium [143]. Similarly to the mammalian gut, ISCs are maintained by Wg/Wnt signaling and divide asymmetrically to give rise to transient cells, the EBs, and new ISCs or divide symmetrically to increase the number of ISCs [149, 150]. In *Drosophila*, transient cells do not undergo any cell division but they differentiate into either an EC or an EE, while mammalian transit amplifying cells also produce the goblet and Paneth cells, which secrete mucus and antimicrobial peptides, respectively [14, 144].

In both *Drosophila* and mammals, a layer of basement membrane underlines and supports the intestinal epithelium and an outer musculature confers intestinal motility. In mammals, however, three additional layers are found in sequence between the outer musculature and the basement membrane: the submucosa, the muscularis mucosae and the lamina propria. The latter contains immune cells and specialized immunity tissues, such as the Peyer's patches [14]. Despite the lack of adaptive immunity as we know it in humans and mice, *Drosophila* phagocytes accumulate outside the adult midgut upon infection contributing to regenerative inflammatory signaling [12]. Moreover, the *Drosophila* tracheal system has been paralleled with the mammalian circulatory system, since both have been characterized as branched tubular networks that transport gasses to all organs, although the *Drosophila* tracheal system does not transport blood as in mammals [151]. In addition, the diversity of gut microbial community in flies is a hundred times lower than in mammals, and is totally devoid of obligate anaerobes [148]. Therefore, flies offer a basic but not the complete inflammation-tumor microenvironment as it occurs in humans. Accordingly, fly models can serve as a point to accelerate the discovery of basic principles

that govern cancer, but the mouse is more suitable for the investigation of specialized aspects of the intestinal inflammation and cancer that depend, for example, on obligate anaerobes, the adaptive immunity, secretion of bile acids and specialized cells of submucosa or lamina propria.

Regenerative inflammatory signaling and tumor modeling in the *Drosophila* intestine reveals synergisms among the host, its microbes and the intestinal chemical environment

The contribution of *Drosophila* to cancer research is instrumental [152, 153]. Up to 75% of genes that associate with human diseases, including cancer, have functional homologues in *Drosophila* [154]. In addition, the *Drosophila* genome has fewer genes compared to the human genome and a lower genetic redundancy, making the identification of disease-related signaling pathways easier. Thus, *Drosophila* studies have identified many genes and signaling pathways before their human counterparts were linked to cancer. For example, Notch pathway mutant flies were first identified due to a phenotype of notched wings. Years after the initial characterization of the notched phenotype in flies, the human homologue Notch1 was found to cause T cell lymphoplastic leukaemia [155]. Likewise, the hedgehog and hippo signaling pathways, which play a role in human tumorigenesis, have been initially studied in *Drosophila* [156]. Pertinent to human leukemia and CRC, fly studies were the first to demonstrate the role of constitutive JAK-STAT signaling pathway activation in hematopoietic disorders and intestinal regeneration [119, 157].

Due to the great availability of genetic tools that enable the modulation of gene expression in a time and tissue specific manner [140], tumor modeling in *Drosophila* is relatively easy and robust. Tumors can be easily induced in larvae and adult flies following constitutive or conditional knockout of tumor suppressor genes, such as cell polarity growth control regulators. For example, loss of *scribbled* and *salvador* tumor suppressors cause the transformation of renal stem cells into dysplastic-like tumors in the adult *Drosophila* malpighian tubules [158]. Carcinogenesis in flies can be modeled also by using gain of function conditions similar to those leading to tumor development in humans [153]. For instance, cancer models combining oncogenic Ras activity and mitochondrial dysfunction lead cooperatively to excessive ROS generation. This in turn activates a Wnt/Wg and JNK signaling pathway which inactivates Hippo and upregulates the IL6-like Upd leading to tumorigenesis [159].

Drosophila studies have also advanced our knowledge on intestinal response to infection and damage and the concomitant intestinal regenerative inflammatory signaling [11, 151]. Under pathogenic conditions, such as EC damage and stress or aging, a series of highly conserved *Drosophila* signaling pathways, including the EGFR, Wnt/Wg, PDGF/PVF2, INSR/InR and the JNK-Hippo-JAK/STAT, induce stem-cell driven regeneration [117, 160-166]. Regeneration necessitates ISC proliferation and differentiation, as a compensatory defense response replenishing damaged cells [70, 117]. Nonetheless, perturbations of this response, due to mutations, aging or imbalances within the microbiota may lead to an overproduction of differentiating cells and tissue dysplasia-like phenotypes [14, 60, 117, 118, 161]. While these phenotypes that accrue during aging are reminiscent of spontaneous tumors [167], they are not invasive and it remains to be established if they are a result of spontaneous mutations as in humans.

Moreover, intestinal infection with *P. aeruginosa* in *Drosophila* activates the c-Jun N-terminal kinase (JNK) pathway, which causes apoptosis of enterocytes and leads to proliferation of ISCs [117]. Strikingly, genetic predisposition *via* a K-Ras/Ras1 oncogene expression in ISCs synergizes with *P. aeruginosa*-induced inflammatory signals promoting stem cell-mediated tumorigenesis. Interestingly, *P. aeruginosa* virulence against *Drosophila* is enhanced when exposed to peptidoglycan derived from human commensal Gram(+) bacteria [168]. Moreover, sustained intestinal infection with *P. aeruginosa* in *Drosophila* induces the NF-κB/Imd pathway, which synergizes with the $Ras1^{V12}$ oncogene to activate the JNK pathway. This synergism leads to invasion and dissemination of oncogenic hindgut cells to distant sites [169, 170]. Another striking example of microbe-gene synergism is the overabundance of the intestinal pathobiont *Gluconobacter morbifer* upon persistent NF-κB/Imd pathway activation, which in turn induces the NADPH oxidase Duox to produce reactive oxygen species and concomitant hyperplasia [58].

Additional studies reveal a role for *Drosophila* phagocytes in solid tumor biology. *Drosophila* phagocytes, named plasmatocytes, are responsible for the engulfment of apoptotic cells and invading pathogens. Tumor models are used for studying the role of these cells in tumor progression [171]. For example, double mutant $Ras^{V12}/scrib^{-/-}$ tumors within the *Drosophila* larval tissues increase the number of circulating plasmatocytes and attract them to the tumor site. Invasive tumors and concomitant tissue damage activates JNK signaling, which in turn induces JAK/STAT pathway-activating cytokines. These cytokines are amplified by additional cytokine expression in circulating plasmatocytes and the fat body [172]. Moreover, expression of the cytokine TNF by circulating plasmatocytes stimulates the JNK pathway and subsequently matrix metalloproteases in malignant cells, which assist tumor invasiveness [173]. While these studies do not address the role of plasmatocytes in the intestine, *Drosophila* phagocytes were recently shown to

Table 1: Examples of detrimental synergisms between the host genetic background and intestinal microbes, nutrients or metabolites

Host genetic background	Microbe(s)	Intestinal Environment	Phenotype
Drosophila (TOR ↑)	*Lactobacillus plantarum* ↓	Nutrient scarcity	Growth retardation
Drosophila (IIS ↓)	*Acetobacter pomorum* ↓	Nutrient scarcity	Growth retardation
Drosophila (IIS ↓)	*Vibrio cholerae*	Acetate ↓	Intestinal steatosis
Drosophila K-Ras/Ras1 ↑	*Pseudomonas aeruginosa*		Virulence ↑, tumorigenesis ↑
Drosophila K-Ras/Ras1 ↑ (NF-κB/Imd ↑)	*Pseudomonas aeruginosa*		Innate Immunity ↑, Tumor cell dissemination
Drosophila NF-κB/Imd ↑	*Gluconobacter morbifer, uracil secretion*		ROS ↑, damage, hyperplasia
Mouse IL-10 ↓	*Bacteroides fragilis* ↓		$CD4^+$ T cells development defects
Mouse IL-10 ↓	*Bacteroides thetaiotaomicron*		Villus capillary formation ↓
Mouse	*Helicobacter hebaticus* *Bacteroides fragilis* ↓		Proinflammatory cytokines ↑, Colitis ↑
Mouse	*Citrobacter rodentium Bacter. thetaiotaomicron* ↓	Mono-saccharides ↑	Inflammation ↑
Mouse IL-10 ↓	*Bilophila wadsworthia*	Saturated (milk-derived) fat ↑	Colitis ↑
Mouse	*Lactobacillus plantarum, Lactobacillus brevis* ↓	DSS	IL-1β, IL-6 INFγ, TNFα ↑, Colitis ↑
Mouse	*Citrobacter rodentium* *Lactobacillus acidophilus* ↓		Colitis ↑
Mouse	Enteric helminthes e.g. *Heligmosmoides polygyrus* ↓	Food allergen	Allergic response ↑
Mouse IL-10 ↓	*Helicobacter spp.*		IBD
Mouse TLR2-Myd88-NF-κB ↓	*Citrobacter rodentum*		Innate Immunity ↓, Inflammation ↑
Mouse Apc ↓	*Citrobacter rodentum or Fusobacterium nucleatum*		Inflammation, tumorigenesis
Mouse IL-10 ↓	*Helicobacter hepaticus*	Azoxymethane	Inflammation, tumorigenesis
Mouse T-bet ↓, Rag2 ↓	colitogenic *Enterobacteriaceae* *Bifidobacterium infantis* ↓	Fermented milk ↓	Colitis ↑

accumulate in the *Drosophila* midgut upon infection or oxidative stress contributing to regenerative inflammatory signaling [12].

Inflammation and tumor modeling in the mouse intestine reveals synergisms among the host, its microbes and the intestinal environment

Historically, the contribution of rodent models in cancer research begun with the generation and maintenance of mouse strains, inbred to the extent of total homozygosity. Spontaneous mutations arising within these inbred strains provided fundamental information regarding basic mechanisms of carcinogenesis. The laboratory mouse *Mus musculus* is the most frequently used animal model in *in vivo* cancer studies primarily because approximately 99% of human genes have murine orthologues [174]. Even more frequently than in flies, human disease genes display an analogous role in mice [175]. Despite the increased complexity as compared to flies, the mouse genome can be manipulated experimentally and carcinogenic, microbial and inflammatory agents can be combined to study inflammation and cancer in the intestine [176]. Available models integrating dysbiosis, inflammation and tumorigenesis broadly fall into 2 groups: (a) Models in which epithelial integrity disruption is the primary event, for example, following administration of the luminal toxin dextran sodium sulfate (DSS), or by genetic ablation of the NF-κB regulatory gene *IKKγ/NEMO*, or by loss of heterozygosity of the *APC* tumor suppressor gene in intestinal epithelial cells. The ensuing tissue damage allows the translocation of bacteria from the lumen into the mucosa triggering a potent colitis-like inflammatory response or in the case of APC, aberrant cell proliferation. (b) Models in which inflammation is the primary pathological event due to either genetic disruption of immunological balance (e.g. IL10 or combined T-bet/Rag2 deficiency) or introduction of pathogenic bacteria (e.g. *Helicobacter hepaticus)* causing dysbiosis. Damage to the epithelium is likely secondary to the microbiota-driven inflammatory response and is mediated by tissue-resident immune cells and their products. Combinations of such models have also been used to further our understanding of intestinal pathologies. Thus, *C. rodentium* and *Fusobacterium nucleatum* infection of *Apc* mutant mice enhances the recruitment of tumor-infiltrating myeloid cells, thereby establishing an inflammatory environment that favors tumor progression [177, 178]. Similarly, *Helicobacter hepaticus* amplifies inflammation-driven tumorigenesis in IL10-deficient mice exposed to the mutagen azoxymethane [179]. Conversely, probiotic bactreria and fermented milk create a nonpermissive environment for colitogenic *Enterobacteriaceae* in T-bet/Rag2 mutant mice [180].

These models have highlighted diverse functions of microbial-sensing pattern recognition receptors (PRRs) in epithelial *versus* innate immune cells [181]. Among them, Toll-like (TLR) and NOD-like (NLR) receptors have attracted particular attention because of the association of *NOD2*, *NLRP3/*inflammasome and *TLR4* genotypic profiles with human IBD. The picture that emerges suggests that upon disruption of the epithelial barrier, PRR signaling in enterocytes is required to restore epithelial architecture and to induce the expression of anti-microbial peptides that dampen microbial effects. NF-κB dominates the protective PRR response [182, 183], while defective PRR signaling in enterocytes results in pathogen outgrowth and exaggerated inflammation. TLR4 is also required for *de novo* expansion of an intestinal cell subpopulation, designated as ISC compartment, in response to microbial products [184].

By contrast, PRR signaling in innate immune cells mediates pathogenic inflammatory responses. Unresolved inflammation establishes a microenvironment conducive to malignant transformation of intestinal epithelium undergoing cycles of damage and regeneration, eventually leading to tumorigenesis. For example, TLR5 signaling activation promotes *Salmonella* Typhimurium pathogenesis [185]. Also, PRR signaling in myeloid cells leads to NF-κB-dependent production of the pro-inflammatory cytokine IL-6, which promotes the survival and proliferation of premalignant intestinal epithelial cells through STAT3 pathway activation [30]. Similarly, IL-22 produced by intestinal inflammation-induced innate lymphoid cells is necessary for STAT3 activation in ECs and tumor maintenance [31]. Therefore, PRR signals must be finely balanced to maintain intestinal homeostasis: diminished PRR activation may compromise epithelial barrier function whereas excessive PRR signaling may lead to pathogenic inflammatory responses to microbiota and malignant transformation of epithelial cells.

Notwithstanding the similarity to humans at the anatomical, histological and genomic level, mouse models are impractical for large-scale studies of the intestinal holo'ome during homeostasis, inflammation and cancer. Experimental limitations aside, there are ethical concerns in using large numbers of mice. Accordingly, simpler organisms, such as fruit flies, provide adjunct systems to identify new genes, pathogenesis mechanisms and drug treatments, wherever the tissues involved are molecularly conserved and cellularly analogous [140].

A reductionist and a systems biology roadmap to the dynamic intestinal holo'ome

One of the major efforts to systematically reveal the role of microbiota in human health and disease is that of the NIH Human Microbiome Project Consortium, the first phase of which (2008-2012) focused on the diversity and composition of human microbiome. Collectively, these

studies demonstrated that the taxonomic composition of the microbiome varies significantly between individuals and could not be used to explain the role of microbiota in health and disease [186]. Studies looking specifically at individuals with inflammatory bowel disease (IBD) showed relative changes in microbial composition, but no simple biomarkers or therapeutic targets were identified. Instead, microbiome metabolic pathways and functions appear to be linked to IBD, prompting the Integrative Human Microbiome Project to gather and analyze in its second phase (2013-2016) personalized, longitudinal multi-omic data on the microbiota, the host, host-microbiota interaction and the role of lifestyle in disease [186]. Similarly to IBD, colon cancer is caused by many factors that act in combination rather than independently. Therefore, it will be pivotal to identify the synergistic activities among the host, its microbes and the systemic and intestinal environment that cause disease. While gene allele combinations, such as between oncogenes and tumor suppressors have been shown to synergize during carcinogenesis [24, 187, 188], combinations between intestinal microbes, the blood and intestinal environment as shaped by lifestyle, and host genetic background may provide a more complete synergistic assessment.

There are various examples of synergisms between the host genetic background and intestinal microbes, nutrients or metabolites using animal models (Table 1). These suggest mechanisms of disease, but unless validated in additional models and in humans they do not provide proof of disease causation. Using different models e.g. different host strains, diets and microbiota is particularly important because quantitative experimental outcome is context-dependent. Similarly, controlling for the genetic polymorphisms, the microbiome and the habits in human individuals necessitates a personalized medicine approach, because the abundance, distribution and virulence of microbes and metabolites, and gene expression in the intestine differs from person to person and may change over time [92, 126]. The lack of sufficient epidemiological data linking specific microbes, gene alleles and diets to intestinal disease may reflect the lack of clinical studies assessing all of these parameters together in each individual (Figure 1). Multi-omic profiling, such as MOPED (http://www.kolkerlab.org/projects/statistics-bioinformatics/moped), that integrates protein and gene expression databases linking them to genes, their pathways and function is an indicative tool towards this direction. Moreover, microbial multi-omics are fairly well established encouraging their adaptation for intestinal microbiota analysis [189]. Nevertheless, host-microbiota-environment interactions are significantly more challenging requiring customized and sophisticated software, integrated data repositories and standardized sampling of blood, colon biopsy and stool. In this respect the Integrative Human Microbiome Project is expected to pave the way. In essence these studies will identify measurable lifestyle and molecular parameters across different platforms calculating their shift between the young (disease free) and the old (disease-prone) state of the same person. Moreover, follow up studies using genetically defined *Drosophila* and mammalian hosts may assess the role of lifestyle and molecular parameters in facilitating intestinal disease, e.g. by assessing the impact of specific microbes or dysbiotic *vs*. symbiotic microbiota, upon different diets in wild type *vs*. genetically predisposed hosts. Lastly, clinical studies can be designed to assess the effectiveness of therapies against dysbiotic combinations of gene alleles, microbes and environmental factors revealed by model organism studies.

To streamline the assessment of causation in CRC we propose that human intestinal holo'omes be tested at various levels: 1) the host genome (e.g. SNPs), transcriptome and proteome (from colon biopsies), 2) the mucosal microbial composition (from colon biopsies) and fecal microbiota metagenome and metatranscriptome, 3) the blood secretome (cytokines, metabolites) and 4) intestinal metabolome and proteome (from stool samples) [190] . Assuming that even a subclinical (histologically defined) deregulation predisposes for CRC, holo'ome analysis will need to be done in stool, blood and normal appearing colonic mucosa samples taken at two points in time for each human individual: (a) at a disease-free age, years before the onset of disease or long after disease remission, and (b) at a disease-prone age, upon the onset of subclinical disease (Figure 2). Collected data should be analyzed to: (i) pinpoint detrimental molecular synergisms correlating with intestinal disease e.g. being present in an individual in the disease-prone *vs*. the disease-free state; (ii) determine if detrimental molecular synergisms promote intestinal disease in the appropriately adapted model hosts (i.e. in genetically manipulated flies or mice fed or injected with specific microbes and metabolites), and (iii) targeted elimination of these synergisms e.g. elimination of the dysbiotic microbiota and/or normalization of the blood cytokines or intestinal metabolites should decrease the prevalence of disease in human clinical trials. Prebiotic, probiotic, fecal transplantation and bacteriophage therapies are some of the treatment options potentially available in the foreseeable future [191-193] (Figure 1). Importantly, one should discriminate between the different stages of tumor development (i.e. initiation *vs*. progression and benign *vs*. invasive), because the detrimental synergisms may differ accordingly.

While primarily an open-ended search, measuring CRC-related homo'ome parameters is expected to shed light into key aspects of the disease [194], such as:

a) The age-related and metabolic factors driving chronic low-grade intestinal inflammation, regeneration and tumorigenesis.

b) The relative contributions of local regenerative inflammatory signaling *vs.* systemic inflammatory factors in driving CRC during aging.

c) Interventions (dietary, nutrition or physical exercise) that can modulate or eliminate the sources of chronic inflammation.

d) Senescent stem cell, progenitor and enterocyte responses to intestinal damage and stress.

CONCLUSIONS

Drosophila is the simplest model organism sharing substantial human disease gene conservation and intestinal epithelium pathophysiology with humans. Thus, fly in addition to mouse models may guide clinical studies in defining basic parameters of intestinal inflammation and cancer, taking into account the multifaceted and highly complex traits of human intestinal holo'omes. Controlling for the complex genetic, epigenetic, microbiota, lifestyle, gender and age background in future experiments will be critical because in most cases the traits that lead to disease emergence are many, a sum of synergies among gene alleles, microbes and diets that change as we age. Molecular prognosis, diagnosis and treatment options regarding intestinal CRC should be more personalized, and take into consideration synergy within evolving holo'omes of disease-prone *vs*. the disease-free individuals, rather than merely tumor specific genetic/epigenetic markers, as is now customary. At the population level detrimental synergies are likely many and diverse, but our current knowledge is not sufficient to explain the emergence and establishment of CRC. Pinpointing novel factors that drive CRC through longitudinally-changing holo'omes might be laborious and expensive, but necessary to improve CRC prognosis, diagnosis and therapy.

Such a holo'ome approach might also be applicable to other cancers influenced by our microbiota and lifestyle-related factors according to the "Second-Expert-Report" (World Cancer Research Fund). Unlike cancers that develop at a very young age, such as retinoblastoma and neuroblastoma, which depend heavily on the genetic background of neonates, other malignancies, such as lung, liver and pancreatic cancer, are influenced by our environment, low-grade chronic inflammation and metabolism. Accordingly, intestinal microbiota may affect our inflammatory and metabolic status and may not only impact CRC, but also other cancers developing at an old age.

ACKNOWLEDGMENTS

AGE acknowledges co-funding of this review by the General Secretariat of Research and Technology of Greece through the Operational Program Competitiveness and Entrepreneurship (OPCII), NSRF 2007-2013, action "SYNERGASIA 2011", Project THERA-CAN (contract number 11_SYN_1_485). YA acknowledges Marie Curie CIG 303586 "InfectionCancer" and Nichole Broderick.

CONFLICTS OF INTEREST

There is no conflict of interest.

REFERENCES

1. Irigaray P, Newby JA, Clapp R, Hardell L, Howard V, Montagnier L, Epstein S, Belpomme D. Lifestyle-related factors and environmental agents causing cancer: an overview. Biomed Pharmacother. 2007; 61:640–58. https://doi.org/10.1016/j.biopha.2007.10.006. [PubMed]

2. Anand P, Kunnumakkara AB, Sundaram C, Harikumar KB, Tharakan ST, Lai OS, Sung B, Aggarwal BB. Cancer is a preventable disease that requires major lifestyle changes. Pharm Res. 2008; 25:2097–116. https://doi.org/10.1007/s11095-008-9661-9. [PubMed]. Erratum in: Pharm Res. 2008 Sep;25(9):2200. Kunnumakara, Ajaikumar B [corrected to Kunnumakkara, Ajaikumar B]. https://doi.org/10.1007/s11095-008-9690-4.

3. Kuper H, Boffetta P, Adami HO. Tobacco use and cancer causation: association by tumour type. J Intern Med. 2002; 252:206–24. https://doi.org/10.1046/j.1365-2796.2002.01022.x. [PubMed]

4. Testino G. The burden of cancer attributable to alcohol consumption. Maedica (Buchar). 2011; 6:313–20. [PubMed]

5. Parkin DM. The global health burden of infection-associated cancers in the year 2002. Int J Cancer. 2006; 118:3030–44. https://doi.org/10.1002/ijc.21731. [PubMed]

6. Conti CM, Angelucci D, Ferri M, Maccauro G, Caraffa A, Doyle R, Fulcheri M, Cianchetti E. Relationship between cancer and psychology: an updated history. J Biol Regul Homeost Agents. 2011; 25:331–39. [PubMed]

7. Calle EE, Rodriguez C, Walker-Thurmond K, Thun MJ. Overweight, obesity, and mortality from cancer in a prospectively studied cohort of U.S. adults. N Engl J Med. 2003; 348:1625–38. https://doi.org/10.1056/NEJMoa021423. [PubMed]

8. Lee J, Jeon JY, Meyerhardt JA. Diet and lifestyle in survivors of colorectal cancer. Hematol Oncol Clin North Am. 2015; 29:1–27. https://doi.org/10.1016/j.hoc.2014.09.005. [PubMed]

9. Flint HJ, Scott KP, Louis P, Duncan SH. The role of the gut microbiota in nutrition and health. Nat Rev Gastroenterol Hepatol. 2012; 9:577–89. https://doi.org/10.1038/nrgastro.2012.156. [PubMed]

10. Balkwill F, Mantovani A. Inflammation and cancer: back to Virchow? Lancet. 2001; 357:539–45. https://doi.org/10.1016/S0140-6736(00)04046-0. [PubMed]

11. Panayidou S, Apidianakis Y. Regenerative inflammation: lessons from Drosophila intestinal epithelium in health and disease. Pathogens. 2013; 2:209–31.

https://doi.org/10.3390/pathogens2020209. [PubMed]

12. Ayyaz A, Li H, Jasper H. Haemocytes control stem cell activity in the Drosophila intestine. Nat Cell Biol. 2015; 17:736–48. https://doi.org/10.1038/ncb3174. [PubMed]

13. Taniguchi K, Wu LW, Grivennikov SI, de Jong PR, Lian I, Yu FX, Wang K, Ho SB, Boland BS, Chang JT, Sandborn WJ, Hardiman G, Raz E, et al. A gp130-Src-YAP module links inflammation to epithelial regeneration. Nature. 2015; 519:57–62. https://doi.org/10.1038/nature14228. [PubMed]

14. Apidianakis Y, Rahme LG. Drosophila melanogaster as a model for human intestinal infection and pathology. Dis Model Mech. 2011; 4:21–30.
https://doi.org/10.1242/dmm.003970. [PubMed]

15. Kinzler KW, Vogelstein B. Cancer-susceptibility genes. Gatekeepers and caretakers. Nature. 1997; 386:761–63, 763. https://doi.org/10.1038/386761a0. [PubMed]

16. Hanahan D, Weinberg RA. Hallmarks of cancer: the next generation. Cell. 2011; 144:646–74.
https://doi.org/10.1016/j.cell.2011.02.013. [PubMed]

17. Arcila M, Lau C, Nafa K, Ladanyi M. Detection of KRAS and BRAF mutations in colorectal carcinoma roles for high-sensitivity locked nucleic acid-PCR sequencing and broad-spectrum mass spectrometry genotyping. J Mol Diagn. 2011; 13:64–73.
https://doi.org/10.1016/j.jmoldx.2010.11.005. [PubMed]

18. de Caestecker MP, Piek E, Roberts AB. Role of transforming growth factor-beta signaling in cancer. J Natl Cancer Inst. 2000; 92:1388–402.
https://doi.org/10.1093/jnci/92.17.1388. [PubMed]

19. Losi L, Bouzourene H, Benhattar J. Loss of Smad4 expression predicts liver metastasis in human colorectal cancer. Oncol Rep. 2007; 17:1095–99.
https://doi.org/10.3892/or.17.5.1095. [PubMed]

20. Schwitalla S, Ziegler PK, Horst D, Becker V, Kerle I, Begus-Nahrmann Y, Lechel A, Rudolph KL, Langer R, Slotta-Huspenina J, Bader FG, Prazeres da Costa O, Neurath MF, et al. Loss of p53 in enterocytes generates an inflammatory microenvironment enabling invasion and lymph node metastasis of carcinogen-induced colorectal tumors. Cancer Cell. 2013; 23:93–106.
https://doi.org/10.1016/j.ccr.2012.11.014. [PubMed]

21. Song MS, Carracedo A, Salmena L, Song SJ, Egia A, Malumbres M, Pandolfi PP. Nuclear PTEN regulates the APC-CDH1 tumor-suppressive complex in a phosphatase-independent manner. Cell. 2011; 144:187–99.
https://doi.org/10.1016/j.cell.2010.12.020. [PubMed]

22. Kato H, Semba S, Miskad UA, Seo Y, Kasuga M, Yokozaki H. High expression of PRL-3 promotes cancer cell motility and liver metastasis in human colorectal cancer: a predictive molecular marker of metachronous liver and lung metastases. Clin Cancer Res. 2004; 10:7318–28.
https://doi.org/10.1158/1078-0432.CCR-04-0485. [PubMed]

23. Martorell Ò, Merlos-Suárez A, Campbell K, Barriga FM, Christov CP, Miguel-Aliaga I, Batlle E, Casanova J, Casali A. Conserved mechanisms of tumorigenesis in the Drosophila adult midgut. PLoS One. 2014; 9:e88413. https://doi.org/10.1371/journal.pone.0088413. [PubMed]

24. Wu M, Pastor-Pareja JC, Xu T. Interaction between Ras(V12) and scribbled clones induces tumour growth and invasion. Nature. 2010; 463:545–48. https://doi.org/10.1038/nature08702. [PubMed]. Erratum in: Corrigendum: Interaction between Ras^{V12} and scribbled clones induces tumour growth and invasion. [Nature. 2017]. https://doi.org/10.1038/nature21397. [PubMed]

25. Doggett K, Grusche FA, Richardson HE, Brumby AM. Loss of the Drosophila cell polarity regulator Scribbled promotes epithelial tissue overgrowth and cooperation with oncogenic Ras-Raf through impaired Hippo pathway signaling. BMC Dev Biol. 2011; 11:57–77.
https://doi.org/10.1186/1471-213X-11-57. [PubMed]

26. Ogura Y, Bonen DK, Inohara N, Nicolae DL, Chen FF, Ramos R, Britton H, Moran T, Karaliuskas R, Duerr RH, Achkar JP, Brant SR, Bayless TM, et al. A frameshift mutation in NOD2 associated with susceptibility to Crohn's disease. Nature. 2001; 411:603–06.
https://doi.org/10.1038/35079114. [PubMed]

27. Franchimont D, Vermeire S, El Housni H, Pierik M, Van Steen K, Gustot T, Quertinmont E, Abramowicz M, Van Gossum A, Devière J, Rutgeerts P. Deficient host-bacteria interactions in inflammatory bowel disease? The toll-like receptor (TLR)-4 Asp299gly polymorphism is associated with Crohn's disease and ulcerative colitis. Gut. 2004; 53:987–92. https://doi.org/10.1136/gut.2003.030205. [PubMed]

28. Cadwell K, Patel KK, Maloney NS, Liu TC, Ng AC, Storer CE, Head RD, Xavier R, Stappenbeck TS, Virgin HW. Virus-plus-susceptibility gene interaction determines Crohn's disease gene Atg16L1 phenotypes in intestine. Cell. 2010; 141:1135–45.
https://doi.org/10.1016/j.cell.2010.05.009. [PubMed]

29. Rad R, Dossumbekova A, Neu B, Lang R, Bauer S, Saur D, Gerhard M, Prinz C. Cytokine gene polymorphisms influence mucosal cytokine expression, gastric inflammation, and host specific colonisation during Helicobacter pylori infection. Gut. 2004; 53:1082–89. https://doi.org/10.1136/gut.2003.029736. [PubMed]

30. Grivennikov S, Karin E, Terzic J, Mucida D, Yu GY, Vallabhapurapu S, Scheller J, Rose-John S, Cheroutre H, Eckmann L, Karin M. IL-6 and Stat3 are required for survival of intestinal epithelial cells and development of colitis-associated cancer. Cancer Cell. 2009; 15:103–13. https://doi.org/10.1016/j.ccr.2009.01.001. [PubMed]

31. Kirchberger S, Royston DJ, Boulard O, Thornton E, Franchini F, Szabady RL, Harrison O, Powrie F. Innate lymphoid cells sustain colon cancer through production

of interleukin-22 in a mouse model. J Exp Med. 2013; 210:917–31. https://doi.org/10.1084/jem.20122308. [PubMed]

32. Levine B, Mizushima N, Virgin HW. Autophagy in immunity and inflammation. Nature. 2011; 469:323–35. https://doi.org/10.1038/nature09782. [PubMed]

33. Jones RM, Luo L, Ardita CS, Richardson AN, Kwon YM, Mercante JW, Alam A, Gates CL, Wu H, Swanson PA, Lambeth JD, Denning PW, Neish AS. Symbiotic lactobacilli stimulate gut epithelial proliferation via Nox-mediated generation of reactive oxygen species. EMBO J. 2013; 32:3017–28. https://doi.org/10.1038/emboj.2013.224. [PubMed]

34. Ayyaz A, Jasper H. Intestinal inflammation and stem cell homeostasis in aging Drosophila melanogaster. Front Cell Infect Microbiol. 2013; 3:98. https://doi.org/10.3389/fcimb.2013.00098. [PubMed]

35. Kim SH, Lee WJ. Role of DUOX in gut inflammation: lessons from Drosophila model of gut-microbiota interactions. Front Cell Infect Microbiol. 2014; 3:116. https://doi.org/10.3389/fcimb.2013.00116. [PubMed]

36. Ferlitsch M, Reinhart K, Pramhas S, Wiener C, Gal O, Bannert C, Hassler M, Kozbial K, Dunkler D, Trauner M, Weiss W. Sex-specific prevalence of adenomas, advanced adenomas, and colorectal cancer in individuals undergoing screening colonoscopy. JAMA. 2011; 306:1352–58. https://doi.org/10.1001/jama.2011.1362. [PubMed]

37. Amos-Landgraf JM, Heijmans J, Wielenga MC, Dunkin E, Krentz KJ, Clipson L, Ederveen AG, Groothuis PG, Mosselman S, Muncan V, Hommes DW, Shedlovsky A, Dove WF, van den Brink GR. Sex disparity in colonic adenomagenesis involves promotion by male hormones, not protection by female hormones. Proc Natl Acad Sci U S A. 2014; 111:16514–19. https://doi.org/10.1073/pnas.1323064111. [PubMed]

38. Saleiro D, Murillo G, Benya RV, Bissonnette M, Hart J, Mehta RG. Estrogen receptor-β protects against colitis-associated neoplasia in mice. Int J Cancer. 2012; 131:2553–61. https://doi.org/10.1002/ijc.27578. [PubMed]

39. Cook LC, Hillhouse AE, Myles MH, Lubahn DB, Bryda EC, Davis JW, Franklin CL. The role of estrogen signaling in a mouse model of inflammatory bowel disease: a Helicobacter hepaticus model. PLoS One. 2014; 9:e94209. https://doi.org/10.1371/journal.pone.0094209. [PubMed]

40. Kane SV, Reddy D. Hormonal replacement therapy after menopause is protective of disease activity in women with inflammatory bowel disease. Am J Gastroenterol. 2008; 103:1193–96. https://doi.org/10.1111/j.1572-0241.2007.01700.x. [PubMed]

41. Coppedè F. The role of epigenetics in colorectal cancer. Expert Rev Gastroenterol Hepatol. 2014; 8:935–48. https://doi.org/10.1586/17474124.2014.924397. [PubMed]

42. Akhtar-Zaidi B, Cowper-Sal-lari R, Corradin O, Saiakhova A, Bartels CF, Balasubramanian D, Myeroff L, Lutterbaugh J, Jarrar A, Kalady MF, Willis J, Moore JH, Tesar PJ, et al. Epigenomic enhancer profiling defines a signature of colon cancer. Science. 2012; 336:736–39. https://doi.org/10.1126/science.1217277. [PubMed]

43. Foran E, Garrity-Park MM, Mureau C, Newell J, Smyrk TC, Limburg PJ, Egan LJ. Upregulation of DNA methyltransferase-mediated gene silencing, anchorage-independent growth, and migration of colon cancer cells by interleukin-6. Mol Cancer Res. 2010; 8:471–81. https://doi.org/10.1158/1541-7786.MCR-09-0496. [PubMed]

44. Lee H, Zhang P, Herrmann A, Yang C, Xin H, Wang Z, Hoon DS, Forman SJ, Jove R, Riggs AD, Yu H. Acetylated STAT3 is crucial for methylation of tumor-suppressor gene promoters and inhibition by resveratrol results in demethylation. Proc Natl Acad Sci U S A. 2012; 109:7765–69. https://doi.org/10.1073/pnas.1205132109. [PubMed]

45. Daniluk J, Liu Y, Deng D, Chu J, Huang H, Gaiser S, Cruz-Monserrate Z, Wang H, Ji B, Logsdon CD. An NF-κB pathway-mediated positive feedback loop amplifies Ras activity to pathological levels in mice. J Clin Invest. 2012; 122:1519–28. https://doi.org/10.1172/JCI59743. [PubMed]

46. Zwiers A, Kraal L, van de Pouw Kraan TC, Wurdinger T, Bouma G, Kraal G. Cutting edge: a variant of the IL-23R gene associated with inflammatory bowel disease induces loss of microRNA regulation and enhanced protein production. J Immunol. 2012; 188:1573–77. https://doi.org/10.4049/jimmunol.1101494. [PubMed]

47. Eckburg PB, Bik EM, Bernstein CN, Purdom E, Dethlefsen L, Sargent M, Gill SR, Nelson KE, Relman DA. Diversity of the human intestinal microbial flora. Science. 2005; 308:1635–38. https://doi.org/10.1126/science.1110591. [PubMed]

48. Gu S, Chen D, Zhang JN, Lv X, Wang K, Duan LP, Nie Y, Wu XL. Bacterial community mapping of the mouse gastrointestinal tract. PLoS One. 2013; 8:e74957. https://doi.org/10.1371/journal.pone.0074957. [PubMed]

49. Mackie RI, Sghir A, Gaskins HR. Developmental microbial ecology of the neonatal gastrointestinal tract. Am J Clin Nutr. 1999; 69:1035S–45S. https://doi.org/10.1093/ajcn/69.5.1035s. [PubMed]

50. Dethlefsen L, McFall-Ngai M, Relman DA. An ecological and evolutionary perspective on human-microbe mutualism and disease. Nature. 2007; 449:811–18. https://doi.org/10.1038/nature06245. [PubMed]

51. Ding T, Schloss PD. Dynamics and associations of microbial community types across the human body. Nature. 2014; 509:357–60. https://doi.org/10.1038/nature13178. [PubMed]

52. Lombardi P, Goldin B, Boutin E, Gorbach SL. Metabolism of androgens and estrogens by human fecal microorganisms. J Steroid Biochem. 1978; 9:795–801. https://doi.org/10.1016/0022-4731(78)90203-0. [PubMed]

53. Ridlon JM, Ikegawa S, Alves JM, Zhou B, Kobayashi A, Iida T, Mitamura K, Tanabe G, Serrano M, De Guzman A, Cooper P, Buck GA, Hylemon PB. Clostridium scindens: a human gut microbe with a high potential to convert glucocorticoids into androgens. J Lipid Res. 2013; 54:2437–49. https://doi.org/10.1194/jlr.M038869. [PubMed]

54. Markle JG, Frank DN, Mortin-Toth S, Robertson CE, Feazel LM, Rolle-Kampczyk U, von Bergen M, McCoy KD, Macpherson AJ, Danska JS. Sex differences in the gut microbiome drive hormone-dependent regulation of autoimmunity. Science. 2013; 339:1084–88. https://doi.org/10.1126/science.1233521. [PubMed]

55. Chandler JA, Lang JM, Bhatnagar S, Eisen JA, Kopp A. Bacterial communities of diverse Drosophila species: ecological context of a host-microbe model system. PLoS Genet. 2011; 7:e1002272. https://doi.org/10.1371/journal.pgen.1002272. [PubMed]

56. Broderick NA, Buchon N, Lemaitre B. Microbiota-induced changes in drosophila melanogaster host gene expression and gut morphology. MBio. 2014; 5:e01117–14. https://doi.org/10.1128/mBio.01117-14. [PubMed]

57. Stein RR, Bucci V, Toussaint NC, Buffie CG, Rätsch G, Pamer EG, Sander C, Xavier JB. Ecological modeling from time-series inference: insight into dynamics and stability of intestinal microbiota. PLOS Comput Biol. 2013; 9:e1003388. https://doi.org/10.1371/journal.pcbi.1003388. [PubMed]

58. Lee KA, Lee WJ. Drosophila as a model for intestinal dysbiosis and chronic inflammatory diseases. Dev Comp Immunol. 2014; 42:102–10. https://doi.org/10.1016/j.dci.2013.05.005. [PubMed]

59. Buffie CG, Pamer EG. Microbiota-mediated colonization resistance against intestinal pathogens. Nat Rev Immunol. 2013; 13:790–801. https://doi.org/10.1038/nri3535. [PubMed]

60. Ryu JH, Kim SH, Lee HY, Bai JY, Nam YD, Bae JW, Lee DG, Shin SC, Ha EM, Lee WJ. Innate immune homeostasis by the homeobox gene caudal and commensal-gut mutualism in Drosophila. Science. 2008; 319:777–82. https://doi.org/10.1126/science.1149357. [PubMed]

61. Flint HJ, Bayer EA, Rincon MT, Lamed R, White BA. Polysaccharide utilization by gut bacteria: potential for new insights from genomic analysis. Nat Rev Microbiol. 2008; 6:121–31. https://doi.org/10.1038/nrmicro1817. [PubMed]

62. Maslowski KM, Vieira AT, Ng A, Kranich J, Sierro F, Yu D, Schilter HC, Rolph MS, Mackay F, Artis D, Xavier RJ, Teixeira MM, Mackay CR. Regulation of inflammatory responses by gut microbiota and chemoattractant receptor GPR43. Nature. 2009; 461:1282–86. https://doi.org/10.1038/nature08530. [PubMed]

63. Storelli G, Defaye A, Erkosar B, Hols P, Royet J, Leulier F. Lactobacillus plantarum promotes Drosophila systemic growth by modulating hormonal signals through TOR-dependent nutrient sensing. Cell Metab. 2011; 14:403–14. https://doi.org/10.1016/j.cmet.2011.07.012. [PubMed]

64. Shin SC, Kim SH, You H, Kim B, Kim AC, Lee KA, Yoon JH, Ryu JH, Lee WJ. Drosophila microbiome modulates host developmental and metabolic homeostasis via insulin signaling. Science. 2011; 334:670–74. https://doi.org/10.1126/science.1212782. [PubMed]

65. Hang S, Purdy AE, Robins WP, Wang Z, Mandal M, Chang S, Mekalanos JJ, Watnick PI. The acetate switch of an intestinal pathogen disrupts host insulin signaling and lipid metabolism. Cell Host Microbe. 2014; 16:592–604. https://doi.org/10.1016/j.chom.2014.10.006. [PubMed]

66. Kelly D, Campbell JI, King TP, Grant G, Jansson EA, Coutts AG, Pettersson S, Conway S. Commensal anaerobic gut bacteria attenuate inflammation by regulating nuclear-cytoplasmic shuttling of PPAR-γ and RelA. Nat Immunol. 2004; 5:104–12. https://doi.org/10.1038/ni1018. [PubMed]

67. Mazmanian SK, Liu CH, Tzianabos AO, Kasper DL. An immunomodulatory molecule of symbiotic bacteria directs maturation of the host immune system. Cell. 2005; 122:107–18. https://doi.org/10.1016/j.cell.2005.05.007. [PubMed]

68. Christensen HR, Frøkiaer H, Pestka JJ. Lactobacilli differentially modulate expression of cytokines and maturation surface markers in murine dendritic cells. J Immunol. 2002; 168:171–78. https://doi.org/10.4049/jimmunol.168.1.171. [PubMed]

69. Fink LN, Zeuthen LH, Christensen HR, Morandi B, Frøkiaer H, Ferlazzo G. Distinct gut-derived lactic acid bacteria elicit divergent dendritic cell-mediated NK cell responses. Int Immunol. 2007; 19:1319–27. https://doi.org/10.1093/intimm/dxm103. [PubMed]

70. Panayidou S, Ioannidou E, Apidianakis Y. Human pathogenic bacteria, fungi, and viruses in Drosophila: disease modeling, lessons, and shortcomings. Virulence. 2014; 5:253–69. https://doi.org/10.4161/viru.27524. [PubMed]

71. Hooper LV. Bacterial contributions to mammalian gut development. Trends Microbiol. 2004; 12:129–34. https://doi.org/10.1016/j.tim.2004.01.001. [PubMed]

72. Chung H, Kasper DL. Microbiota-stimulated immune mechanisms to maintain gut homeostasis. Curr Opin Immunol. 2010; 22:455–60. https://doi.org/10.1016/j.coi.2010.06.008. [PubMed]

73. Hooper LV, Stappenbeck TS, Hong CV, Gordon JI. Angiogenins: a new class of microbicidal proteins involved in innate immunity. Nat Immunol. 2003; 4:269–73. https://doi.org/10.1038/ni888. [PubMed]

74. Chung H, Pamp SJ, Hill JA, Surana NK, Edelman SM, Troy EB, Reading NC, Villablanca EJ, Wang S, Mora JR, Umesaki Y, Mathis D, Benoist C, et al. Gut immune maturation depends on colonization with a host-specific microbiota. Cell. 2012; 149:1578–93. https://doi.org/10.1016/j.cell.2012.04.037. [PubMed]

75. Suzuki K, Meek B, Doi Y, Muramatsu M, Chiba T, Honjo T, Fagarasan S. Aberrant expansion of segmented filamentous bacteria in IgA-deficient gut. Proc Natl Acad Sci U S A. 2004; 101:1981–86.
https://doi.org/10.1073/pnas.0307317101. [PubMed]

76. Round JL, Mazmanian SK. The gut microbiota shapes intestinal immune responses during health and disease. Nat Rev Immunol. 2009; 9:313–23. https://doi.org/10.1038/nri2515. [PubMed]. Erratum in: Nat Rev Immunol. 2009 Aug;9(8):600. https://doi.org/10.1038/nri2614.

77. Bäckhed F, Ding H, Wang T, Hooper LV, Koh GY, Nagy A, Semenkovich CF, Gordon JI. The gut microbiota as an environmental factor that regulates fat storage. Proc Natl Acad Sci U S A. 2004; 101:15718–23.
https://doi.org/10.1073/pnas.0407076101. [PubMed]

78. Xu J, Gordon JI. Honor thy symbionts. Proc Natl Acad Sci U S A. 2003; 100:10452–59.
https://doi.org/10.1073/pnas.1734063100. [PubMed]

79. Mazmanian SK, Round JL, Kasper DL. A microbial symbiosis factor prevents intestinal inflammatory disease. Nature. 2008; 453:620–25.
https://doi.org/10.1038/nature07008. [PubMed]

80. Clarridge JE 3rd. Impact of 16S rRNA gene sequence analysis for identification of bacteria on clinical microbiology and infectious diseases. Clin Microbiol Rev. 2004; 17:840–62.
https://doi.org/10.1128/CMR.17.4.840-862.2004. [PubMed]

81. Manichanh C, Rigottier-Gois L, Bonnaud E, Gloux K, Pelletier E, Frangeul L, Nalin R, Jarrin C, Chardon P, Marteau P, Roca J, Dore J. Reduced diversity of faecal microbiota in Crohn's disease revealed by a metagenomic approach. Gut. 2006; 55:205–11.
https://doi.org/10.1136/gut.2005.073817. [PubMed]

82. Boleij A, Tjalsma H. The itinerary of Streptococcus gallolyticus infection in patients with colonic malignant disease. Lancet Infect Dis. 2013; 13:719–24.
https://doi.org/10.1016/S1473-3099(13)70107-5. [PubMed]

83. Toprak NU, Yagci A, Gulluoglu BM, Akin ML, Demirkalem P, Celenk T, Soyletir G. A possible role of Bacteroides fragilis enterotoxin in the aetiology of colorectal cancer. Clin Microbiol Infect. 2006; 12:782–86. https://doi.org/10.1111/j.1469-0691.2006.01494.x. [PubMed]

84. Swidsinski A, Khilkin M, Kerjaschki D, Schreiber S, Ortner M, Weber J, Lochs H. Association between intraepithelial Escherichia coli and colorectal cancer. Gastroenterology. 1998; 115:281–86.
https://doi.org/10.1016/S0016-5085(98)70194-5. [PubMed]

85. Castellarin M, Warren RL, Freeman JD, Dreolini L, Krzywinski M, Strauss J, Barnes R, Watson P, Allen-Vercoe E, Moore RA, Holt RA. Fusobacterium nucleatum infection is prevalent in human colorectal carcinoma. Genome Res. 2012; 22:299–306.
https://doi.org/10.1101/gr.126516.111. [PubMed]

86. Sartor RB. Microbial influences in inflammatory bowel diseases. Gastroenterology. 2008; 134:577–94.
https://doi.org/10.1053/j.gastro.2007.11.059. [PubMed]

87. Lysenko ES, Ratner AJ, Nelson AL, Weiser JN. The role of innate immune responses in the outcome of interspecies competition for colonization of mucosal surfaces. PLoS Pathog. 2005; 1:e1.
https://doi.org/10.1371/journal.ppat.0010001. [PubMed]

88. Garrett WS, Lord GM, Punit S, Lugo-Villarino G, Mazmanian SK, Ito S, Glickman JN, Glimcher LH. Communicable ulcerative colitis induced by T-bet deficiency in the innate immune system. Cell. 2007; 131:33–45. https://doi.org/10.1016/j.cell.2007.08.017. [PubMed]

89. Guo L, Karpac J, Tran SL, Jasper H. PGRP-SC2 promotes gut immune homeostasis to limit commensal dysbiosis and extend lifespan. Cell. 2014; 156:109–22.
https://doi.org/10.1016/j.cell.2013.12.018. [PubMed]

90. Zackular JP, Baxter NT, Iverson KD, Sadler WD, Petrosino JF, Chen GY, Schloss PD. The gut microbiome modulates colon tumorigenesis. MBio. 2013; 4:e00692–13.
https://doi.org/10.1128/mBio.00692-13. [PubMed]

91. Arthur JC, Perez-Chanona E, Mühlbauer M, Tomkovich S, Uronis JM, Fan TJ, Campbell BJ, Abujamel T, Dogan B, Rogers AB, Rhodes JM, Stintzi A, Simpson KW, et al. Intestinal inflammation targets cancer-inducing activity of the microbiota. Science. 2012; 338:120–23.
https://doi.org/10.1126/science.1224820. [PubMed]

92. Tjalsma H, Boleij A, Marchesi JR, Dutilh BE. A bacterial driver-passenger model for colorectal cancer: beyond the usual suspects. Nat Rev Microbiol. 2012; 10:575–82. https://doi.org/10.1038/nrmicro2819. [PubMed]

93. Lahti L, Salojärvi J, Salonen A, Scheffer M, de Vos WM. Tipping elements in the human intestinal ecosystem. Nat Commun. 2014; 5:4344.
https://doi.org/10.1038/ncomms5344. [PubMed]

94. Howlader N, Noone A, Krapcho M, Garshell J, Miller D, Altekruse S, Kosary C, Yu M, Ruhl J, Tatalovich Z, Mariotto A, Lewis D, Chen H, et al. SEER Cancer Statistics Review, 1975-2009 (Vintage 2009 Populations). 2012.

95. David LA, Maurice CF, Carmody RN, Gootenberg DB, Button JE, Wolfe BE, Ling AV, Devlin AS, Varma Y, Fischbach MA, Biddinger SB, Dutton RJ, Turnbaugh PJ. Diet rapidly and reproducibly alters the human gut microbiome. Nature. 2014; 505:559–63.
https://doi.org/10.1038/nature12820. [PubMed]

96. Turnbaugh PJ, Ridaura VK, Faith JJ, Rey FE, Knight R, Gordon JI. The effect of diet on the human gut microbiome: a metagenomic analysis in humanized gnotobiotic mice. Sci Transl Med. 2009; 1:6ra14.
https://doi.org/10.1126/scitranslmed.3000322. [PubMed]

97. Kamada N, Kim YG, Sham HP, Vallance BA, Puente JL,

Martens EC, Núñez G. Regulated virulence controls the ability of a pathogen to compete with the gut microbiota. Science. 2012; 336:1325–29. https://doi.org/10.1126/science.1222195. [PubMed]

98. Wong AC, Dobson AJ, Douglas AE. Gut microbiota dictates the metabolic response of Drosophila to diet. J Exp Biol. 2014; 217:1894–901. https://doi.org/10.1242/jeb.101725. [PubMed]

99. Kapsetaki SE, Tzelepis I, Avgousti K, Livadaras I, Garantonakis N, Varikou K, Apidianakis Y. The bacterial metabolite 2-aminoacetophenone promotes association of pathogenic bacteria with flies. Nat Commun. 2014; 5:4401. https://doi.org/10.1038/ncomms5401. [PubMed]

100. Bolnick DI, Snowberg LK, Hirsch PE, Lauber CL, Org E, Parks B, Lusis AJ, Knight R, Caporaso JG, Svanbäck R. Individual diet has sex-dependent effects on vertebrate gut microbiota. Nat Commun. 2014; 5:4500. https://doi.org/10.1038/ncomms5500. [PubMed]

101. Devkota S, Wang Y, Musch MW, Leone V, Fehlner-Peach H, Nadimpalli A, Antonopoulos DA, Jabri B, Chang EB. Dietary-fat-induced taurocholic acid promotes pathobiont expansion and colitis in Il10-/- mice. Nature. 2012; 487:104–08. https://doi.org/10.1038/nature11225. [PubMed]

102. Maslowski KM, Mackay CR. Diet, gut microbiota and immune responses. Nat Immunol. 2011; 12:5–9. https://doi.org/10.1038/ni0111-5. [PubMed]

103. Smith PM, Howitt MR, Panikov N, Michaud M, Gallini CA, Bohlooly-Y M, Glickman JN, Garrett WS. The microbial metabolites, short-chain fatty acids, regulate colonic Treg cell homeostasis. Science. 2013; 341:569–73. https://doi.org/10.1126/science.1241165. [PubMed]

104. Furusawa Y, Obata Y, Fukuda S, Endo TA, Nakato G, Takahashi D, Nakanishi Y, Uetake C, Kato K, Kato T, Takahashi M, Fukuda NN, Murakami S, et al. Commensal microbe-derived butyrate induces the differentiation of colonic regulatory T cells. Nature. 2013; 504:446–50. https://doi.org/10.1038/nature12721. [PubMed]. Erratum in: Nature. 2014 Feb 13;506(7487):254. https://doi.org/10.1038/nature13041.

105. Arpaia N, Campbell C, Fan X, Dikiy S, van der Veeken J, deRoos P, Liu H, Cross JR, Pfeffer K, Coffer PJ, Rudensky AY. Metabolites produced by commensal bacteria promote peripheral regulatory T-cell generation. Nature. 2013; 504:451–55. https://doi.org/10.1038/nature12726. [PubMed]

106. Issa JP, Ahuja N, Toyota M, Bronner MP, Brentnall TA. Accelerated age-related CpG island methylation in ulcerative colitis. Cancer Res. 2001; 61:3573–77. [PubMed]

107. Tahara T, Yamamoto E, Suzuki H, Maruyama R, Chung W, Garriga J, Jelinek J, Yamano HO, Sugai T, An B, Shureiqi I, Toyota M, Kondo Y, et al. Fusobacterium in colonic flora and molecular features of colorectal carcinoma. Cancer Res. 2014; 74:1311–18. https://doi.org/10.1158/0008-5472.CAN-13-1865. [PubMed]

108. Williams CD, Satia JA, Adair LS, Stevens J, Galanko J, Keku TO, Sandler RS. Associations of red meat, fat, and protein intake with distal colorectal cancer risk. Nutr Cancer. 2010; 62:701–09. https://doi.org/10.1080/01635581003605938. [PubMed]

109. Sears CL, Garrett WS. Microbes, microbiota, and colon cancer. Cell Host Microbe. 2014; 15:317–28. https://doi.org/10.1016/j.chom.2014.02.007. [PubMed]

110. Gill CI, Rowland IR. Diet and cancer: assessing the risk. Br J Nutr. 2002 (Suppl 1); 88:S73–87. https://doi.org/10.1079/BJN2002632. [PubMed]

111. Mühlbauer M, Allard B, Bosserhoff AK, Kiessling S, Herfarth H, Rogler G, Schölmerich J, Jobin C, Hellerbrand C. Differential effects of deoxycholic acid and taurodeoxycholic acid on NF-kappa B signal transduction and IL-8 gene expression in colonic epithelial cells. Am J Physiol Gastrointest Liver Physiol. 2004; 286:G1000–08. https://doi.org/10.1152/ajpgi.00338.2003. [PubMed]

112. Da Silva M, Jaggers GK, Verstraeten SV, Erlejman AG, Fraga CG, Oteiza PI. Large procyanidins prevent bile-acid-induced oxidant production and membrane-initiated ERK1/2, p38, and Akt activation in Caco-2 cells. Free Radic Biol Med. 2012; 52:151–59. https://doi.org/10.1016/j.freeradbiomed.2011.10.436. [PubMed]

113. Park J, Floch MH. Prebiotics, probiotics, and dietary fiber in gastrointestinal disease. Gastroenterol Clin North Am. 2007; 36:47–63, v. https://doi.org/10.1016/j.gtc.2007.03.001. [PubMed]

114. Nell S, Suerbaum S, Josenhans C. The impact of the microbiota on the pathogenesis of IBD: lessons from mouse infection models. Nat Rev Microbiol. 2010; 8:564–77. https://doi.org/10.1038/nrmicro2403. [PubMed]

115. Lee HS, Han SY, Bae EA, Huh CS, Ahn YT, Lee JH, Kim DH. Lactic acid bacteria inhibit proinflammatory cytokine expression and bacterial glycosaminoglycan degradation activity in dextran sulfate sodium-induced colitic mice. Int Immunopharmacol. 2008; 8:574–80. https://doi.org/10.1016/j.intimp.2008.01.009. [PubMed]

116. Chen CC, Louie S, Shi HN, Walker WA. Preinoculation with the probiotic Lactobacillus acidophilus early in life effectively inhibits murine Citrobacter rodentium colitis. Pediatr Res. 2005; 58:1185–91. https://doi.org/10.1203/01.pdr.0000183660.39116.83. [PubMed]

117. Apidianakis Y, Pitsouli C, Perrimon N, Rahme L. Synergy between bacterial infection and genetic predisposition in intestinal dysplasia. Proc Natl Acad Sci U S A. 2009; 106:20883–88. https://doi.org/10.1073/pnas.0911797106. [PubMed]

118. Buchon N, Broderick NA, Chakrabarti S, Lemaitre B.

Invasive and indigenous microbiota impact intestinal stem cell activity through multiple pathways in Drosophila. Genes Dev. 2009; 23:2333–44. https://doi.org/10.1101/gad.1827009. [PubMed]

119. Jiang H, Patel PH, Kohlmaier A, Grenley MO, McEwen DG, Edgar BA. Cytokine/Jak/Stat signaling mediates regeneration and homeostasis in the Drosophila midgut. Cell. 2009; 137:1343–55. https://doi.org/10.1016/j.cell.2009.05.014. [PubMed]

120. Zhu Y, Michelle Luo T, Jobin C, Young HA. Gut microbiota and probiotics in colon tumorigenesis. Cancer Lett. 2011; 309:119–27. https://doi.org/10.1016/j.canlet.2011.06.004. [PubMed]

121. Zitvogel L, Galluzzi L, Viaud S, Vétizou M, Daillère R, Merad M, Kroemer G. Cancer and the gut microbiota: an unexpected link. Sci Transl Med. 2015; 7:271ps1. https://doi.org/10.1126/scitranslmed.3010473. [PubMed]

122. De Filippo C, Cavalieri D, Di Paola M, Ramazzotti M, Poullet JB, Massart S, Collini S, Pieraccini G, Lionetti P. Impact of diet in shaping gut microbiota revealed by a comparative study in children from Europe and rural Africa. Proc Natl Acad Sci U S A. 2010; 107:14691–96. https://doi.org/10.1073/pnas.1005963107. [PubMed]

123. Looft T, Allen HK. Collateral effects of antibiotics on mammalian gut microbiomes. Gut Microbes. 2012; 3:463–67. https://doi.org/10.4161/gmic.21288. [PubMed]

124. Wohlgemuth S, Haller D, Blaut M, Loh G. Reduced microbial diversity and high numbers of one single Escherichia coli strain in the intestine of colitic mice. Environ Microbiol. 2009; 11:1562–71. https://doi.org/10.1111/j.1462-2920.2009.01883.x. [PubMed]

125. Flanagan JL, Brodie EL, Weng L, Lynch SV, Garcia O, Brown R, Hugenholtz P, DeSantis TZ, Andersen GL, Wiener-Kronish JP, Bristow J. Loss of bacterial diversity during antibiotic treatment of intubated patients colonized with Pseudomonas aeruginosa. J Clin Microbiol. 2007; 45:1954–62. https://doi.org/10.1128/JCM.02187-06. [PubMed]

126. Markou P, Apidianakis Y. Pathogenesis of intestinal Pseudomonas aeruginosa infection in patients with cancer. Front Cell Infect Microbiol. 2014; 3:115. https://doi.org/10.3389/fcimb.2013.00115. [PubMed]

127. Papoff P, Ceccarelli G, d'Ettorre G, Cerasaro C, Caresta E, Midulla F, Moretti C. Gut microbial translocation in critically ill children and effects of supplementation with pre- and pro biotics. Int J Microbiol. 2012; 2012:151393. https://doi.org/10.1155/2012/151393. [PubMed]

128. Löfmark S, Jernberg C, Jansson JK, Edlund C. Clindamycin-induced enrichment and long-term persistence of resistant Bacteroides spp. and resistance genes. J Antimicrob Chemother. 2006; 58:1160–67. https://doi.org/10.1093/jac/dkl420. [PubMed]

129. Sjölund M, Tano E, Blaser MJ, Andersson DI, Engstrand L. Persistence of resistant Staphylococcus epidermidis after single course of clarithromycin. Emerg Infect Dis. 2005; 11:1389–93. https://doi.org/10.3201/eid1109.050124. [PubMed]

130. Blum JE, Fischer CN, Miles J, Handelsman J. Frequent replenishment sustains the beneficial microbiome of Drosophila melanogaster. MBio. 2013; 4:e00860–13. https://doi.org/10.1128/mBio.00860-13. [PubMed]

131. Strachan DP. Hay fever, hygiene, and household size. BMJ. 1989; 299:1259–60. https://doi.org/10.1136/bmj.299.6710.1259. [PubMed]

132. Gent AE, Hellier MD, Grace RH, Swarbrick ET, Coggon D. Inflammatory bowel disease and domestic hygiene in infancy. Lancet. 1994; 343:766–67. https://doi.org/10.1016/S0140-6736(94)91841-4. [PubMed]

133. Wold AE. The hygiene hypothesis revised: is the rising frequency of allergy due to changes in the intestinal flora? Allergy. 1998; 53:20–25. https://doi.org/10.1111/j.1398-9995.1998.tb04953.x. [PubMed]

134. Bach JF. The effect of infections on susceptibility to autoimmune and allergic diseases. N Engl J Med. 2002; 347:911–20. https://doi.org/10.1056/NEJMra020100. [PubMed]

135. Macpherson AJ, Harris NL. Interactions between commensal intestinal bacteria and the immune system. Nat Rev Immunol. 2004; 4:478–85. https://doi.org/10.1038/nri1373. [PubMed]

136. East R. Microbiome: soil science comes to life. Nature. 2013; 501:S18–19. https://doi.org/10.1038/501S18a. [PubMed]

137. Bashir ME, Andersen P, Fuss IJ, Shi HN, Nagler-Anderson C. An enteric helminth infection protects against an allergic response to dietary antigen. J Immunol. 2002; 169:3284–92. https://doi.org/10.4049/jimmunol.169.6.3284. [PubMed]

138. Longo VD, Finch CE. Evolutionary medicine: from dwarf model systems to healthy centenarians? Science. 2003; 299:1342–46. https://doi.org/10.1126/science.1077991. [PubMed]

139. Kostic AD, Howitt MR, Garrett WS. Exploring host-microbiota interactions in animal models and humans. Genes Dev. 2013; 27:701–18. https://doi.org/10.1101/gad.212522.112. [PubMed]

140. Tzelepis I, Kapsetaki SE, Panayidou S, Apidianakis Y. Drosophila melanogaster: a first step and a stepping-stone to anti-infectives. Curr Opin Pharmacol. 2013; 13:763–68. https://doi.org/10.1016/j.coph.2013.08.003. [PubMed]

141. Skaer H. The Alimentary Canal In: Bate M, Arias A (eds). The development of Drosophila melanogaster. Cold Spring Harbor Laboratory Press. NY: Cold Spring Harbor. 1993: 941–1012.

142. Micchelli CA, Perrimon N. Evidence that stem cells

reside in the adult Drosophila midgut epithelium. Nature. 2006; 439:475–79. https://doi.org/10.1038/nature04371. [PubMed]

143. Ohlstein B, Spradling A. The adult Drosophila posterior midgut is maintained by pluripotent stem cells. Nature. 2006; 439:470–74. https://doi.org/10.1038/nature04333. [PubMed]

144. Li L, Clevers H. Coexistence of quiescent and active adult stem cells in mammals. Science. 2010; 327:542–45. https://doi.org/10.1126/science.1180794. [PubMed]

145. Buchon N, Osman D, David FP, Fang HY, Boquete JP, Deplancke B, Lemaitre B. Morphological and molecular characterization of adult midgut compartmentalization in Drosophila. Cell Rep. 2013; 3:1725–38. https://doi.org/10.1016/j.celrep.2013.04.001. [PubMed]. Erratum in: Cell Rep. 2013 May 30;3(5):1755. https://doi.org/10.1016/j.celrep.2013.05.019.

146. Marianes A, Spradling AC. Physiological and stem cell compartmentalization within the Drosophila midgut. Elife. 2013; 2:e00886. https://doi.org/10.7554/eLife.00886. [PubMed]

147. Fox DT, Spradling AC. The Drosophila hindgut lacks constitutively active adult stem cells but proliferates in response to tissue damage. Cell Stem Cell. 2009; 5:290–97. https://doi.org/10.1016/j.stem.2009.06.003. [PubMed]

148. Charroux B, Royet J. Gut-microbiota interactions in non-mammals: what can we learn from Drosophila? Semin Immunol. 2012; 24:17–24. https://doi.org/10.1016/j.smim.2011.11.003. [PubMed]

149. Cordero JB, Stefanatos RK, Scopelliti A, Vidal M, Sansom OJ. Inducible progenitor-derived Wingless regulates adult midgut regeneration in Drosophila. EMBO J. 2012; 31:3901–17. https://doi.org/10.1038/emboj.2012.248. [PubMed]

150. de Navascués J, Perdigoto CN, Bian Y, Schneider MH, Bardin AJ, Martínez-Arias A, Simons BD. Drosophila midgut homeostasis involves neutral competition between symmetrically dividing intestinal stem cells. EMBO J. 2012; 31:2473–85. https://doi.org/10.1038/emboj.2012.106. [PubMed]

151. Kux K, Pitsouli C. Tissue communication in regenerative inflammatory signaling: lessons from the fly gut. Front Cell Infect Microbiol. 2014; 4:49. https://doi.org/10.3389/fcimb.2014.00049. [PubMed]

152. Christofi T, Apidianakis Y. Drosophila and the hallmarks of cancer. Adv Biochem Eng Biotechnol. 2013; 135:79–110. https://doi.org/10.1007/10_2013_190. [PubMed]

153. Gonzalez C. Drosophila melanogaster: a model and a tool to investigate malignancy and identify new therapeutics. Nat Rev Cancer. 2013; 13:172–83. https://doi.org/10.1038/nrc3461. [PubMed]

154. Reiter LT, Potocki L, Chien S, Gribskov M, Bier E. A systematic analysis of human disease-associated gene sequences in Drosophila melanogaster. Genome Res. 2001; 11:1114–25. https://doi.org/10.1101/gr.169101. [PubMed]

155. Ellisen LW, Bird J, West DC, Soreng AL, Reynolds TC, Smith SD, Sklar J. TAN-1, the human homolog of the Drosophila notch gene, is broken by chromosomal translocations in T lymphoblastic neoplasms. Cell. 1991; 66:649–61. https://doi.org/10.1016/0092-8674(91)90111-B. [PubMed]

156. Harvey K, Tapon N. The Salvador-Warts-Hippo pathway - an emerging tumour-suppressor network. Nat Rev Cancer. 2007; 7:182–91. https://doi.org/10.1038/nrc2070. [PubMed]

157. Bina S, Zeidler M. JAK/STAT pathway signalling in Drosophila melanogaster In: Anastasis Stephanou (ed). JAK-STAT Pathway in Disease. Landes Bioscience. 2009; 24–42.

158. Zeng X, Singh SR, Hou D, Hou SX. Tumor suppressors Sav/Scrib and oncogene Ras regulate stem-cell transformation in adult Drosophila malpighian tubules. J Cell Physiol. 2010; 224:766–74. https://doi.org/10.1002/jcp.22179. [PubMed]

159. Ohsawa S, Sato Y, Enomoto M, Nakamura M, Betsumiya A, Igaki T. Mitochondrial defect drives non-autonomous tumour progression through Hippo signalling in Drosophila. Nature. 2012; 490:547–51. https://doi.org/10.1038/nature11452. [PubMed]

160. Lin G, Xu N, Xi R. Paracrine Wingless signalling controls self-renewal of Drosophila intestinal stem cells. Nature. 2008; 455:1119–23. https://doi.org/10.1038/nature07329. [PubMed]

161. Biteau B, Hochmuth CE, Jasper H. JNK activity in somatic stem cells causes loss of tissue homeostasis in the aging Drosophila gut. Cell Stem Cell. 2008; 3:442–55. https://doi.org/10.1016/j.stem.2008.07.024. [PubMed]

162. Choi NH, Kim JG, Yang DJ, Kim YS, Yoo MA. Age-related changes in Drosophila midgut are associated with PVF2, a PDGF/VEGF-like growth factor. Aging Cell. 2008; 7:318–34. https://doi.org/10.1111/j.1474-9726.2008.00380.x. [PubMed]

163. Cronin SJ, Nehme NT, Limmer S, Liegeois S, Pospisilik JA, Schramek D, Leibbrandt A, Simoes RM, Gruber S, Puc U, Ebersberger I, Zoranovic T, Neely GG, et al. Genome-wide RNAi screen identifies genes involved in intestinal pathogenic bacterial infection. Science. 2009; 325:340–43. https://doi.org/10.1126/science.1173164. [PubMed]

164. Buchon N, Broderick NA, Poidevin M, Pradervand S, Lemaitre B. Drosophila intestinal response to bacterial infection: activation of host defense and stem cell proliferation. Cell Host Microbe. 2009; 5:200–11. https://doi.org/10.1016/j.chom.2009.01.003. [PubMed]

165. Amcheslavsky A, Jiang J, Ip YT. Tissue damage-induced intestinal stem cell division in Drosophila. Cell Stem Cell. 2009; 4:49–61. https://doi.org/10.1016/j.stem.2008.10.016. [PubMed]

166. Ren F, Wang B, Yue T, Yun EY, Ip YT, Jiang J. Hippo signaling regulates Drosophila intestine stem cell proliferation through multiple pathways. Proc Natl Acad Sci U S A. 2010; 107:21064–69. https://doi.org/10.1073/pnas.1012759107. [PubMed]

167. Salomon RN, Jackson FR. Tumors of testis and midgut in aging flies. Fly (Austin). 2008; 2:265–68. https://doi.org/10.4161/fly.7396. [PubMed]

168. Korgaonkar A, Trivedi U, Rumbaugh KP, Whiteley M. Community surveillance enhances Pseudomonas aeruginosa virulence during polymicrobial infection. Proc Natl Acad Sci U S A. 2013; 110:1059–64. https://doi.org/10.1073/pnas.1214550110. [PubMed]

169. Bangi E, Pitsouli C, Rahme LG, Cagan R, Apidianakis Y. Immune response to bacteria induces dissemination of Ras-activated Drosophila hindgut cells. EMBO Rep. 2012; 13:569–76. https://doi.org/10.1038/embor.2012.44. [PubMed]

170. Christofi T, Apidianakis Y. Ras-oncogenic Drosophila hindgut but not midgut cells use an inflammation-like program to disseminate to distant sites. Gut Microbes. 2013; 4:54–59. https://doi.org/10.4161/gmic.22429. [PubMed]

171. Wang L, Kounatidis I, Ligoxygakis P. Drosophila as a model to study the role of blood cells in inflammation, innate immunity and cancer. Front Cell Infect Microbiol. 2014; 3:113. https://doi.org/10.3389/fcimb.2013.00113. [PubMed]

172. Pastor-Pareja JC, Wu M, Xu T. An innate immune response of blood cells to tumors and tissue damage in Drosophila. Dis Model Mech. 2008; 1:144–54. https://doi.org/10.1242/dmm.000950. [PubMed]

173. Cordero JB, Macagno JP, Stefanatos RK, Strathdee KE, Cagan RL, Vidal M. Oncogenic Ras diverts a host TNF tumor suppressor activity into tumor promoter. Dev Cell. 2010; 18:999–1011. https://doi.org/10.1016/j.devcel.2010.05.014. [PubMed]

174. Waterston RH, Lindblad-Toh K, Birney E, Rogers J, Abril JF, Agarwal P, Agarwala R, Ainscough R, Alexandersson M, An P, Antonarakis SE, Attwood J, Baertsch R, et al, and Mouse Genome Sequencing Consortium. Initial sequencing and comparative analysis of the mouse genome. Nature. 2002; 420:520–62. https://doi.org/10.1038/nature01262. [PubMed]

175. Peters LL, Robledo RF, Bult CJ, Churchill GA, Paigen BJ, Svenson KL. The mouse as a model for human biology: a resource guide for complex trait analysis. Nat Rev Genet. 2007; 8:58–69. https://doi.org/10.1038/nrg2025. [PubMed]

176. Gkouskou KK, Deligianni C, Tsatsanis C, Eliopoulos AG. The gut microbiota in mouse models of inflammatory bowel disease. Front Cell Infect Microbiol. 2014; 4:28. https://doi.org/10.3389/fcimb.2014.00028. [PubMed]

177. Newman JV, Kosaka T, Sheppard BJ, Fox JG, Schauer DB. Bacterial infection promotes colon tumorigenesis in Apc(Min/+) mice. J Infect Dis. 2001; 184:227–30. https://doi.org/10.1086/321998. [PubMed]

178. Kostic AD, Chun E, Robertson L, Glickman JN, Gallini CA, Michaud M, Clancy TE, Chung DC, Lochhead P, Hold GL, El-Omar EM, Brenner D, Fuchs CS, et al. Fusobacterium nucleatum potentiates intestinal tumorigenesis and modulates the tumor-immune microenvironment. Cell Host Microbe. 2013; 14:207–15. https://doi.org/10.1016/j.chom.2013.07.007. [PubMed]

179. Nagamine CM, Rogers AB, Fox JG, Schauer DB. Helicobacter hepaticus promotes azoxymethane-initiated colon tumorigenesis in BALB/c-IL10-deficient mice. Int J Cancer. 2008; 122:832–38. https://doi.org/10.1002/ijc.23175. [PubMed]

180. Veiga P, Gallini CA, Beal C, Michaud M, Delaney ML, DuBois A, Khlebnikov A, van Hylckama Vlieg JE, Punit S, Glickman JN, Onderdonk A, Glimcher LH, Garrett WS. Bifidobacterium animalis subsp. lactis fermented milk product reduces inflammation by altering a niche for colitogenic microbes. Proc Natl Acad Sci U S A. 2010; 107:18132–37. https://doi.org/10.1073/pnas.1011737107. [PubMed] PMID:20921388. Erratum in: Proc Natl Acad Sci U S A. 2010 Dec 14;107(50):21943. https://doi.org/10.1073/pnas.1017174108.

181. Asquith M, Powrie F. An innately dangerous balancing act: intestinal homeostasis, inflammation, and colitis-associated cancer. J Exp Med. 2010; 207:1573–77. https://doi.org/10.1084/jem.20101330. [PubMed]

182. Greten FR, Eckmann L, Greten TF, Park JM, Li ZW, Egan LJ, Kagnoff MF, Karin M. IKKbeta links inflammation and tumorigenesis in a mouse model of colitis-associated cancer. Cell. 2004; 118:285–96. https://doi.org/10.1016/j.cell.2004.07.013. [PubMed]

183. Nenci A, Becker C, Wullaert A, Gareus R, van Loo G, Danese S, Huth M, Nikolaev A, Neufert C, Madison B, Gumucio D, Neurath MF, Pasparakis M. Epithelial NEMO links innate immunity to chronic intestinal inflammation. Nature. 2007; 446:557–61. https://doi.org/10.1038/nature05698. [PubMed]

184. Lee SH, Hong B, Sharabi A, Huang XF, Chen SY. Embryonic stem cells and mammary luminal progenitors directly sense and respond to microbial products. Stem Cells. 2009; 27:1604–15. https://doi.org/10.1002/stem.75. [PubMed]

185. Uematsu S, Jang MH, Chevrier N, Guo Z, Kumagai Y, Yamamoto M, Kato H, Sougawa N, Matsui H, Kuwata H, Hemmi H, Coban C, Kawai T, et al. Detection of pathogenic intestinal bacteria by Toll-like receptor 5 on intestinal CD11c+ lamina propria cells. Nat Immunol. 2006; 7:868–74. https://doi.org/10.1038/ni1362. [PubMed]

186. Integrative HM, and Integrative HMP (iHMP) Research Network Consortium. The Integrative Human Microbiome Project: dynamic analysis of microbiome-host omics profiles during periods of human health and disease. Cell

Host Microbe. 2014; 16:276–89.
https://doi.org/10.1016/j.chom.2014.08.014. [PubMed]

187. D'Abaco GM, Whitehead RH, Burgess AW. Synergy between Apc min and an activated ras mutation is sufficient to induce colon carcinomas. Mol Cell Biol. 1996; 16:884–91. https://doi.org/10.1128/MCB.16.3.884. [PubMed]

188. Janssen KP, Alberici P, Fsihi H, Gaspar C, Breukel C, Franken P, Rosty C, Abal M, El Marjou F, Smits R, Louvard D, Fodde R, Robine S. APC and oncogenic KRAS are synergistic in enhancing Wnt signaling in intestinal tumor formation and progression. Gastroenterology. 2006; 131:1096–109.
https://doi.org/10.1053/j.gastro.2006.08.011. [PubMed]

189. Zhang W, Li F, Nie L. Integrating multiple 'omics' analysis for microbial biology: application and methodologies. Microbiology. 2010; 156:287–301.
https://doi.org/10.1099/mic.0.034793-0. [PubMed]

190. Segata N, Boernigen D, Tickle TL, Morgan XC, Garrett WS, Huttenhower C. Computational meta'omics for microbial community studies. Mol Syst Biol. 2013; 9:666. https://doi.org/10.1038/msb.2013.22. [PubMed]

191. Borody TJ, Warren EF, Leis S, Surace R, Ashman O. Treatment of ulcerative colitis using fecal bacteriotherapy. J Clin Gastroenterol. 2003; 37:42–47.
https://doi.org/10.1097/00004836-200307000-00012. [PubMed]

192. Hedin C, Whelan K, Lindsay JO. Evidence for the use of probiotics and prebiotics in inflammatory bowel disease: a review of clinical trials. Proc Nutr Soc. 2007; 66:307–15. https://doi.org/10.1017/S0029665107005563. [PubMed]

193. Mills S, Shanahan F, Stanton C, Hill C, Coffey A, Ross RP. Movers and shakers: influence of bacteriophages in shaping the mammalian gut microbiota. Gut Microbes. 2013; 4:4–16. https://doi.org/10.4161/gmic.22371. [PubMed]

194. Howcroft TK, Campisi J, Louis GB, Smith MT, Wise B, Wyss-Coray T, Augustine AD, McElhaney JE, Kohanski R, Sierra F. The role of inflammation in age-related disease. Aging (Albany NY). 2013; 5:84–93.
https://doi.org/10.18632/aging.100531. [PubMed]

cancers

MDPI

Review

Apolipoprotein A-I (ApoA-I), Immunity, Inflammation and Cancer

Konstantina Georgila [1,2,†], Dimitra Vyrla [1,2,†] and Elias Drakos [2,*]

[1] Department of Biology, Medical School, University of Crete, Heraklion, Voutes, 71110 Crete, Greece
[2] Department of Pathology, Medical School, University of Crete, Heraklion, Voutes, 71110 Crete, Greece
* Correspondence: drakil@uoc.gr; Tel.: +30-2810394708
† These authors contributed equally to this work.

Received: 20 June 2019; Accepted: 30 July 2019; Published: 1 August 2019

Abstract: Apolipoprotein A-I (ApoA-I), the major protein component of high-density lipoproteins (HDL) is a multifunctional protein, involved in cholesterol traffic and inflammatory and immune response regulation. Many studies revealing alterations of ApoA-I during the development and progression of various types of cancer suggest that serum ApoA-I levels may represent a useful biomarker contributing to better estimation of cancer risk, early cancer diagnosis, follow up, and prognosis stratification of cancer patients. In addition, recent in vitro and animal studies disclose a more direct, tumor suppressive role of ApoA-I in cancer pathogenesis, which involves anti-inflammatory and immune-modulatory mechanisms. Herein, we review recent epidemiologic, clinicopathologic, and mechanistic studies investigating the role of ApoA-I in cancer biology, which suggest that enhancing the tumor suppressive activity of ApoA-I may contribute to better cancer prevention and treatment.

Keywords: apolipoprotein A-I; HDL; cancer; immunity; inflammation; review

1. Introduction

Apolipoprotein A-I (ApoA-I), the major protein component of high density lipoprotein (HDL), widely known for regulating cholesterol trafficking and for protecting against cardiovascular disease (CVD), may also modulate inflammatory and immune responses [1]. Recent studies suggest that organismal metabolic changes that include shifts in the levels and the quality of ApoA-I, may facilitate cancer initiation and progression [2,3]. Herein, we present and review the findings of various epidemiologic, clinicopathologic, and mechanistic studies implicating ApoA-I in cancer, with emphasis on its connection with inflammatory and immune-modulating effects.

The *ApoA1* gene is regarded to have the same evolutionary origin with the genes of apolipoproteins A-II, A-IV, C-I, C-III, and E, by virtue of duplication and diversification of a basic genetic motif encoding an 11/22 amino acid sequence with a characteristic α-amphipathic helix signature [4–7]. Homologous ApoA-I-encoding genes have been described in mammals, birds, and teleost fish [8].

The regulation of human *ApoA1* gene expression is complex and is controlled at multiple levels. The transcription of human *ApoA1* largely depends on two hormone response elements (HREs) proximal to the transcription start site that bind members of the hormone nuclear receptor superfamily. Among them, peroxisome proliferator-activated receptor-γ (PPARγ) appears to have a prominent role in *ApoA1* transactivation by interacting with HREs as heterodimer with RXRα. Other transcription factors implicated in the regulation of *ApoA1* promoter include the hepatocyte nuclear factor 4 (HNF4), Liver Receptor Homologue 1 (LRH1) and the ApoA-I Regulatory Protein 1 (ARP1/NR2F2) which activate and repress the *ApoA1* promoter, respectively [9]. HNF4 operates together with Sp1 in the

communication of *ApoA1* promoter with enhancer sequences that facilitate the recruitment of the basal transcriptional machinery.

ApoA-I expression is also controlled by a long noncoding RNA, *ApoA1-AS*, which is transcribed in the apolipoprotein gene cluster on chromosome 11q23.3 and modulates suppressive epigenetic marks leading to *ApoA1* transcriptional repression [10]. Interestingly, the liver, small intestine, and colon where ApoA-I is predominantly detected, show approximately 100-fold higher expression levels of *ApoA1* mRNA compared to *ApoA1*-AS, whereas the *ApoA1*/*ApoA1*-AS ratios are less than one in most other tissues [10]. Post-transcriptional mechanisms may also contribute to the regulation of ApoA-I expression in certain conditions. Thus, an enrichment of polysomal fractions with *ApoA1* mRNAs explains the increase in ApoA-I synthesis observed in high fat-fed mice in the absence of an effect on transcription [11].

Following translation and intracellular removal of a N-terminal signal peptide, ApoA-I is secreted as a lipid-poor/free mature protein of 243 amino acids and a molecular weight of approximately 28kDa [6]. Its structure contains ten consecutive helical regions, critical for the biophysical properties of the protein to spontaneously solubilize lipids in aqueous environment [6]. Based, exactly, on the properties of these amphipathic helical motifs, various peptides, without sharing any sequence homology, have been synthesized, known as ApoA-I mimetics, because of their ability to simulate ApoA-I functionality [12–14]. In physiological conditions, the bulk of ApoA-I constitutes approximately 70% of the protein component of HDL, which are microemulsions composed of a nonpolar lipid core, a surface polar lipid monolayer and up to 95 different proteins [15,16].

HDL are heterogeneous and dynamic structures exchanging lipids with cells and other lipoproteins, classified to different subcategories with pre-β1 HDL corresponding to lipid-poor ApoA-I [17,18]. ApoA-I is essential for the assembly of HDL. ApoA-I stabilizes the ATP-binding cassette transporter 1 (ABCA1), a member of the ABC superfamily, at the cell membrane of hepatocytes and enterocytes, enabling it to mediate the efflux of cellular phospholipids and free cholesterol to nascent discoid HDL particles harboring two to four molecules of ApoA-I, leading to the biogenesis of HDL particles. A similar lipid efflux by ABCA1 in cells of peripheral tissues initiates the reverse cholesterol transport (RCT) [17,19] (Figure 1). Also, ApoA-I activates lecithin cholesterol acyl transferase (LCAT), leading to the maturation of HDL particles [20]. Interaction of lipidated ApoA-I in discoid or more mature HDL particles with another transporter of the ABC family, ATP-binding cassette subfamily G member 1 (ABCG1), contributes further to the RCT [21]. HDL particles undergo additional remodeling through interaction with the cholesteryl ester transfer protein (CETP) [22]. Finally, binding of HDL particles to the scavenger receptor class B type 1 (SR-BI), transfers cholesterol down a cholesterol gradient [23,24]. As a result, cholesterol mobilized at peripheral tissues can enter the liver and is catabolized and excreted to the bile [24–26]. ApoA-I itself is mainly catabolized in the liver [27,28] (Figure 1).

Besides promoting RCT, ApoA-I inhibits apoptosis and pro-oxidative and proinflammatory processes in endothelial cells, induces vasodilation, inhibits the activation of platelets, and contributes to innate immunity. Some of these functions are relevant to inflammatory and malignant processes and are discussed below.

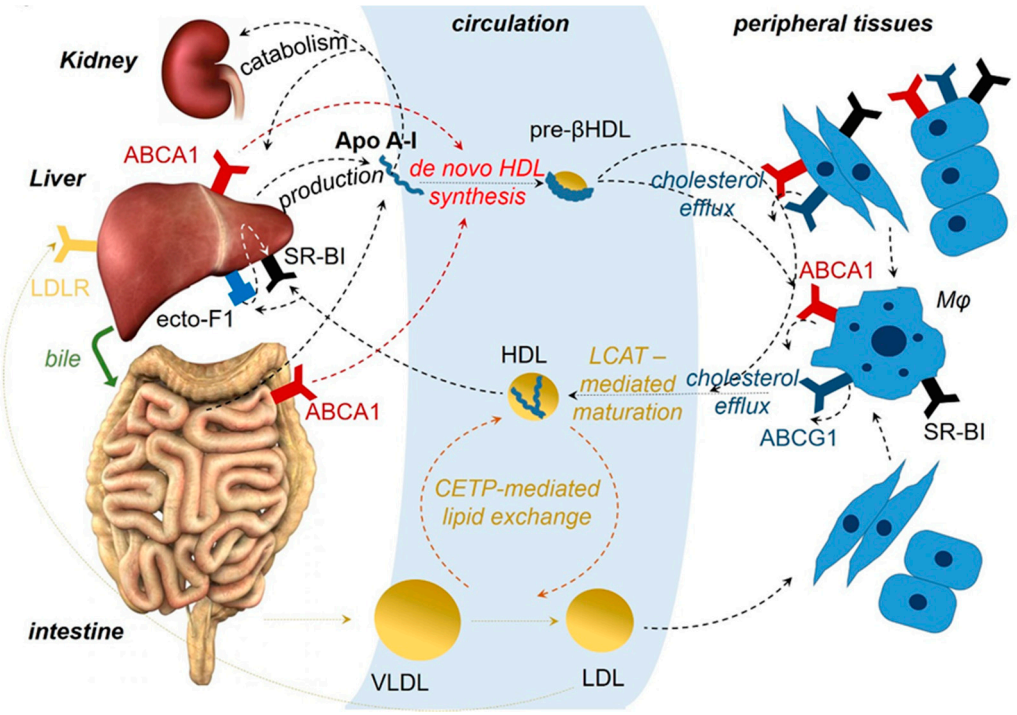

Figure 1. ApoA-I in relation to high-density lipoprotein (HDL) biogenesis and reverse cholesterol transport (RCT). About 75% of the ApoA-I protein is produced by hepatocytes and the remaining 25% by epithelial cells of the small intestine. It has been shown that some ApoA-I is also produced by the most proximal part of the mouse colon, in line with the reported ApoA-I expression in human fetal colon. ApoA-I is mainly catabolized in the liver. In addition, ApoA-I protein unassociated with lipids can be filtered in renal glomeruli, recognized by cubulin, a protein synthesized by distal renal tubular cells, internalized and degraded by renal epithelial cells. Binding of ApoA-I to ABCA1 at the cell membrane of hepatocytes and enterocytes mediates the production of nascent HDL particles. A similar efflux of lipids by ABCA1 and ABCG1 directly in various cells, or indirectly in macrophages (Mφ) of peripheral tissues, contributes to the RCT. LCAT, which catalyzes the esterification of free cholesterol and interaction through CETP transferring cholesterol esters to very low density lipoproteins (VLDL) and low density lipoproteins (LDL) and the phospholipid transfer protein (PLTP) transferring phospholipids from VLDL lipoproteins to HDL, leads to maturation and remodeling of HDL particles. Binding of HDL particles to SR-BI, expressed in hepatocytes, transfers cholesterol esters and other lipids, so that excess cholesterol can be accepted by the liver, catabolized, and excreted via the bile to the intestine. Also, binding of HDL remnants produced after the action of endothelial lipase, or lipid-poor ApoA-I to the beta chain of ATP F1 synthase, expressed at the cell membrane of hepatocytes and other cells (called, also, ecto-F1F0-ATPase that is similar to the F1F0 inner mitochondrial membrane protein complex) promotes cell internalization of HDL particles bound to SR-BI. Abbreviations for various receptors and enzymes are explained in the main text.

2. ApoA-I, Immunity, and Inflammation

Throughout its evolutionary course, ApoA-I/HDL contributes to the humoral part of innate immunity [29]. It has antiviral activity associated with prevention of viral penetration, facilitation of complement-mediating bacterial killing, and protection against trypanosome brucei, a protozoal parasite [30–32]. ApoA-I protects from sepsis by binding to and neutralizing lipopolysaccharide (LPS) and lipoteichoic acid (LTA), components of the Gram-negative and Gram-positive bacterial cell wall, respectively [33,34]. Clearance of LPS through binding of HDL-LPS to SR-BI results in lower activation of the Toll-like receptor 4 (TLR4), the corresponding pathogen-associated molecular pattern (PAMP) recognition receptor, and in decreased production of tumor necrosis factor (TNF), interleukin 1β (IL-1β) and interleukin 6 (IL-6) by the proinflammatory cells that mediate sepsis pathology [29,35,36]. In line

with these experimental findings, reduced serum ApoA-I levels in sepsis patients are associated with poor prognosis [37,38]. Also, ApoA-I was found to increase the levels of pentraxin 3 (PTX3), an acute phase protein, which recognizes PAMPs in viruses, bacteria, and fungi [39,40].

Inflammatory cytokines such as TNF and IL-1β repress the production of ApoA-I from hepatocytes and increase the expression of serum amyloid A (SAA), which becomes the major protein component of HDL in this context [41–43]. Consequently, lipid-poor ApoA-I is rapidly catabolized in the liver and the kidney. These findings could be meaningful if ApoA-I, in addition to its proimmune features, had anti-inflammatory potential. In this way, removal of ApoA-I could intensify the inflammatory response, resulting in a more robust effect. On the other hand, decreased levels of ApoA-I could contribute to destructive chronic inflammation characterizing many autoinflammatory and autoimmune diseases. Indeed, a plethora of studies have shown that ApoA-I exhibits anti-inflammatory features by various mechanisms [1]. In the context of the humoral arm of innate immunity, it has been shown that ApoA-I inhibit the formation of the terminal attack complex of the complement, C5b-9, by interfering with C9 polymerization and incorporation into the membrane and contributes to complement clearance [44]. Also, ApoA-I-mediated increase of PTX3 levels could contribute to a better healing, given that PTX3 can promote efficient tissue repair [45].

In a seminal study, it was shown that mice deficient for the receptors Abca1 and Abcg1 display marked leukocytosis and a transplantable myeloproliferative disease, which can be suppressed by transgenic overexpression of ApoA-I [46]. These findings suggest an inhibitory role of ApoA-I in cellular components of the immune system which has been postulated to relate to the lipid-modulating function of ApoA-I. One potential mechanism involves modulation of cholesterol-enriched lipid raft microdomains that function as docking sites for several receptors, coreceptors, and costimulatory molecules in neutrophils, monocytes/macrophages, dendritic cells (DC), and B and T lymphocytes [47–49]. ApoA-I, via ABCA1, reduces the abundance of lipid rafts and lowers the levels of CD11b expression leading to downregulation of neutrophil activation, migration, and adhesion [50]. A similar mechanism has been proposed for downregulation of TLR signaling in macrophages and major histocompatibility (MHC) class II molecule expression in antigen presenting cells with consequent attenuation of adaptive immune responses [51]. Inhibition of dendritic cell maturation and differentiation by ApoA-I is associated with elevated secretion of prostaglandin E2 (PGE2) and IL-10 and downregulation of IL-12 and IFN-γ [52]. Similarly, inhibition of dendritic cell maturation and downregulation of Th1 and Th17 cell reactivity by ApoA-I/HDL leads to attenuation of arthritis in an antigen-induced murine arthritis model [53].

In contrast, a recent study provided evidence that the ability of ApoA-I/HDL to suppress the TLR-mediated secretion of proinflammatory cytokines IL-6 and TNF in monocytes was dependent on transcriptional events mediated by the induction of activating transcription factor 3 (ATF3) and independent of TLR signaling and cholesterol modulation in lipid rafts, implying "outside-in" signaling events induced by ApoA-I/HDL that remain obscure [54]. Another anti-inflammatory mechanism was recently proposed. It was observed that ApoA-I/HDL decreased the expression of inflammasome components, including NLR family pyrin domain containing 3 (NLRP3) and IL-1β, as well as caspase 1 activation in human macrophages [55]. In addition, by using a murine model of atherosclerosis, it was shown that myeloid Abca1/g1 deficiency enhanced caspase-1 activation in monocytes, macrophages, and neutrophils, resulting in enhanced atherogenesis that was suppressed by Nlrp3 or Caspase-1/11 deficiency [56,57]. Also, the link between ApoA-I/HDL and inflammasome activation in dendritic cells and has been recently reported in a systemic lupus erythematosus-like murine model [58]. These findings suggested that accumulation of cholesterol in macrophages, or dendritic cells acting as a "danger signal", could activate the inflammasome leading to chronic inflammation, something that can be opposed by ApoA-I/HDL.

Additional effects on specific cellular compartments of the immune system by ApoA-I have been discovered. Thus, administration of ApoA-I suppressed inflammation in autoimmune-prone mice lacking both LDL-receptor and ApoA-I, an effect that was associated with expansion of regulatory

T cells (Treg) and a decrease of effector/effector memory T cells [59]. Another study showed that ApoA-I and ABCA1 play a pivotal role in the extracellular release of isopentenyl pyrophosphate and the consequent activation of Vγ9Vδ2 T cells, a specialized type of lymphocytes that recognize phosphor-antigens in a TCR-dependent but MCH-independent manner [60].

Deregulated immunity against microorganisms and pathogenic chronic inflammation can be viewed as different aspects of the same process. A recent study showed that mice deficient in ApoA-I exhibit exaggerated colitis, while administration of an ApoA-I mimetic peptide attenuated gut inflammation, which was associated with decreased secretion of IL-6 by epithelial enterocytes in response to LPS, abundant in the gut lumen [61]. In agreement with these findings, another study reported that the intensified chemically-induced colitis observed in the setting of selective deletion of transcription factor EB (Tfeb) in the murine intestinal epithelium was associated with reduced ApoA-I expression [62]. It has been suggested that part of the anti-inflammatory properties of ApoA-I/HDL may be due to its contribution to innate immunity mechanisms including its ability to neutralize bacterial products [61]. Given that chronic inflammatory conditions may predispose to various types of malignancy, the anti-inflammatory effects of ApoA-I may impinge on cancer-related processes as discussed below in Section 6.

It must be added that the anti-inflammatory properties of ApoA-I depend not only on the levels of the protein but also on its functionality [63–65]. Many epigenetic alterations of ApoA-I, including oxidative modifications, observed in chronic inflammation may erase its anti-inflammatory features or even transform it to a proinflammatory agent [66].

3. A Potential Protective Role of ApoA-I against Cancer: Evidence by Association

Accumulating evidence suggests that regulation of the ApoA-I/HDL axis is derailed in cancer. Our mining of transcriptome microarray data registered in the Oncomine database (https://www.oncomine.org) and of recently published RNAseq data [67] uncovers reduced *ApoA1* mRNA levels in hepatocellular carcinoma (HCC) compared to normal liver tissue, the main source of ApoA-I. The transcriptional repression of *ApoA1* in HCC remains mechanistically unexplored but it is in line with the reported reduction in protein levels of ApoA-I in both cancerous liver tissue [68] and in the serum of HCC patients [69,70]. HDL itself is also reduced in HCC [71]. Collectively, the reduction in *ApoA1* transcription, intracellular and secreted ApoA-I, and circulating HDL levels in HCC hint to a putative tumor suppressor role of this pathway. Indeed, numerous studies have discovered associations between the levels of serum ApoA-I/HDL and various parameters of the natural history of many types of cancer (summarily presented in Table 1).

The Alpha-Tocopherol, Beta-Carotene (ATBC) cancer prevention study showed inverse association between HDL-associated cholesterol (HDL-c) levels and the risk for the development of lung, liver, and hematologic malignancies [72]. The Women's Health Study investigating the cancer risk in female health workers, found that lower levels of HDL were associated with higher risk for the development of lung and colorectal cancer [73]. The Malmo Diet and Cancer Study revealed an inverse association between the risk for the development of colorectal, lung, and breast cancer and the levels of HDL-c and ApoA-I [74]. The correlation between lower levels of HDL/ApoA-I and higher risk for colorectal cancer was also reported in a Korean cross-sectional study, while premalignant lesions of colorectal cancer (colon adenomas) were shown to be associated with lower HDL levels in a cohort of patients examined by colonoscopy [75,76]. Similar associations have been reported for prostate cancer by a Swedish cohort study and for Hodgkin and non-Hodgkin lymphoma by the Cancer Research Network lymphoma study [77,78]. The latter found that the more pronounced drop in HDL levels was observed 3–4 years prior to lymphoma diagnosis [77].

Table 1. Clinicopathologic associations of Apo A-I in cancer.

Organ	Type of Cancer	Association of ApoA-I Levels with:				References
		Risk for the Development of Cancer	Cancer at Primary Diagnosis	Cancer Progression/ Metastasis	Cancer Prognosis	
head & neck	squamous cell cancer			+		[79]
	nasopharyngeal carcinoma			–	–	[80–82]
lung	non-small cell carcinoma	–	–	– (+)	–	[74,83–87]
esophagus	squamous cell carcinoma		–		–	[88,89]
stomach	gastric cancer		– (+)			[90,91]
colon	adenocarcinoma	–	–	– (+)	–	[76,92–97]
liver	hepatocellular carcinoma		–	–	–	[69,70,98–102] [69,70,98–102]
gallbladder	adenocarcinoma		–			[103]
pancreas	adenocarcinoma		–			[104,105]
breast	adenocarcinoma	– (+)	–	–	–	[106–116]
ovary	ovarian carcinoma		–		–	[117–122]
uterus	endometrial carcinoma		–			[123–125]
cervix	cervical squamous cell carcinoma		–	–		[126,127]
prostate	adenocarcinoma	–	–			[78,128,129]
bladder	transitional cell carcinoma,		– (+)	–	–	[130–133]
kidney	renal cell carcinoma				–	[134,135]
hematopoietic/ lymphoid system	leukemia/lymphoma	–	–	–		[77,136,137]
neural tumors	neuroblastoma		–		–	[138]
	retinoblastoma	+				[139]

– indicates reported inverse association of Apo A-I levels with the specific parameter; + indicates positive association of Apo A-I levels with the specific parameter, reported in a minority of studies or in an isolated study.

In line with these risk association studies, reduced serum levels of HDL/ApoA-I have been reported in cancer patients at first diagnosis, indicating that HDL/ApoA-I may be a potential biomarker for early cancer detection. A study analyzing serum lipid profiles of patients diagnosed with any type of solid tumor and healthy controls showed decreased HDL/ApoA-I levels, specifically, in the cancer group [140]. Similarly, relatively decreased levels of HDL/ApoA-I have been reported in many cancers of the gastrointestinal tract including adenocarcinomas of the stomach, the colon, the pancreas, and hepatocellular carcinoma (HCC) [70,76,83,92–94,98,104,105]. A serum proteomic analysis of patients with chronic liver disease associated with hepatitis C virus (HCV) infection showed that the development of HCC was associated with lower levels of ApoA-I [69]. Also, relatively reduced serum HDL/ApoA-I levels have been found in patients with lung and breast adenocarcinoma, early stage ovarian and cervical cancer, and acute lymphoblastic leukemia [84,106,117–120,126,136].

The levels of HDL/ApoA-I have also been associated with the progression of the neoplastic disease and the response to therapy. Reduced serum ApoA-I levels correlate with the progression of lung, liver, breast, kidney, endometrial, and cervical cancer, associated with the appearance of metastases [99,107,123–125,127,137,141]. A postoperative serum proteomics analysis of high-risk breast cancer patients also showed that low expression of ApoA-I was associated with metastatic relapse [107,134]. Other studies reported that ApoA-I serum levels were significantly decreased in HCC patients with recurrent disease, as compared to patients in remission, and patients with acute

lymphoblastic leukemia who achieved remission after receiving chemotherapy displayed significant increases in ApoA-I levels [100,137].

An overall association of HDL/ApoA-I levels with the prognosis of cancer patients treated with surgery, chemotherapy, radiotherapy, or immunotherapy has been concluded in a recent meta-analysis [142]. Indeed, an association with prognosis has been reported in patients with nasopharyngeal carcinoma, non-small cell lung carcinoma, invasive breast ductal adenocarcinoma, esophageal squamous cell carcinoma, colorectal adenocarcinoma, HCC, renal cell carcinoma, and transitional cell carcinoma of the bladder [80–82,85,86,88,89,95,101,102,108,109,135,143]. Likewise, ApoA-I has been proposed as a putative prognostic biomarker in neuroblastoma patients, since ApoA-I serum levels were found significantly lower in patients with high risk tumors [138]. Interestingly, post-treatment ApoA-I levels also seem to confer prognostic significance. A retrospective study of colorectal cancer patients treated with surgery and adjuvant chemotherapy showed that relatively increased levels of HDL-c and ApoA-I, one month after the completion of chemotherapy, were associated with better prognosis [144]. ApoA-I levels have been especially evaluated in response to chemosensitivity. Higher serum ApoA-I were found to be associated to better response to chemotherapy in patients with colorectal cancer, while higher ApoA-I levels secreted in the interstitial fluid of breast tumors were associated with more chemosensitive tumors [145,146]. In another study, ApoA-I levels were found to predict response to IMA901, the first therapeutic vaccine used in a randomized phase 2 trial for the treatment of patients with advanced renal cell carcinoma. Specifically, high levels of ApoA-I were associated with better overall survival [147].

Possible associations of ApoA-I genetic variations with cancer parameters have also been noted. A positive association was found between the ApoA-I (−75) A allele and breast cancer risk, and between the ApoA-I (+83) T allele and the development of lymph node metastasis [110]. Another study showed that breast cancer patients carrying an ApoA-I-rs670 A allele showed a less favorable phenotype at presentation, with absence of hormone receptor expression and lymph node metastases in comparison to G/G carriers. Moreover, rs670 A/A carrying patients had more frequent recurrences and inferior survival in comparison to patients with no A alleles [111].

Although the majority of studies have shown an inverse association of ApoA-I levels with the development and progression of various cancers, positive correlations have been reported. For example, ApoA-I levels are upregulated in the serum of patients with early stage gastric adenocarcinoma, recurrent head and neck squamous cell carcinoma and retinoblastoma and in the urine of patients with transitional cell carcinoma of the bladder, while a nested case-control study reported that HDL-c/ApoA-I levels were positively associated with the risk for the development of breast cancer [79,90,112,113,130,131,139]. Also, pro-ApoA-I levels were found upregulated in the serum of lung cancer patients with brain metastases and overexpressed at transcriptional level in metastases of colon adenocarcinoma to the liver suggesting that, in these particular situations, ApoA-I levels could be used as a biomarker for the extension of the disease to the brain and the liver, respectively [87,96,148]. It is unclear whether the positive correlation between ApoA-I levels and cancer parameters reported in a minority of studies are specific reflecting, in these particular situations, tumor promoting processes, associated with increased cholesterol uptake of malignant cells through the HDL/SR-BI pathway, as proposed by some studies [149–151].

Even though the bulk of data suggest that increased levels of ApoA-I/HDL could be protective against cancer development and progression, the reported ApoA-I/HDL alterations could be a consequence and not a cause of the carcinogenesis process. In such a case, ApoA-I could still be a useful biomarker for early cancer detection, or for better management stratification and follow up of cancer patients. However, a causative role would imply that interventions aiming at increasing the levels and functionality of ApoA-I could contribute to better cancer prevention and therapy.

4. ApoA-I Exhibits Tumor Suppressive Activity: Evidence from In Vitro Studies

A number of in vitro studies suggest that ApoA-I affects the proliferative, survival, and migratory behavior of various carcinoma cells, largely through cell-autonomous mechanisms (summarily presented in Table 2).

Table 2. In vitro studies of ApoA-I in cancer.

Type of Cancer	In Vitro System	Apo A-I Manipulation	Biologic Effect and Associated Mechanisms	Ref.
ovarian carcinoma (OC)	murine ovarian cell line ID8	treatment with human ApoA-I or ApoA-I mimetics (L-5F and L-4F)	↓ viability and proliferation ↓ LPA-induced viability	[152]
	murine ovarian cell line ID8	treatment with the ApoA-I mimetic D-4F	↓ viability and proliferation ↓ oxidative stress ↑ MnSOD expression and activity	[153]
	cis-platinum–resistant human ovarian cell lines (OVCAR5, SKOV3, OV2008, and A2780)	treatment with the ApoA-I mimetic L-4F	↓ viability and invasiveness ↓ AKT activation	[154]
	cis-platinum-resistant human ovarian cell lines (SKOV3, OV2008)	treatment with the ApoA-I mimetic L-5F	↓ LPA-induced cell viability and VEGF production	[155]
	human ovarian cancer cell lines (OV2008, CAOV-3 and SKOV3)	treatment with the ApoA-I mimetics L-4F and L-5F	↑ proteasome-dependent protein degradation of HIF 1α ↓ ROS production	[156]
hepatocellular carcinoma (HCC)	human HCC cell lines (MHCC97H and Huh7)	treatment with recombinant ApoA-I	↓ proliferation (cell cycle arrest) ↑ apoptosis ↓ MMP2/9 ↓ VEGF inhibition of the MAPK signaling pathway	[100]
colon adenocarcinoma (CA)	human CA cell lines (DLD-1 and Caco-2) overexpressing ABCA1	transgenic overexpression of ApoA-I, treatment with recombinant ApoA-I or apabetalone (a BET inhibitor, inducer of ApoA-I production)	↓ cell proliferation, migration and invasion modulation of ABCA1 expression through COX-2 downregulation compensation for ABCA1-dependent excessive export of cholesterol	[157]
	murine CA cell line, CT26	treatment with the ApoA-I mimetic L-4F	↓ viability and proliferation ↓ cyclin D1 and cyclin A protein levels ↓ LPA-induced viability	[158]
breast adenocarcinoma (BA)	human CA cell line, MCF-7	treatment with the ApoA-I mimetic D-4F	↓ oxLDL-induced proliferation	[159]
pancreatic adenocarcinoma (PA)	murine PA cell line P7	treatment with the ApoA-I mimetic L-4F	none	[160]

↑ indicates increase, while ↓ indicates decrease; ABCA1: ATP-binding cassette transporter 1; COX-2: Cyclooxygenase 2; HIF-1α: Hypoxia induced factor 1α; LPA: lysophosphatidic acid; MAPK: Mitogen-activated protein kinases; MMP2/9: Matrix metalloproteinases 2 and 9; MnSOD: Manganese superoxide dismutase; oxLDL: Oxidized low-density lipoprotein; ROS: Reactive oxygen species; VEGF: Vascular endothelial growth factor.

HCC cells treated with recombinant ApoA-I undergo G0/1 cell cycle arrest and apoptosis associated with downregulation of mitogen-activated protein kinases 1 and 3 (MAPK1, MAPK3), known for their antiapoptotic function, and upregulation of proapoptotic genes including caspase 5 (casp5), tumor necrosis factor receptor superfamily 10B (TNFRSF10B), and apoptosis protease activating factor 1 (APAF-1) [100]. ApoA-I also induced downregulation of vascular growth factor (VEGF) and matrix metalloproteinases 2 and 9 (MMP2, MMP9) genes, suggesting that ApoA-I may decrease the angiogenetic potential and the ability of HCC cells to remodel extracellular matrix, inhibiting in this way their metastatic potential [100].

A recent study showed that human colon adenocarcinoma (CA) cells stably transfected with ABCA1, exhibit increased proliferative, invasive and migratory behavior, which could be inhibited by simultaneous, transgenic overexpression of ApoA-I, or by exogenous treatment with human recombinant ApoA-I [157]. This inhibition was associated with downregulation of cyclooxygenase 2 (COX-2), a known promoter of colon adenocarcinoma involved in proinflammatory processes. In the same study, apabetalone, a small molecule BET-inhibitor, used in experimental therapeutics of atherosclerosis and known to induce production of ApoA-I, reduced the ABCA1-driven proliferative and invasive behavior of CA cells [157]. Another study showed that treatment of CA cells with the ApoA-I-mimetic peptide L-4F induced G0/1 cell cycle arrest, associated with decreased expression levels of cyclins D1 and A and decreased cell viability [158]. Also, it reduced the survival of CA cells stimulated by lysophosphatidic acid (LPA), a potent bioactive phospholipid, known to decrease its free concentration in the cell culture media [158].

In ovarian carcinoma (OC) cells, treatment with ApoA-I-mimetic peptides D-4F or L-4F was also found to impact proliferation, survival, and migratory behavior associated with reduced lipid peroxidation and hydrogen hyperoxide levels, and to decrease VEGF production and expression of the hypoxia induced factor-1α (HIF-1α) transcription factor [152,153,155,156]. Moreover, administration of ApoA-I or various ApoA-I mimetic peptides increases the sensitivity of human OC cells to cisplatin, a classical chemotherapeutic agent, associated with decreased activation of AKT [154]. Also, the ApoA-I mimetic D-4F was shown to reduce the proliferative response of human breast adenocarcinoma cells, stimulated by oxidized low-density lipoprotein (oxLDL) [159].

5. The Tumor Suppressive Function of ApoA-I: Evidence from Animal Studies

Accumulating evidence suggests that ApoA-I inhibits the growth of tumors and the metastatic progression of the disease in various animal cancer models (summarily presented in Table 3).

In a melanoma model, mice deficient for ApoA-I showed increased tumor burden and reduced survival. Conversely, transgenic overexpression of human ApoA-I or exogenous administration of ApoA-I protein reduced malignant burden, decreased metastases and increased mouse survival [161]. Melanomas in transgenic mice expressing high levels of ApoA-I showed decreased angiogenesis, reduced expression of MMP9, a matrix-degrading enzyme contributing to the invasive behavior of tumor cells, and reduced levels of survivin, an important antiapoptotic molecule.

Table 3. Animal studies of ApoA-I in cancer.

Type of Cancer	Animal Model	Apo A-I Manipulation	Biologic Effect and Associated Alterations	Ref.
melanoma and non-small lung carcinoma	syngeneic murine melanoma (B16F10L), human melanoma (A375) and Lewis lung (murine) carcinoma cells engrafted subcutaneously or injected intravenously in a metastatic cancer mouse model	human ApoA-I transgenic overexpression or injection of human ApoA-I	↓ tumor growth and metastasis ↑ survival ↓ tumor angiogenesis ↓ MMP-9 ↓ surviving modulation of the tumor immune microenvironment: ↓ M2 Mφ ↑ M2 Mφ ↓ MDSCs ↑ TILs	[161]
		ApoA-I KO	the opposite effects	
ovarian carcinoma	syngeneic murine ovarian carcinoma cells (ID-8) engrafted subcutaneously or injected intraperitoneally in mice	transgenic overexpression of human ApoA-I, or treatment with ApoA-I mimetic peptides (L-5F, L-4F, D-4F)	↓ tumor growth ↑ survival	[152]
ovarian carcinoma	syngeneic murine ovarian carcinoma cells (ID-8) engrafted subcutaneously in mice	treatment with ApoA-I mimetic peptides (L-5F, L-4F, D-4F)	↓ tumor growth ↓ LPA serum levels ↓ tumor angiogenesis ↓ VEGF (L-5F) ↓ HIF-1α expression (L-4F) ↑ MnSOD (D-4F) ↓ oxidized phospholipids	[152, 153, 155, 156]
colon adenocarcinoma	AOM/DSS-induced murine colorectal adenocarcinomas	ApoA-I haploinsufficiency Apo A-I$^{(+/-)}$	↑ tumor growth and altered tumor distribution (proximal extension) ↓ survival ↑ inflammation ↑ tumor cell proliferation ↑ IL-6, pSTAT3, NF-kB signaling	[61]
colon adenocarcinoma	syngeneic murine colon adenocarcinoma cells CT26 engrafted subcutaneously in mice	treatment with the ApoA-I mimetic peptide L-4F	↓ tumor growth ↓ LPA serum levels	[158]
	a murine model for familial adenomatous polyposis (APC$^{-/+}$)		↓ number and size of colon polyps	
colon adenocarcinoma and non-small lung carcinoma	syngeneic murine colon adenocarcinoma (CT26) and Lewis lung carcinoma cells injected intravenously in a metastatic lung mouse carcinoma model	treatment with a concentrate of transgenic tomatoes expressing the ApoA-I mimetic peptide 6F	↓ number of tumors in the lung ↓ Notch signaling ↓ oxidized phospholipids ↑ osteopontin ↓ MDSCs in lung and intestine tissues	[162]
colon and ovarian adenocarcinoma	syngeneic murine ovarian carcinoma cells (ID-8) engrafted intraperitoneally and colon adenocarcinoma cells (CT26) injected intravenously in a metastatic lung carcinoma mouse model	treatment with a concentrate of transgenic tomatoes expressing the ApoA-I mimetic peptide 6F	↓ tumor growth in the abdomen ↓ number of tumors in the lung	[163]
pancreatic adenocarcinoma	syngeneic murine pancreatic adenocarcinoma cells line P7 orthotopically engrafted in mice	treatment with the ApoA-I mimetic peptide L-4F	↓ tumor growth in the abdomen ↓ M2 Mφ in tumors	[160]
breast adenocarcinoma	mammary tumour virus-polyoma middle T-antigen transgenic (PyMT) mice	treatment with the ApoA-I mimetic peptide D-4F	↑ latency of tumor appearance ↓ tumor growth ↓ oxidized LDL plasma levels	[159]
		transgenic overexpression of human ApoA-I in PyMT mice	none	

↑ indicates increase, while ↓ indicates decrease; AOM: azoxymethane; DSS: dextran sodium sulfate; HIFα: Hypoxia induced factor-1α; LPA: Lysophosphatidic acid; MnSOD: Manganese superoxide dismutase; MMP-9: Matrix metalloproteinases 9; Mφ: macrophages; NF-kB: Nuclear factor kappa-light-chain-enhancer of activated B cells; TIL: tumor infiltrating lymphocytes; MDSC: myeloid-derived suppressor cells; pSTAT3: phosphorylated signal transducer and activator of transcription 3; PyMT: mammary tumour virus-polyoma middle T-antigen transgenic; VEGF: Vascular endothelial growth factor.

In line with the reported in vitro effects of ApoA-I mimetic peptides in OC, transgenic overexpression of human ApoA-I in a murine model of OC, or exogenous administration of D4-F, L5-F, and L4-F decreased tumor burden and increased survival [152]. The levels of LPA, VEGF, and HIF-1α in mice treated with ApoA-I mimetic peptides were found significantly reduced relative to control animals [152,155,156,163]. Another study showed that the inhibitory effects of the ApoA-I mimetic peptide D4-F was dependent on the upregulation of the antioxidant enzyme manganese superoxide dismutase (MnSOD), as silencing of the gene in the engrafted cells by a MnSOD-specific shRNA abolished the D4-F-tumor suppressing effects, suggesting that the antioxidant activity downstream of ApoA-I may be essential for its tumor suppressor properties in OC [153].

Patients with inflammatory bowel disease have increased risk for the development of CA [164]. In both humans with ulcerative colitis and mouse models of colitis-associated carcinogenesis, CA develops predominantly in the distal part of the large intestine. Intriguingly, ApoA-I$^{-/-}$ and ApoA-I$^{+/-}$ mice develop more numerous and larger tumors that display extension to the proximal part of the colon [61]. These differences were accompanied by a higher tumor cell proliferation rate in the ApoA-I$^{+/-}$ group and by elevated expression levels of activated STAT3 [61], a transcription factor involved in inflammatory and tumor-promoting processes [165]. In another study, treatment with the ApoA-I mimetic peptide L-4F significantly reduced the size and number of polyps in Adenomatosis Polyposis Coli (APC)$^{-/+}$ mice, a mouse model for human familial adenomatous polyposis [158]. Interestingly, the administration of ApoA-I mimetic peptides or the overexpression of ApoA-I not only reduced primary tumor burden but also metastasis of CA cells in the lung [161,162].

The tumor suppressive activity of ApoA-I has also been demonstrated in an orthotopically implanted mouse model of pancreatic adenocarcinoma and in a breast cancer mouse model, the latter being associated with reduction in plasma oxLDL [159,160]. Interestingly, dysfunctional, oxidized ApoA-I/HDL has been reported to promote breast cancer metastasis in mice [166]. Other animal studies have reported inverse association of serum ApoA-I levels with the progression of lung and gastric cancer in the mouse [167–170].

6. Anti-Inflammatory and Immune-Modulating Mechanisms Are Involved in the Tumor Suppressive Activity of ApoA-I

Collectively, the aforementioned in vitro and animal studies provide convincing evidence that ApoA-I affects many of the originally proposed hallmarks of cancer [171], including sustained proliferative signaling, resistance to cell death, angiogenesis, and activation of invasion and metastasis (Figure 2).

Accumulating findings suggest that ApoA-I also targets one of the more recently proposed hallmarks of cancer, that of tumor promoting inflammation. Chronic inflammation, caused by dysbiosis, plays a pivotal role in cancer promotion in the liver and colon [172,173], tissues known to produce ApoA-I, and inflammatory mechanisms emanating from TLR4 stimulation on cancer cells contribute to malignant growth in this context [172,174]. The concept that the anti-inflammatory properties of ApoA-I participate in the protection against colon cancer is highlighted by the fact that ApoA-I ameliorates colitis-promoted colon carcinogenesis in parallel with the attenuation of TLR4-mediated activation of key inflammatory regulators, including NF-$_K$B, STAT3, and IL-6 [61]. This is further supported by studies demonstrating reduction of various oxidized lipids and enzymes involved in inflammation, such as COX-2, by ApoA-I in models of colon or ovarian cancer [156,157].

Given the role of ApoA-I/HDL in RCT (see Section 1), deregulation of this pathway may have systemic effects on lipid and cholesterol accumulation which, in turn, may impact on immune cell homeostasis and inflammatory reactions that are linked to malignancy [175,176]. Moreover, modulation of the integrity of cholesterol-enriched microdomains in the plasma membrane, which function as docking sites for several receptors, may alter the activation of signaling pathways in many cells of the immune system [47]. Additionally, ligation of HDL particles to specific ApoA-I receptors (ABCA1, ABCG1 etc.) promoting the RCT may result in broader "outside-in" signaling events which have

been reported to enable macrophages to convey anti-inflammatory effects [177]. It is also possible that ApoA-I, internalized by the responsive cells may further modify signaling mechanisms.

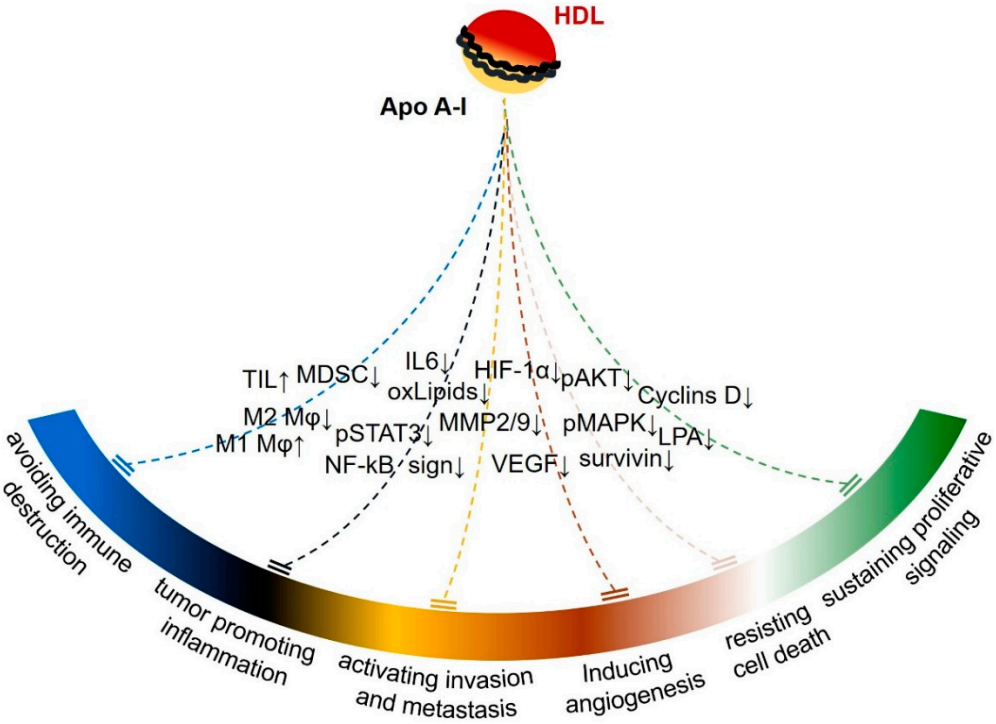

Figure 2. The antitumor activity of ApoA-I in relation to the proposed hallmarks of cancer. Cancer hallmarks affected by ApoA-I, in association with some of the corresponding molecular or cellular mediators reported by various in vitro and animal studies, are shown. It is possible that some mediators may affect more than one hallmark and additional hallmark features, not yet investigated, such as deregulated cellular energetic and genome instability and mutation, may be affected by the tumor suppressive activity of ApoA-I. Abbreviations for various molecules and cell types are explained in the main text. ↑ increase; ↓ decrease.

As the modulation of the inflammatory tumor microenvironment is exploited by cancer cells to buffer the attack of the immune system, the effects of ApoA-I on cancer inflammatory and immuno-editing processes seem interconnected [178,179]. Indeed, the ability of ApoA-I to inhibit melanoma growth is attenuated, although not abolished, in mice lacking the humoral and the cellular components of specific immunity [161]. Immuno-phenotyping of tumors developed in ApoA-I transgenic mice showed a reduction in myeloid derived suppressor cells (MDSCs), a heterogeneous immature myeloid cell population of granulocytic or monocytic origin capable of inhibiting the immune response, but an increase in tumor infiltrating cytotoxic T cells (TIL) and CD11b+ macrophages [161,180]. The latter is of particular interest as ApoA-I has been implicated in the conversion of tumor associated macrophages (TAM) from M2 to M1 phenotype that associates with enhanced antitumor properties [161]. Along these lines, administration of the ApoA-I mimetic peptide L4-F resulted in decreased recruitment of M2 macrophages to the tumors [160]. However, the exact mechanisms involved in the regulation of MDSC and M1/2 phenotype by ApoA-I remain elusive.

One mechanism by which ApoA-I mimetic peptides impact on antitumor immunity entails an increase in the levels of specific oxidized lipids to activate Notch signaling in the intestine which, in turn, leads to higher numbers of patrolling monocytes in lamina propria. This treatment also reduces 25-hydroxycholesterol with concomitant decrease in osteopontin expression in enterocytes and lower numbers of MDSCs in lamina propria [162].

The notion that the tumor suppressive properties of ApoA-I are connected to the modulation of anticancer immunity is further supported by recent animal studies that investigated the effects of the

ApoA-I receptors, Abcg1 and Abca1, on cancer growth in connection with parameters of anticancer immunity [181,182]. It was shown that myeloid specific deficiency of Abcg1 or Abca1 was associated with decreased tumor growth, increased polarization of TAMs towards M1 phenotype, and decreased numbers of specific MDSCs subsets in the tumors [181,182].

7. Tools for Therapeutic Targeting of ApoA-I

The tools for therapeutic targeting of ApoA-I originated from an effort to discover strategies exploiting the atheroprotective properties of HDL [183]. Some of these strategies aim to indirectly augment the ApoA-I and HDL-c levels by inhibiting endothelial lipase and CETP or to augment RCT by activating LCAT or the liver X receptors (LXRs), members of the nuclear receptor superfamily that orchestrate the activation of many genes promoting RCT and intestinal HDL production [183–187]. None of these approaches have been thoroughly tested in cancer studies.

However, strategies aiming in directly augmenting ApoA-I, or mimicking ApoA-I functionality have already been used successfully in preclinical cancer studies (Tables 2 and 3). The first of these approaches can be accomplished by intravenous administration of autologous delipidated HDL, purified native ApoA-I, or recombinant ApoA-I Milano protein, a mutated "hyperfunctional" ApoA-I variant discovered in a cohort of Italian patients, in complexes with phosphatidylcholine [188,189]. Although administration of such reconstituted HDL has shown antitumor activity in various preclinical models, it is a laborious and expensive strategy, difficult for a broad application in cancer patients.

Another approach utilizes ApoA-I mimetic peptides, synthesized on the basis of α-amphipathic helical repeating structure of ApoA-I, aiming to mimic the function of ApoA-I [190]. Many of them are 18 amino acids long and modified in various ways for augmenting stability and lipid-binding properties. Some of them including peptides composed of D-amino acids, being resistant to protease degradation, can be given orally, and have been expressed transgenically in tomatoes, in an effort to increase their practical utility [191]. Their action in small intestine tissues has been shown to be critical for their anti-atherogenic value in animal models [192]. These agents can produce HDL-like particles that promote cholesterol efflux and have shown antiatherogenic, antioxidant, anti-inflammatory, and antitumor activity in preclinical models [190,193]. Their function is not exactly equivalent to ApoA-I, since some are designed to better mimic one or another function of ApoA-I. For example, some of them have far superior ability, in comparison to ApoA-I, to neutralize pathogenic lipids such as LPA [190,192]. This may explain the discrepancy in the findings regarding alterations of LPA levels among various cancer studies using ApoA-I mimetics and ApoA-I [152,161] as well as differences in the antitumor activity [159].

Although ApoA-I mimetics have shown promising therapeutic potential in various preclinical models, recent clinical trials in the context of CVD have failed to demonstrate clear clinical benefit [194]. However, all clinical trials so far have been performed in the setting of acute coronary syndrome regarding patients with advanced disease in need for aggressive intervention. It is possible that future, carefully designed clinical trials, investigating a longer period of administration time in combination with established chemotherapeutic or immunotherapeutic agents, could be more informative for the therapeutic potential of ApoA-I mimetics in cancer.

8. Open Questions for Future Research

In vitro and in vivo experimental studies have shown that the tumor suppressive activity of ApoA-I targets cell-autonomous and cell-nonautonomous survival mechanisms (Figure 2). Which mechanism is pivotal for the antitumor activity of ApoA-I has not been fully elucidated. The prevailing view is that the anti-inflammatory action of ApoA-I is important for the enhanced antitumor immunity. Recent studies have shown that chronic inflammation is an essential mechanism contributing to the attenuation of innate and specific immunity against cancer [195]. Although there is evidence that ApoA-I may modify the anticancer immune response, detailed investigation of the effects of ApoA-I on immune checkpoints (for example programmed death ligand-1, PD-L1) in cancer cells or the cells of

tumor microenvironment and on anticancer immunity has not been performed [161]. The effects of ApoA-I on the outcome of cancer immunotherapy also remains to be elucidated.

Whilst the anti-inflammatory action of ApoA-I has attracted most attention, additional hallmarks of cancer may be influenced by ApoA-I. Findings showing that ApoA-I can affect the expression levels of transcription factors, such as HIF-1α, suggest that ApoA-I may have profound effects on metabolic pathways in cancer cells [156,196]. However, detailed alterations in energetic metabolism of cancer cells, including lipid metabolism, after treatment with ApoA-I or ApoA-I mimetic peptides have not been explored. The antioxidative function of ApoA-I has been demonstrated in various cancer models [153,156]. Although it is known that increased oxidation stress may contribute to DNA damage and increased mutational burden, the effects of ApoA-I on DNA damage response mechanisms have not been explored. ApoA-I itself is subject to oxidative damage and carbonylation which have been linked to apolipoprotein dysfunction and a pathogenic role in Alzheimer disease [197]. Whether these modifications may also have a role in immunity, inflammation and cancer remain obscure.

Most efforts to clarify the mechanism of the anti-inflammatory and antitumor activity of ApoA-I have focused on the interaction of ApoA-I with the receptors ABCA1, ABCG1, and SR-BI. For example, it has been shown that mice deficient in ABCG1 and ABCA1, when fed a "western"-type diet, display reduced growth of tumors derived from subcutaneously engrafted melanoma or bladder carcinoma cells, while other studies have attempted to associate ABCA1 with epithelial mesenchymal transition in breast cancer [181,182,198,199]. Although deficiency of ABCA1 or ABCG1 transporters does not always mirror the ApoA-I effect, at first glance, it seems counterintuitive that deficiency of ABCA1 and excess of ApoA-I, which affect RCT in opposite directions, both may contribute to tumor suppression. However, it is possible that some of the anti-inflammatory and antitumor activities of ApoA-I may be mediated by other receptors. For example, the beta-chain of ATP F1 synthase was discovered to represent a high affinity receptor of lipid poor ApoA-I at the cell membrane (known also as ecto-F1F0-ATPase; Figure 1) [25]. Binding of ApoA-I to this receptor was found to stimulate the hydrolysis of extracellular ATP to ADP and phosphate, implying that ApoA-I may affect signaling emanating from cell membrane P2 purinergic receptors, many of which have been shown to modify inflammatory and immune responses and tumor growth [26,200]. Although one of these receptors, P2Y13, was shown to mediate the signal from ecto-F1F0-ATPase to SR-BI for promoting HDL cell internalization, ecto-F1F0-ATPase-mediated effects of ApoA-I on P2 purinergic receptor signaling important for immune responses and cancer biology have not been investigated.

ApoA-I levels have been shown to be affected by chemotherapy. Examination of serum lipid profiles in breast cancer patients revealed a significant reduction of ApoA-I and HDL levels upon completion of chemotherapy [141,201]. ApoA-I protein levels were reduced by doxorubicin, while they remained unaffected by cyclophosphamide and paclitaxel treatment, in agreement with in vitro experimental findings [201]. Postchemotherapy infections are an important complication of cancer patients, and the ability of ApoA-I to neutralize bacterial products represents an important aspect of innate immunity [202]. However, the impact of ApoA-I on the incidence and outcome of postchemotherapy bacterial infections has not been investigated in epidemiologic or preclinical studies.

9. Conclusions

In conclusion, combined epidemiologic, clinicopathologic, and preclinical experimental research has shown that ApoA-I could represent not only a useful cancer biomarker, but a biochemical variable of the organism that could be modified for more effective cancer prevention and treatment. The exact mechanisms involved in the antitumor activity of ApoA-I and the evaluation of its antitumor therapeutic potential merits further investigations.

Author Contributions: Conceptualization and Literature review, K.G., D.V. and E.D.; Writing—Original Draft Preparation, K.G. and D.V.; Writing—Review & Editing and Supervision, E.D. All authors have read and approved the submitted version of the manuscript.

Funding: This study has been co-financed by the Operational Program "Human Resources Development, Education and Lifelong Learning" (KA 10071) and is co-financed by the European Union (European Social Fund) and Greek national funds.

Acknowledgments: We thank Aristides G Eliopoulos (Dept. of Biology, Medical School, National and Kapodistrian University of Athens) for constructive discussions and comments on the manuscript.

Conflicts of Interest: The authors declare no conflict of interest.

References

1. Gordon, S.M.; Hofmann, S.; Askew, D.S.; Davidson, W.S. High density lipoprotein: It's not just about lipid transport anymore. *Trends Endocrinol. Metab.* **2011**, *22*, 9–15. [CrossRef] [PubMed]
2. Levine, A.J.; Puzio-Kuter, A.M. The control of the metabolic switch in cancers by oncogenes and tumor suppressor genes. *Science* **2010**, *330*, 1340–1344. [CrossRef] [PubMed]
3. Zamanian-Daryoush, M.; DiDonato, J.A. Apolipoprotein A-I and Cancer. *Front. Pharmacol.* **2015**, *6*, 265. [CrossRef] [PubMed]
4. Barker, W.C.; Dayhoff, M.O. Evolution of lipoproteins deduced from protein sequence data. *Comp. Biochem. Physiol. B Comp. Biochem.* **1977**, *57*, 309–315. [CrossRef]
5. Fitch, W.M. Phylogenies constrained by the crossover process as illustrated by human hemoglobins and a thirteen-cycle, eleven-amino-acid repeat in human apolipoprotein A-I. *Genetics* **1977**, *86*, 623–644. [PubMed]
6. Li, W.H.; Tanimura, M.; Luo, C.C.; Datta, S.; Chan, L. The apolipoprotein multigene family: Biosynthesis, structure, structure-function relationships, and evolution. *J. Lipid Res.* **1988**, *29*, 245–271. [PubMed]
7. McLachlan, A.D. Repeated helical pattern in apolipoprotein-A-I. *Nature* **1977**, *267*, 465–466. [CrossRef] [PubMed]
8. Bashtovyy, D.; Jones, M.K.; Anantharamaiah, G.M.; Segrest, J.P. Sequence conservation of apolipoprotein A-I affords novel insights into HDL structure-function. *J. Lipid Res.* **2011**, *52*, 435–450. [CrossRef] [PubMed]
9. Kardassis, D.; Mosialou, I.; Kanaki, M.; Tiniakou, I.; Thymiakou, E. Metabolism of HDL and its regulation. *Curr. Med. Chem.* **2014**, *21*, 2864–2880. [CrossRef]
10. Halley, P.; Kadakkuzha, B.M.; Faghihi, M.A.; Magistri, M.; Zeier, Z.; Khorkova, O.; Coito, C.; Hsiao, J.; Lawrence, M.; Wahlestedt, C. Regulation of the apolipoprotein gene cluster by a long noncoding RNA. *Cell Rep.* **2014**, *6*, 222–230. [CrossRef]
11. Azrolan, N.; Odaka, H.; Breslow, J.L.; Fisher, E.A. Dietary fat elevates hepatic apoA-I production by increasing the fraction of apolipoprotein A-I mRNA in the translating pool. *J. Biol. Chem.* **1995**, *270*, 19833–19838. [CrossRef] [PubMed]
12. Bloedon, L.T.; Dunbar, R.; Duffy, D.; Pinell-Salles, P.; Norris, R.; DeGroot, B.J.; Movva, R.; Navab, M.; Fogelman, A.M.; Rader, D.J. Safety, pharmacokinetics, and pharmacodynamics of oral apoA-I mimetic peptide D-4F in high-risk cardiovascular patients. *J. Lipid Res.* **2008**, *49*, 1344–1352. [CrossRef] [PubMed]
13. Reddy, S.T.; Navab, M.; Anantharamaiah, G.M.; Fogelman, A.M. Apolipoprotein A-I mimetics. *Curr. Opin. Lipidol.* **2014**, *25*, 304–308. [CrossRef] [PubMed]
14. Reddy, S.T.; Navab, M.; Anantharamaiah, G.M.; Fogelman, A.M. Searching for a successful HDL-based treatment strategy. *Biochim. Biophys. Acta* **2014**, *1841*, 162–167. [CrossRef] [PubMed]
15. Shah, A.S.; Tan, L.; Long, J.L.; Davidson, W.S. Proteomic diversity of high density lipoproteins: Our emerging understanding of its importance in lipid transport and beyond. *J. Lipid Res.* **2013**, *54*, 2575–2585. [CrossRef]
16. Shao, B.; Heinecke, J.W. Quantifying HDL proteins by mass spectrometry: How many proteins are there and what are their functions? *Expert Rev. Proteom.* **2018**, *15*, 31–40. [CrossRef] [PubMed]
17. Duong, P.T.; Weibel, G.L.; Lund-Katz, S.; Rothblat, G.H.; Phillips, M.C. Characterization and properties of pre beta-HDL particles formed by ABCA1-mediated cellular lipid efflux to apoA-I. *J. Lipid Res.* **2008**, *49*, 1006–1014. [CrossRef] [PubMed]
18. Rosenson, R.S.; Brewer, H.B., Jr.; Chapman, M.J.; Fazio, S.; Hussain, M.M.; Kontush, A.; Krauss, R.M.; Otvos, J.D.; Remaley, A.T.; Schaefer, E.J. HDL measures, particle heterogeneity, proposed nomenclature, and relation to atherosclerotic cardiovascular events. *Clin. Chem.* **2011**, *57*, 392–410. [CrossRef] [PubMed]

19. Wang, N.; Silver, D.L.; Costet, P.; Tall, A.R. Specific binding of ApoA-I, enhanced cholesterol efflux, and altered plasma membrane morphology in cells expressing ABC1. *J. Biol. Chem.* **2000**, *275*, 33053–33058. [CrossRef] [PubMed]
20. Liang, H.Q.; Rye, K.A.; Barter, P.J. Cycling of apolipoprotein A-I between lipid-associated and lipid-free pools. *Biochim. Biophys. Acta* **1995**, *1257*, 31–37. [CrossRef]
21. Sankaranarayanan, S.; Oram, J.F.; Asztalos, B.F.; Vaughan, A.M.; Lund-Katz, S.; Adorni, M.P.; Phillips, M.C.; Rothblat, G.H. Effects of acceptor composition and mechanism of ABCG1-mediated cellular free cholesterol efflux. *J. Lipid Res.* **2009**, *50*, 275–284. [CrossRef] [PubMed]
22. Rye, K.A.; Hime, N.J.; Barter, P.J. Evidence that cholesteryl ester transfer protein-mediated reductions in reconstituted high density lipoprotein size involve particle fusion. *J. Biol. Chem.* **1997**, *272*, 3953–3960. [CrossRef] [PubMed]
23. Acton, S.; Rigotti, A.; Landschulz, K.T.; Xu, S.; Hobbs, H.H.; Krieger, M. Identification of scavenger receptor SR-BI as a high density lipoprotein receptor. *Science* **1996**, *271*, 518–520. [CrossRef] [PubMed]
24. Kozarsky, K.F.; Donahee, M.H.; Rigotti, A.; Iqbal, S.N.; Edelman, E.R.; Krieger, M. Overexpression of the HDL receptor SR-BI alters plasma HDL and bile cholesterol levels. *Nature* **1997**, *387*, 414–417. [CrossRef] [PubMed]
25. Martinez, L.O.; Jacquet, S.; Esteve, J.P.; Rolland, C.; Cabezon, E.; Champagne, E.; Pineau, T.; Georgeaud, V.; Walker, J.E.; Terce, F.; et al. Ectopic beta-chain of ATP synthase is an apolipoprotein A-I receptor in hepatic HDL endocytosis. *Nature* **2003**, *421*, 75–79. [CrossRef] [PubMed]
26. Martinez, L.O.; Najib, S.; Perret, B.; Cabou, C.; Lichtenstein, L. Ecto-F1-ATPase/P2Y pathways in metabolic and vascular functions of high density lipoproteins. *Atherosclerosis* **2015**, *238*, 89–100. [CrossRef] [PubMed]
27. Christensen, E.I.; Gburek, J. Protein reabsorption in renal proximal tubule-function and dysfunction in kidney pathophysiology. *Pediatr. Nephrol.* **2004**, *19*, 714–721. [CrossRef]
28. Glass, C.; Pittman, R.C.; Weinstein, D.B.; Steinberg, D. Dissociation of tissue uptake of cholesterol ester from that of apoprotein A-I of rat plasma high density lipoprotein: Selective delivery of cholesterol ester to liver, adrenal, and gonad. *Proc. Natl. Acad. Sci. USA* **1983**, *80*, 5435–5439. [CrossRef] [PubMed]
29. Catapano, A.L.; Pirillo, A.; Bonacina, F.; Norata, G.D. HDL in innate and adaptive immunity. *Cardiovasc. Res.* **2014**, *103*, 372–383. [CrossRef]
30. Biedzka-Sarek, M.; Metso, J.; Kateifides, A.; Meri, T.; Jokiranta, T.S.; Muszynski, A.; Radziejewska-Lebrecht, J.; Zannis, V.; Skurnik, M.; Jauhiainen, M. Apolipoprotein A-I exerts bactericidal activity against Yersinia enterocolitica serotype O:3. *J. Biol. Chem.* **2011**, *286*, 38211–38219. [CrossRef]
31. Perez-Morga, D.; Vanhollebeke, B.; Paturiaux-Hanocq, F.; Nolan, D.P.; Lins, L.; Homble, F.; Vanhamme, L.; Tebabi, P.; Pays, A.; Poelvoorde, P.; et al. Apolipoprotein L-I promotes trypanosome lysis by forming pores in lysosomal membranes. *Science* **2005**, *309*, 469–472. [CrossRef] [PubMed]
32. Singh, I.P.; Chopra, A.K.; Coppenhaver, D.H.; Ananatharamaiah, G.M.; Baron, S. Lipoproteins account for part of the broad non-specific antiviral activity of human serum. *Antivir. Res.* **1999**, *42*, 211–218. [CrossRef]
33. Jiao, Y.L.; Wu, M.P. Apolipoprotein A-I diminishes acute lung injury and sepsis in mice induced by lipoteichoic acid. *Cytokine* **2008**, *43*, 83–87. [CrossRef] [PubMed]
34. Wurfel, M.M.; Kunitake, S.T.; Lichenstein, H.; Kane, J.P.; Wright, S.D. Lipopolysaccharide (LPS)-binding protein is carried on lipoproteins and acts as a cofactor in the neutralization of LPS. *J. Exp. Med.* **1994**, *180*, 1025–1035. [CrossRef] [PubMed]
35. Levine, D.M.; Parker, T.S.; Donnelly, T.M.; Walsh, A.; Rubin, A.L. In vivo protection against endotoxin by plasma high density lipoprotein. *Proc. Natl. Acad. Sci. USA* **1993**, *90*, 12040–12044. [CrossRef]
36. Wang, Y.; Zhu, X.; Wu, G.; Shen, L.; Chen, B. Effect of lipid-bound apoA-I cysteine mutants on lipopolysaccharide-induced endotoxemia in mice. *J. Lipid Res.* **2008**, *49*, 1640–1645. [CrossRef] [PubMed]
37. Morin, E.E.; Guo, L.; Schwendeman, A.; Li, X.A. HDL in sepsis - risk factor and therapeutic approach. *Front. Pharmacol.* **2015**, *6*, 244. [CrossRef] [PubMed]
38. Wendel, M.; Paul, R.; Heller, A.R. Lipoproteins in inflammation and sepsis. II. Clinical aspects. *Intensive Care Med.* **2007**, *33*, 25–35. [CrossRef]
39. Bottazzi, B.; Doni, A.; Garlanda, C.; Mantovani, A. An integrated view of humoral innate immunity: Pentraxins as a paradigm. *Annu. Rev. Immunol.* **2010**, *28*, 157–183. [CrossRef]

40. Norata, G.D.; Marchesi, P.; Pirillo, A.; Uboldi, P.; Chiesa, G.; Maina, V.; Garlanda, C.; Mantovani, A.; Catapano, A.L. Long pentraxin 3, a key component of innate immunity, is modulated by high-density lipoproteins in endothelial cells. *Arterioscler. Thromb. Vasc. Biol.* **2008**, *28*, 925–931. [CrossRef]
41. Cabana, V.G.; Siegel, J.N.; Sabesin, S.M. Effects of the acute phase response on the concentration and density distribution of plasma lipids and apolipoproteins. *J. Lipid Res.* **1989**, *30*, 39–49. [PubMed]
42. Van Leeuwen, H.J.; Heezius, E.C.; Dallinga, G.M.; Van Strijp, J.A.; Verhoef, J.; Van Kessel, K.P. Lipoprotein metabolism in patients with severe sepsis. *Crit. Care Med.* **2003**, *31*, 1359–1366. [CrossRef] [PubMed]
43. Van Lenten, B.J.; Hama, S.Y.; De Beer, F.C.; Stafforini, D.M.; McIntyre, T.M.; Prescott, S.M.; La Du, B.N.; Fogelman, A.M.; Navab, M. Anti-inflammatory HDL becomes pro-inflammatory during the acute phase response. Loss of protective effect of HDL against LDL oxidation in aortic wall cell cocultures. *J. Clin. Investig.* **1995**, *96*, 2758–2767. [CrossRef] [PubMed]
44. Hamilton, K.K.; Zhao, J.; Sims, P.J. Interaction between apolipoproteins A-I and A-II and the membrane attack complex of complement. Affinity of the apoproteins for polymeric C9. *J. Biol. Chem.* **1993**, *268*, 3632–3638. [PubMed]
45. Doni, A.; D'Amico, G.; Morone, D.; Mantovani, A.; Garlanda, C. Humoral innate immunity at the crossroad between microbe and matrix recognition: The role of PTX3 in tissue damage. *Semin Cell Dev. Biol.* **2017**, *61*, 31–40. [CrossRef] [PubMed]
46. Yvan-Charvet, L.; Pagler, T.; Gautier, E.L.; Avagyan, S.; Siry, R.L.; Han, S.; Welch, C.L.; Wang, N.; Randolph, G.J.; Snoeck, H.W.; et al. ATP-binding cassette transporters and HDL suppress hematopoietic stem cell proliferation. *Science* **2010**, *328*, 1689–1693. [CrossRef] [PubMed]
47. Fessler, M.B.; Parks, J.S. Intracellular lipid flux and membrane microdomains as organizing principles in inflammatory cell signaling. *J. Immunol.* **2011**, *187*, 1529–1535. [CrossRef]
48. Gupta, N.; DeFranco, A.L. Lipid rafts and B cell signaling. *Semin Cell Dev. Biol.* **2007**, *18*, 616–626. [CrossRef]
49. Kabouridis, P.S.; Jury, E.C. Lipid rafts and T-lymphocyte function: Implications for autoimmunity. *FEBS Lett.* **2008**, *582*, 3711–3718. [CrossRef]
50. Murphy, A.J.; Woollard, K.J.; Suhartoyo, A.; Stirzaker, R.A.; Shaw, J.; Sviridov, D.; Chin-Dusting, J.P. Neutrophil activation is attenuated by high-density lipoprotein and apolipoprotein A-I in in vitro and in vivo models of inflammation. *Arterioscler. Thromb. Vasc. Biol.* **2011**, *31*, 1333–1341. [CrossRef]
51. Wang, S.H.; Yuan, S.G.; Peng, D.Q.; Zhao, S.P. HDL and ApoA-I inhibit antigen presentation-mediated T cell activation by disrupting lipid rafts in antigen presenting cells. *Atherosclerosis* **2012**, *225*, 105–114. [CrossRef] [PubMed]
52. Kim, K.D.; Lim, H.Y.; Lee, H.G.; Yoon, D.Y.; Choe, Y.K.; Choi, I.; Paik, S.G.; Kim, Y.S.; Yang, Y.; Lim, J.S. Apolipoprotein A-I induces IL-10 and PGE2 production in human monocytes and inhibits dendritic cell differentiation and maturation. *Biochem. Biophys. Res. Commun.* **2005**, *338*, 1126–1136. [CrossRef] [PubMed]
53. Tiniakou, I.; Drakos, E.; Sinatkas, V.; Van Eck, M.; Zannis, V.I.; Boumpas, D.; Verginis, P.; Kardassis, D. High-density lipoprotein attenuates Th1 and Th17 autoimmune responses by modulating dendritic cell maturation and function. *J. Immunol.* **2015**, *194*, 4676–4687. [CrossRef] [PubMed]
54. De Nardo, D.; Labzin, L.I.; Kono, H.; Seki, R.; Schmidt, S.V.; Beyer, M.; Xu, D.; Zimmer, S.; Lahrmann, C.; Schildberg, F.A.; et al. High-density lipoprotein mediates anti-inflammatory reprogramming of macrophages via the transcriptional regulator ATF3. *Nat. Immunol.* **2014**, *15*, 152–160. [CrossRef] [PubMed]
55. Thacker, S.G.; Zarzour, A.; Chen, Y.; Alcicek, M.S.; Freeman, L.A.; Sviridov, D.O.; Demosky, S.J., Jr.; Remaley, A.T. High-density lipoprotein reduces inflammation from cholesterol crystals by inhibiting inflammasome activation. *Immunology* **2016**, *149*, 306–319. [CrossRef] [PubMed]
56. Tall, A.R.; Westerterp, M. Inflammasomes, neutrophil extracellular traps, and cholesterol. *J. Lipid Res.* **2019**, *60*, 721–727. [CrossRef] [PubMed]
57. Westerterp, M.; Fotakis, P.; Ouimet, M.; Bochem, A.E.; Zhang, H.; Molusky, M.M.; Wang, W.; Abramowicz, S.; La Bastide-van Gemert, S.; Wang, N.; et al. Cholesterol Efflux Pathways Suppress Inflammasome Activation, NETosis, and Atherogenesis. *Circulation* **2018**, *138*, 898–912. [CrossRef] [PubMed]
58. Westerterp, M.; Gautier, E.L.; Ganda, A.; Molusky, M.M.; Wang, W.; Fotakis, P.; Wang, N.; Randolph, G.J.; D'Agati, V.D.; Yvan-Charvet, L.; et al. Cholesterol Accumulation in Dendritic Cells Links the Inflammasome to Acquired Immunity. *Cell Metab.* **2017**, *25*, 1294–1304. [CrossRef]

59. Wilhelm, A.J.; Zabalawi, M.; Owen, J.S.; Shah, D.; Grayson, J.M.; Major, A.S.; Bhat, S.; Gibbs, D.P., Jr.; Thomas, M.J.; Sorci-Thomas, M.G. Apolipoprotein A-I modulates regulatory T cells in autoimmune LDLr-/-, ApoA-I-/- mice. *J. Biol. Chem.* **2010**, *285*, 36158–36169. [CrossRef]
60. Castella, B.; Kopecka, J.; Sciancalepore, P.; Mandili, G.; Foglietta, M.; Mitro, N.; Caruso, D.; Novelli, F.; Riganti, C.; Massaia, M. The ATP-binding cassette transporter A1 regulates phosphoantigen release and Vgamma9Vdelta2 T cell activation by dendritic cells. *Nat. Commun.* **2017**, *8*, 15663. [CrossRef]
61. Gkouskou, K.K.; Ioannou, M.; Pavlopoulos, G.A.; Georgila, K.; Siganou, A.; Nikolaidis, G.; Kanellis, D.C.; Moore, S.; Papadakis, K.A.; Kardassis, D.; et al. Apolipoprotein A-I inhibits experimental colitis and colitis-propelled carcinogenesis. *Oncogene* **2016**, *35*, 2496–2505. [CrossRef] [PubMed]
62. Murano, T.; Najibi, M.; Paulus, G.L.C.; Adiliaghdam, F.; Valencia-Guerrero, A.; Selig, M.; Wang, X.; Jeffrey, K.; Xavier, R.J.; Lassen, K.G.; et al. Transcription factor TFEB cell-autonomously modulates susceptibility to intestinal epithelial cell injury in vivo. *Sci. Rep.* **2017**, *7*, 13938. [CrossRef] [PubMed]
63. Khera, A.V.; Cuchel, M.; De la Llera-Moya, M.; Rodrigues, A.; Burke, M.F.; Jafri, K.; French, B.C.; Phillips, J.A.; Mucksavage, M.L.; Wilensky, R.L.; et al. Cholesterol efflux capacity, high-density lipoprotein function, and atherosclerosis. *N. Engl. J. Med.* **2011**, *364*, 127–135. [CrossRef] [PubMed]
64. Pan, B.; Ren, H.; Lv, X.; Zhao, Y.; Yu, B.; He, Y.; Ma, Y.; Niu, C.; Kong, J.; Yu, F.; et al. Hypochlorite-induced oxidative stress elevates the capability of HDL in promoting breast cancer metastasis. *J. Transl. Med.* **2012**, *10*, 65. [CrossRef] [PubMed]
65. Pirillo, A.; Catapano, A.L.; Norata, G.D. Biological Consequences of Dysfunctional HDL. *Curr. Med. Chem.* **2019**, *26*, 1644–1664. [CrossRef] [PubMed]
66. Huang, Y.; DiDonato, J.A.; Levison, B.S.; Schmitt, D.; Li, L.; Wu, Y.; Buffa, J.; Kim, T.; Gerstenecker, G.S.; Gu, X.; et al. An abundant dysfunctional apolipoprotein A1 in human atheroma. *Nat. Med.* **2014**, *20*, 193–203. [CrossRef] [PubMed]
67. Jiang, Y.; Sun, A.; Zhao, Y.; Ying, W.; Sun, H.; Yang, X.; Xing, B.; Sun, W.; Ren, L.; Hu, B.; et al. Proteomics identifies new therapeutic targets of early-stage hepatocellular carcinoma. *Nature* **2019**, *567*, 257–261. [CrossRef] [PubMed]
68. Ai, J.; Tan, Y.; Ying, W.; Hong, Y.; Liu, S.; Wu, M.; Qian, X.; Wang, H. Proteome analysis of hepatocellular carcinoma by laser capture microdissection. *Proteomics* **2006**, *6*, 538–546. [CrossRef]
69. Mustafa, M.G.; Petersen, J.R.; Ju, H.; Cicalese, L.; Snyder, N.; Haidacher, S.J.; Denner, L.; Elferink, C. Biomarker discovery for early detection of hepatocellular carcinoma in hepatitis C-infected patients. *Mol. Cell. Proteom.* **2013**, *12*, 3640–3652. [CrossRef]
70. Steel, L.F.; Shumpert, D.; Trotter, M.; Seeholzer, S.H.; Evans, A.A.; London, W.T.; Dwek, R.; Block, T.M. A strategy for the comparative analysis of serum proteomes for the discovery of biomarkers for hepatocellular carcinoma. *Proteomics* **2003**, *3*, 601–609. [CrossRef]
71. Jiang, J.; Nilsson-Ehle, P.; Xu, N. Influence of liver cancer on lipid and lipoprotein metabolism. *Lipids Health Dis.* **2006**, *5*, 4. [CrossRef] [PubMed]
72. Ahn, J.; Lim, U.; Weinstein, S.J.; Schatzkin, A.; Hayes, R.B.; Virtamo, J.; Albanes, D. Prediagnostic total and high-density lipoprotein cholesterol and risk of cancer. *Cancer Epidemiol. Biomark. Prev.* **2009**, *18*, 2814–2821. [CrossRef] [PubMed]
73. Chandler, P.D.; Song, Y.; Lin, J.; Zhang, S.; Sesso, H.D.; Mora, S.; Giovannucci, E.L.; Rexrode, K.E.; Moorthy, M.V.; Li, C.; et al. Lipid biomarkers and long-term risk of cancer in the Women's Health Study. *Am. J. Clin. Nutr.* **2016**, *103*, 1397–1407. [CrossRef] [PubMed]
74. Borgquist, S.; Butt, T.; Almgren, P.; Shiffman, D.; Stocks, T.; Orho-Melander, M.; Manjer, J.; Melander, O. Apolipoproteins, lipids and risk of cancer. *Int. J. Cancer* **2016**, *138*, 2648–2656. [CrossRef] [PubMed]
75. Bayerdorffer, E.; Mannes, G.A.; Richter, W.O.; Ochsenkuhn, T.; Seeholzer, G.; Kopcke, W.; Wiebecke, B.; Paumgartner, G. Decreased high-density lipoprotein cholesterol and increased low-density cholesterol levels in patients with colorectal adenomas. *Ann. Intern. Med.* **1993**, *118*, 481–487. [CrossRef]
76. Jung, Y.S.; Ryu, S.; Chang, Y.; Yun, K.E.; Park, J.H.; Kim, H.J.; Cho, Y.K.; Sohn, C.I.; Jeon, W.K.; Kim, B.I.; et al. Associations Between Parameters of Glucose and Lipid Metabolism and Risk of Colorectal Neoplasm. *Dig. Dis. Sci.* **2015**, *60*, 2996–3004. [CrossRef] [PubMed]
77. Alford, S.H.; Divine, G.; Chao, C.; Habel, L.A.; Janakiraman, N.; Wang, Y.; Feigelson, H.S.; Scholes, D.; Roblin, D.; Epstein, M.M.; et al. Serum cholesterol trajectories in the 10 years prior to lymphoma diagnosis. *Cancer Causes Control.* **2018**, *29*, 143–156. [CrossRef]

78. Van Hemelrijck, M.; Walldius, G.; Jungner, I.; Hammar, N.; Garmo, H.; Binda, E.; Hayday, A.; Lambe, M.; Holmberg, L. Low levels of apolipoprotein A-I and HDL are associated with risk of prostate cancer in the Swedish AMORIS study. *Cancer Causes Control.* **2011**, *22*, 1011–1019. [CrossRef] [PubMed]
79. Gourin, C.G.; Zhi, W.; Adam, B.L. Proteomic identification of serum biomarkers for head and neck cancer surveillance. *Laryngoscope* **2009**, *119*, 1291–1302. [CrossRef] [PubMed]
80. Chang, H.; Wei, J.W.; Chen, K.; Zhang, S.; Han, F.; Lu, L.X.; Xiao, W.W.; Gao, Y.H. Apolipoprotein A-I Is a Prognosticator of Nasopharyngeal Carcinoma in the Era of Intensity-modulated Radiotherapy. *J. Cancer* **2018**, *9*, 702–710. [CrossRef] [PubMed]
81. Jiang, R.; Yang, Z.H.; Luo, D.H.; Guo, L.; Sun, R.; Chen, Q.Y.; Huang, P.Y.; Qiu, F.; Zou, X.; Cao, K.J.; et al. Elevated apolipoprotein A-I levels are associated with favorable prognosis in metastatic nasopharyngeal carcinoma. *Med Oncol.* **2014**, *31*, 80. [CrossRef] [PubMed]
82. Luo, X.L.; Zhong, G.Z.; Hu, L.Y.; Chen, J.; Liang, Y.; Chen, Q.Y.; Liu, Q.; Rao, H.L.; Chen, K.L.; Cai, Q.Q. Serum apolipoprotein A-I is a novel prognostic indicator for non-metastatic nasopharyngeal carcinoma. *Oncotarget* **2015**, *6*, 44037–44048. [CrossRef]
83. Zablocka-Slowinska, K.; Placzkowska, S.; Skorska, K.; Prescha, A.; Pawelczyk, K.; Porebska, I.; Kosacka, M.; Grajeta, H. Oxidative stress in lung cancer patients is associated with altered serum markers of lipid metabolism. *PLoS ONE* **2019**, *14*, e0215246. [CrossRef]
84. Chang, Y.K.; Lai, Y.H.; Chu, Y.; Lee, M.C.; Huang, C.Y.; Wu, S. Haptoglobin is a serological biomarker for adenocarcinoma lung cancer by using the ProteomeLab PF2D combined with mass spectrometry. *Am. J. Cancer Res.* **2016**, *6*, 1828–1836. [PubMed]
85. Cheng, T.; Dai, X.; Zhou, D.L.; Lv, Y.; Miao, L.Y. Correlation of apolipoprotein A-I kinetics with survival and response to first-line platinum-based chemotherapy in advanced non-small cell lung cancer. *Med. Oncol.* **2015**, *32*, 407. [CrossRef]
86. Shi, H.; Huang, H.; Pu, J.; Shi, D.; Ning, Y.; Dong, Y.; Han, Y.; Zarogoulidis, P.; Bai, C. Decreased pretherapy serum apolipoprotein A-I is associated with extent of metastasis and poor prognosis of non-small-cell lung cancer. *Onco Targets Ther.* **2018**, *11*, 6995–7003. [CrossRef] [PubMed]
87. Marchi, N.; Mazzone, P.; Fazio, V.; Mekhail, T.; Masaryk, T.; Janigro, D. ProApolipoprotein A1: A serum marker of brain metastases in lung cancer patients. *Cancer* **2008**, *112*, 1313–1324. [CrossRef] [PubMed]
88. Li, C.; Xia, G.; Jianqing, Z.; Mei, Y.; Ge, B.; Li, Z. Serum differential protein identification of Xinjiang Kazakh esophageal cancer patients based on the two-dimensional liquid-phase chromatography and LTQ MS. *Mol. Biol. Rep.* **2014**, *41*, 2893–2905. [CrossRef]
89. Wang, X.P.; Li, X.H.; Zhang, L.; Lin, J.H.; Huang, H.; Kang, T.; Mao, M.J.; Chen, H.; Zheng, X. High level of serum apolipoprotein A-I is a favorable prognostic factor for overall survival in esophageal squamous cell carcinoma. *BMC Cancer* **2016**, *16*, 516. [CrossRef] [PubMed]
90. Shi, F.; Wu, H.; Qu, K.; Sun, Q.; Li, F.; Shi, C.; Li, Y.; Xiong, X.; Qin, Q.; Yu, T.; et al. Identification of serum proteins AHSG, FGA and APOA-I as diagnostic biomarkers for gastric cancer. *Clin. Proteom.* **2018**, *15*, 18. [CrossRef] [PubMed]
91. Wu, J.Y.; Cheng, C.C.; Wang, J.Y.; Wu, D.C.; Hsieh, J.S.; Lee, S.C.; Wang, W.M. Discovery of tumor markers for gastric cancer by proteomics. *PLoS ONE* **2014**, *9*, e84158. [CrossRef] [PubMed]
92. Lim, L.C.; Looi, M.L.; Zakaria, S.Z.; Sagap, I.; Rose, I.M.; Chin, S.F.; Jamal, R. Identification of Differentially Expressed Proteins in the Serum of Colorectal Cancer Patients Using 2D-DIGE Proteomics Analysis. *Pathol. Oncol. Res.* **2016**, *22*, 169–177. [CrossRef] [PubMed]
93. Van Duijnhoven, F.J.; Bueno-De-Mesquita, H.B.; Calligaro, M.; Jenab, M.; Pischon, T.; Jansen, E.H.; Frohlich, J.; Ayyobi, A.; Overvad, K.; Toft-Petersen, A.P.; et al. Blood lipid and lipoprotein concentrations and colorectal cancer risk in the European Prospective Investigation into Cancer and Nutrition. *Gut* **2011**, *60*, 1094–1102. [CrossRef] [PubMed]
94. Zhang, X.; Zhao, X.W.; Liu, D.B.; Han, C.Z.; Du, L.L.; Jing, J.X.; Wang, Y. Lipid levels in serum and cancerous tissues of colorectal cancer patients. *World J. Gastroenterol.* **2014**, *20*, 8646–8652. [CrossRef] [PubMed]
95. Sirnio, P.; Vayrynen, J.P.; Klintrup, K.; Makela, J.; Makinen, M.J.; Karttunen, T.J.; Tuomisto, A. Decreased serum apolipoprotein A1 levels are associated with poor survival and systemic inflammatory response in colorectal cancer. *Sci. Rep.* **2017**, *7*, 5374. [CrossRef] [PubMed]

96. Sayagues, J.M.; Corchete, L.A.; Gutierrez, M.L.; Sarasquete, M.E.; Del Mar Abad, M.; Bengoechea, O.; Ferminan, E.; Anduaga, M.F.; Del Carmen, S.; Iglesias, M.; et al. Genomic characterization of liver metastases from colorectal cancer patients. *Oncotarget* **2016**, *7*, 72908–72922. [CrossRef] [PubMed]
97. Sakaguchi, Y.; Yamamichi, N.; Tomida, S.; Takeuchi, C.; Kageyama-Yahara, N.; Takahashi, Y.; Shiogama, K.; Inada, K.I.; Ichinose, M.; Fujishiro, M.; et al. Identification of marker genes and pathways specific to precancerous duodenal adenomas and early stage adenocarcinomas. *J. Gastroenterol.* **2018**, *54*, 131–140. [CrossRef]
98. Fye, H.K.; Wright-Drakesmith, C.; Kramer, H.B.; Camey, S.; Nogueira da Costa, A.; Jeng, A.; Bah, A.; Kirk, G.D.; Sharif, M.I.; Ladep, N.G.; et al. Protein profiling in hepatocellular carcinoma by label-free quantitative proteomics in two west African populations. *PLoS ONE* **2013**, *8*, e68381. [CrossRef]
99. Qin, X.; Chen, Q.; Sun, C.; Wang, C.; Peng, Q.; Xie, L.; Liu, Y.; Li, S. High-throughput screening of tumor metastatic-related differential glycoprotein in hepatocellular carcinoma by iTRAQ combines lectin-related techniques. *Med Oncol.* **2013**, *30*, 420. [CrossRef]
100. Ma, X.L.; Gao, X.H.; Gong, Z.J.; Wu, J.; Tian, L.; Zhang, C.Y.; Zhou, Y.; Sun, Y.F.; Hu, B.; Qiu, S.J.; et al. Apolipoprotein A1: A novel serum biomarker for predicting the prognosis of hepatocellular carcinoma after curative resection. *Oncotarget* **2016**, *7*, 70654–70668. [CrossRef]
101. Mao, M.; Wang, X.; Sheng, H.; Liu, Y.; Zhang, L.; Dai, S.; Chi, P.D. A novel score based on serum apolipoprotein A-1 and C-reactive protein is a prognostic biomarker in hepatocellular carcinoma patients. *BMC Cancer* **2018**, *18*, 1178. [CrossRef] [PubMed]
102. Xu, X.; Wei, X.; Ling, Q.; Cheng, J.; Zhou, B.; Xie, H.; Zhou, L.; Zheng, S. Identification of two portal vein tumor thrombosis associated proteins in hepatocellular carcinoma: Protein disulfide-isomerase A6 and apolipoprotein A-I. *J. Gastroenterol. Hepatol.* **2011**, *26*, 1787–1794. [CrossRef] [PubMed]
103. Zuo, M.; Rashid, A.; Wang, Y.; Jain, A.; Li, D.; Behari, A.; Kapoor, V.K.; Koay, E.J.; Chang, P.; Vauthey, J.N.; et al. RNA sequencing-based analysis of gallbladder cancer reveals the importance of the liver X receptor and lipid metabolism in gallbladder cancer. *Oncotarget* **2016**, *7*, 35302–35312. [CrossRef] [PubMed]
104. Ehmann, M.; Felix, K.; Hartmann, D.; Schnolzer, M.; Nees, M.; Vorderwulbecke, S.; Bogumil, R.; Buchler, M.W.; Friess, H. Identification of potential markers for the detection of pancreatic cancer through comparative serum protein expression profiling. *Pancreas* **2007**, *34*, 205–214. [CrossRef] [PubMed]
105. Liu, X.; Zheng, W.; Wang, W.; Shen, H.; Liu, L.; Lou, W.; Wang, X.; Yang, P. A new panel of pancreatic cancer biomarkers discovered using a mass spectrometry-based pipeline. *Br. J. Cancer* **2017**, *117*, 1846–1854. [CrossRef] [PubMed]
106. Chung, L.; Moore, K.; Phillips, L.; Boyle, F.M.; Marsh, D.J.; Baxter, R.C. Novel serum protein biomarker panel revealed by mass spectrometry and its prognostic value in breast cancer. *Breast Cancer Res.* **2014**, *16*, R63. [CrossRef] [PubMed]
107. Goncalves, A.; Esterni, B.; Bertucci, F.; Sauvan, R.; Chabannon, C.; Cubizolles, M.; Bardou, V.J.; Houvenaegel, G.; Jacquemier, J.; Granjeaud, S.; et al. Postoperative serum proteomic profiles may predict metastatic relapse in high-risk primary breast cancer patients receiving adjuvant chemotherapy. *Oncogene* **2006**, *25*, 981–989. [CrossRef] [PubMed]
108. His, M.; Zelek, L.; Deschasaux, M.; Pouchieu, C.; Kesse-Guyot, E.; Hercberg, S.; Galan, P.; Latino-Martel, P.; Blacher, J.; Touvier, M. Prospective associations between serum biomarkers of lipid metabolism and overall, breast and prostate cancer risk. *Eur. J. Epidemiol.* **2014**, *29*, 119–132. [CrossRef]
109. Lin, X.; Hong, S.; Huang, J.; Chen, Y.; Chen, Y.; Wu, Z. Plasma apolipoprotein A1 levels at diagnosis are independent prognostic factors in invasive ductal breast cancer. *Discov. Med.* **2017**, *23*, 247–258.
110. Hamrita, B.; Ben Nasr, H.; Gabbouj, S.; Bouaouina, N.; Chouchane, L.; Chahed, K. Apolipoprotein A1 -75 G/A and +83 C/T polymorphisms: Susceptibility and prognostic implications in breast cancer. *Mol. Biol. Rep.* **2011**, *38*, 1637–1643. [CrossRef]
111. Hsu, M.C.; Lee, K.T.; Hsiao, W.C.; Wu, C.H.; Sun, H.Y.; Lin, I.L.; Young, K.C. The dyslipidemia-associated SNP on the APOA1/C3/A5 gene cluster predicts post-surgery poor outcome in Taiwanese breast cancer patients: A 10-year follow-up study. *BMC Cancer* **2013**, *13*, 330. [CrossRef] [PubMed]
112. Martin, L.J.; Melnichouk, O.; Huszti, E.; Connelly, P.W.; Greenberg, C.V.; Minkin, S.; Boyd, N.F. Serum lipids, lipoproteins, and risk of breast cancer: A nested case-control study using multiple time points. *J. Natl. Cancer Inst.* **2015**, *107*, 32. [CrossRef] [PubMed]

113. Zografos, E.; Anagnostopoulos, A.K.; Papadopoulou, A.; Legaki, E.; Zagouri, F.; Marinos, E.; Tsangaris, G.T.; Gazouli, M. Serum Proteomic Signatures of Male Breast Cancer. *Cancer Genom. Proteom.* **2019**, *16*, 129–137. [CrossRef] [PubMed]
114. Cine, N.; Baykal, A.T.; Sunnetci, D.; Canturk, Z.; Serhatli, M.; Savli, H. Identification of ApoA1, HPX and POTEE genes by omic analysis in breast cancer. *Oncol. Rep.* **2014**, *32*, 1078–1086. [CrossRef] [PubMed]
115. Liu, J.X.; Yuan, Q.; Min, Y.L.; He, Y.; Xu, Q.H.; Li, B.; Shi, W.Q.; Lin, Q.; Li, Q.H.; Zhu, P.W.; et al. Apolipoprotein A1 and B as risk factors for development of intraocular metastasis in patients with breast cancer. *Cancer Manag. Res.* **2019**, *11*, 2881–2888. [CrossRef]
116. Pendharkar, N.; Gajbhiye, A.; Taunk, K.; RoyChoudhury, S.; Dhali, S.; Seal, S.; Mane, A.; Abhang, S.; Santra, M.K.; Chaudhury, K.; et al. Quantitative tissue proteomic investigation of invasive ductal carcinoma of breast with luminal B HER2 positive and HER2 enriched subtypes towards potential diagnostic and therapeutic biomarkers. *J. Proteom.* **2016**, *132*, 112–130. [CrossRef]
117. Clarke, C.H.; Yip, C.; Badgwell, D.; Fung, E.T.; Coombes, K.R.; Zhang, Z.; Lu, K.H.; Bast, R.C., Jr. Proteomic biomarkers apolipoprotein A1, truncated transthyretin and connective tissue activating protein III enhance the sensitivity of CA125 for detecting early stage epithelial ovarian cancer. *Gynecol. Oncol.* **2011**, *122*, 548–553. [CrossRef]
118. Kozak, K.R.; Amneus, M.W.; Pusey, S.M.; Su, F.; Luong, M.N.; Luong, S.A.; Reddy, S.T.; Farias-Eisner, R. Identification of biomarkers for ovarian cancer using strong anion-exchange ProteinChips: Potential use in diagnosis and prognosis. *Proc. Natl. Acad. Sci. USA* **2003**, *100*, 12343–12348. [CrossRef]
119. Kozak, K.R.; Su, F.; Whitelegge, J.P.; Faull, K.; Reddy, S.; Farias-Eisner, R. Characterization of serum biomarkers for detection of early stage ovarian cancer. *Proteomics* **2005**, *5*, 4589–4596. [CrossRef]
120. Wegdam, W.; Argmann, C.A.; Kramer, G.; Vissers, J.P.; Buist, M.R.; Kenter, G.G.; Aerts, J.M.; Meijer, D.; Moerland, P.D. Label-free LC-MSe in tissue and serum reveals protein networks underlying differences between benign and malignant serous ovarian tumors. *PLoS ONE* **2014**, *9*, e108046. [CrossRef]
121. Cruz, I.N.; Coley, H.M.; Kramer, H.B.; Madhuri, T.K.; Safuwan, N.A.; Angelino, A.R.; Yang, M. Proteomics Analysis of Ovarian Cancer Cell Lines and Tissues Reveals Drug Resistance-associated Proteins. *Cancer Genom. Proteom.* **2017**, *14*, 35–51. [CrossRef] [PubMed]
122. Tuft Stavnes, H.; Nymoen, D.A.; Hetland Falkenthal, T.E.; Kaern, J.; Trope, C.G.; Davidson, B. APOA1 mRNA expression in ovarian serous carcinoma effusions is a marker of longer survival. *Am. J. Clin. Pathol.* **2014**, *142*, 51–57. [CrossRef] [PubMed]
123. Farias-Eisner, G.; Su, F.; Robbins, T.; Kotlerman, J.; Reddy, S.; Farias-Eisner, R. Validation of serum biomarkers for detection of early- and late-stage endometrial cancer. *Am. J. Obstet. Gynecol.* **2010**, *202*, 73. [CrossRef] [PubMed]
124. Rizner, T.L. Discovery of biomarkers for endometrial cancer: Current status and prospects. *Expert Rev. Mol. Diagn.* **2016**, *16*, 1315–1336. [CrossRef] [PubMed]
125. Takano, M.; Kikuchi, Y.; Asakawa, T.; Goto, T.; Kita, T.; Kudoh, K.; Kigawa, J.; Sakuragi, N.; Sakamoto, M.; Sugiyama, T.; et al. Identification of potential serum markers for endometrial cancer using protein expression profiling. *J. Cancer Res. Clin. Oncol.* **2010**, *136*, 475–481. [CrossRef]
126. Chen, Y.; Xiong, X.; Wang, Y.; Zhao, J.; Shi, H.; Zhang, H.; Wang, Y.; Wei, Y.; Xue, W.; Zhang, J. Proteomic Screening for Serum Biomarkers for Cervical Cancer and Their Clinical Significance. *Med. Sci. Monit. Int. Med. J. Exp. Clin. Res.* **2019**, *25*, 288–297. [CrossRef] [PubMed]
127. Guo, X.; Hao, Y.; Kamilijiang, M.; Hasimu, A.; Yuan, J.; Wu, G.; Reyimu, H.; Kadeer, N.; Abudula, A. Potential predictive plasma biomarkers for cervical cancer by 2D-DIGE proteomics and Ingenuity Pathway Analysis. *Tumour Biol.* **2015**, *36*, 1711–1720. [CrossRef]
128. Alaiya, A.A.; Al-Mohanna, M.; Aslam, M.; Shinwari, Z.; Al-Mansouri, L.; Al-Rodayan, M.; Al-Eid, M.; Ahmad, I.; Hanash, K.; Tulbah, A.; et al. Proteomics-based signature for human benign prostate hyperplasia and prostate adenocarcinoma. *Int. J. Oncol.* **2011**, *38*, 1047–1057. [CrossRef]
129. Davalieva, K.; Kiprijanovska, S.; Komina, S.; Petrusevska, G.; Zografska, N.C.; Polenakovic, M. Proteomics analysis of urine reveals acute phase response proteins as candidate diagnostic biomarkers for prostate cancer. *Proteome Sci.* **2015**, *13*, 2. [CrossRef]
130. Chen, C.L.; Lin, T.S.; Tsai, C.H.; Wu, C.C.; Chung, T.; Chien, K.Y.; Wu, M.; Chang, Y.S.; Yu, J.S.; Chen, Y.T. Identification of potential bladder cancer markers in urine by abundant-protein depletion coupled with quantitative proteomics. *J. Proteom.* **2013**, *85*, 28–43. [CrossRef]

131. Chen, Y.T.; Chen, C.L.; Chen, H.W.; Chung, T.; Wu, C.C.; Chen, C.D.; Hsu, C.W.; Chen, M.C.; Tsui, K.H.; Chang, P.L.; et al. Discovery of novel bladder cancer biomarkers by comparative urine proteomics using iTRAQ technology. *J. Proteome Res.* **2010**, *9*, 5803–5815. [CrossRef] [PubMed]
132. Li, H.; Li, C.; Wu, H.; Zhang, T.; Wang, J.; Wang, S.; Chang, J. Identification of Apo-A1 as a biomarker for early diagnosis of bladder transitional cell carcinoma. *Proteome Sci.* **2011**, *9*, 21. [CrossRef] [PubMed]
133. Shang, Z.; Wang, J.; Wang, X.; Yan, H.; Cui, B.; Jia, C.; Wang, Q.; Cui, X.; Li, J.; Ou, T. Preoperative serum apolipoprotein A-I levels predict long-term survival in non-muscle-invasive bladder cancer patients. *Cancer Manag. Res.* **2018**, *10*, 1177–1190. [CrossRef] [PubMed]
134. Chinello, C.; Stella, M.; Piga, I.; Smith, A.J.; Bovo, G.; Varallo, M.; Ivanova, M.; Denti, V.; Grasso, M.; Grasso, A.; et al. Proteomics of liquid biopsies: Depicting RCC infiltration into the renal vein by MS analysis of urine and plasma. *J. Proteom.* **2019**, *191*, 29–37. [CrossRef] [PubMed]
135. Guo, S.; He, X.; Chen, Q.; Yang, G.; Yao, K.; Dong, P.; Ye, Y.; Chen, D.; Zhang, Z.; Qin, Z.; et al. The Effect of Preoperative Apolipoprotein A-I on the Prognosis of Surgical Renal Cell Carcinoma: A Retrospective Large Sample Study. *Medicine* **2016**, *95*, e3147. [CrossRef] [PubMed]
136. Halton, J.M.; Nazir, D.J.; McQueen, M.J.; Barr, R.D. Blood lipid profiles in children with acute lymphoblastic leukemia. *Cancer* **1998**, *83*, 379–384. [CrossRef]
137. Scribano, D.; Baroni, S.; Pagano, L.; Zuppi, C.; Leone, G.; Giardina, B. Return to normal values of lipid pattern after effective chemotherapy in acute lymphoblastic leukemia. *Haematologica* **1996**, *81*, 343–345.
138. Egler, R.A.; Li, Y.; Dang, T.A.; Peters, T.L.; Leung, E.; Huang, S.; Russell, H.V.; Liu, H.; Man, T.K. An integrated proteomic approach to identifying circulating biomarkers in high-risk neuroblastoma and their potential in relapse monitoring. *Proteom. Clin. Appl.* **2011**, *5*, 532–541. [CrossRef]
139. Naru, J.; Aggarwal, R.; Mohanty, A.K.; Singh, U.; Bansal, D.; Kakkar, N.; Agnihotri, N. Identification of differentially expressed proteins in retinoblastoma tumors using mass spectrometry-based comparative proteomic approach. *J. Proteom.* **2017**, *159*, 77–91. [CrossRef]
140. Muntoni, S.; Atzori, L.; Mereu, R.; Satta, G.; Macis, M.D.; Congia, M.; Tedde, A.; Desogus, A.; Muntoni, S. Serum lipoproteins and cancer. *Nutr. Metab. Cardiovasc. Dis.* **2009**, *19*, 218–225. [CrossRef]
141. Li, X.; Liu, Z.L.; Wu, Y.T.; Wu, H.; Dai, W.; Arshad, B.; Xu, Z.; Li, H.; Wu, K.N.; Kong, L.Q. Status of lipid and lipoprotein in female breast cancer patients at initial diagnosis and during chemotherapy. *Lipids Health Dis.* **2018**, *17*, 91. [CrossRef] [PubMed]
142. Wu, J.; Zhang, C.; Zhang, G.; Wang, Y.; Zhang, Z.; Su, W.; Lyu, J. Association Between Pretreatment Serum Apolipoprotein A1 and Prognosis of Solid Tumors in Chinese Population: A Systematic Review and Meta-Analysis. *Cell. Physiol. Biochem.* **2018**, *51*, 575–588. [CrossRef] [PubMed]
143. Zhang, Y.; Yang, X. Prognostic Significance of Pretreatment Apolipoprotein A-I as a Noninvasive Biomarker in Cancer Survivors: A Meta-Analysis. *Dis. Markers* **2018**, *2018*, 1034037. [CrossRef] [PubMed]
144. Wang, Y.; Wang, Z.Q.; Wang, F.H.; Lei, X.F.; Yan, S.M.; Wang, D.S.; Zhang, F.; Xu, R.H.; Wang, L.Y.; Li, Y.H. Predictive value of chemotherapy-related high-density lipoprotein cholesterol (HDL) elevation in patients with colorectal cancer receiving adjuvant chemotherapy: An exploratory analysis of 851 cases. *Oncotarget* **2016**, *7*, 57290–57300. [CrossRef] [PubMed]
145. Cortesi, L.; Barchetti, A.; De Matteis, E.; Rossi, E.; Della Casa, L.; Marcheselli, L.; Tazzioli, G.; Lazzaretti, M.G.; Ficarra, G.; Federico, M.; et al. Identification of protein clusters predictive of response to chemotherapy in breast cancer patients. *J. Proteome Res.* **2009**, *8*, 4916–4933. [CrossRef] [PubMed]
146. Zhang, J.; Cai, Y.; Hu, H.; Lan, P.; Wang, L.; Huang, M.; Kang, L.; Wu, X.; Wang, H.; Ling, J.; et al. Nomogram basing pre-treatment parameters predicting early response for locally advanced rectal cancer with neoadjuvant chemotherapy alone: A subgroup efficacy analysis of FOWARC study. *Oncotarget* **2016**, *7*, 5053–5062. [CrossRef] [PubMed]
147. Walter, S.; Weinschenk, T.; Stenzl, A.; Zdrojowy, R.; Pluzanska, A.; Szczylik, C.; Staehler, M.; Brugger, W.; Dietrich, P.Y.; Mendrzyk, R.; et al. Multipeptide immune response to cancer vaccine IMA901 after single-dose cyclophosphamide associates with longer patient survival. *Nat. Med.* **2012**, *18*, 1254–1261. [CrossRef] [PubMed]
148. Zhang, T.; Guo, J.; Gu, J.; Wang, Z.; Wang, G.; Li, H.; Wang, J. Identifying the key genes and microRNAs in colorectal cancer liver metastasis by bioinformatics analysis and in vitro experiments. *Oncol. Rep.* **2019**, *41*, 279–291. [CrossRef] [PubMed]

149. Danilo, C.; Gutierrez-Pajares, J.L.; Mainieri, M.A.; Mercier, I.; Lisanti, M.P.; Frank, P.G. Scavenger receptor class B type I regulates cellular cholesterol metabolism and cell signaling associated with breast cancer development. *Breast Cancer Res.* **2013**, *15*, R87. [CrossRef] [PubMed]
150. Gutierrez-Pajares, J.L.; Ben Hassen, C.; Chevalier, S.; Frank, P.G. SR-BI: Linking Cholesterol and Lipoprotein Metabolism with Breast and Prostate Cancer. *Front. Pharmacol.* **2016**, *7*, 338. [CrossRef]
151. Zheng, Y.; Liu, Y.; Jin, H.; Pan, S.; Qian, Y.; Huang, C.; Zeng, Y.; Luo, Q.; Zeng, M.; Zhang, Z. Scavenger receptor B1 is a potential biomarker of human nasopharyngeal carcinoma and its growth is inhibited by HDL-mimetic nanoparticles. *Theranostics* **2013**, *3*, 477–486. [CrossRef] [PubMed]
152. Su, F.; Kozak, K.R.; Imaizumi, S.; Gao, F.; Amneus, M.W.; Grijalva, V.; Ng, C.; Wagner, A.; Hough, G.; Farias-Eisner, G.; et al. Apolipoprotein A-I (apoA-I) and apoA-I mimetic peptides inhibit tumor development in a mouse model of ovarian cancer. *Proc. Natl. Acad. Sci. USA* **2010**, *107*, 19997–20002. [CrossRef] [PubMed]
153. Ganapathy, E.; Su, F.; Meriwether, D.; Devarajan, A.; Grijalva, V.; Gao, F.; Chattopadhyay, A.; Anantharamaiah, G.M.; Navab, M.; Fogelman, A.M.; et al. D-4F, an apoA-I mimetic peptide, inhibits proliferation and tumorigenicity of epithelial ovarian cancer cells by upregulating the antioxidant enzyme MnSOD. *Int. J. Cancer* **2012**, *130*, 1071–1081. [CrossRef] [PubMed]
154. Marinho, A.T.; Lu, H.; Pereira, S.A.; Monteiro, E.; Gabra, H.; Recchi, C. Anti-tumorigenic and Platinum-Sensitizing Effects of Apolipoprotein A1 and Apolipoprotein A1 Mimetic Peptides in Ovarian Cancer. *Front. Pharmacol.* **2018**, *9*, 1524. [CrossRef] [PubMed]
155. Gao, F.; Vasquez, S.X.; Su, F.; Roberts, S.; Shah, N.; Grijalva, V.; Imaizumi, S.; Chattopadhyay, A.; Ganapathy, E.; Meriwether, D.; et al. L-5F, an apolipoprotein A-I mimetic, inhibits tumor angiogenesis by suppressing VEGF/basic FGF signaling pathways. *Integr. Biol.* **2011**, *3*, 479–489. [CrossRef] [PubMed]
156. Gao, F.; Chattopadhyay, A.; Navab, M.; Grijalva, V.; Su, F.; Fogelman, A.M.; Reddy, S.T.; Farias-Eisner, R. Apolipoprotein A-I mimetic peptides inhibit expression and activity of hypoxia-inducible factor-1alpha in human ovarian cancer cell lines and a mouse ovarian cancer model. *J. Pharmacol. Exp. Ther.* **2012**, *342*, 255–262. [CrossRef] [PubMed]
157. Aguirre-Portoles, C.; Feliu, J.; Reglero, G.; Ramirez de Molina, A. ABCA1 overexpression worsens colorectal cancer prognosis by facilitating tumour growth and caveolin-1-dependent invasiveness, and these effects can be ameliorated using the BET inhibitor apabetalone. *Mol. Oncol.* **2018**, *12*, 1735–1752. [CrossRef]
158. Su, F.; Grijalva, V.; Navab, K.; Ganapathy, E.; Meriwether, D.; Imaizumi, S.; Navab, M.; Fogelman, A.M.; Reddy, S.T.; Farias-Eisner, R. HDL mimetics inhibit tumor development in both induced and spontaneous mouse models of colon cancer. *Mol. Cancer Ther.* **2012**, *11*, 1311–1319. [CrossRef]
159. Cedo, L.; Garcia-Leon, A.; Baila-Rueda, L.; Santos, D.; Grijalva, V.; Martinez-Cignoni, M.R.; Carbo, J.M.; Metso, J.; Lopez-Vilaro, L.; Zorzano, A.; et al. ApoA-I mimetic administration, but not increased apoA-I-containing HDL, inhibits tumour growth in a mouse model of inherited breast cancer. *Sci. Rep.* **2016**, *6*, 36387. [CrossRef]
160. Peng, M.; Zhang, Q.; Cheng, Y.; Fu, S.; Yang, H.; Guo, X.; Zhang, J.; Wang, L.; Zhang, L.; Xue, Z.; et al. Apolipoprotein A-I mimetic peptide 4F suppresses tumor-associated macrophages and pancreatic cancer progression. *Oncotarget* **2017**, *8*, 99693–99706. [CrossRef]
161. Zamanian-Daryoush, M.; Lindner, D.; Tallant, T.C.; Wang, Z.; Buffa, J.; Klipfell, E.; Parker, Y.; Hatala, D.; Parsons-Wingerter, P.; Rayman, P.; et al. The cardioprotective protein apolipoprotein A1 promotes potent anti-tumorigenic effects. *J. Biol. Chem.* **2013**, *288*, 21237–21252. [CrossRef] [PubMed]
162. Chattopadhyay, A.; Yang, X.; Mukherjee, P.; Sulaiman, D.; Fogelman, H.R.; Grijalva, V.; Dubinett, S.; Wasler, T.C.; Paul, M.K.; Salehi-Rad, R.; et al. Treating the Intestine with Oral ApoA-I Mimetic Tg6F Reduces Tumor Burden in Mouse Models of Metastatic Lung Cancer. *Sci. Rep.* **2018**, *8*, 9032. [CrossRef] [PubMed]
163. Chattopadhyay, A.; Grijalva, V.; Hough, G.; Su, F.; Mukherjee, P.; Farias-Eisner, R.; Anantharamaiah, G.M.; Faull, K.F.; Hwang, L.H.; Navab, M.; et al. Efficacy of tomato concentrates in mouse models of dyslipidemia and cancer. *Pharmacol. Res. Perspect.* **2015**, *3*, e00154. [CrossRef] [PubMed]
164. Ungaro, R.; Mehandru, S.; Allen, P.B.; Peyrin-Biroulet, L.; Colombel, J.F. Ulcerative colitis. *Lancet* **2017**, *389*, 1756–1770. [CrossRef]
165. Lin, Q.; Lai, R.; Chirieac, L.R.; Li, C.; Thomazy, V.A.; Grammatikakis, I.; Rassidakis, G.Z.; Zhang, W.; Fujio, Y.; Kunisada, K.; et al. Constitutive activation of JAK3/STAT3 in colon carcinoma tumors and cell lines: Inhibition of JAK3/STAT3 signaling induces apoptosis and cell cycle arrest of colon carcinoma cells. *Am. J. Pathol.* **2005**, *167*, 969–980. [CrossRef]

166. Cedo, L.; Reddy, S.T.; Mato, E.; Blanco-Vaca, F.; Escola-Gil, J.C. HDL and LDL: Potential New Players in Breast Cancer Development. *J. Clin. Med.* **2019**, *8*, 853. [CrossRef] [PubMed]
167. Borlak, J.; Langer, F.; Chatterji, B. Serum proteome mapping of EGF transgenic mice reveal mechanistic biomarkers of lung cancer precursor lesions with clinical significance for human adenocarcinomas. *Biochim. Et Biophys. Acta Mol. Basis Dis.* **2018**, *1864*, 3122–3144. [CrossRef] [PubMed]
168. Chong, P.K.; Lee, H.; Zhou, J.; Liu, S.C.; Loh, M.C.; So, J.B.; Lim, K.H.; Yeoh, K.G.; Lim, Y.P. Reduced plasma APOA1 level is associated with gastric tumor growth in MKN45 mouse xenograft model. *J. Proteom.* **2010**, *73*, 1632–1640. [CrossRef] [PubMed]
169. Lozano-Pope, I.; Sharma, A.; Matthias, M.; Doran, K.S.; Obonyo, M. Effect of myeloid differentiation primary response gene 88 on expression profiles of genes during the development and progression of Helicobacter-induced gastric cancer. *BMC Cancer* **2017**, *17*, 133. [CrossRef]
170. Takaishi, S.; Wang, T.C. Gene expression profiling in a mouse model of Helicobacter-induced gastric cancer. *Cancer Sci.* **2007**, *98*, 284–293. [CrossRef]
171. Hanahan, D.; Weinberg, R.A. Hallmarks of cancer: The next generation. *Cell* **2011**, *144*, 646–674. [CrossRef] [PubMed]
172. Dapito, D.H.; Mencin, A.; Gwak, G.Y.; Pradere, J.P.; Jang, M.K.; Mederacke, I.; Caviglia, J.M.; Khiabanian, H.; Adeyemi, A.; Bataller, R.; et al. Promotion of hepatocellular carcinoma by the intestinal microbiota and TLR4. *Cancer Cell* **2012**, *21*, 504–516. [CrossRef] [PubMed]
173. Terzic, J.; Grivennikov, S.; Karin, E.; Karin, M. Inflammation and colon cancer. *Gastroenterology* **2010**, *138*, 2101–2114. [CrossRef] [PubMed]
174. Fukata, M.; Chen, A.; Vamadevan, A.S.; Cohen, J.; Breglio, K.; Krishnareddy, S.; Hsu, D.; Xu, R.; Harpaz, N.; Dannenberg, A.J.; et al. Toll-like receptor-4 promotes the development of colitis-associated colorectal tumors. *Gastroenterology* **2007**, *133*, 1869–1881. [CrossRef] [PubMed]
175. Mineo, C.; Shaul, P.W. Novel biological functions of high-density lipoprotein cholesterol. *Circ. Res.* **2012**, *111*, 1079–1090. [CrossRef] [PubMed]
176. Tall, A.R.; Yvan-Charvet, L. Cholesterol, inflammation and innate immunity. *Nat. Rev. Immunol.* **2015**, *15*, 104–116. [CrossRef] [PubMed]
177. Tang, C.; Liu, Y.; Kessler, P.S.; Vaughan, A.M.; Oram, J.F. The macrophage cholesterol exporter ABCA1 functions as an anti-inflammatory receptor. *J. Biol. Chem.* **2009**, *284*, 32336–32343. [CrossRef] [PubMed]
178. Chen, D.S.; Mellman, I. Oncology meets immunology: The cancer-immunity cycle. *Immunity* **2013**, *39*, 1–10. [CrossRef] [PubMed]
179. Schreiber, R.D.; Old, L.J.; Smyth, M.J. Cancer immunoediting: Integrating immunity's roles in cancer suppression and promotion. *Sci.* **2011**, *331*, 1565–1570. [CrossRef] [PubMed]
180. Gabrilovich, D.I.; Nagaraj, S. Myeloid-derived suppressor cells as regulators of the immune system. *Nat. Rev. Immunol.* **2009**, *9*, 162–174. [CrossRef] [PubMed]
181. Sag, D.; Cekic, C.; Wu, R.; Linden, J.; Hedrick, C.C. The cholesterol transporter ABCG1 links cholesterol homeostasis and tumour immunity. *Nat. Commun.* **2015**, *6*, 6354. [CrossRef] [PubMed]
182. Zamanian-Daryoush, M.; Lindner, D.J.; DiDonato, J.A.; Wagner, M.; Buffa, J.; Rayman, P.; Parks, J.S.; Westerterp, M.; Tall, A.R.; Hazen, S.L. Myeloid-specific genetic ablation of ATP-binding cassette transporter ABCA1 is protective against cancer. *Oncotarget* **2017**, *8*, 71965–71980. [CrossRef] [PubMed]
183. Degoma, E.M.; Rader, D.J. Novel HDL-directed pharmacotherapeutic strategies. *Nat. Rev. Cardiol.* **2011**, *8*, 266–277. [CrossRef] [PubMed]
184. Bradley, M.N.; Hong, C.; Chen, M.; Joseph, S.B.; Wilpitz, D.C.; Wang, X.; Lusis, A.J.; Collins, A.; Hseuh, W.A.; Collins, J.L.; et al. Ligand activation of LXR beta reverses atherosclerosis and cellular cholesterol overload in mice lacking LXR alpha and apoE. *J. Clin. Investig.* **2007**, *117*, 2337–2346. [CrossRef] [PubMed]
185. Goodman, K.B.; Bury, M.J.; Cheung, M.; Cichy-Knight, M.A.; Dowdell, S.E.; Dunn, A.K.; Lee, D.; Lieby, J.A.; Moore, M.L.; Scherzer, D.A.; et al. Discovery of potent, selective sulfonylfuran urea endothelial lipase inhibitors. *Bioorg. Med. Chem. Lett.* **2009**, *19*, 27–30. [CrossRef] [PubMed]
186. Hoeg, J.M.; Santamarina-Fojo, S.; Berard, A.M.; Cornhill, J.F.; Herderick, E.E.; Feldman, S.H.; Haudenschild, C.C.; Vaisman, B.L.; Hoyt, R.F., Jr.; Demosky, S.J., Jr.; et al. Overexpression of lecithin:cholesterol acyltransferase in transgenic rabbits prevents diet-induced atherosclerosis. *Proc. Natl. Acad. Sci. USA* **1996**, *93*, 11448–11453. [CrossRef] [PubMed]

187. Okamoto, H.; Yonemori, F.; Wakitani, K.; Minowa, T.; Maeda, K.; Shinkai, H. A cholesteryl ester transfer protein inhibitor attenuates atherosclerosis in rabbits. *Nature* **2000**, *406*, 203–207. [CrossRef] [PubMed]
188. Nissen, S.E.; Tsunoda, T.; Tuzcu, E.M.; Schoenhagen, P.; Cooper, C.J.; Yasin, M.; Eaton, G.M.; Lauer, M.A.; Sheldon, W.S.; Grines, C.L.; et al. Effect of recombinant ApoA-I Milano on coronary atherosclerosis in patients with acute coronary syndromes: A randomized controlled trial. *J. Am. Med. Assoc.* **2003**, *290*, 2292–2300. [CrossRef] [PubMed]
189. Waksman, R.; Torguson, R.; Kent, K.M.; Pichard, A.D.; Suddath, W.O.; Satler, L.F.; Martin, B.D.; Perlman, T.J.; Maltais, J.A.; Weissman, N.J.; et al. A first-in-man, randomized, placebo-controlled study to evaluate the safety and feasibility of autologous delipidated high-density lipoprotein plasma infusions in patients with acute coronary syndrome. *J. Am. Coll. Cardiol.* **2010**, *55*, 2727–2735. [CrossRef]
190. Navab, M.; Anantharamaiah, G.M.; Reddy, S.T.; Fogelman, A.M. Apolipoprotein A-I mimetic peptides and their role in atherosclerosis prevention. *Nat. Clin. Pract. Cardiovasc. Med.* **2006**, *3*, 540–547. [CrossRef]
191. Chattopadhyay, A.; Navab, M.; Hough, G.; Gao, F.; Meriwether, D.; Grijalva, V.; Springstead, J.R.; Palgnachari, M.N.; Namiri-Kalantari, R.; Su, F.; et al. A novel approach to oral apoA-I mimetic therapy. *J. Lipid Res.* **2013**, *54*, 995–1010. [CrossRef] [PubMed]
192. Getz, G.S.; Reardon, C.A. The structure/function of apoprotein A-I mimetic peptides: An update. *Curr. Opin. Endocrinol. Diabetesand Obes.* **2014**, *21*, 129–133. [CrossRef] [PubMed]
193. Ditiatkovski, M.; D'Souza, W.; Kesani, R.; Chin-Dusting, J.; De Haan, J.B.; Remaley, A.; Sviridov, D. An apolipoprotein A-I mimetic peptide designed with a reductionist approach stimulates reverse cholesterol transport and reduces atherosclerosis in mice. *PLoS ONE* **2013**, *8*, e68802. [CrossRef] [PubMed]
194. Karalis, I.; Jukema, J.W. HDL Mimetics Infusion and Regression of Atherosclerosis: Is It Still Considered a Valid Therapeutic Option? *Curr. Cardiol. Rep.* **2018**, *20*, 66. [CrossRef] [PubMed]
195. Shalapour, S.; Lin, X.J.; Bastian, I.N.; Brain, J.; Burt, A.D.; Aksenov, A.A.; Vrbanac, A.F.; Li, W.; Perkins, A.; Matsutani, T.; et al. Inflammation-induced IgA+ cells dismantle anti-liver cancer immunity. *Nature* **2017**, *551*, 340–345. [CrossRef] [PubMed]
196. Jia, D.; Lu, M.; Jung, K.H.; Park, J.H.; Yu, L.; Onuchic, J.N.; Kaipparettu, B.A.; Levine, H. Elucidating cancer metabolic plasticity by coupling gene regulation with metabolic pathways. *Proc. Natl. Acad. Sci. USA* **2019**, *116*, 3909–3918. [CrossRef] [PubMed]
197. Korolainen, M.A.; Nyman, T.A.; Nyyssonen, P.; Hartikainen, E.S.; Pirttila, T. Multiplexed proteomic analysis of oxidation and concentrations of cerebrospinal fluid proteins in Alzheimer disease. *Clin. Chem.* **2007**, *53*, 657–665. [CrossRef] [PubMed]
198. Revilla, G.; Corcoy, R.; Moral, A.; Escola-Gil, J.C.; Mato, E. Cross-Talk between Inflammatory Mediators and the Epithelial Mesenchymal Transition Process in the Development of Thyroid Carcinoma. *Int. J. Mol. Sci.* **2019**, *20*, 2466. [CrossRef] [PubMed]
199. Zhao, W.; Prijic, S.; Urban, B.C.; Tisza, M.J.; Zuo, Y.; Li, L.; Tan, Z.; Chen, X.; Mani, S.A.; Chang, J.T. Candidate Antimetastasis Drugs Suppress the Metastatic Capacity of Breast Cancer Cells by Reducing Membrane Fluidity. *Cancer Res.* **2016**, *76*, 2037–2049. [CrossRef] [PubMed]
200. Idzko, M.; Ferrari, D.; Eltzschig, H.K. Nucleotide signalling during inflammation. *Nature* **2014**, *509*, 310–317. [CrossRef] [PubMed]
201. Sharma, M.; Tuaine, J.; McLaren, B.; Waters, D.L.; Black, K.; Jones, L.M.; McCormick, S.P. Chemotherapy Agents Alter Plasma Lipids in Breast Cancer Patients and Show Differential Effects on Lipid Metabolism Genes in Liver Cells. *PLoS ONE* **2016**, *11*, e0148049. [CrossRef] [PubMed]
202. Feingold, K.R.; Grunfeld, C. The role of HDL in innate immunity. *J. Lipid Res.* **2011**, *52*, 1–3. [CrossRef] [PubMed]

© 2019 by the authors. Licensee MDPI, Basel, Switzerland. This article is an open access article distributed under the terms and conditions of the Creative Commons Attribution (CC BY) license (http://creativecommons.org/licenses/by/4.0/).